



University
of Glasgow

Abdalahaman, Naiemh (2017) *The assessment of bone health in young women with childhood-onset type one diabetes mellitus*. PhD thesis.

<http://theses.gla.ac.uk/8413/>

Copyright and moral rights for this work are retained by the author

A copy can be downloaded for personal non-commercial research or study, without prior permission or charge

This work cannot be reproduced or quoted extensively from without first obtaining permission in writing from the author

The content must not be changed in any way or sold commercially in any format or medium without the formal permission of the author

When referring to this work, full bibliographic details including the author, title, awarding institution and date of the thesis must be given

Enlighten:Theses
<http://theses.gla.ac.uk/>
theses@gla.ac.uk

**The Assessment of Bone Health
In Young Women with Childhood-Onset Type
One Diabetes Mellitus**

Dr Naiemh Abdalrahaman
MBChB & MSc (paediatrics)

Submitted in fulfilment of the requirements for the degree of Doctor
of Philosophy



Department of Child Health
Royal Hospital for Sick Children
Faculty of Medicine University of Glasgow

August 2017

Abstract

The risk of hip fracture in people with type one diabetes mellitus (T1DM) is reported to be 7 to 12 times greater than in those without T1DM, and this increased risk is evident in both children and young adults. This fracture risk is higher than expected bone mineral density (BMD) measurements, which indicates the likelihood that other skeletal factors, not captured by DXA, may contribute toward increased fracture risk. There is increasing evidence that alteration in trabecular bone microarchitecture and increased bone marrow adiposity (BMA) are causes for excess skeletal fragility, yet these data are lacking in people with T1DM. Recent technological advances in magnetic resonance imaging (MRI) have allowed the quantification of trabecular bone architecture. In addition, MRI can quantify the amount of intra-abdominal fat, and magnetic resonance spectroscopy (MRS) can also be used to assess BMA. These advances may enhance our understanding of the underlying causes of diabetic osteopathy which may lead to improved fracture risk predictors and preventive measures in patients with T1DM beyond that provided by dual energy x-ray absorptiometry (DXA).

The overall objective of this thesis was to improve the understanding of the bone pathology of young adult women with childhood-onset T1DM by using high resolution MRI.

A cross-sectional study was first carried out to assess trabecular bone microarchitecture of the tibia, vertebral BMA and abdominal adiposity in patients with childhood onset T1DM (n=30) compared with healthy controls (n=28). Additionally, the biochemical markers of bone turnover, adiposity and GH/IGF-1 axis (IGF-1, IGFBP3, and ALS) were examined to evaluate the underlying mechanism that might result in bone deficit in this group of people. We found that young women with childhood onset T1DM had reduced apparent trabecular bone volume (appBV/TV) and apparent trabecular number (appTbN) and greater apparent trabecular separation (appTbSp) than women without T1DM. Interestingly, these differences remained significant after adjustment for multiple confounders. Furthermore, these abnormalities were markedly obvious in those with microvascular complication compared with those without microvascular complication. Although women with T1DM had greater abdominal adiposity compared with healthy controls, there was no significant difference in BMA between the groups. However, BMA showed positive significant association with current glycaemic control ($r=0.45$, $p=0.02$). Women with T1DM had lower bone turnover and decreased GH/IGF axis compared with healthy controls. Osteocalcin and ALS were negatively correlated with trabecular separation in women with T1DM.

Next, a one-year prospective study was conducted in a subset (n=28) of the participants involved in the cross-sectional study. The aim of this study was to compare one year changes in trabecular bone microarchitecture and BMA in women with and without T1DM. Additionally, the study aimed to evaluate the effect of glycaemic control on these changes over this period. After adjustment for relevant confounders, the cases (n=17) had a lower median appTbN and a higher median appTbSp at baseline and 12 months compared with healthy controls (n=11). Although the sample size was small at follow-up, the trabecular bone deficits were clearly noticeable in those with retinopathy compared with those without retinopathy. Similarly, there was no difference in median BMA which was 26.2% (12.1, 62.1) and 22.4% (9.6, 41.9) in cases and controls, respectively ($p=0.57$). Additionally, over the 12 month period, there was no significant change in MRI-measured parameters in cases or in controls, and no differences in the change of these variables between the two groups. Mixed model effect analysis showed that age was a negative predictor of percent changes of appBV/TV, appTbN and appTbSp in both cases and controls ($p=0.02$, $p=0.02$, $p=0.002$, respectively). Interestingly, there was a strong correlation between change in HbA1c and change in BMA ($r=0.8$; $p=0.002$).

In the third study, we aimed to assess adiposity-based determinants of bone mineral density and bone microarchitecture in healthy young women and women with T1DM.

Additionally, we aimed to compare the feasibility of using DXA and MRI-measured bone parameters to differentiate women with and without T1DM. In addition to high resolution MRI we used DXA scans to measure BMD and body composition from the same participants (n=26) involved in the longitudinal study. Vertebral BMA was positively correlated with VAT. Additionally, we demonstrated evidence of an inverse association of vertebral BMA and DXA-measured bone parameters of femoral neck, lumbar spine and total body independent of demographics and body composition in healthy young women and women with T1DM. These findings support the hypothesis that BMA is linked with low bone density, and may contribute to excess bone fragility. Moreover, this study suggested that MRI-measured trabecular bone measurements were able to differentiate between T1DM with and without microvascular complication compared with DXA-measured BMD.

In summary, differences in MRI-measured trabecular microarchitecture parameters identified in this body of work provide preliminary explanations for elevated fracture risk in young women with childhood onset T1DM. Additionally, these findings provide potential insight into a number of possible underlying mechanisms of diabetic osteopathy.

Table of Contents

Abstract	II
List of Tables	VI
List of Figures	VII
List of Accompanying Material	X
Acknowledgement	XII
Dedication	XII
Author’s Declaration	XIV
Abbreviations	XV
Chapter 1	19
Introduction	19
1.1 Bone development and its Components	20
1.2 Osteoporosis	30
1.3 T1DM	37
1.4 T1DM and abnormalities of bone health	38
1.5 Imaging Modalities for assessment of bone health	56
1.6 The rationale for the present work	79
1.7 Key Aims and hypothesis	80
Chapter 2	83
Methodology	83
2.1 Introduction	84
2.2 MRI scanning	84
2.3 Dual-Energy X-ray Absorptiometry (DXA)	95
2.4 Blood analysis	96
2.5 Statistical Analysis	97
Chapter 3	98
Deficits in Trabecular Bone Microarchitecture in Young Women With Type 1 Diabetes Mellitus	98
3.1 Abstract	99
3.2 Introduction	100
3.3 Material and method	101
3.4 Results	104
3.5 Discussion	119
3.6 Conclusion	122
Chapter 4	123
Longitudinal Changes In Bone Marrow Adiposity And Its Relationship To Diabetes Control In Young Women With Type 1 Diabetes Mellitus	123
4.1 Abstract	124

4.2	Introduction	125
4.3	Research Design & Methods.....	126
4.4	Results	128
4.5	Discussion	143
4.6	Conclusion	145
Chapter 5		146
An assessment of adiposity-based determinants of bone density and microarchitecture in healthy young women and women with T1DM.....		146
5.1	Abstract:	147
5.2	Introduction	148
5.3	Subjects and methods	149
5.4	Result	151
5.5	Discussion	162
5.6	Conclusion	164
Chapter 6		165
Discussion, conclusion and future perspective		165
6.1	General discussion	166
6.2	Final conclusion	172
6.3	Strengths and Limitations	174
6.4	Future Perspectives	176
List of References		178
Appendices		221
7.1	Appendix A: Study protocol	222
7.2	Appendix B: Pilot Study Of Bone Health In Young People With Type 1 Diabetes Mellitus, Case Report Form.	231

List of Tables

Table 1.1: Showing WHO BMD T-Score criteria	32
Table 1.2: Studies that evaluated fracture risk in people with Type 1 Diabetes Mellitus (T1DM).	48
Table 1.3: Bone densitometry studies in children with T1DM.....	51
Table 1.4: Bone densitometry studies in adults with Type 1 diabetes.	52
Table 1.5: Summary of MRI studies which report assessment of trabecular bone microarchitecture in different population.....	70
Table 1.6: Summary of MRI studies which report assessment of bone marrow composition in different populations. Variety in MRI protocols is reported; including adiposity used technique, magnetic field strength and anatomical location.	75
Table 2.1: Pulse sequence parameters for tibia imaging.....	85
Table 2.2: Pulse sequence (PRESS) parameters for MRS	91
Table 2.3: Pulse sequence parameters for abdominal imaging	93
Table 3.1: Clinical and biochemical details of study participants.	105
Table 3.2: MRI-based measures of abdominal adiposity, bone microarchitecture and vertebral bone marrow adiposity at L3	108
Table 4.1: Descriptive characteristic of study participants who were enrolled at baseline and follow-up. All continuous variables are described as median and range	129
Table 4.2: Differences in MRI baseline data for who dropout and completed the study ..	130
Table 4.3: MRI-based measures of abdominal adiposity, bone microarchitecture and vertebral bone marrow adiposity at L3 for controls and participants with T1DM (diabetes) at baseline and one year.	132
Table 5.1: Clinical characteristic of study participants.....	151
Table 5.2: Bone and body composition parameters in women with T1DM and matched controls.....	152
Table 5.3: Correlations among body fat measures in T1DM and Matched Controls	153
Table 5.4: Correlation among bone measures in T1DM and matched controls.....	154
Table 5.5: Correlations among bone measures, BMA, and body composition in T1DM and Matched Controls	157
Table 5.6: Regression model with BMD and FN-BMC as the dependent variable.....	158

List of Figures

Figure 1.1: Schematic diagram illustrates the hierarchical structures of cortical and trabecular bone (12).	21
Figure 1.2: Illustrating Remodelling pathway and how the bone cells communicate through signalling pathways.	25
Figure 1.3: Microarchitecture of normal and osteoporotic bone.	31
Figure 1.4: Determinants of bone strength including bone mineral density (BMD), structural properties and material properties. The bone remodelling has influences on the bone strength parameters (165).	34
Figure 1.5: Illustrating the relationship between adipose tissue and bone. The connection can be via peripheral fat and fat within bone marrow milieu.	36
Figure 1.6: Pathophysiological mechanisms of diabetes bone disease.	55
Figure 1.7: Illustration of spin alignment a) with no external magnetic field and b) in the presence of an external magnetic field (393).	59
Figure 1.8: Illustration of transfer of net magnetisation (M) from the longitudinal plane to the transverse plane	60
Figure 1.9: Illustration of a) T_1 and b) T_2 relaxation curves for fat, muscle and fluid(395).	61
Figure 1.10: Illustration of a) slice selection and b) localisation in the frequency and phase directions using linear magnetic field gradients (395).	61
Figure 1.11: Images of the tibia acquired with voxel sizes of a) 2.2x2.2x3.0, b) 1.1x1.1x3.0 and c) 0.4x0.4x3.0 mm.	62
Figure 1.12: Example of an MRI pulse sequence diagram. The RF pulses are shown on the top line, and the magnetic field gradients are shown on the lines marked G_s , G_p , and G_f , where the subscripts refer to the slice, phase and frequency directions.	63
Figure 1.13: Sagittal MR image of the tibia.	64
Figure 1.14: Typical MRS spectrum within the brain.	65
Figure 1.15: Axial MRI image of the tibia.	66
Figure 1.16: The resulting spectrum shows peaks corresponding to water and lipid peaks	71
Figure 1.17: Example of T1-weighted axial magnetic resonance images acquired in abdomen at the level of the L3 vertebrae demonstrating the typical high signal intensities of fatty tissues (arrows) in contrast to other darker muscles and organs. Data were acquired on a 3 Tesla MRI scanner.	78
Figure 2.1: Representative MR image of the knee. Scan locations are shown, (A) showing the placement of the reference line and the region of interest captured in the coronal image, (B) The region of interest captured in the axial image.	85
Figure 2.2: Illustrating a median filter applied to MR image, a 3x3 filter was used (A). An example of the output of a 3x3 filter (B).	86
Figure 2.3: Illustrate estimation of the marrow-equivalent intensity	87
Figure 2.4: Representative MR Image through an axial section in the proximal tibia using MRI.	90
Figure 2.5: Representative MR image of spine showing the scan localisation at L3 vertebrae.	91
Figure 2.6: The method of frequency domain fitting using Gaussian line shape. The white line illustrates the original spectrum; the red line illustrates the fitting model.	92
Figure 2.7: Representative MR Image through axial slice of abdomen at L3 vertebrae showing example of Slice-O-matic segmentation to delineate the subcutaneous (Green) and visceral (Blue) adipose tissue depots.	94
Figure 3.1: Pathway outlining participant recruitment and enrolment in the study.	102
Figure 3.2: Box plot of serum CTX, IGF-1 and ALS in women with T1DM (Green box) and controls (Blue box).	107

Figure 3.3: Box plot of MRI-measured abdominal adiposity parameters in women with T1DM (Green box) and controls (Blue box).....	109
Figure 3.4: Boxplot of MRI-measured trabecular bone parameters in women with T1DM (Green box) and controls (Blue box).	111
Figure 3.5: The relationship between apparent trabecular separation (appTbSp) as assessed by MRI and serum acid labile subunit (ALS) (A) and serum osteocalcin (OC) (B) in women with T1DM (filled circles) and controls (open circles).	112
Figure 3.6: Apparent bone volume/total volume (appBV/TV) in women with T1DM with and without retinopathy and compared with control women.....	113
Figure 3.7: Unadjusted correlation of apparent trabecular separation (appTbSp) and appBV/TV with disease duration (A, B, respectively) and age of the patients (C, D, respectively) in women with T1DM.	114
Figure 3.8: App BV/TV in relation to age of diagnosis. T1DM women with earlier age of diagnosis showed trend toward lower bone volume compared with women with later age of diagnosis (p=0.08).	115
Figure 3.9 The relationship between vertebral bone marrow adiposity (FF%) as assessed by MRS and cross sectional area (CSA) (A), subcutaneous adipose tissue (SCAT) (B), visceral adipose tissue (VAT) (C) and total adipose tissue (TAT) (D) in women with T1DM (filled circles) and controls (open circles).....	116
Figure 3.10: The relationship between vertebral bone marrow adiposity (FF%) as assessed by MRS and serum acid labile subunit (ALS) (A) and serum osteocalcin (OC) (B) in women with T1DM (filled circles) and controls (open circles).....	117
Figure 3.11: The relationship between vertebral BMA (FF %) and current HbA1c. Positive significant association was observed.	118
Figure 3.12 VBMA in relation to current HbA1c of >7% or ≤7%.....	118
Figure 4.1: Path outlining study participant recruitment, enrollment and followup from baseline to follow-up assessment.	127
Figure 4.2: The absolute changes in the abdominal adiposity parameters over the one year period in both women with T1DM and controls.....	134
Figure 4.3: The median percentage changes in the abdominal adiposity parameters over the one year period in both T1DM (black circles) and controls (black squares).	135
Figure 4.4: The relationship between % changes in CSA, SCAT and TAT as assessed by MRI and % change in BMI in women with T1DM (filled circles) and controls (open circles).	136
Figure 4.5: Absolute and median % changes in fat fraction (%FF) over one year period in both women with T1DM and controls. (A) absolute changes in FF% in T1DM, (B) absolute changes in FF% in controls and (C) % changes in FF% in both T1DM (Black circles) and controls (Black squares)	137
Figure 4.6: The relationship between percentage (%) change in fat fraction as a measure of vertebral Bone Marrow Adiposity (BMA) and % change in HbA1c measured within the 4 weeks prior to MRI scan at baseline and follow-up visit at 1 yr (A) and average HbA1c for the year prior to MRI scan at baseline and follow-up visit at 1 yr (B).	138
Figure 4.7: Percentage change (%) in fat fraction as a measure of vertebral Bone Marrow Adiposity (BMA) for each participant in relation to the extent of change in HbA1c from baseline to 12 months.....	138
Figure 4.8: The median percentage changes in the bone microarchitecture parameters over the one year period in both women with T1DM and control groups.	141
Figure 4.9: The median % changes in the bone microarchitecture parameters over one year period in both women with T1DM (Black circles) and controls (Black squares).....	142
Figure 5.1: The relationship between apparent trabecular separation (appTbSp) as assessed by MRI and total body BMD (TB-BMD g/cm ²), Total body BMC (TB-BMC (g)), Femoral neck BMD (FN-BMD (g/cm ²)) and Femoral neck-BMC (FN-BMC (g)) in women with T1DM (filled circles) and controls (open circles).....	155

Figure 5.2: The relationship between VBMA and BMD and BMC at different measured sites (Whole body, FN, L2-L4).....160

Figure 5.3: The relationship between visceral adipose tissue (VAT) as assessed by MRI and vertebral bone marrow adiposity (FF %) and Total body BMD (TB-BMD (g/cm²)) in women with T1DM (filled circles) and controls (open circles).....161

List of Accompanying Material

Relevant Papers

Abdalrahaman N, McComb C, Foster JE, McLean J, Lindsay RS, McClure J, McMillan M, Drummond R, Gordon D, McKay GA, Shaikh MG, Perry CG, Ahmed SF. Deficits in Trabecular Bone Microarchitecture in Young Women With Type 1 Diabetes Mellitus. *J Bone Miner Res.* 2015 Aug;30(8):1386-93.

Abdalrahman, N., Suet Ching Chen, Jessie Ruijun Wang and Syed Faisal Ahmed. An update on diabetes related skeletal fragility. *Expert Review of Endocrinology & Metabolism*, 2015. 10(2): p. 193-210.

Abdalrahaman N, McComb C, Foster JE, Lindsay RS, Drummond R, McKay GA, Perry CG, Ahmed SF. The Relationship Between Adiposity, Bone Density And Microarchitecture Is Maintained In Young Women Irrespective Of Diabetes Status. *Clin Endocrinol (Oxf)*. 2017 Jun 28

Relevant Conference Abstracts

Abdalrahaman N, McComb C, Foster JE, McMillan M, Drummond R, Gordon D, Lindsay R, Mackay G, Perry C, Shaikh MG, Ahmed SF. Bone Microarchitecture And Vertebral Bone Marrow Adiposity In Young Women With Childhood-Onset Type 1 Diabetes Mellitus (T1DM). *European Society for Paediatric Endocrinology (ESPE)/ 9th joint meeting, Milan, Italy, 2013.*

Abdalrahaman N, McComb C, Foster JE, McMillan M, Drummond R, Gordon D, Lindsay R, Mackay G, Perry C, Shaikh MG, Ahmed SF. Bone Microarchitecture And Vertebral Bone Marrow Adiposity In Young Women With Childhood-Onset Type 1 Diabetes Mellitus (T1DM). *Yorkhill research day, Glasgow, UK, 29th Nov 2013*

Abdalrahaman N, McComb C, Foster JE, Lindsay RS, McClure J, McMillan M, Drummond R, Gordon D, McKay GA, Shaikh MG, Perry CG, Ahmed SF. Abnormalities In Bone Microarchitecture And Bone Marrow Adiposity In Young Women With Type 1 Diabetes Mellitus. *Endocrine society (ICE/ENDO), Chicago, USA, 22nd June 2014*

Abdalrahaman N, McComb C, Foster JE, McLean J, Lindsay RS, Boroujerdi M, Drummond R, McKay GA, Perry CG, Ahmed SF. Longitudinal Changes In Bone Marrow Adiposity And Its Relationship To Diabetes Control In Young Women With Type 1 Diabetes Mellitus. *Diabetes UK Professional Conference, Glasgow, UK, 2-4 March 2016.*

Abdalrahaman N, McComb C, Foster JE, McLean J, Lindsay RS, Boroujerdi M, Drummond R, McKay GA, Perry CG, Ahmed SF. Longitudinal Changes In Bone Marrow Adiposity And Its Relationship To Diabetes Control In Young Women With Type 1 Diabetes Mellitus. *Glasgow Paediatric Research Day, Glasgow, UK, 9th October 2015.*

SC Chen, N **Abdalahaman**, C McComb, J Foster, SF Ahmed. The Precision of Partial Image Analysis of Trabecular Bone Microarchitecture by High-resolution Magnetic Resonance Imaging (hrMRI). International Conference of Children's Bone Health /7th, Salzburg, Austria, 27-30 June 2015

Achievement

Helmley Charitable Trust Travel Award in Type 1 Diabetes in conjunction with ICE/ENDO toward attending ICE/ENDO 2014, Chicago, USA, 22nd June 2014

Acknowledgement

First and foremost, I am most thankful to Allah, the Almighty, for giving me the strength to complete this thesis.

Most of the results described in this thesis would not have been possible without the help and support of many people. I am deeply indebted to those who contributed in many ways to the achievement of this study and made it an unforgettable experience for me. It is my pleasure that I have now the opportunity to express my gratitude to all of them.

First of all, I would like to express my deep and sincere gratitude to my supervisors. My principal supervisor, Professor Faisal Ahmed, for the patient guidance, encouragement and advice he has provided me throughout my PhD and my second supervisor, Dr John foster, for supporting me with his great knowledge and guidance. They have provided me with continued positive support and feedback. Without their help and encouragement I would not have reached this stage.

Along with Dr John Foster, I must express my gratitude particularly to Dr Christie McComb who gave me support and an understanding of the MRI work carried out by her that is described in the thesis and she has been very kind to my day-to-day needs in the MRI department.

I would also like to thank all the members of the MRI department for their helping in scanning the study participants.

I also gratefully acknowledge the help of diabetic team at Stobhill hospital for all their assistance in the recruitment of patients and I would like to thank all participants who took part in this thesis. I owe a great deal of appreciation and gratitude to Dr Sheila Shepherd for carrying out DXA scanning and Mr. Martin McMillan for analysing blood samples.

I am indebted to my many colleagues for providing a stimulating and fun filled environment. My thanks go in particular to Dr Mabrouka and Dr Mahjouba, for standing always beside me during the happy and hard moments to push me and motivate me. I would like to thank all members of research and development research group and staff in department of child health. I wish to express my sincere gratitude in particular to Mrs. Karyn Cooper for her continued support at various stages of the PhD, her co-operation and for assisting in several administrative matters.

Finally, I must express my gratitude for the unconditional love and support given by my family, thanks to you.

Dedication

This thesis is dedicated to my husband Fawzi Pousopaa and my children Ammar, Odey, Muammar and Qusay for they gave me values; enjoyment and love. I was continually amazed by the patience of my husband who experienced all of the ups and downs of my research. Without their encouragement and understanding it would have been impossible for me to finish this work. I dedicate this work to them.

This thesis is also dedicated to all member of my family in Libya who have all supported me and given me the strength to complete this thesis.

Author's Declaration

I declare, except where reference is made to the contribution of others that all work presented in this thesis was performed entirely by myself and has not been submitted for any other degree at the University of Glasgow or any other institution.

Dr Naiemh Abdalrahaman

I certify that the work reported in this thesis has been performed by Dr Naiemh Abdalrahaman and that during the period of study she has fulfilled the conditions of the ordinances and regulations governing the Degree of Doctor of Philosophy, University of Glasgow.

Prof SF Ahmed

Abbreviations

ALS	Acid labile subunits
AGEs	Advanced glycation end-products
ALP	Alkaline phosphatase
aBMD	Areal bone mineral density
APN	Adiponectin
APN-KO	APN-knockout
ADC	Apparent diffusion coefficient
AN	Anorexia nervosa
AlloHSCT	Allogenic haematopoietic stem cell transplantation
AppBV/TV	Apparent bone volume to total volume ratio
App TbTh	Apparent trabecular thickness
App TbN	Apparent trabecular number
App TbSp	Apparent trabecular spacing
BMI	Body mass index
BMA	Bone marrow adiposity
BAT	Brown adipose tissue
BMF	Bone marrow fat
BALP	Bone alkaline phosphatase
BA	Bone area
BMAD	Bone mineral apparent density
BMC	Bone mineral content
BMD	Bone mineral density
BMPs	Bone morphogenic proteins
BSU	Basic structural unit
BTMs	Bone turnover markers
BMUs	Basic multicellular units
BGLAP	Bone δ -carboxyglutamic acid-containing protein
β -cells	Beta cells
BSAP	Bone-specific alkaline phosphatase
β 2-AR	β 2-adrenergic receptor
BUA	Broadband ultrasound attenuation
b-SSFP	Balanced- steady-state free precession
b-SSSE	Balanced- steady state spin echo sequence
CBA	Cortical bone area

CP	Cerebral palsy
CSA	Cross sectional area
CTX	Cross-linked C-terminal telopeptides
C3	Cervical vertebrae 3
DPP-4	Dipeptidyl peptidase-4
DXA	Dual energy X-ray absorptiometry
DWI	Diffusion-weighted magnetic resonance imaging
DR	Distal radius
3-D	3-Dimensional
ELISA	Enzyme-linked immunosorbent assay
%FF	Percentage fat fraction
FA	Forearm
FN	Femoral neck
FLASE	Fast Large-Angle Spin-Echo
FRAX	Fracture risk assessment tool
FOV	Field of view
INF- γ	Gamma interferon
GH	Growth hormone
GH/IGF-1	Growth hormone/insulin-like growth factor-1
GHBP	Growth hormone binding protein
GHD	Growth hormone deficiency
γ -carboxylation	Gamma- carboxylation
HBSC	Haematopoietic stem cells
HtSDS	Height standard deviation scores
HO-1	Heme oxygenase-1
HR-pQCT	High resolution peripheral quantitative computed tomography
IGFBP	Insulin-like growth factor -binding protein
IAP	Intestinal alkaline phosphatase
IL	Interleukin
ICAM-1	Intracellular adhesion molecule-1
% IBW	Ideal body weight
IRs	Insulin receptors
JMRUI	Java-based magnetic resonance user interface
LS	Lumbar spine
LS-BMC	Lumbar spine BMC

LS-BMD	Lumbar spine BMD
LWR	Lipid to water ratio
MHz	Megahertz
MIL	Mean Intercept Length
MVD	Microvascular diseases
MRI	Magnetic resonance imaging
MRS	Magnetic resonance spectroscopy
MSCs	Mesenchymal stem cells
M-CSF	Macrophage clonally stimulating factor
mRNA	Massenger ribonucleic acid
μ CT	Micro-computed tomography
NTX	Cross-linked N-terminal telopeptide of type I collagen
OC	Osteocalcin
OI	Osteogenesis imperfect
OPG	Osteoprotegerin
OSX	Osterix
p.QCT	Peripheral quantitative computed tomography
PICP	Carboxy-terminal propeptide of type I procollagen
PINP	Amino-terminal propeptide of type I procollagen
PRESS	Point-REsolved Spectroscopy
PTH	Parathyroid hormone
PPAR γ	Peroxisome proliferator-activated receptor gamma
PCR	Polymerase chain reaction
PVE	Partial volume effects
PDFF	Proton density fat fraction:
QUS	Quantitative ultrasound
QCT	Quantitative computed tomography
RANK	Receptor activator of nuclear factor $\kappa\beta$
RANKL	Receptor activator of nuclear factor $\kappa\beta$ ligand
ROI	Region of interest
Runx2	Runt-related protein
ROS	Reactive oxygen species
RF	Radiofrequency
SDS	Standard deviation score
SNS	Sympathetic nervous system

SOS	Speed of sound
SNR	Signal noise ratio
SRCT	Synchrotron radiation computed tomography
SAT	Subcutaneous adipose tissue
TB-BMC	Total Body BMC
TB-BMD	Total Body BMD
TBF	Total body fat
TNF- α	Tumour necrosis factors- α
TNAP	Tissue nonspecific alkaline phosphatase
TAT	Total adipose tissue
TR	Repetition Time
TE	Echo Time
TA	Acquisition Time
TZDs	Thiazolidinediones
T1DM	Type 1 diabetes mellitus
T2DM	Type 2 diabetes mellitus
T	Time
Tetramethylsilane	TMS
ucOC	Uncarboxylated osteocalcin
vBMD	Volumetric BMD
VIT-D	Vitamin D
VDR	Vitamin D receptor
VF _s	Vertebral fracture
VAT	Visceral adipose tissue
WHO	World Health Organization
WT	Wild type
WB-FM	Whole body fat mass
WAT	White adipose tissue

Chapter 1

Introduction

1.1 Bone development and its Components

1.1.1 Bone architecture

Bone is a multifunctional organ organized in a hierarchical way that enables it to perform its functions. Structurally, the bone is formed of two tissues: cortical and trabecular bone (Figure 1.1). Cortical bone is found in the diaphysis of long bones and outer surfaces of flat bones, and trabecular bone is found mainly at the end of long bones and in the inner parts of flat bones. Different skeletal sites have different proportions of cortical to trabecular bone (1). Both types of bone will be discussed in detail below.

1.1.1.1 Trabecular bone

Trabecular bone is a porous type of bone tissue found inside the bone, and known as cancellous or spongy bone. Trabecular bone constitutes 20% of total bone mass in the skeleton. The greatest volumes of trabecular bone are at the skeletal sites where the majority of osteoporotic or fragility fractures occur (2). Trabecular bone is identifiable by the sponge-like appearance of calcified tissue, with spaces filled with bone marrow, giving them the alternative name of spongy bones. The bone marrow spaces of trabecular bone provide vascular and neural access and create the large surface area through which bone remodelling occurs (3). Trabecular bone is unlike cortical bone in that the osteon does not contain a central Haversian canal, but has lacunae filled with bone cells, and canaliculi which connect these lacunae and the trabecular surface, through which the nutrition of bone cells is facilitated (4). The trabecular structure resembles a honeycomb of mineralized trabeculae in the shape of rod-like structures connected by plate-like structures. Each individual trabecula is approximately 100-300 μm thick and trabeculae are separated by spaces of 300–1500 μm (5). The trabecular tissue properties are determined by the orientation and the connectivity of the trabeculae (6). Furthermore, the trabecular tissue properties are determined by the total amount of mineralized trabecular tissue and the morphological characterization of these trabeculae. The most important morphological parameters are Bone Volume (BV/TV), Trabecular Number (Tb.N), Trabecular Thickness (Tb.Th), and Trabecular Separation (Tb.Sp). These parameters are typically determined using histomorphometry (7), or by 3D imaging techniques(8, 9).

1.1.1.2 Cortical bone

Cortical bone is the solid thick outer shell of bones often referred to as “compact” bone. It constitutes about 80% of the total bone mass in the skeleton, but it accounts for a considerably smaller surface area than trabecular bone because of its high cellularity that in turn give rise to its higher mass to volume ratio (1, 10). The basic structure in the cortical bone is the osteons, which are cylindrical structures oriented with the long axis of the bone, forming the Haversian system (1). The spaces between the harversian systems are filled with the interstitial bone. Each osteon consists of a central canal (Haversian canal) through which vascular access is facilitated. The Haversian canals are oriented with the long axis of the bone, surrounded by layers of calcified bone matrix called concentric lamellae. The concentric lamellae contain collagen fibres oriented in a specific direction to provide strength to the tissue. Between these concentric circles there are specific interconnected canals (lacunae and canaliculi) through which bone cells communicate. In fact, cortical bone is not solid; it typically contains about 5% cavities to its total volume, including cellular lacunae and canaliculi (1). The cortical volumetric bone mineral density (vBMD) is determined by the number and average size of the cavities (osteonal canals) (porosity) and the mineralization density of the cortical tissue (11).

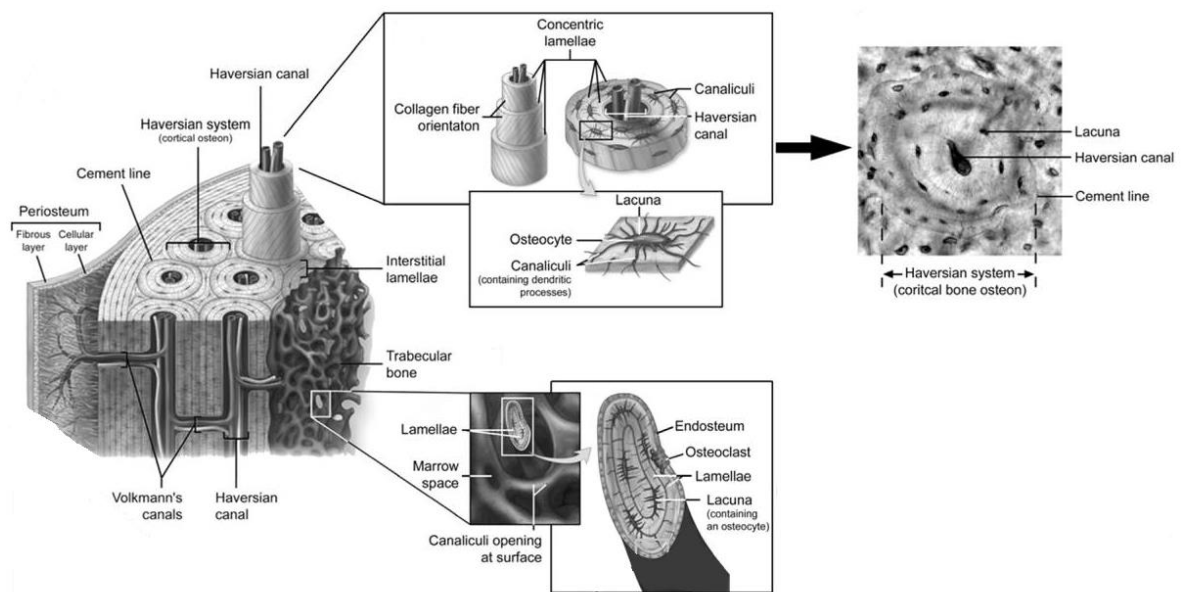


Figure 1.1: Schematic diagram illustrates the hierarchical structures of cortical and trabecular bone (12).

1.1.3 Bone cells and matrix

Within both trabecular and cortical bone there are three main types of bone cells: osteoclasts, osteoblasts, and osteocytes. Osteoclasts are terminally differentiated multinucleated cells derived from hematopoietic stem cells and are responsible for bone resorption (13). Once osteoclasts are differentiated they are capable of secreting enzymes that dissolve the bone matrix. Additionally, they secrete factors to promote osteoblast precursor recruitment and differentiation and thereby promote bone formation (14, 15). Osteoblasts are derived from mesenchymal stem cells (MSCs) and are responsible for building the organic bone matrix and regulating mineral deposition on the matrix (16). The commitment of MSCs towards the osteoprogenitor lineage requires expression of specific genes (17-22). Runx2 is a master gene of osteoblast differentiation, as demonstrated by the fact that Runx2-null mice are devoid of osteoblasts (23). Osteocytes are the most abundant and long-lived cells derived from MSC lineage through osteoblast differentiation. Osteocytes act as Master Orchestrator of skeletal activity, regulating both bone formation and resorption to govern the skeletal response to mechanical forces (24-26). These cells are embedded within the bone matrix which is composed of organic materials (20%), inorganic materials (70%) and water (10%) (27, 28). The organic portion is mainly composed of type 1 collagen (90%), which forms an extracellular matrix where the inorganic materials can be deposited to strengthen the collagen structure. The most abundant inorganic material in bone is calcium and phosphate ions, which nucleate to form hydroxyapatite crystals (27, 29). The water content of the matrix binds to the collagen and minerals. Collagen-bound water influences its three-dimensional structure, which can be visualised by magnetic resonance imaging (MRI) (30). Each of these bone matrix components plays a critical role in the biomechanical properties and functional integrity of bone (29, 31-38).

1.1.5 Bone turnover and remodelling

Bone remodelling is a life-long process that involves cyclical removal of discrete packets of old bone (bone resorption) and replacement of these packets with newly synthesized bone (bone formation) (39-41). To maintain the structural integrity of the skeleton, it is of crucial importance that the amount of bone resorbed matches the amount of newly formed bone in each remodelling site. This requires that the processes of bone resorption and bone formation are linked in a temporally and spatially coordinated manner within the remodelling cycle and form a coupling mechanism (42-44). To maintain the balance, bone cells communicate directly, and indirectly through signalling pathways (45). However, the specific signals that maintain the coupling process are still not well understood. It is clear, however, that the osteocyte acts as an orchestrator in regulating bone remodelling (46, 47). Additionally, there are several systemic factors (genetic, mechanical, vascular, nutritional, and hormonal) and locally produced growth factors suggested to modulate the balance between bone resorption and formation (3, 48). Any defect in the coupling process results in bone loss (13, 49-51). The bone remodelling cycle is precisely coupled in the third decade at the time of the peak bone mass attainment, and this is maintained with small variations until the age of 50. After that, resorption dominates, resulting in bone loss in both sexes, with dramatic bone loss in women around the time of the menopausal transition making them more susceptible to osteoporosis (52, 53). With aging, men as well as postmenopausal women demonstrate gradual increase in bone loss (54, 55).

Remodelling takes place within bone area that need to be remodelled. In this bone area, all bone cells are organized with their precursors cells, nerve cells and blood vessels in temporary specialized unite called basic multicellular unite (BMUs). The BMU is a mediator mechanism for bone remodelling via connecting individual cellular activity to whole bone morphology (56-58). Bone remodelling occurs both in trabecular and cortical bone, but the metabolic rate is ten times higher in trabecular bone compared to cortical bone due to the greater surface area to volume ratio of trabecular bone. Bone remodelling occurs on trabecular surfaces in the form of shallow irregular Howship's lacunae, whereas in cortical bone it occurs as a cylinder to form the Haversian canal, which is then replaced to form an osteon. The cortical remodelling cycle lasts approximately four months, compared with almost seven months in trabecular bone (3, 56).

The remodelling cycle is composed of three consecutive phases (Figure 1.2): an initiation phase, which consists of bone resorption by osteoclasts, followed by a transition (or reversal) phase, and finally a phase of bone formation by osteoblasts. In the initiation phase, hematopoietic stem cells are recruited to specific bone surface areas and

differentiate into mature osteoclasts that initiate bone resorption. This is achieved under the action of osteoclastogenic cytokine factors including RANKL and M-CSF. They are one of the key signalling molecules that facilitate crosstalk between the osteoblasts and osteoclasts and help coordinate bone remodelling. This system is held in balance by the production of a decoy receptor, osteoprotegerin (OPG), which is a key factor inhibiting the differentiation and activation of osteoclasts (59, 60). Osteoprotegerin inhibits the binding of RANK to RANKL and thus inhibits the recruitment, proliferation, and activation of osteoclasts. Abnormalities in the balance of the RANK/OPG system lead to the increased bone resorption that underlies the bone damage of postmenopausal osteoporosis (60, 61). This resorption takes approximately one month. During the reversal phase, osteoblast precursors appear at the same resorption site. Finally, during the formation phase, which lasts for a period of approximately five months, the preosteoblast grouping phenomenon occurs and starts bone formation (3). The preosteoblasts synthesize a cementing substance upon which the new tissue is attached and express bone morphogenic proteins (BMPs) responsible for differentiation. A few days later, the already differentiated osteoblasts synthesize the osteoid matrix which fills the resorption cavity. Subsequently, mineralisation of this matrix occurs and a basic structural unit (BSU) of new bone is formed. The remaining osteoblasts continue to synthesize bone until they eventually stop and transform to quiescent lining cells that completely cover the newly formed bone surface and connect with the osteocytes in the bone matrix through a network of canaliculi (62-65).

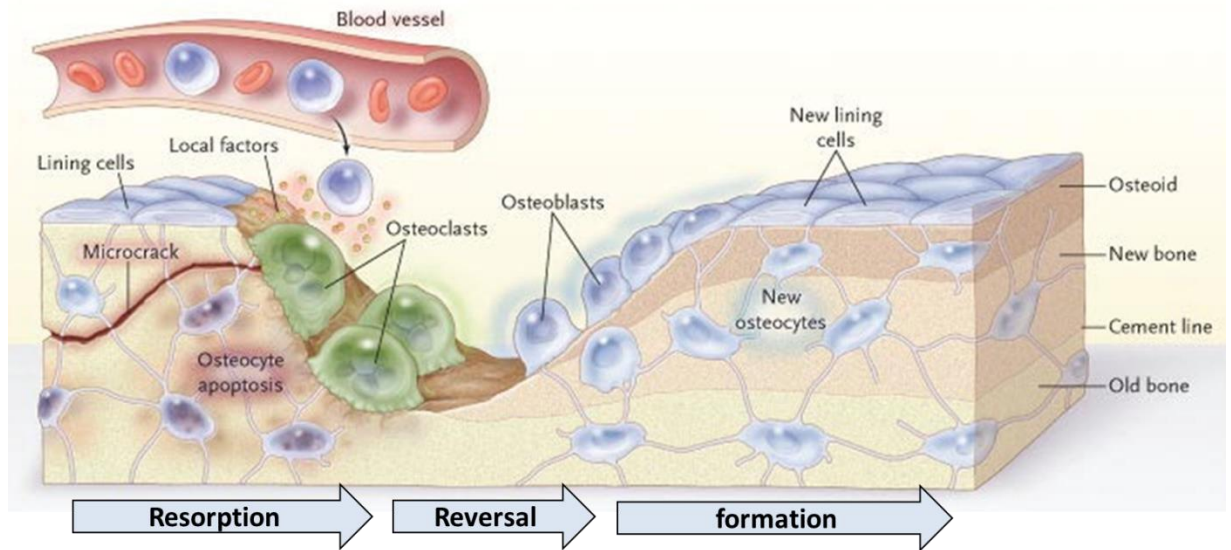


Figure 1.2: Illustrating Remodelling pathway and how the bone cells communicate through signalling pathways.

The osteocyte acts as an orchestrator in regulating bone remodelling, by its lacunocanalicular system the osteocytes act as mechanosensors can detect mechanical pressures and microcrack which cause osteocyte apoptosis and thus signals osteoclast to resorb the bone matrix. Lining cells and osteocytes release local factors that attract cells from blood and marrow into the remodeling compartment (BMU) in which osteoclastogenesis occurs. Consequently, groups of osteoblasts deposit new bone. Osteoblasts that are trapped in the matrix become new osteocytes; others die or form new, flattened osteoblast lining cells (65).

1.1.6 Bone turnover markers (BTMs)

Bone turnover markers (BTMs) represent different processes in bone turnover from collagen synthesis (procollagen type 1 amino terminal propeptide (P1NP)) and degradation (C-terminal cross-linked telopeptide of type-I collagen (CTX)) to markers released by bone cells (osteocalcin (OC) and bone specific alkaline phosphatase (BAP)). These markers can be broadly classified as reflecting either bone formation (OC, BAP, P1NP) or bone resorption (CTX and N-terminal cross-linked telopeptide of type-I collagen (NTX)) (66). In addition, non-classical bone biochemical markers are more specific regulators of bone turnover, including specific cell signalling markers (RANKL, OPG, PTH, VIT-D and Sclerostin), and one could also include markers of other metabolic pathways (Insulin, IGF-1, adiponectin and pentosidine) (67). Bone strength is highly dependent on its structural and material properties. The balance between bone formation and resorption greatly influences the structural and material properties of bone (bone strength parameters). Consequently, it has been suggested that bone strength may be reflected in part, independent of BMD levels, by measuring bone turnover using specific serum and urinary markers of bone formation and resorption. Recently, CTX and P1NP have been proposed as standardised reference markers of bone resorption and bone formation, respectively (68). Irrespective of BMD, an increase in fracture risk is approximately 20% per standard deviation increase in s-PINP or s-CTX (69). Although technical advances have greatly enhanced assay performance, resulting in reliable, rapid, non-invasive cost-effective assays with improved sensitivity and specificity, BTMs still have limited clinical utility. Lack of adopted international reference standards is the main reason for uncertainties over their clinical use. In addition, several biological and external factors cause measurement variability, and poor quality control of measurement techniques is also a problem (68). Not all components of bone markers are bone-specific markers. For example, BAP is one of several isoenzymes in the alkaline phosphatase family and is present in the liver, kidney, and bone tissue. Additionally, biochemical markers of bone resorption are based principally on type I collagen, which is not bone-specific and is widely distributed in several tissues of the body. Furthermore, the systemic levels of BTMs reflect overall bone metabolism and do not provide particular information on the remodelling process of each bone tissue individually, although their relative contribution may vary with aging, disease and treatment. Moreover, BTMs reflect quantitative changes of bone turnover and do not offer any information on the structural abnormalities of bone matrix materials, which are an important determinant of bone fragility. The existing evidence indicates that the diagnostic value of BTMs in predicting osteoporosis is low, and their use in osteoporosis

treatment decisions and monitoring of individual therapy is not well established (70). However, their utility in providing insight into the pathophysiology of osteoporosis and the presence of secondary bone pathology, and their changes following various osteoporosis treatments are well defined (71). It has been shown that u-NTX and s-CTX are the most responsive BTMs following antiresorptive treatment (72). The following are descriptions of bone turnover markers which will be examined in this study.

1.1.6.1 Bone Formation Biomarkers

1.1.6.1.1 Osteocalcin and undercarboxylated osteocalcin

Osteocalcin, also known as bone δ -carboxyglutamic acid-containing protein (BGLAP), is the most abundant non-collagenous protein in bone, comprising about 20% of non-collagenous matrix protein, and is produced exclusively by differentiated osteoblasts in the later period of bone formation and stored in the extracellular matrix (57, 73). Therefore, osteocalcin is considered one of specific markers of bone formation. To generate the mature form of osteocalcin, the OC gene is regulated at transcriptional level by Vitamins D and K as essential cofactors for γ -carboxylation of OC, resulting in an increase in the affinity for Ca and hydroxyapatite, allowing mature carboxylated osteocalcin deposition in mineralized bone matrix (74-77). In contrast, noncarboxylated osteocalcin (ucOC) has a low affinity for hydroxyapatite and is more easily released into the circulation.

Carboxylated, as well as total osteocalcin forms, can be also detectable in the peripheral blood, and measured as markers of bone formation. Approximately 10–40% of carboxylated osteocalcin is released into the circulation and is considered a reliable marker of bone formation (78). In normal individuals, an immunoassay analysis can identify up to 50% of osteocalcin as the undercarboxylated form. The levels of undercarboxylated osteocalcin are influenced by vitamin K status. However, total circulating concentrations of osteocalcin are influenced by bone cell activity independent of vitamin K (78).

Osteocalcin has some disadvantages: it is an unstable molecule and therefore might cause some problems in the specificity and sensitivity of the osteocalcin assay, and it has circadian variability and a short half-life of a few minutes, is influenced by Vitamin K status, and is released during formation and resorption. While osteocalcin is secreted by osteoblasts and deposited within the mineralized bone matrix [2], its physiological role in bone mineralization has not been fully explained (79-81). Recently, it was shown that in addition to acting as a marker of bone formation, several experimental studies in rodent models showed that circulating undercarboxylated osteocalcin (ucOC) acts as a hormone which regulates the whole body's metabolism and reproduction (82, 83). It stimulates

insulin production and secretion by pancreatic β -cells and adiponectin by adipocytes (84-90). Additionally, osteocalcin has the ability to induce testosterone production by stimulating the Leydig cells of the testes (91).

1.1.6.1.2 Bone Alkaline Phosphatase (BAP)

BAP is a member of the alkaline phosphatase (AP) family which are common enzymes distributed among different tissues throughout the body. In humans, four genes encode AP enzyme isoforms: tissue nonspecific AP (TNAP), intestinal AP (IAP), placental AP, and germ cell AP (92). TNAP is mainly expressed in liver, bone, and kidney but is also found in circulating leukocytes and the colon and its expression within the intestine is increased during inflammation (93, 94). Most of the total ALP isoenzymes are derived from the bones and liver, and each represent approximately 50% of the total effect of all isoenzymes in each organ. Although total ALP is not a specific bone marker, ALP level increases in patients with bone disorders such as Paget's disease or osteomalacia (95-97). Bone-specific ALP (BSAP) levels provide more selective bone formation data than that provided by measurements of total enzyme activity. BAP is present in the osteoblast plasma membrane, and it is probably cleaved off from the membrane and released into circulation. It is expressed in the early period of osteoblastic differentiation and is produced in high amounts during the cycle of bone formation. Therefore, BAP represents the most frequently used marker of bone formation (98). It is specific for bone, but with some cross-reactivity with the liver isoform (up to 20%). Cheap assays are available that detect more specifically the bone-derived isoform, bone-specific ALP. The main advantages of bone-specific alkaline phosphatase is that it has a very small circadian rhythm, low intra-individual variability of less than 10%, long circulatory half-life of 1–2 days, and sample stability (99, 100).

1.1.6.2 Bone Resorption Biomarkers

1.1.6.2.1 C-terminal cross-linking telopeptide of type 1 collagen (CTX)

Carboxy terminal cross-linked telopeptide of type 1 collagen (CTX) is currently considered the marker of choice for measuring bone resorption. It is generated from type 1 collagen by cathepsin-K during bone resorption (101). The CTX exists in an isomerised beta-CTX form and a non-isomerised alpha-CTX form. The α -form converts to the β -form as the bone ages. CTX can be measured in urine and blood, and because serum CTX is one of the most responsive BTMs following antiresorptive treatment it is therefore widely used in clinical practice (102). However, it has some disadvantages: it has intra individual

variability with a large circadian variation with the highest level between 01:30 – 04:30, which is approximately twice the level of the nadir between 11:00–15:00. This inconsistency necessitates a morning fasting sample for accurate interpretation (103). Physical activity (104) and the menstrual status are also significant factors affecting the CTX level (105). Additionally, CTX level has inter individual variability as it may be attenuated by several factors such as age, gender, ethnicity, menopausal status and osteoporotic stage (106). However, currently there are some studies being carried out to establish reference intervals classified by age, gender and, in women, menopausal state (107).

1.1.7 Bone marrow and its composition

Bone marrow is soft, sponge-like tissue that occupies approximately 85% of the bone cavity scattered within a mesh of trabecular bone (108). It is a complex environment, in which a variety of cell types share a common space. The main cellular components within the bone marrow include two types of stem cells: haematopoietic stem cells which develop into blood cells, and marrow stromal cells (MSCs) which develop into bone mass-regulating cells, and marrow adipocytes (108, 109). Bone marrow provides an environment for controlling both haematopoiesis and bone remodelling through a variety of autocrine, paracrine and endocrine activities of its different cellular components (109). Based on the composition, two types of bone marrow exist: red (hematopoietic, active) and yellow (fatty, inactive) marrow. Hematopoietic marrow is red because of the presence of haemoglobin within erythrocytes and their precursor cells, and is actively involved in haematopoiesis. It is found primarily in flat bones and at the rounded ends of long bones. In contrast, fatty yellow marrow is yellow due to its high lipid content, consisting mainly of adipocytes (95%), and it is found in the medullary cavity of long bones. Red and yellow bone marrows contain multiple chemical components, but predominantly water, lipids/triglycerides (TG) and proteins. The concentration of these chemical components varies according to the type of marrow present. Red marrow is 40–60% lipid, 30–40% water, and 10–20% proteins. In contrast, yellow marrow is 80% lipid, 15% water, and 5% protein (108, 110-112). The MRI signal of bone marrow reflects its chemical composition: the major determinants of the MRI appearance of bone marrow are the fat and water content (113). Therefore, the bone marrow fat can be visualized and quantified by MRI; this is discussed in greater detail below (Section 1.5.2.3).

The cellular proportion of bone marrow in term of red and fatty marrow varies significantly over time depending on age, gender, location, homeostatic requirements and

concomitant disease (114, 115). Although both hematopoietic and stromal cells are present during the embryonic and early stages of life, at birth the bone marrow is entirely red and the fatty marrow only reaches significant levels during the second decade of life at the peak bone mass acquisition (116). The conversion in the direction of fatty bone marrow follows an anticipated pattern, which starting in the appendicular skeleton, followed by the axial skeleton (117). By age 10 to 20 years, the shafts of long bones are predominantly filled with yellow marrow. By the age of 25 years, red marrow is limited to the axial skeleton. The process of progressive fatty infiltration of the bone marrow space increases with aging until finally it occupies a major proportion of the bone marrow in the axial skeleton (118, 119). Detailed knowledge of the speed and anatomical pattern of bone marrow conversion allows MRI to detect the expected bone marrow changes throughout the skeleton (111, 113, 120, 121).

Predisposition of bone marrow MSCs to the adipocyte versus osteoblast lineage is the main contributing factor for progressive fatty infiltration of bone marrow. However, the master controls over MSCs lineage allocation are still not well defined (119). This process will be discussed in more details in section 1.2.5. In contrast to the other body fat depots (BAT, WAT), the metabolic function of yellow marrow fat is largely unknown (122). Marrow fat may participate in lipid metabolism; it acts as localized reservoir for triglycerides which can then be released during demand, for example during bone fracture healing (123). It has been suggested that bone marrow fat is acting as energy source activating the bone remodelling process (82, 122). On the other hand, a large number of studies documented the detrimental effect of marrow fat on bone mass in different metabolic disease as they enhance bone marrow adipogenesis. This will be discussed in sections 1.2.4 and 1.4.1.4.

1.2 Osteoporosis

1.1.1 Epidemiology of osteoporosis

Osteoporosis is a weakening of bone microarchitecture which results in low bone density, reduced bone strength, increased fragility and consequently increased risk of fracture (124). The osteoporotic deficit of bone microarchitecture is illustrated in Figure 1.3. It is usually asymptomatic unless osteoporotic fracture and secondary changes of bone structure occur. It is estimated that approximately 30% of all postmenopausal women are affected and up to 40% will develop a fragility fracture within their lifetime (125). It is estimated that one in four men over the age of 50 years will develop at least one osteoporosis-related fracture in their lifetime (126). A recent report from 27 countries of the European Union

(EU27) estimated that nearly 22 million women and 5.5 million men in these 27 countries were expected to have osteoporosis, and 3.5 million new fragility fractures were sustained, comprising 610,000 hip fractures, 520,000 vertebral fractures, 560,000 forearm fractures and 1,800,000 other fractures (127). Given the aging population, the annual occurrence of hip fracture worldwide has been predicted to reach 8.2 million by 2050 (128).

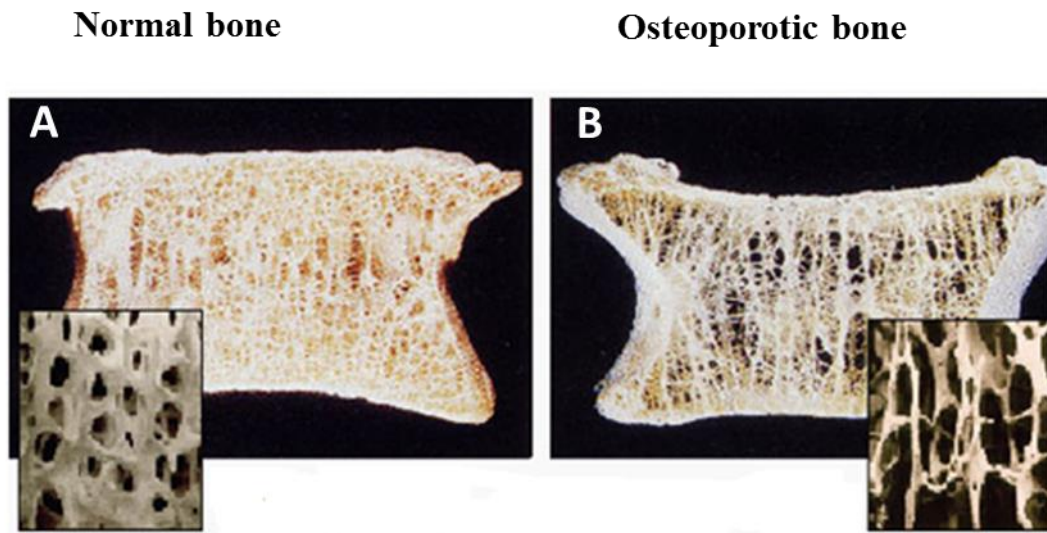


Figure 1.3: Microarchitecture of normal and osteoporotic bone.

(A) Healthy vertebral bone (B) Compressed osteoporotic vertebra with reduced trabecular number, connectivity and density and more trabecular spaces (129).

1.2.1 Risk factors for osteoporosis

Osteoporosis can occur in both men and women and at any age but it is most common in elderly people and postmenopausal women (primary osteoporosis/senile) (61), due to an increased rate of bone resorption compared with the rate of bone formation (130).

Osteoporosis may arise from secondary causes (secondary osteoporosis), such as endocrine (Type 1 diabetes mellitus (T1DM)), drug use, malignancy, chronic disease, or medication (129). Other risk factors for osteoporosis include lifestyle and dietary factors, late onset of sexual development, early menopause, family history of osteoporosis and low body weight, race (Caucasian or Asian postmenopausal women), and immobilisation (20).

1.2.3 Diagnosis of osteoporosis

Currently, the clinical diagnosis of osteoporosis is made on the basis of the widely accepted Bone Mineral Density (BMD) T-score criteria established by the World Health Organization (WHO) as shown in (Table 1.1) (131). The T-score is based on the studies that evaluated postmenopausal women. . More details about DXA measured BMD will be explained in (Section 2.4.1).

Table 1.1: Showing WHO BMD T-Score criteria

	T-score
Normal	> -1.0 SD
Osteopenia	Between -1.0 and -2.5 SD
Osteoporosis	≤ -2.5 SD
Severe osteoporosis	≤ -2.5 SD with one or two fragility fracture

SD;standard deviation. T-score is the number of SD's away from the young adult mean.

Although dual-energy X-ray absorptiometry (DXA)-measured BMD remains the important determinant of fracture risk and osteoporosis in the clinical setting, BMD alone does not fully explain and predict fracture risk of bone (132-135). There exists considerable overlap in T-scores in adults with and without fragility fractures (136, 137). Some studies reported that over half of trauma fractures occur in people with non-osteoporotic BMD (BMD T-score > -2.5) (134, 138-141). Furthermore, BMD does not adequately explain the effect of therapeutic interventions on fracture risk (142). A new paradigm fracture risk assessment tool (FRAX) which includes clinical risk factors for fracture risk prediction has been implemented for the assessment of osteoporosis (129). FRAX is a diagnostic tool that is used to evaluate the 10- year probability of fracture. Along with femoral neck T-score, age, gender, prior fracture, and use of systemic glucocorticoids, additional risk factors that influence the risk of fracture are implemented into this tool. In FRAX, T1DM has been recognized as a secondary cause of osteoporosis and increases the probability of fracture independent of BMD (143, 144). Kanis *et al.* (145) stated that the prediction of fractures with the use of clinical risk factors alone in FRAX is comparable to the use of BMD alone to predict fracture. However, in spite of methods for the refinement of DXA indication and interpretation via FRAX scoring (146), the 1994 WHO criteria are still used as a diagnostic gold standard (131).

1.2.4 Determinants of bone strength and their clinical implications for osteoporosis diagnosis

The definition of osteoporosis emphasizes bone strength as the predictor of fracture risk (147-149). In addition to BMD, which accounts for approximately 60–70% of the variation in bone strength (150), there are other skeletal factors that influence bone strength (Bone quality parameters) (Figure 1.4). They encompass the spatial distribution of bone mass (structural properties) and the intrinsic properties of the materials that comprise the bone. Some of the important structural characteristics are bone size and shape, trabecular bone microarchitecture and cortical bone thickness and porosity. The intrinsic material properties of bone include the accumulation or removal of microdamage, matrix mineralization and crystallinity, collagen denaturation and covalent cross-links between collagen microfibrils (151). Additionally, changes in the amount of bone remodelling resulting in alterations in tissue degree of mineralization and trabecular microarchitecture. Therefore, any factors impact bone remodelling will influence the bone strength. An impairment of trabecular microarchitecture with loss of connectivity between trabeculae and cortical thinning is the characteristic feature of osteoporosis (148, 149). Therefore, assessment of the extent of compromised bone strength is of particular importance to predict the magnitude of fracture risk which cannot be assessed by BMD alone. However, there is currently no accurate measure of overall bone strength. There is an increasing body of evidence suggesting that indices of trabecular structure and cortical measures are better than DXA-derived bone measures in separating men and women with and without fractures (152, 153), and the apparent trabecular bone volume (BV/TV) has been found to be the best morphometric strength predictor (154). In a research context, new imaging techniques such as High Resolution Peripheral Quantitative Computed Tomography (HR-pQCT) and micro-MRI have provided greater dimensions to assessment of fracture risk and skeletal health in a variety of diseases related to bone abnormalities irrespective of DXA-measured BMD (155-159). T1DM was one of disorders for which newer approaches to evaluating skeletal health has been introduced. The existing data showed that DXA-measured BMD did not explain the higher fracture risk in this group of the population (160-162). QCT and HR-pQCT (163, 164) showed that deficits in cortical and trabecular bone vBMD and microarchitecture are greater in patients with T1DM compared with healthy controls. These promising results achieved by applying 3-dimensional imaging techniques will give insights into bone strength determinants of fracture risk that cannot be fully studied by DXA alone.

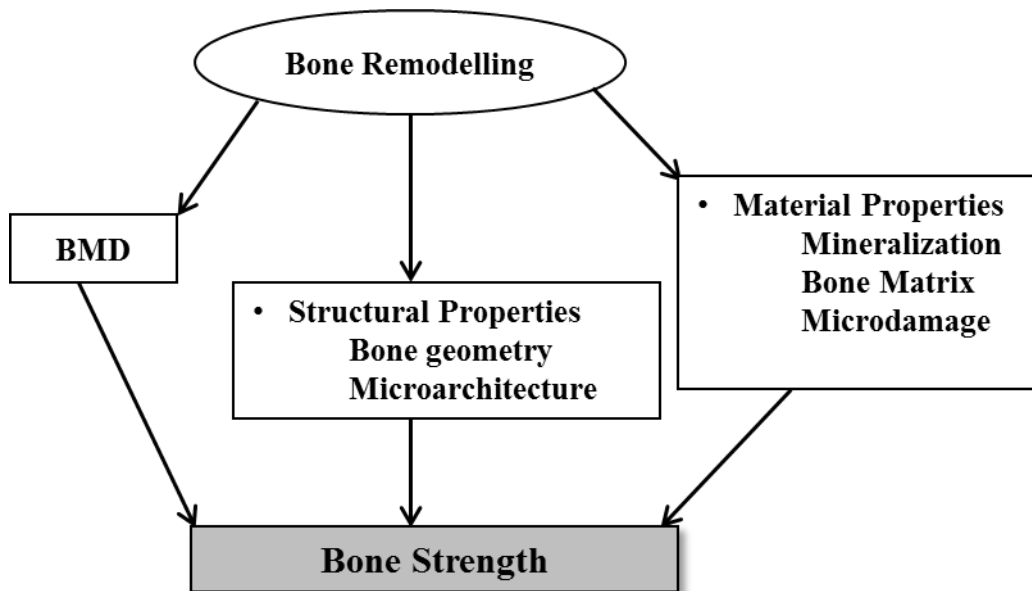


Figure1.4: Determinants of bone strength including bone mineral density (BMD), structural properties and material properties. The bone remodelling has influences on the bone strength parameters (165).

1.2.5 The relationship between adiposity and osteoporosis

More recently, evidence has accumulated to suggest another mechanism for osteoporosis involving the relationship between osteoporosis and excess adiposity (166-172). A number of potential mechanisms have been proposed to explain the complex relationship between adipose tissue and bone (Figure 1.5), yet precise mechanisms underlying this relationship remain unclear (169). The existing literature suggests that the fat bone connection can be either due to the effect of peripheral adipose tissue (e.g., abdominal fat) or the fat present within the bone marrow (bone marrow adipogenesis). However, the role of BMF is distinct from that of other fat depots as demonstrated in the patients with anorexia nervosa who display extreme low body fat mass with high vertebral BMA (173). The adverse effect of peripheral adipose tissues on bone metabolism is elucidated partially through the influence of the biochemical factors that are secreted by adipocytes. These factors include inflammatory cytokines such as resistin (174), tumour necrosis factor- α (TNF- α), interleukin (IL-1, IL-6) (175, 176), and endocrine hormones such as leptin (177-179) and adiponectin (180, 181), which modulate bone remodelling by enhancing bone resorption or suppressing bone formation. On the other hand, adipose tissue is the source of other hormones such as oestrogen which play a key role in the maintenance of skeletal homeostasis (182, 183). Indeed, there is increasing evidence that the developmental origins of various fat depots are different (184, 185), which explains why various adipose tissues themselves have individual characteristics in terms of production of biochemical factors,

which are thought to have different effects on bone metabolism (186-189). There is some discrepancy regarding the effect of peripheral adipose tissue on bone metabolism, and both positive and negative effects have been reported (190-193). Although a growing number of *in vivo* and *in vitro* studies examine the effect of peripheral adipose tissue on bone metabolism, the mechanism of this effect is not yet understood. The local activity of fat within the bone marrow milieu and its interaction with other bone cells is better understood. An extensive body of literature suggests that the first local connection between bone and fat is demonstrated by the finding that the differentiation programmes of osteoblasts and adipocytes share a common progenitor, the mesenchymal stem cells (MSCs). This balanced differentiation programme is under the tight control of multiple transcription factors including the peroxisome proliferator-activated receptor (PPAR)- γ and RUNX2, with many regulating pathways and additional factors being directly or indirectly involved (119, 194-199). The commitment of MSCs towards adipocyte lineages (adipogenesis) depends on PPAR- γ (i.e., PPAR- γ 2) (200), whereas RUNX2 promotes osteoblast differentiation and inhibiting adipogenic differentiation (201). In addition to bone marrow adipogenesis, adipocytes secrete lipotoxic substances (paracrine factors) which affect the bone cells in the vicinity of the bone marrow (202). The existing data indicate that there are certain conditions such as ageing (203), and other osteoporosis-induced diseases, e.g., diabetes mellitus (204), that can be considered adipocytic risk factors and induce the alteration of MSC commitment. This will be explained in more detail in sections 1.4.1.4 and 1.5.2.4.2.

In conclusion, the ultimate effect of adiposity on bone mass is emphasized through these opposing pathways. However, the relationship of marrow adipose tissue to other fat depots is complex and might play a very distinct role in bone metabolism and thus remains to be explored. Understanding the relationship between bone and fat at the marrow level provides us not only with the pathophysiology of disease-related osteoporosis, but also with a novel approach to the diagnosis and treatment of osteoporosis (205).

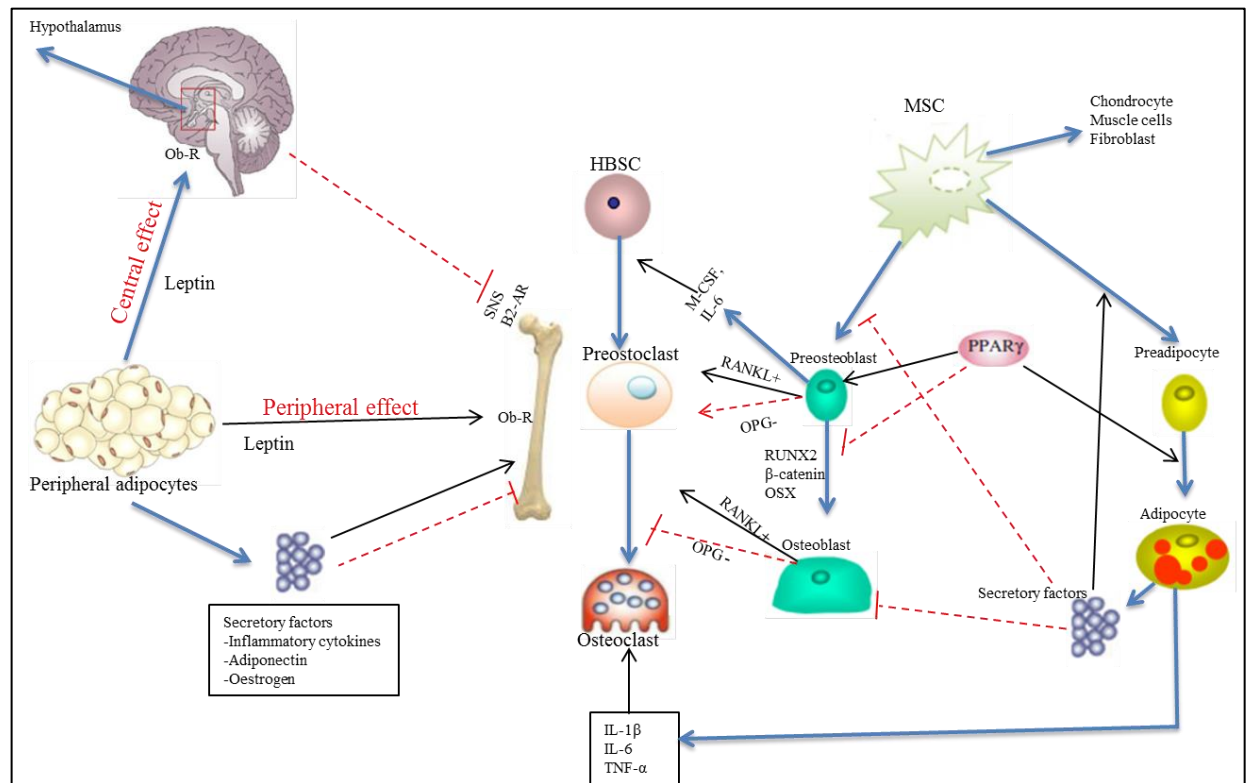


Figure 1.5: Illustrating the relationship between adipose tissue and bone. The connection can be via peripheral fat and fat within bone marrow milieu.

The Peripheral fat can affect the bone mass either through Leptin or other secretory factors (Inflammatory cytokines, fatty acids, adiponectin and oestrogen). Osteoblasts, osteoclasts and MSCs express the leptin receptor. The direct peripheral action of leptin on bone occurs via binding to the Ob-R on bone cells (MSCs, osteoblasts, and osteoclast). Leptin suppresses adipogenic differentiation of MSCs and promotes osteoblastic differentiation. In addition, leptin increases OPG production in association with reducing that of RANKL, thereby inhibiting osteoclastic differentiation. Leptin also exhibits a central indirect effect on bone by binding to its receptor in the hypothalamus and activating the SNS, enabling binding of noradrenalin to β_2 -AR on osteoblasts and thus inhibiting bone formation. It also increases RANKL expression and promotes the differentiation of osteoclasts. However, to date the precise mechanisms of leptin action on skeletal homeostasis remain unknown. Other secretory factors produced by adipocytes can positively or negatively regulate skeletal mass. In the bone marrow setting, activation of PPAR- γ causes bone loss in part through altering the fate of MSCs towards adipogenesis and away from osteogenesis. Activation of PPAR γ also results in recruitment of hematopoietic cells that can differentiate into osteoclasts under the influence of m-CSF and RANKL, which are produced by preosteoblasts, thereby ensuring a coupled process. Furthermore, secretory factors released by marrow adipocytes are toxic and block osteoblast differentiation and enhancing adipogenesis, whereas secretion of pro-inflammatory cytokines ($IL-1\beta$, $IL-6$, $TNF-\alpha$) can stimulate osteoclast activity thereby enhancing bone resorption processes. HBSC, haematopoietic stem cells; MSC, mesenchymal stem cell; RANKL, receptor activator for nuclear factor κ B ligand; OPG, osteoprotegerin; PPAR γ , peroxisome proliferator-activated receptor γ ; Runx2, runt-related protein; OSX, osterix; IL, interleukin; $TNF-\alpha$, tumour necrosis factor; M-CSF, macrophage clonally stimulating factor; SNS, sympathetic nervous system; β_2 -AR, β_2 -adrenergic receptor; Ob-R, leptin receptor. Red line indicate inhibitory action; black arrow indicate stimulatory action (206).

1.4 T1DM

1.4.1 Background

T1DM is a chronic metabolic disorder characterized by hypoinsulinemia and chronic hyperglycaemia due to the autoimmune destruction of insulin-producing pancreatic β cells (207, 208). T1DM account for 10% of all diabetes, and the overall incidence of T1DM seems to be increasing in recent decades up to 4.8% per year, an increase which is attributed to a number of possible immune-modulatory factors which include social changes in hygiene, infectious exposures and nutritional factors (209, 210). If these trends continue, the incidence of people with type 1 diabetes will increase in coming years (211, 212). It is one of the most common chronic diseases of childhood. The peak age of presentation is school entry (5 -7 years), and at puberty (10-14 years), but the disease can also be diagnosed at any age. In adults, it constitutes approximately 5% of all diagnosed cases of diabetes (213, 214). Diagnosis of diabetes is generally given when fasting blood glucose is equal or higher than 7 mmol/L (126 mg/dL), any blood glucose of 11.1 mmol/L (200 mg/dL) or higher with symptoms of hyperglycaemia, or an abnormal 2h oral glucose-tolerance test. In addition, recently HBA1C has been set as a standard of diagnosing diabetes. If an individual has an HA1C of 6.5% (47.5 mmol/mol) or higher, they meet the criteria for the diagnosis of diabetes (215). Some cases of T1DM are misdiagnosed as T2DM. Therefore, pancreatic autoantibodies are considered characteristic of type 1 diabetes, and more than 90% of individuals with newly diagnosed T1DM have autoantibodies at disease onset (216). The management of T1DM is by exogenous insulin replacement which is usually delivered by multiple daily injections or by using an insulin pump. An adjustment of the insulin dose is made according to the number of carbohydrates in each meal, which is what is known as carb counting (217). Regular monitoring of average blood glucose over a period of 6-10 weeks by using glycated haemoglobin HBA1C is essential to tightly regulate the glycaemic control and in turn decrease the risk of developing complications. Additionally, a regular screening programme for people with diabetes is imperative to prevent the long term complications that develop as a result of chronic hyperglycaemia.

1.4.2 Complications of diabetes

Long term complications of diabetes include microvascular disease, nephropathy, neuropathy, retinopathy, and macrovascular disease, cardiovascular and peripheral vascular complications (218). Recently, fragility fracture is another common complication of diabetes (161, 219). The interaction of advanced glycation end-products (AGEs) with their receptors on different body tissues are thought to play a significant role in the pathogenesis of diabetic complications via activation of pro-inflammatory pathways (220). AGEs are generated by the non-enzymatic addition of reduced sugar moieties to amine groups on both tissue-specific and circulating proteins. In the presence of hyperglycaemia, AGEs accumulate within various organs including the kidney, retina, and the cardiovascular system. These AGEs may also accumulate in bone and contribute to diabetic bone disease; this will be discussed in more details in the following section (Section 1.4.1.1).

1.5 T1DM and abnormalities of bone health

In addition to the many target organs that are typically associated with dysfunction, the skeleton has been recognized as another organ that is adversely affected in diabetes mellitus with fragility fractures being increasingly recognized in people with diabetes mellitus (161, 162, 221). An extensive volume of clinical data supports altered bone structure and biochemical markers of bone turnover in people with both Type 1 and Type 2 diabetes (T1D and T2D)(222-224). In addition, a series of experimental studies have reported several possible mechanisms that could explain the link between diabetes and adverse bone health. In the following section, we review the pathophysiological mechanisms of diabetic bone loss and the evidence that exists for abnormalities of bone health in people with T1DM.

1.5.1 Pathogenesis of altered bone metabolism in T1DM

1.5.1.1 Hyperglycemia

Several in vivo and in vitro studies indicate that hyperglycemia contributes to bone loss through a variety of mechanisms: direct glucose toxicity to osteoblast through polyol pathway activity affecting osteoblast numbers and function (225, 226); osmotic and nonosmotic pathways which independently suppress osteoblast maturation and mineralization (227, 228); down regulation of vitamin D receptor thus indirectly impairing

osteoblast maturation in response to 1,25(OH)D₃ (226); oxidative stress(229); and formation of glycation products (230). Hyperglycemia leads to increased nonenzymatic protein glycation and excessive formation of these modified proteins called advanced glycosylation end-products (AGEs). AGEs appear to be the common biochemical entity accumulating in individuals with long term diabetic complications. They are seen in various sites such as vascular tissues, kidneys and bones(231, 232). The accumulation of AGEs increases formation of collagen cross-links which results in increased stiffness of the collagen network in the cortical bone, but this has no overall effect on the stiffness of the mineralized bone(233). Accumulation of pentosidine, a well-characterized AGE, is negatively correlated to trabecular bone volume and the structural strength of the trabecular bone, which may explain how AGEs contribute to bone fragility (234-236). In support of this hypothesis, *in vivo* studies in both T1D and T2D rats have confirmed that an increase in AGE production is negatively correlated with bone mineral density (BMD) and bone strength (237, 238). Moreover, AGE was found at higher concentration in cortical and cancellous bones of people with femoral neck fracture compared to post-mortem controls (235, 237). Higher pentosidine levels and AGE products have been found to reduce bone strength and elevated vertebral fracture risks in T2D (235, 239). In addition to affecting bone physical properties, AGEs also have direct effects on bone cells. There is a growing body of evidence suggested that linking of AGEs with their receptor (RAGE) causes oxidative stress generation and induces inflammatory reactions in a variety of bone forming cells, including osteoblasts, osteoclasts, and mesenchymal stem cells (MSCs). *In vitro* and *ex vivo* findings suggest that elevated AGE can inhibit proliferation and differentiation of osteoblast (240, 241) in mouse and human mesenchymal stem cells (MSCs). It is also associated with reduced osteocalcin mRNA expression as seen in rodents with diabetes (238, 242). Furthermore, Okazaki et al. demonstrated that the inhibition of osteoblastic differentiation by AGEs can occur independently of hyperglycemia (243). AGEs can also cause osteoblast death by provoking inflammation and generation of reactive oxygen species (ROS) which in turn lead to cell apoptosis as a result of oxidative stress (229, 242, 244, 245). However, reports regarding the influence of AGEs on osteoclasts and bone resorption show inconsistent effects with some evidence of increased(246), decreased (247) as well as no effect of AGE on bone resorption (240). MSCs are pluripotent stem cells capable of differentiating into bone, muscle, cartilage and adipose tissues. Emerging evidence suggests that hyperglycemia may also alter the differentiation of the MSCs promoting adipogenesis instead of osteogenesis via AGE-RAGE oxidative stress system (241, 248). Mice with spontaneously and pharmacologically

induced diabetes with bone loss have shown increased marrow adiposity, determined by histology and by mRNA markers of adipogenesis (PPAR γ and aP2)(249). Hyperglycemia diverts the MSC differentiation signaling pathways toward adipogenesis at the expense of osteogenesis. This effect is achieved via ERK-1/-2-activated P13K/Akt-regulated pathway in mouse MSCs (250), and via suppression of HO-1 expression (251) and Wnt/protein kinase C noncanonical pathway in human MSCs (252), evidenced by increased PPAR γ expression in high glucose stimuli and reduction of osteocalcin levels. Wang et al. demonstrated that hyperglycemia can also promote adipogenesis through synthesis of hyaluronan matrix which promotes an inflammatory response culminating in demineralization of trabecular bones (253).

1.5.1.2 Insulin, IGF-1 & other growth factors

Insulin is increasingly recognized to have an anabolic effect on bone that is distinct from the effect of its analogue IGF-1. This effect is mediated either indirectly through its control of blood glucose concentration while maintaining the levels of parathyroid hormone (PTH), IGF-1, vitamin D (254, 255), or directly on bone cells through specific insulin receptors (IRs) and IGF-1 receptors in osteoblast. IRs are present on osteoblasts and its expression varies with differentiation status of the osteoblast both in vivo and in vitro (256, 257). In vitro studies on primary osteoblasts and clonal osteoblast cell lines show insulin promotes glucose uptake (258), alkaline phosphatase activity, collagen synthesis (259, 260) and osteoblast proliferation (261) of these cells. Maor et al. demonstrated reduced IRs in the skeletal growth centers of mice with streptozocin (STZ)-induced diabetes and these were reversed with insulin therapy (262). Evidence for a direct link between insulin action and bone formation in vivo can be observed in IR knock out mice which show altered bone formation (86), abnormal trabecular microarchitecture (263) and reduced bone strength (264). Insulin positively regulates bone formation by stimulating osteocalcin production. Observational studies in people with T1D and T2D, with insulin deficiency and resistance respectively, demonstrate reduced osteocalcin levels compared with controls (265, 266). Furthermore, there is a positive correlation between insulin dose and BMD (267, 268). The dichotomy of lower BMD in T1D with insulinopenia and higher BMD in T2D with clinical hyperinsulinemia further implicates a causal anabolic effect of insulin on bone. The direct effect on bone may also be mediated by the IGF-1 pathway. IGF-binding protein (IGFBP) serves as a carrier protein for IGF1. Insulin inhibits IGFBP-1, 4 expression in osteoblasts and therefore lack of insulin leads to an increase in IGFBP-1 and 4 levels, accordingly decreasing the availability of unbound IGF-1 for anabolic effects on bone (269). In

addition to insulin deficiency, T1D individuals and animal models demonstrate dysregulation of a variety of endocrine factors including reduced amylin (162) and IGF-1 (270). Amylin is another osteotropic factor that is cosecreted by pancreatic beta-cells and absent in T1D (271). Amylin-deficient mice displayed low bone mass with increased number of osteoclast (272) and that treatment with amylin in diabetic rat result in increased BMD and bone strength (271). Similarly, diabetic animals with low blood IGF-1 and knock-out mice for its receptor displayed diminished bone formation (273, 274). Also, serum IGF-I level was another predictor of prevalent VFs in postmenopausal women with T2D (275).

1.5.1.3 Calcium, vitamin D & calciotropic hormones

It is well known that calcium homeostasis plays a major role in regulating bone metabolism, Therefore, imbalance in systemic factors which are capable of regulating calcium balance have been found to influence diabetic bone loss (276). Similar to diabetic patients, several but not all studies demonstrate that diabetic animal models have reduced levels of PTH, vitamin D, calcium, magnesium and phosphate (277). The effect of DM on calcium metabolism is complex, but essentially it is associated with a negative calcium balance hallmark by both bone and renal loss (278). There is a growing body of evidence which demonstrate exacerbation of osteopenia and osteoporosis in animals and humans with vitamin D deficiency and T1D or T2D (279-281). Verhaegae et al. found that diabetic rats have higher urinary calcium excretion and significantly lower serum concentrations of both 1,25-dihydroxyvitamin D₃ and vitamin D-binding protein (280). Frazer et al. demonstrated that alteration in vitamin D metabolism in young insulin-dependent diabetics aged 7–18 years old, who have markedly reduced 1,25-dihydroxyvitamin–D but normal serum calcium, phosphate and PTH concentrations, could be related to their observed decrease in cortical bone mass (281). More recently, Zhang et al. aimed to explain the mechanism involved by demonstrating that male STZ-induced diabetic mice have high urinary calcium excretion and decreased BMD (276). Quantified PCR results showed alteration of vitamin D metabolic enzyme expression and down regulation of mRNA expression levels for renal calcium transporter receptors, plasma membrane Ca-ATPase, and vitamin D receptor. In support of this, treatment with calcitriol in STZ-induced rats demonstrated recovery of BMD (282). In terms of PTH, several in vivo and in vitro studies indicate that an imbalance in PTH was associated with bone loss and increase fracture risk (283, 284). PTH encourages bone formation and turnover by increasing the expression of osteocalcin, IGF-1, IGFBP-3, bFGF, MMP-1 and MMP-13 in rat osteoblasts in vitro (285),

as well as MMP-13 in mice *in vivo* (286). Moreover, treatment with PTH to T1D and T2D mice demonstrated reversal of trabecular bone parameters through its anabolic effects on osteoblasts differentiation and maturation (284, 287). PTH-treatment was also associated with reduced TUNEL-staining of osteoblast suggesting its antiapoptotic effect on osteoblasts. It has been suggested that PTH promotes repair of DNA damage by increasing PCNA and Foxo3a (288), hence prolonging osteoblast survival. Intermittent PTH-treatment reversed bone loss to baseline in mice compared to only partial reversal in continuous PTH-treatment, although this effect may be due to underlying differences between the T1D and T2D mouse models (284, 287). Similarly, treatment with PTH-related protein, which is produced at high levels by differentiating osteoblasts, also reverses trabecular bone loss in STZ-induced diabetic mice suggesting its modulatory effect on osteoblast function and role in diabetic osteopenia (289).

1.5.1.4 Marrow adiposity & adipokines

There is a growing body of evidence that suggests that the fat bone connection plays an important role in the pathophysiology of bone loss. Osteoblasts and adipocytes share a common precursor, both derived from the pluripotent MSCs located in the bone marrow suggesting a mutually exclusive and reciprocal lineage selection of one or the other. The main lineage-specific transcription factors that direct the differentiation of MSC are the runt-related transcription factor 2 (Runx2) for osteoblastogenesis and the PPAR γ for adipogenesis (199). It has been suggested that lineage selection could regulate bone density and result in bone loss when MSCs commit to the adipocytes at the expense of osteoblasts (251, 290, 291). Botolin et al., 2005 were the first to report an increase in the expression of PPAR γ and an increase in visible adipocytes in tibia of T1D mouse models compared with control (292). Subsequently, several experimental animal studies have demonstrated an increase in bone marrow adiposity in both spontaneously and STZ-induced T1D mice compared to controls (249, 289, 293). As described earlier, hyperglycemia is capable of promoting adipogenesis by altering the lineage commitment of MSCs to adipocytes through various signaling pathways contributing to the diabetic osteopenia (250, 253, 294). Rzonca et al. demonstrated *in vivo* that rosiglitazone (PPAR γ agonist) administration results in significant bone loss whilst Cock et al. 2004 demonstrated that congenitally PPAR γ deficient mice had increased BMD and bone trabecular microarchitecture parameter including BV/TV and trabecular thickness (295). However, Botolin and McCabe found that inhibition of PPAR γ by administration of an antagonist to insulin deficient T1D mice prevented bone marrow adiposity but not bone loss (249). This inability in preventing

bone loss in T1D mice suggested that bone marrow adiposity may only be partially responsible for diabetic bone loss. Bone marrow adiposity can also have direct effect on osteoblasts as demonstrated by several coculture studies in mouse and human cells (296-298). The presence of adipocytes inhibit osteoblast proliferation (296) through the lipotoxic effect of free fatty acid in the bone marrow microenvironment (297). Coe et al. demonstrated that the diabetic bone marrow itself is a mediator for osteoblast death with an increase in caspase-3 activity, a marker for extrinsic apoptotic pathway which are activated by extracellular ligands such as TNF α , in bone marrows of both spontaneous and pharmacologically-induced diabetic mice. By treating the cocultures with TNF α antibodies, they prevented osteoblast death further supporting the negative correlation of diabetic bone marrow adiposity and bone mass. In addition to releasing large amounts of free fatty acid, adipocytes in the bone marrow also secrete cytokines including leptin, resistin and TNF α , the last of which will be discussed in the next section. Leptin is an adipokine which has a complex regulatory role on bone metabolism, with an indirect inhibitory effect on osteoclastogenesis and a direct stimulatory effect on osteoblastogenesis through a central (hypothalamic) and peripheral pathway (299-301). Despite being an adipokine, in vitro studies indicate that leptin promotes an osteoblast rather than adipocyte lineage (300, 301). In contrast to T1D patients who demonstrate increased (302) or slightly decreased leptin level (303), leptin levels were found to be significantly suppressed in T1D mice, its absence results in reducing bone mass with increasing marrow adiposity (299)[83]. T2D is typically associated with obesity, which has been associated with higher leptin level and higher BMD. Vasilkova et al., however, demonstrated that leptin has an independent positive correlation to BMD, irrespective of BMI (304). In addition, interventional studies in mice have demonstrated that leptin administration reduces bone marrow adiposity and increase bone mass (305, 306). However, similar to their work on PPAR γ antagonist, Motyl and McCabe concluded that leptin administration to T1D mice modify and prevent marrow adiposity but did not prevent diabetic bone loss (307). Adiponectin (APN), the most abundant adipocyte-secreted adipokine, regulates energy homeostasis and exerts well-characterized insulin sensitizing properties. The peripheral and central effects of APN on bone metabolism are beginning to be explored but are still not clearly understood. APN-knockout (APN-KO) mice fed a normal diet exhibit decreased trabecular structure and mineralization and increased bone marrow adiposity and central administration of APN decreased osteoclast numbers, whereas osteoblast osteogenic marker expression and trabecular bone mass increased both, in APN-KO and WT mice (308). The insulin-sensitising effect of OC is known be due to the upregulation of the expression of the

insulin-sensitizing APN gene in adipocytes (89) but there is some suggestion that in humans the link between OC and APN may be gender specific (309).

1.5.1.5 Chronic inflammation

The pathogenesis of both T1D and T2D are associated with activation of the immune system, especially so in T1D which involves an autoimmune destruction of pancreatic β -cells whilst T2D involves a more chronic low-grade inflammatory process (310, 311). Several experimental studies using T1D mice model indicate that systemic and local inflammatory cytokines are increased at the onset of diabetes with rapid suppression of osteoblast markers and increase in adipocyte markers, indicating that bone inflammation may be another contributing factor to the diabetic bone pathology (298, 312, 313). Serum cytokine levels (TNF α , IFN- γ , IL-1Ra and LT-b) and corresponding bone cytokine mRNA expression were increased from as early as 5 days after induction of diabetes in mouse models (249, 312) with decrease in osteocalcin mRNA expression in bone RNA extracts, and it remains suppressed at 40 days post induction. mTNF α can either directly suppress osteoblast maturation as well as promote osteoblast death in vitro (313) or act indirectly by contributing to elevation of ROS causing osteoblast apoptosis from oxidative stress (229, 245). Coe et al. also found that TNF α in the bone marrow microenvironment directly mediate osteoblast death with increase in increased expression of proapoptotic factors and osteoblast TUNEL staining, further contributing to T1D bone loss (298). Inhibition of the cytokines with TNF α neutralizing antibodies prevented osteoblast apoptosis (298) but transgenic mice with IFN- γ KO proceeded to have diabetic bone pathology (312), supporting the idea that diabetic inflammatory bone loss involves an interplay of more than one cytokine and/or a combinations of other factors. Apart from proinflammatory cytokines, abnormal hyaluronan production in bones of diabetic rodents also induced monocyte and macrophage infiltration into the bone collagen matrix, promoting adipogenesis at the expense of osteogenesis (253). The concept of T2D as an inflammatory disease is relatively new with increased fat depots in T2D implicated as the source for more proinflammatory cytokines and adipokines (310). However, a large prospective population study (EPIC) in Germany found that systemic inflammatory markers are independent predictors for the development of T2D, independent of degree of insulin resistance and obesity (314).

1.5.1.6 Vasculopathy

Similar to other diabetic microvascular complications of retinopathy, nephropathy and neuropathy, bone microangiopathy has been insinuated as another possible mechanism for diabetic bone loss. In hypoxic condition (2% oxygen), the bone marrow shifts toward adipogenic lineage by enhancing expression of genes associated with adipogenic/lipogenic phenotype (C/EBP β , PPAR γ 2, and aP2) and by suppressing expression of genes associated with osteoblast differentiation (alkaline phosphatase, AP) (315). Oikawa et al. found that the cumulative vascular density was reduced by three fold in bone marrow of STZ-induced diabetic mice compared to control, along with reduction in blood flow (316). In addition, there is also evidence of reduction in bone marrow volume and bone marrow remodeling with cell depletion mainly affecting the osteoblastic niche secondary to hypoperfusion and oxidative stress (316). Correspondingly, boosting the antioxidative pentose phosphate pathway with benfotiamine supplementation prevented microangiopathy and hypoperfusion in the bone marrow with reduction in cell apoptosis, providing further compelling evidence for vasculopathy in diabetic bone pathology. Regenerating mouse tibia has reduction in blood vessels with lower expression of VEGF, a signaling protein which regulate angiogenesis, and its receptor (289). Clinically, histomorphometric evaluation of iliac crest bone biopsy in 118 diabetic patients revealed evidence of diabetic bone microangiopathy in 82% with significant osteopenia and reduction in the sinusoidal capillaries (317).

1.5.1.7 Anti-diabetic medications

Although insulin has a clear anabolic role on bone as reported earlier, the skeletal effects of insulin treatment remain controversial with increased risk of falls from hypoglycemic attacks resulting in fractures (318). Total daily insulin requirement has a positive predictive value for low BMD, although the need for higher insulin dose may reflect the presence of more severe disease (319). Different classes of anti-diabetic medication, such as thiazolidinediones (TZDs), metformin and glycogen-like peptide 1 inhibitors have been reported to have both varying effects on bone. TZDs such as pioglitazone and rosiglitazone have been shown to increase adipocyte differentiation and decreased osteoblast differentiation through activation of PPAR γ activity (295, 320, 321). Consistent with these preclinical observations, a meta-analysis clearly indicate that TZD use is associated with a higher risk of fracture, particularly in women (321). In contrast, metformin and sulfonylurea have been reported to be bone protective with a reduction in risk of fractures in patients treated with these agents (322, 323). Both compounds exert a direct osteogenic

effect in vitro by stimulating proliferation and differentiation of osteoblast (324-328) through preventing AGE-induced deleterious effects in osteoblastic cells (329) and various signaling pathways including the PI3K/Akt pathway (327), ERK-1/2 (324) and AMPK activation (326, 328). Zhen et al. also demonstrated an indirect effect of metformin on osteoblast survival through reduction of intracellular ROS (330). In addition to its osteoblastogenic potency in vitro, metformin can further prevent bone loss by inhibiting osteoclastic differentiation (331). However, ovariectomized rodents treated with metformin demonstrated inconsistent radiological findings of no change in bone microarchitecture (332) to increased BMD (331). A newer class of oral antidiabetic agent, the dipeptidyl peptidase-4 (DPP-4) inhibitors, such as sitagliptin, has been observed to have anabolic effects on the bone (333) but the long-term skeletal consequences of these drugs are yet unclear. Lastly, dapagliflozin, a highly selective inhibitor of sodium-glucose cotransporter 2 which reduces hyperglycemia and weight in patients with T2D by increasing urinary glucose excretion has also been studied for its effects on bone metabolism but no clear effects have been described (334, 335).

1.5.2 Clinical evidence of fracture

Although fracture data for T1D is scarce, the existing evidence indicates that people with T1D have a higher fracture risk compared to the general population and these fractures occur more frequently in the lower limbs (161, 336-338). More recently, vertebral fractures have been also reported (160, 339). The risk of hip fractures in those with T1D is reported to be 7–12 times greater (336, 340) and this increased risk is also evident in young adults (221). Recent population-based cohort study used data from The Health Improvement Network (THIN) in the U.K. in which 30,394 participants aged 0-89 years with type 1 diabetes were compared with 303,872 randomly selected age-, sex-, and practice-matched participants without diabetes. They found that T1DM was associated with increased risk of incident fracture that began in childhood and extended across the life span. HR were lowest in males and females age <20 years, with HR 1.14 (95% CI 1.01-1.29) and 1.35 (95% CI 1.12-1.63), respectively. Risk was highest in men 60-69 years (HR 2.18 [95% CI 1.79-2.65]), and in women 40-49 years (HR 2.03 [95% CI 1.73-2.39]). The majority of these fractures were lower extremity fracture(219). The increased fracture risk was much higher than expected based on BMD assessed by dual energy x-ray absorptiometry (DXA), which was only 10% lower than normal (162). In a meta-analysis that highlighted the fracture rates and the discrepant relationship with BMD, the relative risk for hip fracture amongst T1D studies was almost 7 (161). Poor glycemic control and disease duration have

also been reported to play a contributory role in this raised fracture risk irrespective of BMD (322, 340, 341). The fracture risk could also be attributed to the microvascular complications of diabetes such as neuropathy, retinopathy and nephropathy (336, 342). Recently, elevated AGEs and pentosidine levels has been found to impair bone strength and cause fragility fractures in T1D (339). Studies that have evaluated fracture risk in patients with T1DM are summarized in (Table 1.2).

Table 1.2: Studies that evaluated fracture risk in people with Type 1 Diabetes Mellitus (T1DM).

Author and year	Study design	Sex	Study population	Age (mean±SD) or range	Fracture site and assessed outcome	Comments
Nicodemus, 2001 (336)	Prospective cohort	F	30377	55-69	Hip	Women were 12.25 times more likely to report an incident hip fracture than women without diabetes.
Miao, 2005 (342)	Prospective cohort	F/M	24,605	20.7± 10.9	Hip	Elevated risks were observed in both sexes (standardized hospitalization ratios =7.6 [95% CI 5.9 –9.6] and 9.8 [7.3–12.9], respectively), increasing with follow-up time. Ophthalmic, nephropathic, neurological, and cardiovascular complications were indicators of particularly high risks.
Ahmed, 2006 (338)	Prospective cohort	F/M	12,639	25-98	All non-vertebral and hip	Men had an increased risk of all non-vertebral [RR, 3.1(95% CI 1.3–7.4)] and hip fractures [RR 17.8 (95% CI 5.6–56.8)]. Men and women using insulin had increased hip fracture risk. Duration of disease did not alter hip fracture risk
Janghorbani, 2007 (222)	Prospective cohort	F	101343	54.7 ± 9.3	Hip	RR of hip fracture was 7.1 (95% CI 4.4 –11.4), after adjustment for BMI, smoking, physical activity, menopausal status, intake of calcium, vitamin D and protein, and postmenopausal hormone use, RR for T1D was 6.4 (3.9 –10.3).
Zhukouskaya, 2013 (160)	Cross-sectional	F/M	82/82	31.1 6 8.6	VFs	No association between VF and lumbar spine BMD in the T1D group. No effect of age of diagnosis, disease duration, HBA1c and related complication on the prevalence of VF.
Neumann, 2014 (339)	Cross-sectional	F/M	128/77	43.4±8.8	Fractures of ribs, fingers and toes were excluded	Those with prevalent fractures had higher HbA1c, pentosidine level and more diabetes-related complications. BMD was lower in those with prevalent fractures.

BMD; bone mineral density; CI; confidence interval; RR, relative risk; VF; vertebral fractures.

1.5.3 Bone turnover studies

In people with T1D, an assessment of markers of bone turnover often shows a state of reduced bone formation which may be associated to factors such as deficiency of insulin and chronic hyperglycemia but this needs further investigation (224). Abnormalities in the growth hormone–IGF-1 axis may also play a contributory role but this needs further investigation. Among the markers of bone turnover, serum osteocalcin level has often been reported to be low whereas bone alkaline phosphatase has been found to be increased in some studies (343, 344). This imbalance of bone formation markers (Increased ALP, decreased osteocalcin) may reflect an impairment of osteoblast differentiation and maturation as bone ALP is expressed early in development of osteoblast and osteocalcin is released from the mature osteoblast. Reports on markers of bone resorption are scarce and conflicting, with studies reporting either normal or reduced circulating levels bone resorption markers (341, 345, 346). Serum PTH has been found to be increased or normal (341). Though levels of the Wnt signaling antagonist, sclerostin, are reported to be higher, its link to other markers of bone metabolism has not been confirmed yet (339). Only one longitudinal study showed that bone turnover returned to normal after improved glycemic control (347).

1.5.4 Bone imaging studies in DM

The association between DM and bone changes has become a subject of extensive research, but the results so far are inconclusive. There is still an open question of whether the effect of diabetes on bone health is primarily due to changes in bone density or changes in the inherent material properties of bone tissue. The majority of BMD studies in children with T1DM have reported either a slightly low BMD or a normal BMD (Table 1.3) (348-351). In adults with T1D, the most consistent observation is that BMD is reported to be significantly decreased at lumbar spine and femoral neck (Table 1.4) (319, 346, 348, 349, 352-359). In one meta-analysis, a significantly lower BMD Z-score at the hip (-0.37 ± 0.16) and spine (-0.22 ± 0.01) [1] was observed. These findings have been confirmed by several subsequent studies (356, 357) but there are also a small number of studies that have reported no abnormalities in BMD (352, 355, 360). The effect of T1D on cortical and trabecular bone structure in humans has not been as well characterized as it has in rodent models (234, 276). Studies that have evaluated bone mass and structure by using pQCT show reduced total and cortical cross sectional area and lower muscle mass in children and adolescence with T1D compared to healthy control (361-365). Another pQCT study by

(366) indicated that as T1D adolescents reached 14 and 15 years of age, their cortical CSA normalized, becoming equivalent to the cortical CSA of nondiabetics at the same age. However, T1D was associated with a decreased bone CSA at the radius at the end of pubertal growth comparing to controls (367). Recently, few studies have analysed cortical and trabecular bone structure measured with high-resolution quantitative computed tomography (HR-pQCT) (163) and QCT(164), and measured trabecular bone score derived from DXA (368). QCT has shown that young and middle aged people with T1DM have lower cortical thickness and lower vBMD compared to healthy controls (164). A single study recently evaluated HR-pQCT in patients with T1D compared to controls concluded that the presence of MVD was associated with deficits in cortical and trabecular bone microarchitecture that could partly explain the increased bone frailty in those group of people (163). TBS which is a measure of bone texture has been found to be lower in T1D patients with prevalent fractures, suggesting an alteration of bone microarchitecture in this subgroup of patients(368). In light of the emerging importance of the interactions between marrow fat and bone and the evidence for the negative effects of marrow fat on bone density, marrow fat as an independent surrogate for bone quality has also been recently assessed by MRI (369). The factors that may be associated with BMD in T1D are not well-known yet. Some studies have documented a decreased BMD in those with a recent onset of T1D (354, 362, 370) indicating the existence of mechanisms before the appearance of clinical symptoms such as autoimmune and inflammatory mechanism (350). However, others studies have not detected an abnormality of BMD in recently diagnosed children indicating that the metabolic consequence of the disease over time may play an important role than a predisposing covariant. Some studies have suggested that metabolic control, including its effect on the growth hormone/ IGF-1 axis, plays a strong role in the genesis of osteopenia (164, 319, 358, 362, 370-373). These findings are supported by a study of intensive insulin therapy that stabilized BMD (345). However, others have failed to show this association (161, 353, 374-378). Vikram V Shanbhogue, et al suggested that the presence of MVD was associated with deficits in cortical and trabecular bone microarchitecture comparing to patient without MVD (163). In summary, the available data on the structural quality of bone in T1D are still scarce and controversial. There are limitations such as small sample sizes, different techniques to measure and interpret data and inadequate adjustment of confounders such as age, disease duration and metabolic status.

Table 1.3: Bone densitometry studies in children with T1DM.

Author, year	N(f/m)	Age (yrs) (range or means \pm SD)	Dis duration (yrs) (range, means \pm SD)	Modality	Site	Major finding in cases vs controls	Comments
Gunczler 1998 (375)	26(11/15)	12.1 \pm 3.1	4 yrs	DXA	LS, FN	\downarrow LS BMD	Adjusted for age, sex and pubertal status. No association with disease duration, glycaemic control, 24 h urinary calcium excretion or bone turnover markers.
Pascual 1998 (374)	55(29/26)	5-15	1-13.8	DXA	LS, FA	No abnormalities	No effect of glycaemic control or disease duration. Adjusted for age and sex.
Heap 2004 (361)	55(25/35)	12-17	6.7 \pm 3.6	pQCT DXA	Tibia LS, FN	$\downarrow\downarrow$ Tibia and FN BMD	Inverse association to HbA1c. Adjusted for sex, maturation, and body size
Léger 2006 (377)	127(54/73)	6-20	4.1-8.6	DXA	LS, TB	$\downarrow\downarrow$ Total BMC and BMD	Only present in girls. Adjusted for age, sex, pubertal stage, and BMI SDS.
Brandao 2007 (351)	44 (22/22)	8.8 \pm 4.4	6.6 \pm 3.9	DXA	LS	No abnormalities	After adjustment for weight, height and pubertal development, the BMD was \leq 2.0 S.D. in only two diabetic patients (4.5%). Longer duration and poor metabolic control may have a negative impact on bone mass,
Moyer-Mileur 2008 (363)	11(11/0)	12.9 \pm 1.0	5.9 \pm 3.7	PQCT DXA	Tibia LS, FN	\downarrow Tibial and FN BMD	Altered markers of GH/IGF-1 axis associated with low BMD. The results were adjusted for height and puberty.
Heilman 2009 (371)	30 (11/19)	4.7-18.6	5.4 \pm 3.4	DXA	LS, TB	$\downarrow\downarrow$ Total BMC and LS BMD	Only present in boys. Inverse association to urinary markers of oxidative stress, plasma ICAM-1 levels and HbA1c. The result was adjusted for age, sex and BMI.
Saha 2009 (364)	48 (26/22)	12-17.8	1-13.5	pQCT DXA	Tibia LS, FN	\downarrow BMC \downarrow CSA	Only present in girls. Adjusted for height, weight, age and sex.
Roggen 2013 (367)	56 (23/33)	17.2-24.8	10.6 \pm 3.9	pQCT	DR	Similar Trabecular BMD, \downarrow CSA	Adjusted for age, gender, height score and BMI. In girls, the CSA SDS correlated negatively with the BMI SDS and positively with the height SDS.
Molina 2014 (350)	75((39/36)	6-20	-	DXA	LS (L1- L4)	$\downarrow\downarrow$ LS BMD	Children and adolescents with early onset T1D presented with low BMD associated with poorer glycaemic control. BMD was not adjusted for any variables.

BMD: Bone mineral density; BMC: bone mineral content; BMI: body mass index; CSA: cross sectional area; DR: distal radius; DXA: dual X-ray absorptiometry; FA: forearm; FN: femoral neck; GH/IGF-1: growth hormone/ Insulin-like growth factor-I; LS: lumbar spine ;pQCT- peripheral quantitative computed tomography ; ICAM-1: intercellular adhesion molecule-1 (ICAM-1).

Table 1.4: Bone densitometry studies in adults with Type 1 diabetes.

Reference	Subject N(f/m)	Age, Yrs (range or means± SD)	Disease Duration, Yrs (mean±SD)	Modalities	Site	Major findings in cases	Comments
Kayath 1994 [152]	90	18-54	2–20	DXA	LS, FN	↓ BMD in 34% of IDDM patients.	Positive correlation with glucose levels duration of disease and insulin dosage.
Lunt 1998 [156]	99 (99/0)	42median	27median	DXA	LS FN	No difference in BMD from control	Positive correlation with BMI and height.
Kemink 2000 [157]	35 (14/21)	37.6±9.9	8.5±3.5	DXA	LS, FN	↓FN BMD, ↓LS BMD, Osteopenia in 67% of men 57% of women	
Lopez-Iberra 2001 [158]	32 (10/22)	20–39	At diagnosis	DXA	LS, FN	↓LS BMD, ↓FN BMD.	
Liu 2003 [153]	33 (33/0)	20–37	14..5±5.7	DXA	FN, LS, wrist, TB.	↓LS BMD, ↓FN BMD	
Bridges 2005 [159]	35 (0/35)	49.3	20	DXA	DR	No difference in BMD from control	
Strotmeyer 2006 [160]	67 (67/0)	35-55	32.2 ±5.3	DXA QUS	Total hip FN, TB, LS	↓ total hip BMD p<0.001 ↓ FN BMD P<0.001 ↓ TB BMD P<0.01 ↓ Calcaneal BUA P<0.001	
Hamilton 2009 [161]	102 (52/50)	20–71	5.5-23.6	DXA	FA, FN, LS	↓BMD at LS, FN and FA	Only present in women, Lower BMD was associated with impaired bone formation.
Danielson 2009 [162]	75 (75/0)	28	16	DXA	Calcaneus FA, FN, LS	↓ BMD at FA and FN	Inverse correlation with HbA1c and markers of bone formation in patients with ↓BMD.
Eller-Vainicher 2011 [104]	175 (104/71)	32±8.4	13 8.4	DXA	LS FN	↓ BMD at LS and FN	Low BMD is associated with low BMI; chronic complications have a negative association with BMD.
Botushanov 2014 [163]	162 (97/ 65)	29.17	/	DXA	LS FN	↓BMD at FN and LS	LS BMD negatively correlated with marker of bone formation.
Shanbhogue et al. 2015 (163)	55 (27/28)	45.6± 11.7	17 median	HR-pQCT DXA	Distal radius and tibia. Total hip, LS	↓ Trabecular vBMD and cortical vBMD at the radius and tibia.	The presence of MVD was associated with deficits in cortical and trabecular bone microarchitecture comparing to patient without MVD.

2 year prospective (Mastrandrea et al 2008) [139]	63(63/0)	15-39	DXA	LS, FN, FA, TB	↓ BMD at FN and TB	Statistically significant in women ≥ 20 years of age.
---	----------	-------	-----	-------------------	--------------------	---

↓: Decrease in BMD; ↑: Increase in BMD; BMD: Bone mineral density; BMI: Body mass index; BUA: Broadband ultrasound attenuation; CSA: Cross sectional area; DR: Distal radius;
DXA: Dual X-ray absorptiometry; FA: Forearm; FN: Femoral neck; LS: Lumbar spine; QUS: Quantitative ultrasound; T1D: Type 1 diabetes; TB: Total body

1.5.5 Conclusion

Figure 1.6 showing the factors that might play significant role in pathogenesis of bone disease in T1DM. In summary, the evidence from experimental studies, with supporting evidence from bone marker and bone density data, suggest that adults with diabetes are at increased risk for fractures. Patients with T1D are at a higher risk for osteoporotic fractures compared to T2D patients or general population. This may be explained by the initial period of insulin deficiency which results in impaired bone formation and prevents accrual of an adequate peak bone mass. This maybe complicated further by subsequent poor glycaemic control. T1D is typically associated with reduced BMD, whereas those with T2D usually have normal or elevated BMD. This inconsistency indicates that impaired bone quality may further explain the higher fracture risk in addition to frequent falls and associated comorbidities. There are several mechanisms by which diabetes could affect bone mass and strength, including insulin level, hyperglycemia, AGE accumulation which influences collagen characteristics, increased marrow adiposity and increased bone inflammation. In addition, associated diabetic complications and treatment with TZDs may increase fracture risk. Future studies are needed to clarify the impact of different aspects of diabetes metabolism, glycemic control and specific treatments for diabetes on bone. Given that DXA related BMD is a poor predictor of bone morbidity in this group of patients, there is a need to explore novel approaches to assessing bone quality. A better understanding of how diabetes affects bone will improve our ability to protect bone health and prevent fractures in the growing population of adults with diabetes.

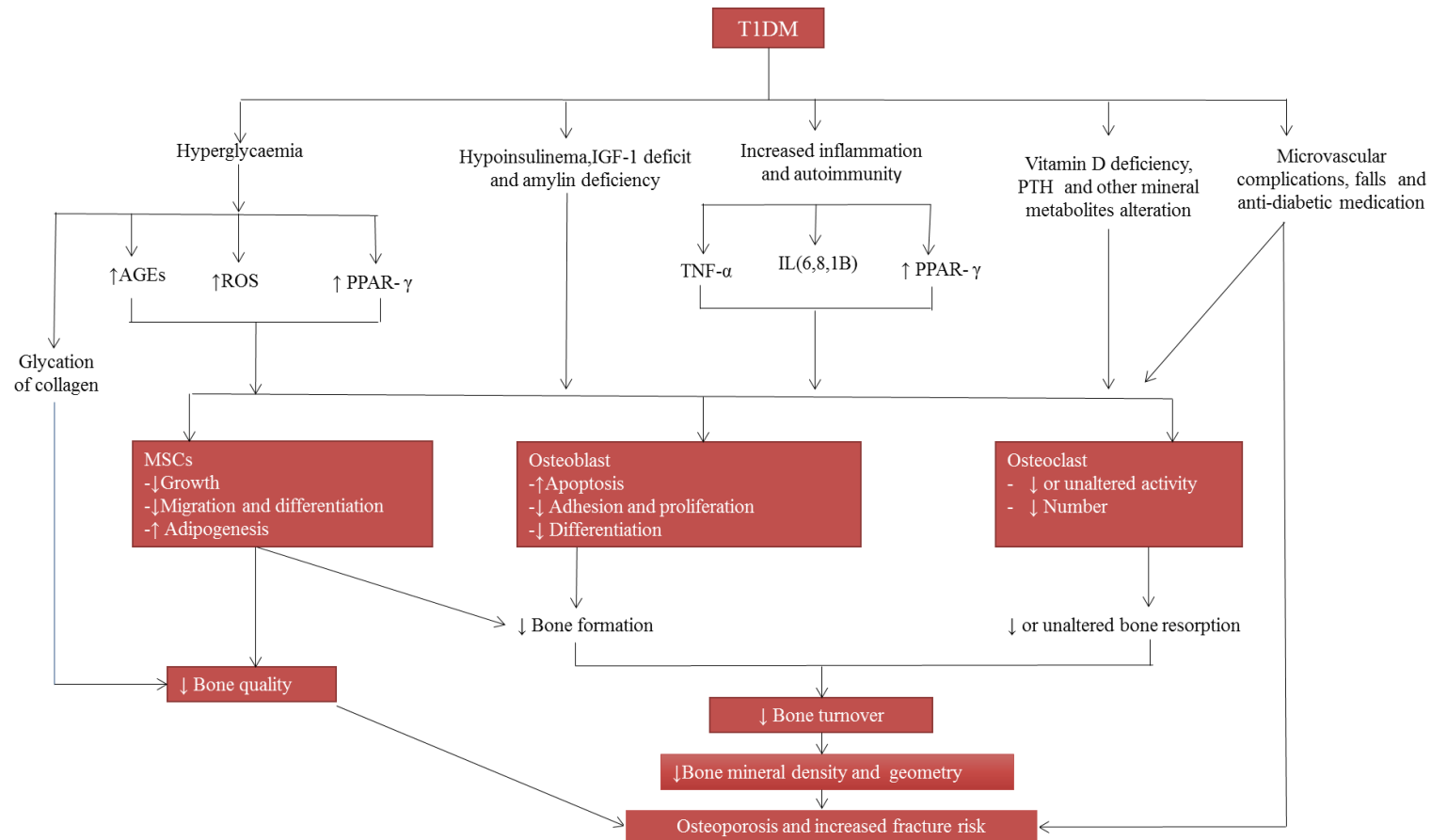


Figure 1.6: Pathophysiological mechanisms of diabetes bone disease.

T1DM leads to hyperglycaemia, increased inflammation, formation of AGEs, generation of ROS, activation of PPAR- γ , alteration of Vitamin D, PTH and other mineral metabolites. This dysregulation as well as reduced insulin signalling and IGF-1 deficit may adversely affect bone cells (MSC, osteoblast, and osteoclast), and induce adipogenesis, low bone turnover and consequently resulting in reduced BMD and bone quality. These abnormalities in addition to associated complications and the use of antidiabetic medications lead altogether to osteoporosis and increasing fracture risk. T1DM; Type 1 diabetes mellitus; IGF-1; insulin growth factor-1; PTH; parathyroid hormone; AGEs; advanced glycation end products; ROS; reactive oxygen species; PPAR- γ ; peroxisome proliferator-activated receptor-gamma; TNF- α ; tumour necrosis factor-alpha; IL(6,8,1B); interleukin-(6,8,beta).

1.6 Imaging Modalities for assessment of bone health

1.6.1 Overview

Dual-energy X-ray absorptiometry (DXA) is by far the most widely used densitometry technique for quantifying bone mass. It is a quick and non-invasive procedure with a low radiation dose of around 0.5-35 μSv . However, it has several major limitations because it provides two-dimensional projected area of a three-dimensional structure, it cannot measure true volumetric BMD and cannot reliably differentiate between cortical and trabecular bone. Furthermore, DXA provides minimal information on bone shape and cannot provide any information on microarchitecture, supporting views that DXA by itself is not reliable in predicting risk of osteoporotic fractures (379)

Quantitative ultrasound (QUS)) represents an alternative method for studying bone tissue and managing patients presenting with osteoporosis or other metabolic bone diseases (380). Although QUS does not directly measure bone mass, it measures bone quality which depends on bone density, bone size, and trabecular architecture (381). It is a method developed on the basis of physical changes that ultrasonic waves undergo while they pass through bone mass. Bone elasticity and hardness could be demonstrated by QUS. Two measures are important in QUS; speed of sound (SOS) and broadband attenuation (BUA). The major advantages of QUS are low cost, accessibility, ease of application, and no radiation exposure allowing it to be used in a large number of disorders such as relatively immobile patient as preterm babies or children (382, 383). The most important limitation of QUS is that it can be used to measure bone quality only on single superficial bones such as the patella, tibia, and calcaneus. Also, clinical interpretation of bone measurements is challenging (384).

More recently, advanced radiological modalities have facilitated assessment of trabecular bone microarchitecture. Micro-computed tomography (μCT), synchrotron radiation computed tomography (SRCT), peripheral quantitative computed tomography (pQCT) and magnetic resonance imaging (MRI) can be used to image and measure trabecular bone microarchitecture (5, 8, 157, 385, 386). Due to high levels of radiation exposure with μCT and SRCT, these methods are currently reserved for ex vivo studies only.

Quantitative computed tomography (QCT) allows for three-dimensional imaging and results in accurate quantification of bone density, but it is more costly and delivers more radiation dose of around 100 μSv (387).

pQCT and HR-pQCT are suitable tools for investigating trabecular bone microarchitecture because they produce images of bone at appendicular sites. However, there are limitations with using pQCT and HR-pQCT for clinical research. There is radiation exposure associated with the scan. The scans are also susceptible to motion artifact causing measurement error. Additionally, because trabeculae size is similar to image resolution, pQCT is limited by partial volume effects which decrease measurement accuracy. To increase image resolution, there are many factors should be taken in amount, higher radiation exposure, more operating costs, longer scan time and processing time for image analysis. Despite these limitations, several research groups have shown the feasibility of pQCT and HR-pQCT to explore changes in cortical and trabecular bone microarchitecture during growth and to differentiate patients with and without established fragility fractures irrespective of their BMD (388-390).

Magnetic resonance imaging (MRI) and magnetic resonance spectroscopy (MRS) have shown great potential in studying bone parameters without any radiation burden to the patient as would be encountered in pQCT, and are currently used in research settings. In the following section detailed description about the basics of MRI and use of MRI in quantification of bone parameters.

1.6.3 The Use of MRI and MRS for the Assessment of Bone Health

1.6.3.1 Overview

Imaging of bones is an important topic of research in identifying abnormalities based on its structure and composition. Different imaging methods are available for measurement of bone properties, but very few modalities are capable of quantifying both structure and composition. Quantitative computed tomography (QCT), peripheral quantitative computed tomography (pQCT) and MRI are suitable imaging techniques that are commonly employed for the non-destructive measurement of trabecular bone microarchitecture and cortical bone. However, QCT and pQCT both require radiation exposure. Magnetic resonance (MR) is a technique that is capable of providing bone information related to both bone quantity and quality from the whole-body without the burden of ionizing radiation to the patient. Additionally, magnetic resonance is emerging as a comprehensive tool for fat quantification, bone marrow adiposity and abdominal adiposity can be measured with MRI, which may contribute to a more complete assessment of bone health. With no ionizing radiation, MRI allows for multislice volume imaging and indefinite repeatability in longitudinal studies and in children. In addition, the signal intensity of fat from CT scans is very low and is similar to that of air and bowel gas. Conversely, the strong bright signal intensity of fat on MR images and the absence of signals from bowel gases permit accurate distinction among fat, other tissues, and gas.

1.6.3.2 Introduction to Magnetic Resonance Imaging (MRI)

The fundamentals of magnetic resonance imaging (MRI) are based on the intrinsic magnetic properties of atomic nuclei. Atomic nuclei with an odd number of protons and neutrons such as ^1H , ^{13}C , ^{19}F , ^{23}Na , ^{31}P have a property known as “spin” and possess a nuclear magnetic moment, which means that they produce a small magnetic field. Hydrogen is present within water (H_2O) and fat (CH_3 etc.) and is the most abundant element within the body, and hence hydrogen nuclei (^1H) generate the strongest MR signal (391, 392). MRI uses a strong external magnetic field (B_0) to align the nuclear magnetic moments of hydrogen atoms in the tissues of the body. Due to the spin characteristics of protons (hydrogen nuclei), when no external magnetic field is present the spins are randomly aligned, and the net magnetic field (M) generated is zero. When an external magnetic field is applied, the spins are aligned either parallel or anti-parallel to the external magnetic field, and the magnetic fields from each pair of parallel and anti-parallel spins cancel out, except for a tiny excess of spins that exist in the low energy state which

generates a small equilibrium magnetisation in the direction of the static field This is illustrated in (Figure 1.7) (393).

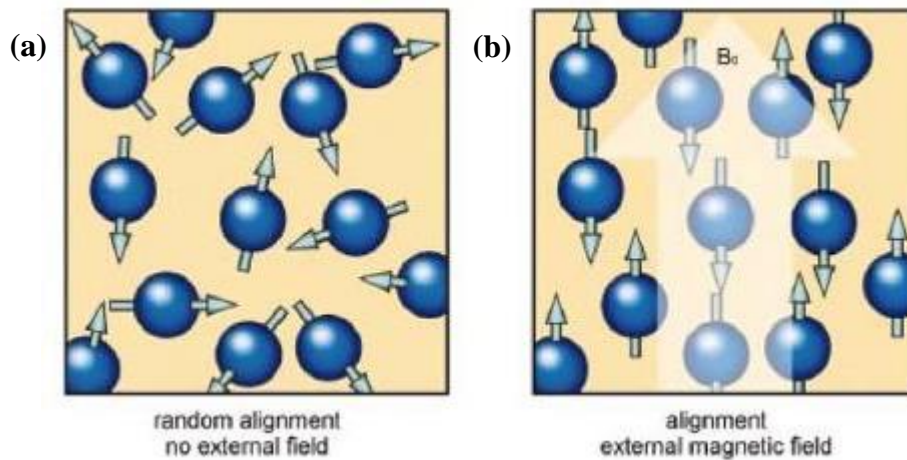


Figure 1.7: Illustration of spin alignment a) with no external magnetic field and b) in the presence of an external magnetic field (393).

Similarly, at body temperature, there is a slightly higher likelihood of spins being aligned parallel to B_0 , which results in a small net magnetic field (M) in the same direction as B_0 . In order to distinguish between M and B_0 , it is necessary to rotate M from being aligned with B_0 (longitudinal plane) to being perpendicular to B_0 (transverse plane). The individual spins rotate, or “precess”, around the axis of the magnetic field at a special frequency called the Larmor frequency, which depends on the strength of the external magnetic field. Typical clinical MRI scanners have a magnetic field strength of 1.5 or 3 Tesla (T), which have corresponding Larmor frequencies of 64 MHz and 128 MHz respectively(394). By applying radiofrequency (RF) pulses of the same resonant frequency as the Larmor frequency and orthogonal to both the B_0 field and the direction of motion of the magnetisation into the x-y plane, energy is transferred to the spins and the net magnetisation deviates from the longitudinal plane into the transverse plane. This is illustrated in (Figure 1.8).

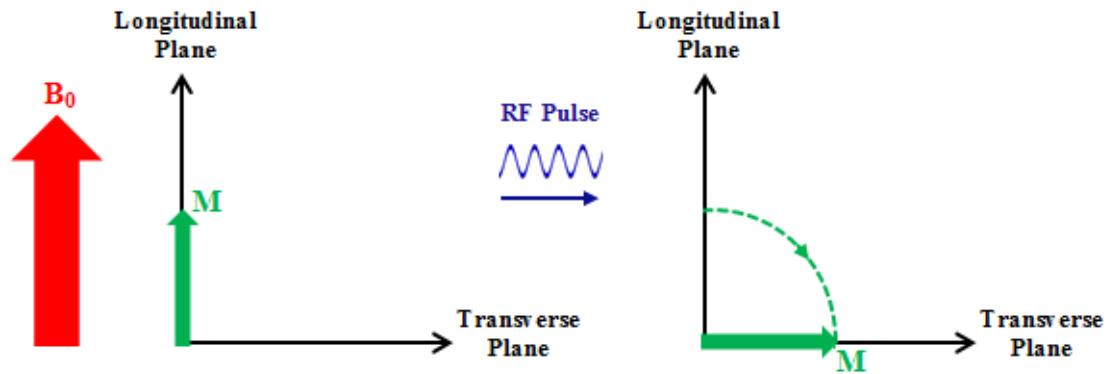


Figure 1.8: Illustration of transfer of net magnetisation (M) from the longitudinal plane to the transverse plane

When the RF pulse is turned off, the spins re-emit the RF energy that they absorbed and the net magnetisation moves, or “relax”, back into the longitudinal plane. The RF energy emitted by the spins can be measured in the transverse plane using an RF receiver known as a “coil”. RF energy is not directly measured by the RF coil. The coil actually measures an induced sinusoidal electric current as a result of the oscillating magnetic field associated with the proton spins. This is Faraday’s law of induction.

The relaxation process can be divided into two parts, called T_1 and T_2 relaxation. T_1 relaxation, which is also known as spin-lattice relaxation, describes the recovery of longitudinal magnetisation, and occurs due to the transfer of energy between the spins and the surrounding environment (lattice). T_2 relaxation, which is also known as spin-spin relaxation, describes the decay of transverse magnetisation, and occurs due to interactions between adjacent spins. T_1 and T_2 relaxation curves are illustrated in (Figure 1.9)(395). In Figure 1.9, longitudinal magnetisation is denoted as M_z and transverse magnetisation is denoted as M_{xy} . The time taken for T_1 and T_2 relaxation to occur varies between tissues, and so at a given time t , the signal intensity available to create the MRI image will be different for each tissue.

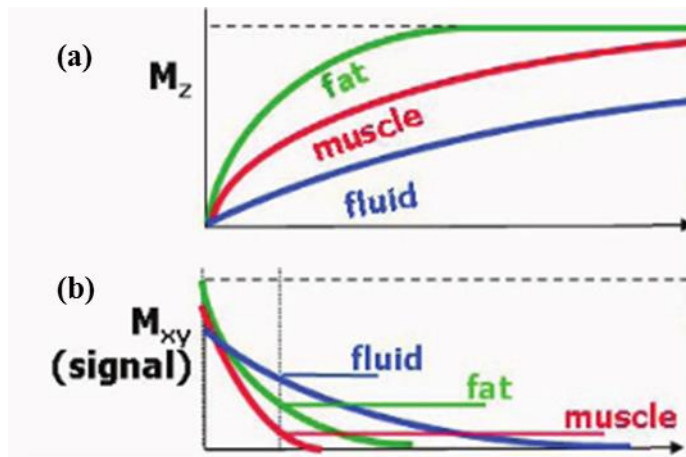


Figure 1.9: Illustration of a) T_1 and b) T_2 relaxation curves for fat, muscle and fluid(395).

Before an MRI image can be created, it is necessary to know where in the body the measured signals originated from. This is achieved by applying linear magnetic field gradients in three orthogonal directions (head-foot, left-right and anterior-posterior). Selection of an imaging slice is performed by applying an RF pulse which contains a small range of frequencies, and only spins which are precessing at those frequencies will contribute to the net magnetisation in the transverse plane. Localisation in the other two planes (denoted as *frequency* and *phase*) is determined according to the frequencies of individual signals – since the magnetic field gradient is linear, the difference in frequency between two spins is directly related to their spatial separation. The area of the body over which data is acquired to form an image is called the *field of view* (FOV). This is illustrated in (Figure 1.10) (395).

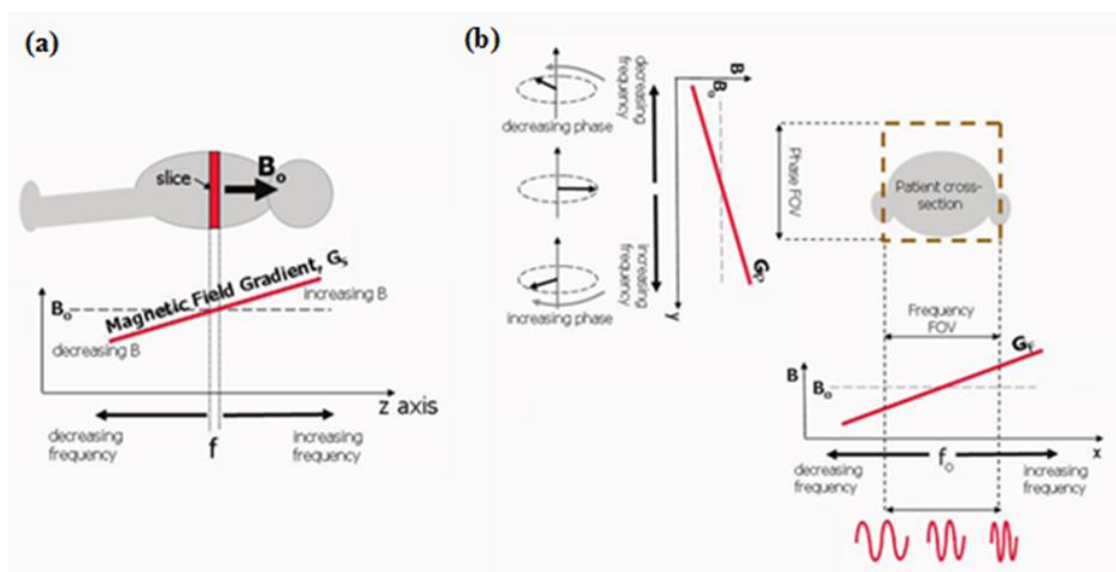


Figure 1.10: Illustration of a) slice selection and b) localisation in the frequency and phase directions using linear magnetic field gradients(395).

The FOV is separated into an array of three-dimensional elements known as voxels. The signal intensity in a given voxel depends on the abundance of hydrogen within the region of the body which contributes to the signal in that voxel. A large voxel will contain more spins and therefore a higher signal, while a small voxel will contain fewer spins and a lower signal. However, a large voxel is not suitable for obtaining images of small structures, and so a balance must be achieved between the required image resolution and an acceptable level of signal intensity. Examples of axial images of the tibia acquired with different voxel sizes are shown in (Figure 1.11).

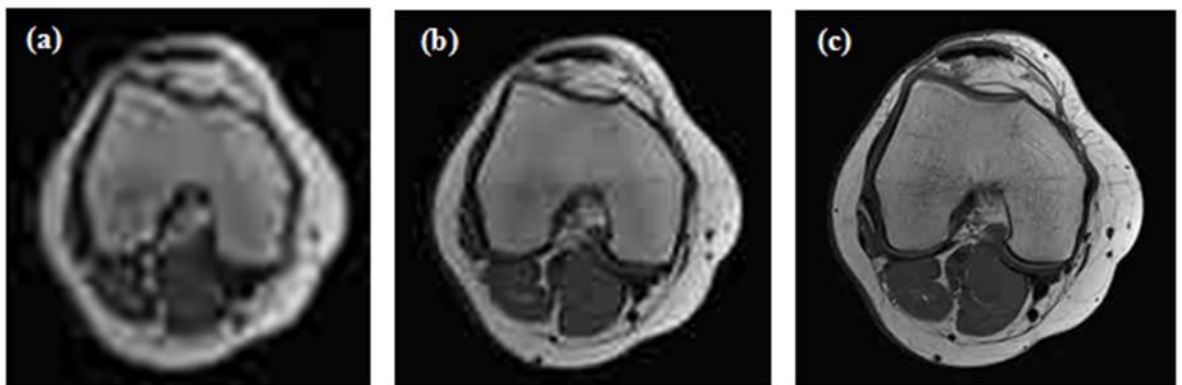


Figure 1.11: Images of the tibia acquired with voxel sizes of a) 2.2x2.2x3.0, b) 1.1x1.1x3.0 and c) 0.4x0.4x3.0 mm

The sequence of RF pulses and magnetic field gradients used to generate an MR image is called a pulse sequence. A pulse sequence will be applied many times in order to build up a single MR image. An example of a typical MRI pulse sequence is shown in (Figure 1.12) (396).

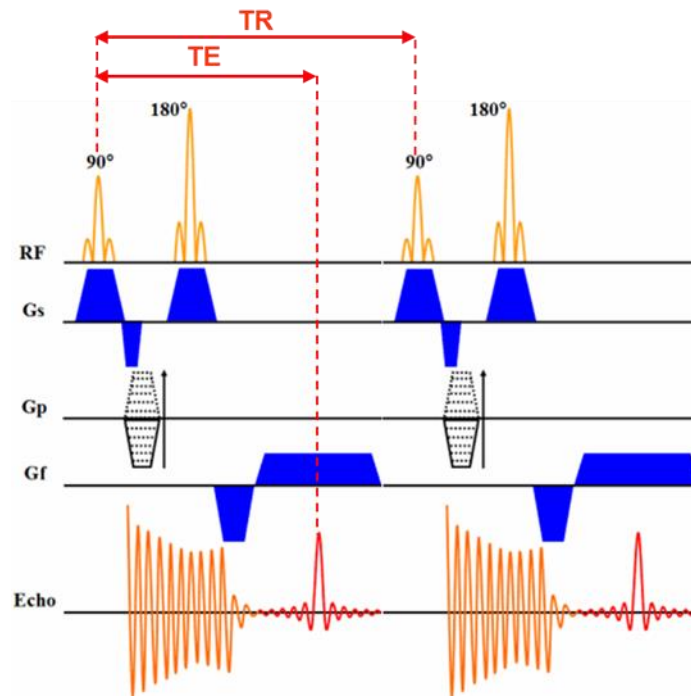


Figure 1.12: Example of an MRI pulse sequence diagram. The RF pulses are shown on the top line, and the magnetic field gradients are shown on the lines marked Gs, Gp, and Gf, where the subscripts refer to the slice, frequency and phase directions.

The important timing parameters shown in the pulse sequence diagram are the repetition time (TR) and the echo time (TE). TR is the time between subsequent applications of the pulse sequence, and TE is the time between the application of the first RF pulse and the measurement of the signal in the transverse plane (396).

The intensity values of the acquired image are generally influenced by the underlying properties of the tissues from which the RF signal is generated. One of the main advantages of MRI compared with other imaging modalities is that the contrast between different biological tissues may be tuned by varying the acquisition parameters. These parameters are either intrinsic or extrinsic parameters. Intrinsic parameters cannot be changed because they are inherent to the body tissues (e.g. T_1 and T_2 values), while extrinsic parameters are those that can be changed and which depend on the pulse sequences parameters used (e.g. TR, TE)(397). An example MRI image of the tibia is shown in (Figure 1.13), which illustrates the differences in signal intensities between bone, bone marrow, muscle and subcutaneous fat. The signal intensities of bone and fatty marrow are very different, which makes MRI ideal for imaging trabecular structure. This will be discussed in more detail in (Section 1.6.3.4.1).

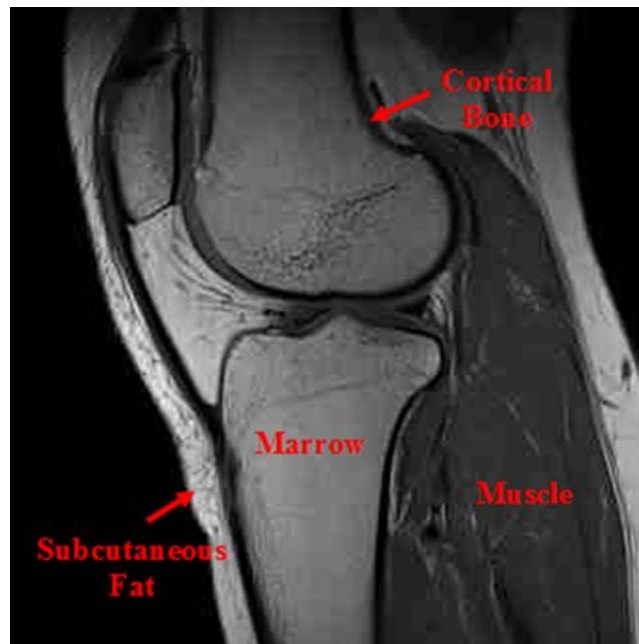


Figure 1.13: Sagittal MR image of the tibia

1.6.3.3 Introduction to Magnetic Resonance Spectroscopy (MRS)

Magnetic Resonance Spectroscopy (MRS) is similar to MRI, but instead of using hydrogen nuclei (^1H) mainly within water and fat to produce anatomical images, MRS measures the abundance of ^1H within a range of molecules (including water and fat).

As mentioned previously, the resonant frequency of a ^1H nucleus is determined by the strength of the magnetic field it is exposed to. ^1H nuclei within molecules are surrounded by orbiting electrons whose motion induces small magnetic fields. This alters the strength of the magnetic field experienced by the ^1H nuclei, and causes a shift in the resonant frequency. The magnitude of the frequency shift varies between different molecules, and plotting a spectrum of signal amplitude against frequency shift allows the relative abundance of molecules to be assessed(393). The frequency shift is expressed in “parts per million” (ppm) rather than Hz to allow comparison between MRS acquisitions obtained at different main magnetic field strengths, and is typically calculated relative to a reference metabolite (tetramethylsilane (TMS) at 0 ppm)(398). MRS data is acquired in a similar way to MRI data i.e. by using a suitable pulse sequence, typically with a single voxel. In a clinical setting, MRS is most commonly performed in the brain, and an example of a typical brain spectrum is shown in (Figure 1.14).

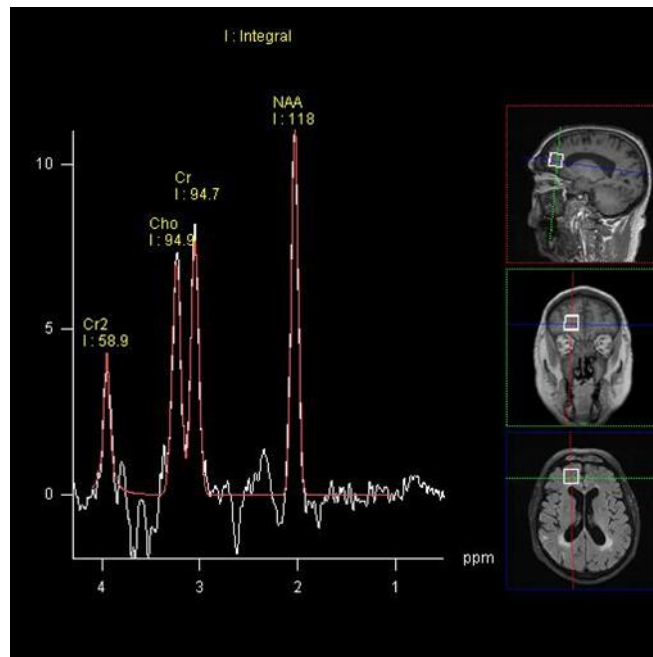


Figure 1.14: Typical MRS spectrum within the brain

The total area under a particular metabolite peak is directly proportional to the concentration of the metabolite. Absolute quantification in biochemical units, e.g. mm/kg, requires calibration using an external solution containing a known concentration of a metabolite, which can be impractical in a clinical setting. Relative quantification is often used instead, which involves defining one metabolite to be the reference metabolite and then calculating the ratio of all other metabolites relative to this (399).

1.6.3.4 Quantification of Bone Structure and Adiposity using MRI and MRS

1.6.3.4.1 Trabecular Bone Microarchitecture

In recent years, MRI has evolved into a powerful tool for non-invasive in vivo visualisation of trabecular bone microarchitecture, using a high resolution technique which is often referred to as micro-MRI. As discussed previously (Section 1.5.2.2), the variations in signal intensity of the imaged tissues depend upon the density of hydrogen nuclei and their T_1 and T_2 relaxation times. Bone has an extremely short T_2 which causes the signal to decay before it can be measured, and consequently bone yields a low MR signal. The MR signal of bone marrow on the contrary is relatively high, and hence bone structures can be indirectly visualised against the fatty background marrow signal, and information on the microarchitecture of the bone can be extracted from the acquired data(400, 401). An example axial image of the tibia which illustrates the high signal intensity from marrow and the low signal intensity from bone is shown in (Figure 1.15).



Figure 1.15: Axial MRI image of the tibia

The most relevant morphological values in the characterization of trabecular bone are the bone volume to total volume ratio (BV/TV), trabecular thickness (Tb.Th), trabecular separation (Tb.Sp) and trabecular number (Tb.N) (394, 402). The methods developed to obtain such morphological parameters are presented in methodology (Section 2.2.1.2).

However, quantification of trabecular bone parameters is limited by partial volume effects (PVE), which overestimate trabecular bone microarchitecture measures in particular Tb.Th (403, 404). The susceptibility of the image to PVEs depends on the alignment of the image plane with respect to trabecular alignment, the size of the trabeculae, spatial resolution, and voxel size (405). Anisotropic bones (vertebrae) are more vulnerable to PVEs than isotropic bone (tibia), due to more random trabecular alignments.

Fundamentally, when the trabecular thickness is greater than image resolution, absolute values of trabecular scale can be reported, while if the trabecular thickness is comparable to or smaller than image resolution, the reported parameters are typically denoted as ‘apparent’ rather than absolute scalar values. Each individual trabeculae are approximately 100-300 μm thickness separated by spaces of 300–1500 μm . In order to accurately resolve small features like trabeculae and reduce PVEs, we need to increase MR image resolution and the slice thickness (voxel size) should be similar to the thickness of the trabeculae. High field strengths and improved coil technology have made it possible to achieve an in-plane resolution of 150 μm (406). However, because of current signal-to-noise constraints, minimal slice thickness is usually about 300 μm . Although this resolution is larger than trabecular thickness, trabecular spacing (800–1000 μm) is still much larger than the size of

a single MR voxel, so that trabecular parameters can be reasonably measured or estimated with MRI.

There are obstacles associated with improving MR image resolution. For example, in order to avoid partial volume effects, voxel sizes less than the size of the trabeculae are desirable. This is not feasible, as voxel sizes are associated with lower SNR (a measure of signal strength relative to background noise). Conversely, thicker slices are associated with an increase in partial volume effects. Consequently, the poorer SNR of small voxel size can be compensated to some extent by increasing the number of acquisitions or by a longer TR to get adequate signals. However, this is accomplished only at the expense of the overall image acquisition time. Consequently, with longer imaging time patients are more likely to move during a longer scan and increasing the susceptibility to motion artefacts. To avoid that we need to reduce the patient movement, this is often done by patient immobilization; for example, padding can be applied around the limb of the participant being scanned to prevent motion, or by using alternative methods (e.g. sedation).

Higher magnetic field strengths are preferred for bone imaging since with a stronger magnetic field, image resolution can be increased with the same scan acquisition time, or acquisition time can be decreased with the same resolution. Various magnetic field strengths e.g. 7 T, 9.4 T, 11.74 T, 14.1 T, and 17.6 T have been used in vitro (405), however in vivo imaging is usually performed at magnetic field strengths ranging from 1 T to 7 T (152, 153, 407-411). The majority of these studies have been performed at 1.5 T, but recent studies (412) have shown practical utility of 3T and 7 T scanners for in vivo imaging of trabecular bone.

Several different pulse sequences have been used to image trabecular microarchitecture, such as spoiled gradient-echo (394) and Fast Large-Angle Spin-Echo (FLASE) (413). FLASE has been shown to provide detailed and reproducible visual delineation of trabecular networks in three dimensions at both anisotropic ($137 \times 137 \times 410 \mu\text{m}^3$) and isotropic ($160 \times 160 \times 160 \mu\text{m}^3$) resolutions in the human distal tibia in vivo (413). However, this pulse sequence was developed by a research group in the US and is not available on standard clinical MRI scanners. Recently, balanced steady-state free precession (b-SSFP) has been used as an alternative technique. It uses RF excitation pulses with small flip angles, which consequently shortens the repetition time (TR) and the total scan time (414, 415). Because of improved SNR, the majority of the studies which have used MRI to investigate trabecular microarchitecture have been done at the peripheral sites e.g. distal radius, distal tibia and calcaneus (402, 416-419). More recently, in vivo

MRI of individual trabeculae within the deeper regions e.g. proximal femur has become possible (411, 420-422).

With the recent advances in high-resolution MRI methods, a large number of studies have documented the feasibility of MRI in quantification of trabecular bone microarchitecture to highlight normal and pathological conditions in a variety of clinical applications. Table 1.5 summarizes some studies using MRI to study trabecular bone microarchitecture in different populations. Variety in MRI protocols was reported, including different magnetic field strength, image resolution; scan time, anatomical location, pulse sequence and immobilisation technique. The early publications by (402, 419, 423, 424) have documented the feasibility and potential of MRI-derived measures of trabecular bone microarchitecture in studying osteoporosis. Furthermore, MRI has been used to explore age and gender-related differences in trabecular bone microarchitecture (425-432). MR-derived structural parameters of trabecular bone microarchitecture are better than DXA at differentiating men and women with and without vertebral fracture (152, 403, 419, 433). Additionally, Change et al., (153) demonstrated the feasibility of 3 Tesla MRI to detect deterioration in proximal femur microarchitecture in long-term glucocorticoid users compared with controls who do not differ by BMD (153).

A study using 1.5 Tesla MRI in children with quadriplegic cerebral palsy (CP) revealed that appBV/TV, appTb.N, and appTb.Th were lower (30, 21, and 12%, respectively) and appTb.Sp was higher (52%) ($p \leq 0.001$) in children with CP than in controls. Distance from the growth plate was inversely related to appBV/TV and appTb.N and was positively related to appTb.Sp at the same distance in children with CP and controls (all $p < 0.01$) (429).

The MRI Department in Glasgow and the Developmental Endocrinology Research Group (DERG) have successfully performed some pilot studies exploring the utility of 1.5T and 3.0T MRI in assessing the microarchitecture of bone in healthy volunteers and some young adults with concerns about bone health (434). They found that people with OI or GHD had a significantly lower appBV/TV and appTb.N and a significantly higher appTb.Sp than the control group.

Moreover, numerous longitudinal studies have demonstrated that MRI-measured trabecular bone parameters found to be more sensitive than BMD in monitoring the response to; different therapeutic effects (435-437), physical activity (438) and diseases progression (439). In a prospective study over 24 months, hypogonadal men who received testosterone replacement therapy, showed the largest changes in surface to curve ratio (+11.2%) and erosion index (- 7.5%), compared to BV/TV (5%) or Tb.Th (1.5%) despite

good reproducibility of BV/TV and Tb.Th (437). Additionally, a 2-year longitudinal study of 91 post-menopausal women receiving either calcitonin nasal spray or placebo studied MRI of trabecular micro-architecture at the distal radius and calcaneus revealed preservation of apparent BV/TV, apparent TbN and app TbSp for the calcitonin group, compared to significant loss in the placebo group. Over the same time, no significant change in DXA BMD was observed among either group (436). Folkesson and Goldenstein, (435) evaluated 2 years longitudinal effects of alendronate on MRI-based trabecular bone structure parameters at distal tibia, distal radius, and proximal femur. They reported significant changes in trabecular bone microarchitecture at the distal tibia but not the radius after 2 years treatment when compared to BMD. These studies suggest that changes are detectable in some, but not all, trabecular bone microarchitecture measures and more apparent at some but not all the skeletal sites. Therefore, the site of assessment may also influence whether changes are apparent.

Concerning diabetes, a small number of recent studies used MR based techniques to investigate bone architecture in patients with diabetes. Pritchard et al., (159) were the first to use high-resolution MRI of the distal radius to compare trabecular bone microarchitecture of postmenopausal women with and without T2DM. They concluded that in women with T2DM, the average pore size within the trabecular bone network at the distal radius is greater compared to controls and hypothesized that this may explain the elevated fracture risk in women with T2DM. A recent study in T2DM aimed to compare 2-year changes in trabecular bone microarchitecture in women with and without T2DM. By using 1 T MRI, they did not find significant differences in the change of trabecular bone microarchitecture variables at the distal radius between the two groups (439).

In summary, trabecular bone microarchitecture may be an important structural bone quality to consider in bone fragility. BMD measurements may not be sensitive enough to detect changes in microarchitectural integrity that impact bone strength. There is abundant evidence now from clinical studies suggested the feasibility of MRI-measured trabecular bone microarchitecture to differentiate between individuals with different bone abnormalities. Additionally, the existing evidence shows a good correlation of MRI measured parameters with the standard quantitative techniques like pQCT and HR-pQCT. While these tools are not yet used in clinical practice for assessing trabecular bone microarchitecture and osteoporosis, recent researches provide evidences of the validity, reproducibility and feasibility of use in clinical settings in the future.

Table 1.5: Summary of MRI studies which report assessment of trabecular bone microarchitecture in different population.

Author, year.	Population (cases/controls)	Techniques	Field strength	Resolution (mm)	Anatomical location,	Scan time (M/S)	Pulse sequence	Immobilisation technique
McComb, C., et al.2014 (434)	GHD, OI (17/22)	MRI	3 T	0.3 × 0.3 × 0.3	Proximal tibia	10 min.	bSSFP	Achieved by placing additional padding within the extremity coil.
Chang, G., et al.2015(153)	long-term glucocorticoid use (6/6)	MRI, DXA	3T	0.234×0.234×1.5	Proximal femur	15:18	3D FLASH	The hip was immobilized by a sandbag laterally secured by a large Velcro strap.
Issever, A.S., et al. 2010 (440)	postmenopausal women (51/0)	MRI, QCT	3T	/	DR, tibia, and calcaneus	20 min. for each	bSSFP	Custom-built immobilization devices were used.
Pritchard, J.M., et al.2012 (159)	T2DM (30/30)	MRI, DXA	1 T	0.195×0.195×0.1	DR	12:9	A spoiled 3-D gradient-echo sequenc	Bracing and padding were applied.
Modlesky, C., et al. 2015(429)	CP (12/12)	MRI	1.5 T	/	Distal femur	/	3D fast gradient echo sequence	The Body FIX (was used to limit motion of the children from the waist down during the scan.
Krug, R., et al. 2008 (408)	10 healthy controls	MRI, HR-pQCT	7T, 3T	/	Distal tibia	9:10(7T), 9:25 (3T).	bSSFP and bSSSE	/
Kazakia, G.J., et al. 2008(441)	Postmenopausal women (53/0)	MRI, (HR)-pQCT, DXA	3 T	0.156 × 0.156 × 0.2	DR and tibia	10 min (Radius) and 15 min (Tibia)	bSSFP	Custom-built immobilization devices were used.
Ladinsky, G.A., et al. 2008(442)	Postmenopausal women (98/0)	MRI, DXA, pQCT, heel QUS	1.5 T	0.137 × 0.137 × 0.410	Distal tibia, DR	16:23 for tibia and 12:18 for DR.	3D FLASE	/
Pritchard, J.M., et al. 2013(439)	T2DM (15/22)	MRI,DXA	1 T	0.195×0.195×0.1	DR.	12:9	A spoiled 3-D gradient-echo sequence	Bracing and padding were applied.

GHD; growth hormone deficiency; OI; osteogenesis imperfecta; T2DM; type 2 diabetes mellitus; MRI, magnetic resonance imaging; DXA; Dual X-ray absorptiometry; pQCT; peripheral quantitative computed tomography; (HR)-pQCT; high resolution peripheral quantitative computed tomography; QUS; quantitative ultrasonography; DR; distal radius; bSSFP; balanced steady-state free precession; bSSSE; balanced steady-state spin-echo sequence; 3D FLASH; 3 Dimension Fast Large-Angle Spin-Echo.

1.6.3.4.2 Bone Marrow Adiposity

As discussed in (Section 1.5.2.3), MRS can be used to quantify the relative abundance of hydrogen nuclei within different molecules. MRS is typically used to investigate metabolites within organs such as the brain and heart; however it can also be used to assess bone marrow adiposity. The majority of clinical studies on BMA have used MRS to analyse separate water and fat signals of BMA at the vertebrae or hip (443-446). The resulting spectrum shows peaks corresponding to water and fat (444) as shown in (Figure 1.16). In MRS measurements, BMA is expressed as a percentage fat fraction FF%.

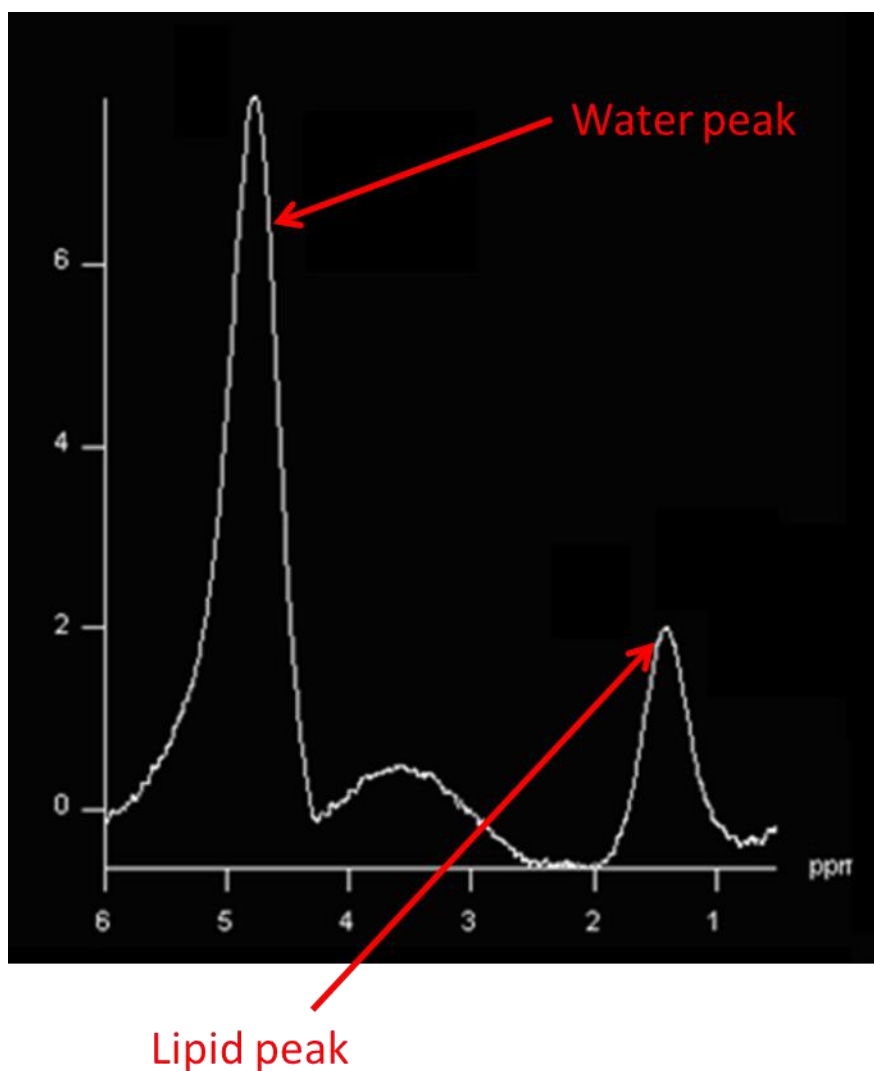


Figure 1.16: The resulting spectrum shows peaks corresponding to water and lipid peaks

Li et al. (445) examined the reproducibility of ¹H-MRS for assessing vertebral bone marrow fat content at 3T. They found that the average CoV of fat content measured was 1.7% (fat content ranged from 45.5% to 66.1%). This lower CoV indicates that ¹H-MRS is a highly reproducible method for quantitatively and noninvasively evaluating fat contents in vertebral bone marrow. Such assessment is critical during interpretation of ¹H-MRS results for both cross-sectional and longitudinal studies. Additionally, they showed variation of marrow adiposity at different vertebral levels and feasibility for identifying patients with low bone density. In addition to quantifying overall bone marrow fat at 3 T, they were also able to selectively quantify the unsaturation level of the bone marrow fat.

Examining and understanding the connection between BMA and bone loss has emerged as an exciting area of research. The study of bone marrow composition for diagnosis of bone abnormalities has been proposed by many groups (443, 447-453). Table 1.6 reviews some of the literature which has used bone marrow composition for diagnosis of bone abnormalities. Variety in MRI protocols was reported; including used technique, magnetic field strength and anatomical location.

Several studies of healthy populations have shown the feasibility of MRS to detect age and gender related differences in marrow adiposity (454-461). Additionally, higher BMA with lower BMD has been reported in patients with osteoporosis (443-445), as well as in individuals with metabolic diseases such as obesity (462) and anorexia nervosa (173). Moreover, studies have reported a relationship between higher BMA and prevalent vertebral fracture (463-465).

It is well known that diabetes is an independent risk factor for fragility fractures, BMA may be altered by diabetes as observed in mouse models of diabetes (Section 1.4.1.4), however, the role of BMA, including the underlying mechanisms of its relationship to bone strength, remains poorly understood. Specifically by using MRS in patients with diabetes mellitus, it was shown that vertebral bone marrow fat content correlated significantly with HbA1c and visceral adipose tissue in patients with T2DM (466) and that decreased unsaturated bone marrow lipids were found to be associated with T2DM and fragility fractures (158). In summary, these results demonstrate that altered bone marrow fat composition (lower unsaturation level) is linked with fragility fractures and diabetes. The authors suggested that MRS of spinal bone marrow fat may therefore serve as a novel tool for BMD-independent fracture risk assessment.

In T1DM, there is only one clinical study which examined the relationship between BMA and diabetes. A study of 16 adult men and women with T1DM and 12 healthy controls, vertebral BMA did not differ by diabetes status but there was a striking positive correlation

between vertebral, femur, and tibia marrow adiposity and serum lipid levels. Also BMA increased with age and was reciprocally related to bone density. Taken together, these data suggest that marrow adiposity may be an indicator of elevated serum lipid levels and decreased bone density (369).

To summarize, there is an accumulating amount of evidence that supports a relationship between higher BMA, lower bone density, and increased prevalence of vertebral fracture in variety of populations. These cross-sectional studies focus on the relationship between bone marrow adiposity and DXA measured BMD, but a limited number of studies also show an association between BMA and bone microstructure (467). Additionally, longitudinal data on these relationships are limited, therefore, prospective data are needed to determine the relationship between changes in BMA and bone, particularly in context of populations of individuals with metabolic diseases (eg, diabetes) in which BMA abnormalities have been demonstrated. A better understanding of the role of BMA in humans may lead to new avenues to promote bone formation and hence prevent and treat osteoporosis.

Table 1.6: Summary of MRI studies which report assessment of bone marrow composition in different populations. Variety in MRI protocols was reported; including adiposity used technique, magnetic field strength and anatomical location.

Author, year	Population type , age	Adiposity measure, anatomical site	Technique, field strength	Bone measures	Adjustment
Kugel, H., et al. 2001(454)	154 healthy men and women (11- 95 yrs.)	FF% of L3	MRS, 1.5 T	None	None
Tang, G.Y., et al. 2010(444)	78postmenopausal women (55-81 yrs.)	FF% and ADC of L3.	MRS and DWI, 1.5 T	BMD of LS by DXA	None
Griffith, J.F., et al. 2012(455)	259 healthy men and women (62-90 yrs.)	FF% of L3	MRS, 1.5 T	BMD of LS by DXA	None
Baum, T., et al. 2012(466)	13 postmenopausal women with T2DM and 13 age- and body mass index-matched healthy controls	FF% and unsaturated lipid fraction of l2-l3	MRS, 3T	VBMD of L1–L3 (QCT).	None
Slade, J.M., et al. 2012 (369)	16 adult men and women with T1DM compared to 12 adult men and women without T1DM.	FF% of femur, tibia and L4.	Ideal MRI, 3 T	BMD by DXA	None
Patsch, J.M., et al. 2013(464)	33 postmenopausal women with T2DM, with and without fragility fracture compared to 36 postmenopausal women with and without fragility fracture.	FF% and composition of L3	MRS, 3 T	BMD of the hip and LS by DXA and QCT	Age, race, and spine BMD
Shen, W., et al. 2014(461)	181 healthy children (5-17yr.) and 495 healthy adults (\geq 18yr.)	Pelvic BMA (ilium, sacrum, ischium, pubis, coccyx and femoral heads)	Whole-body MRI, 1.5T	Pelvic BMD by DXA, pelvic vBMD calculated by dividing BMC by the pelvic bone volume (BV) determined by MRI.	Age, weight, TBF, SAT, VAT, skeletal muscle, sex, ethnicity and menopausal status
Bredella, M.A., et al.2014 (173),	14 women with AN (29.5 \pm 1.9yrs) and 12 age-matched normal-weight	Total marrow fat content and marrow fat composition of the femoral diaphysis and soleus	MRS, 3 T	BMD of LS and hip by DXA	%IBW

	controls	intramyocellular lipids and unsaturated muscle lipid				
Gao, Y., et al. 2015 (453)	185 healthy children (76 females and 109 males, aged 5-18 yrs.)	BMA (cm ²) of femur	Whole body MRI, 1.5 T	Femoral-CBA by whole body MRI	Weight, TBF, SCAT, VAT, and skeletal muscle	
Baum, T., et al. 2015(468)	28 healthy young subjects (26 ± 4 yrs.)	PDFF of C3-L5.	Chemical shift encoding based water-fat MRI, 3T	None	None	
Agrawal, K., et al. 2015(449)	50 postmenopausal women (40-73 yrs.)	FF% and ADC of L3	MRS and DWI, 1.5T	BMD of L3 by DXA	None	
Mostoufi-Moab, S., et al. 2015 (469)	25 alloHSCT survivors (12-25 yrs.) compared to 25 age-, race-, and sex-matched healthy controls.	FF% for the five lumbar vertebrae	MRSI, 1.5 T	Digital topological parameters were acquired at distal tibia by using 1.5-T whole-body scanner	Sex, VAT, SAT, and muscle density, WB-FM	
Huovinen, V., et al. 2015(462),	18 normal-weight (BMI <25kg/m ² ; 2 males, 16 females) and 17 overweight (BMI ≥25kg/m ² ; 9 males, 8 females) (15-27 yrs.).	BMA unsaturation index (UI) of the tibia	MRS, 3 T	None	Age, gender, physical activity and blood glucose	

T1DM; Type 1 diabetes mellitus: T2DM; type 2 diabetes mellitus: AN; anorexia nervosa: alloHSCT; Allogeneic hematopoietic stem-cell transplantation (alloHSCT): BMI; body mass index: FF%; fat fraction: ADC; apparent diffusion coefficient: PDFF; Proton density fat fraction: BMA; bone marrow adiposity: L3, L4, L5; lumbar vertebrae: C3; third cervical vertebrae: LS; lumbar spine: MRS; magnetic resonance spectroscopy: MRI; magnetic resonance imaging: DWI; Diffusion-weighted magnetic resonance imaging: DXA; Dual-energy x-ray absorptiometry: QCT; quantitative computed tomography: CBA; cortical bone area: %IBW; ideal body weight: BMD; bone mineral density: VBMD; volumetric bone mineral density: TBF; total body fat: WB-FM; whole body fat mass: SAT; subcutaneous adipose tissue: VAT; visceral adipose tissue.

1.6.3.4.3 Abdominal Adiposity

Compared to other methods (470), MRI is currently the gold standard for non-invasive direct accurate quantitative measurement of intra-abdominal adipose tissue (470-475). There are several MRI methods for abdominal fat quantification, T1-weighted imaging, magnetic resonance spectroscopy (MRS), and chemical-shift imaging (CSI). In this thesis T1-weighted imaging has been used.

T1-weighted sequences are very common in clinical MRI. They are available as standard software on all commercial MRI scanners (GE, Philips, Siemens, Hitachi, and Toshiba) and can be easily applied. It is based on relaxation rates of fat and water proton signals as they recover after radio-frequency excitation. T1-weighted MRI is mainly used for white adipose tissue (WAT) quantification because fat is characteristically bright in contrast to other lean tissues and organs owing to its rapid T1 recovery rate (Figure 1.17)(476, 477). Thus bright fat can be easily identified and delineated by simple signal thresholding from darker structures. by using partially automated software, the sharp contrast between the bright adipose and dark water-containing lean tissues creates the visual basis that enable the segmentation of each image, consequently, the distribution of adipose tissue in terms of total(TAT), visceral (VAT) and subcutaneous (SAT) were semi-automatically calculated.

Another method for quantifying abdominal fat adiposity is by the use of the Dixon technique. The technique acquires two separate images with two TE settings such that one image has the water and fat signals in-phase and the other has the water and fat signals 180° out-of-phase. Dixon showed that from these two images, a water-only image and a fat-only image can be generated. The availability of both the water-only and fat-only images allows direct image based water and fat quantitation (478).

A consistent body of literature suggests that the arrangement of regional fat deposition into the subcutaneous and visceral compartments to be a stronger predictor of disease risk than overall fat mass (479-482). Therefore, a frequent approach is to only scan the trunk region. Methods range from a single slice at a predefined abdominal level to the whole trunk that includes intrathoracic, intra-abdominal, and intra-pelvic cavities and associated adipose tissues (483). The multislice imaging is generally considered a gold standard reference for measuring total and regional adipose tissue volumes (484). However, with the cost involved with multislice imaging for volumetric analysis, single-slice images can be used as representative measures of VAT (483). One major concern in using single-slice analysis for MRI is that soft-tissue structures are continuously moving and may adversely affect the

reliability of the visceral fat measurement, as movement of these tissues will change the location of VAT in a particular single slice. The commonly used technique to overcome this limitation is by using breath holding technique which has been applied in the presented thesis.

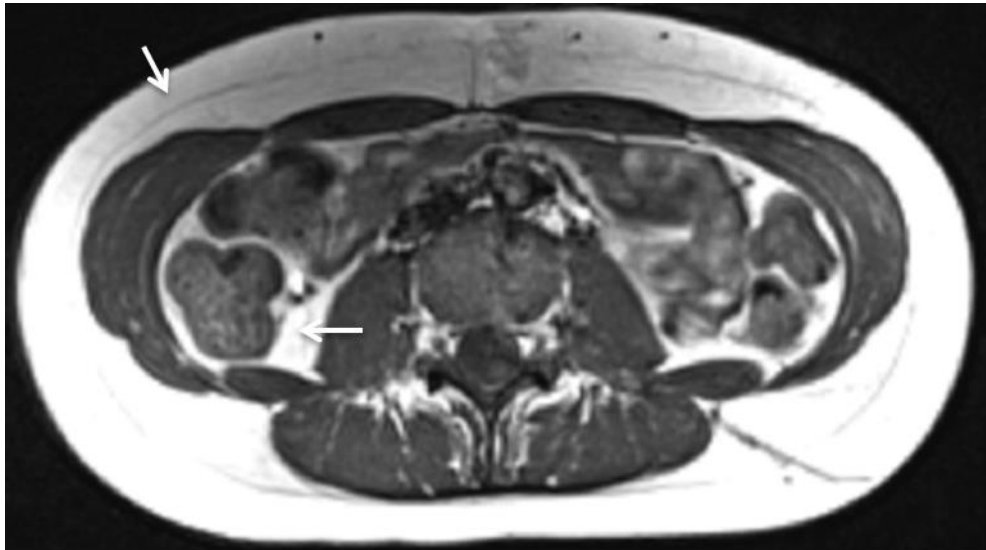


Figure 1.17: Example of T1-weighted axial magnetic resonance images acquired in abdomen at the level of the L3 vertebrae demonstrating the typical high signal intensities of fatty tissues (arrows) in contrast to other darker muscles and organs. Data were acquired on a 3 Tesla MRI scanner using T1 weighted turbo-spin-echo sequence.

The feasibility of MRI in accurate quantification of abdominal adiposity has been shown by several studies (473, 485). The differential effect of abdominal adiposity measures (VAT, SCAT) on metabolic risk factors is well described, yet it is uncertain whether abdominal adiposity measures protects against osteoporosis or adiposity is harmful to bone as different adipose tissues express different biochemical factors and in varying concentrations (482, 486, 487). Studies using direct measures of VAT appear to provide more consistent finding on the association between VAT and BMD (486, 488-493) than those using surrogate measure (360, 494-496). These studies were limited by the use of crude measures (e.g. DXA) of abdominal adiposity that are unable to separate VAT from other soft tissues; therefore, the contribution of VAT on bone is difficult to define in these studies.

In summary, direct accurate quantitative assessment of abdominal adiposity measures are essential to evaluate their influence on bone health. In particular, there is a need to use this technique in diabetic patient and this may contribute to a more complete assessment of bone health.

1.7 The rationale for the present work

Based on the current fracture risk predictors the explanation for the higher fracture risk in patients with T1DM is yet unclear. Although, numerous studies have assessed the bone structure and turnover markers in patients with T1DM, these studies have not provided a consensus. Detailed trabecular bone microarchitectural assessments are lacking, and it is not known whether patients with T1DM have altered bone microarchitecture compared to healthy controls without T1DM. Further, considering the possibility that bone deficit may be related to adiposity measures (BMA, abdominal adiposity), which may contribute to the increased bone fragility, studies in rodent models of T1DM have suggested that diabetic bone loss is associated with increasing bone marrow adiposity. However, whether bone marrow adiposity is different and associated with bone deficit in people with T1DM is not known. In addition, how trabecular bone microarchitecture and bone marrow adiposity changes over time in patients with T1DM is not known. Further, as noted earlier in the introduction, numerous studies have investigated the possible underlying mechanisms that might be affecting the bone health in those groups of people, however, these studies have not provided a consensus and the results are inconclusive yet.

1.9 Key Aims and hypothesis

Primary hypothesis:

1. There are differences in the measurements of key bone parameters and bone adiposity parameters obtained using micro-MRI images and MRS and biochemical markers of bone metabolism and adiposity in patients with T1DM compared to healthy women without T1DM.
2. The expected deficit in bone parameters in patients with T1DM is associated with increasing bone marrow adiposity and abnormal levels of biochemical markers of bone metabolism and adiposity.
3. There would be changes in the measures of bone microarchitecture and adiposity in women with T1DM compared to women without T1DM.

Secondary hypothesis:

1. Different body adiposity measures have different effects on DXA and MRI - measured bone parameters.
2. Abdominal adipose tissue is positively correlated with vertebral bone marrow adiposity, and negatively with DXA and MRI -measured bone parameters.
3. The MRI- measured bone parameters demonstrate good correlation with DEXA data and are able to differentiate between people with and without T1DM.
4. Markers of diabetic control are inversely associated with the bone and adiposity measured parameters.

Thesis Aims:

To study the measurements of trabecular bone microarchitecture, bone marrow adiposity and abdominal adiposity obtained by MRI, and the biochemical markers of bone metabolism and adiposity in group of young women with childhood onset T1DM compared to healthy women without T1DM (chapter 3).

1. To explore the differences in trabecular bone microarchitecture and bone marrow adiposity parameters between a group of young adult women with childhood-onset T1DM and controls without T1DM.
2. To examine differences in the biochemical markers of bone metabolism and adiposity between women with T1DM and women without T1DM.
3. To evaluate whether the bone marrow adiposity, abdominal adiposity and the biochemical parameters of bone metabolism and adiposity are associated with bone deficit in patients with T1DM.
4. To evaluate the relationship between the all these measured parameters with markers of diabetes control and disease parameters.

To examine the longitudinal changes in the measurements of bone microarchitecture and adiposity parameters in young adult women with childhood onset T1DM compared to healthy controls (chapter 4).

1. To compare the prospective changes in trabecular bone microarchitecture and adiposity parameters over one year period in the same groups of women who were enrolled in the first study.
2. To evaluate whether there is any association between the changes in trabecular bone microarchitecture with vertebral bone marrow adiposity and abdominal adiposity in the studied group.
3. To evaluate whether the expected changes in these measurements are associated with the changes of markers of diabetic control.

To study the adiposity based determinants of bone density and microarchitecture in healthy young women and women with T1DM (chapter 5).

1. To compare adiposity and bone parameters measured by DXA and MRI in healthy young women and women with T1DM,
2. To determine the associations between the markers of diabetic controls and disease related parameters and these measured outcomes.
3. To ascertain which adiposity measure (s) is most strongly associated with bone measured parameters in healthy young women and women with T1DM.
4. To compare the feasibility of DXA and MRI measured parameters to differentiate between women with and without T1DM.

Chapter 2

Methodology

2.1 Introduction

This chapter provides details of the image acquisition and analysis protocols for the study procedures that are presented in this thesis. Further analysis was performed for specific investigations, and the details will be provided in the relevant chapters. The procedures involved in this study are MRI of the right knee and abdominal adiposity, MRS of L3, a DXA scan of the lumbar spine, hip and total body, venous blood sampling and biochemical assays.

2.2 MRI scanning

All imaging was performed using a 3 Tesla (T) Siemens VerioMRI scanner (Siemens, Erlangen, Germany) using a transmit/receive (Tx/Rx) extremity coil for the knee, an 8-element spine coil for MRS of L3 and surface body coils for the abdominal scanning. All MR imaging was performed during a single scanning session, more details are shown in appendix A.

2.2.1 Proximal Tibia Imaging

2.2.1.1 Acquisition

MRI images of the proximal tibia were acquired using an extremity coil positioned over the knee. During scanning, the participants were positioned supine with legs extended; immobilisation of the leg was achieved by placing additional padding within the extremity coil. Following immobilisation, three localiser scans were performed in the sagittal, axial and coronal planes to identify the region of interest using a T1-weighted spin-echo sequence. Scan locations are shown in (Figure 2.1). The pulse sequence parameters used to provide 3D volume of isotropic resolution using a fully balanced steady state free precession (bSSFP) pulse sequence is shown in (Table 2.1). Thirty axial Micro-MRI images (0.3mm thick) of the metaphysis were collected immediately below the growth plate. Analysis was performed using the slice that was located at the insertion point of the patellar ligament.

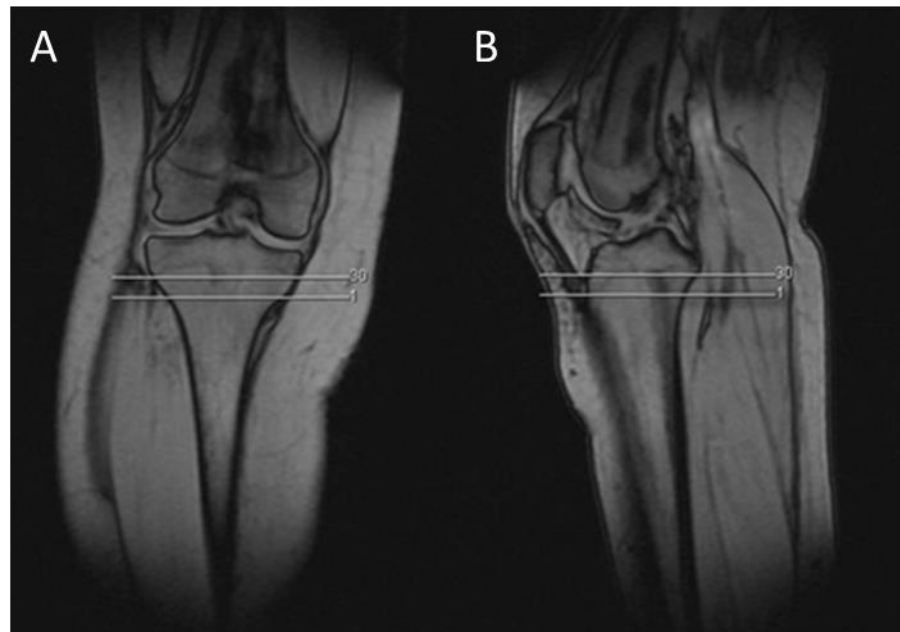


Figure 2.1: Representative MR image of the knee. Scan locations are shown, (A) showing the placement of the reference line and the region of interest captured in the coronal image, (B) The region of interest captured in the sagittal image.

Table 2.1: Pulse sequence parameters for tibia imaging

Parameter	Used value
Resolution	0.3 mm x 0.3 mm
Slice thickness	0.3 mm
Repetition time (TR)	10.19 ms
Echo time (TE)	4.39 ms
Flip angle	60°
Bandwidth	180 Hz/pixel
Matrix size	384x384
Field of view	100 mm x 100 mm
Scan time	10 minutes

2.2.1.2 Image processing and Analysis

Following scanning, images were coded and analysed using IDL software that was developed in-house (Research Systems Inc, Boulder, CO, USA), based on a method that was described by Majumdar et al(402), which give measures for apparent bone volume to total volume ratio (appBV/TV), apparent trabecular number (appTbN), apparent trabecular thickness (appTbTh) and apparent trabecular spacing (appTbSp). The proportion and location of magnetic resonance images that need to be processed to yield representative

estimates of trabecular bone microarchitecture have been assessed by our group (509), and also by Modlesky et al (497). The image processing steps required for quantifying trabecular bone microarchitecture parameters are shown in (Figure 2.4).

2.2.1.2.1 Image processing

A median filter is applied to the MR image to reduce the effects of noise. A 3x3 filter was used as shown in Figure 2.2, which means that the intensity of each pixel from the original image is replaced with the median value of the intensities of that pixel plus its eight nearest neighbours. An example of the output of a 3x3 filter can be appreciated in figure 2.2.

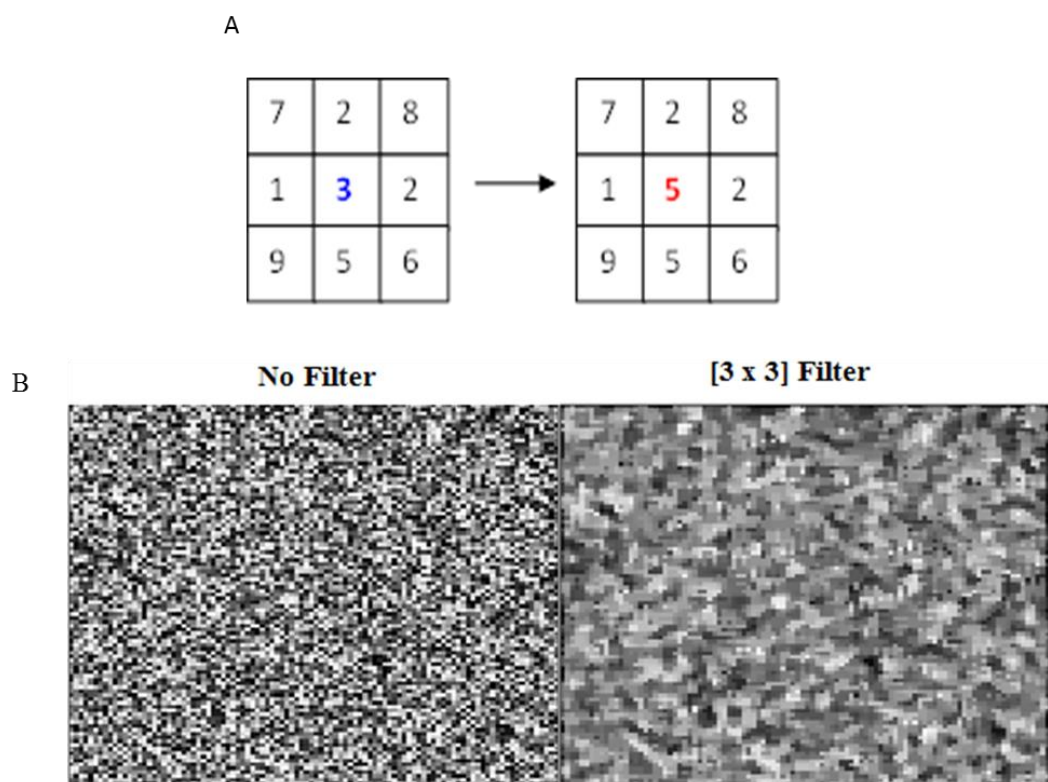


Figure 2.2: Illustrating a median filter applied to MR image, a 3x3 filter was used (A). An example of the output of a 3x3 filter (B).

2.2.1.2.2 Image analysis

After image filtering, the MR image was analysed to give the measures of bone parameters.

Calculate Apparent Trabecular Bone Volume Fraction (appBV/TV)

Regions of Interest (ROIs) were drawn within the trabecular bone region, in the area which is to be analysed, and within the cortical bone. The regions of Interest (ROIs) were defined manually using the cortical bone boundary as reference point to ensure that the analysed ROI consisted only of the trabecular bone and bone marrow (Figure 2.4). To extend the standard stereological techniques and quantify the trabecular bone microarchitecture, the images were thresholded and segmented into a trabecular bone and a bone marrow phase. The mean signal intensity within the trabecular bone region, I_{ROI} , was calculated, and a histogram of the distribution of signal intensities in the ROI was plotted. The ROI within the trabecular bone region contained both bone and marrow. If the pixel dimensions were less than the trabecular width, then a histogram of the intensities within the ROI would show two distinct peaks one for bone and one for marrow. However, since the pixel dimensions were similar to or greater than the trabecular width, a single pixel might contain signals from bone and from marrow, and this mixture results in a histogram with a single peak (Figure 2.4). By using the cortical bone as standard, the bone intensity I_{bone} was calculated as the mean value within the cortical bone ROI. Estimation of the marrow-equivalent intensity was made by finding the maximum value, N_{max} , in the histogram, and setting a threshold value, $N_{thresh} = 0.5 * N_{max}$. The marrow-equivalent intensity I_{marrow} is calculated from the upper intensity value at which N_{thresh} was reached (Figure 2.3).

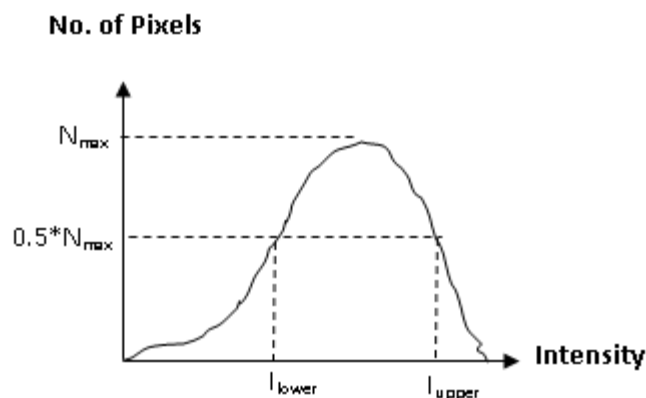


Figure 2.3: Illustrate estimation of the marrow-equivalent intensity

The apparent trabecular bone volume fraction was then calculated to satisfy the following equation:

$$I_{ROI} = (appBV / TV)I_{bone} + (1 - appBV / TV)I_{marrow}$$

$$\Rightarrow appBV / TV = \frac{I_{ROI} - I_{marrow}}{I_{bone} - I_{marrow}}$$

Equation 2-1

Binary image

The apparent trabecular bone volume fraction is also defined as “number of bone pixels/total number of pixels”. The total number of pixels in the ROI is known, and so the number of bone pixels and marrow pixels corresponding to the calculated value of appBV/TV can be calculated:

$$N_{bone} = appBV / TV * N_{total}$$

$$N_{marrow} = N_{total} - N_{bone}$$

Equation 2-2

Bone has a lower intensity than marrow, and hence the pixels which appear in the left hand side of the intensity histogram are more likely to contain pure bone, or a large percentage of bone. The intensity value at which the fractional trabecular bone content in the ROI corresponded to the calculated app BV/TV was selected as the threshold, and the images were binarized into a bone and a marrow phase. Finally, the region of interest (ROI) was binarised to produce an image of a pure bone phase and a pure marrow phase (Figure 2.4).

Calculation Mean Intercept Length (MIL)

The MIL at a given angle θ was calculated by counting the number of trabeculae-marrow boundaries that cross a set of parallel rays oriented at a given angle θ through the binarized image.

A grid of parallel lines, each one pixel thick and separated by 10 pixels, is used as a mask, so that only the sections of the image which lie along the lines are considered and the rest of the image was set to zero. For each line in turn, a starting value corresponding to the value of the first pixel in the line was established. Each pixel along the line was then examined in turn, and the number of times that a change from bone to marrow (1 to 0) or

marrow to bone (0 to 1) occurs was counted, and defined as $P_L(\theta)$. The number of pixels which correspond to bone, P_P was also counted, and the MIL was calculated using:

$$MIL(\theta) = 2 \cdot \frac{P_P}{P_L(\theta)}$$

Equation 2-3

Calculation of Apparent Trabecular Thickness (appTbTh)

The MIL is calculated for all angles between 0° and 360° in steps of 10° . The apparent trabecular thickness (in mm) was then calculated using:

$$appTbTh(mm) = 0.5 * \text{mean}(MIL(\theta)_{\theta=0,360}) * \text{Pixel Resolution}(mm)$$

Equation 2-4

Calculation of Apparent Trabecular Number (appTbN)

Apparent trabecular number (in mm^{-1}) was calculated using the following equation:

$$appTbN(mm^{-1}) = \frac{appBV / TV}{appTbTh}$$

Equation 2-5

Calculation of Apparent Trabecular Spacing (appTbSp)

Apparent trabecular spacing (in mm) was calculated using the following equation:

$$appTbSp(mm) = \frac{1}{appTbN} - appTbTh$$

Equation 2-6

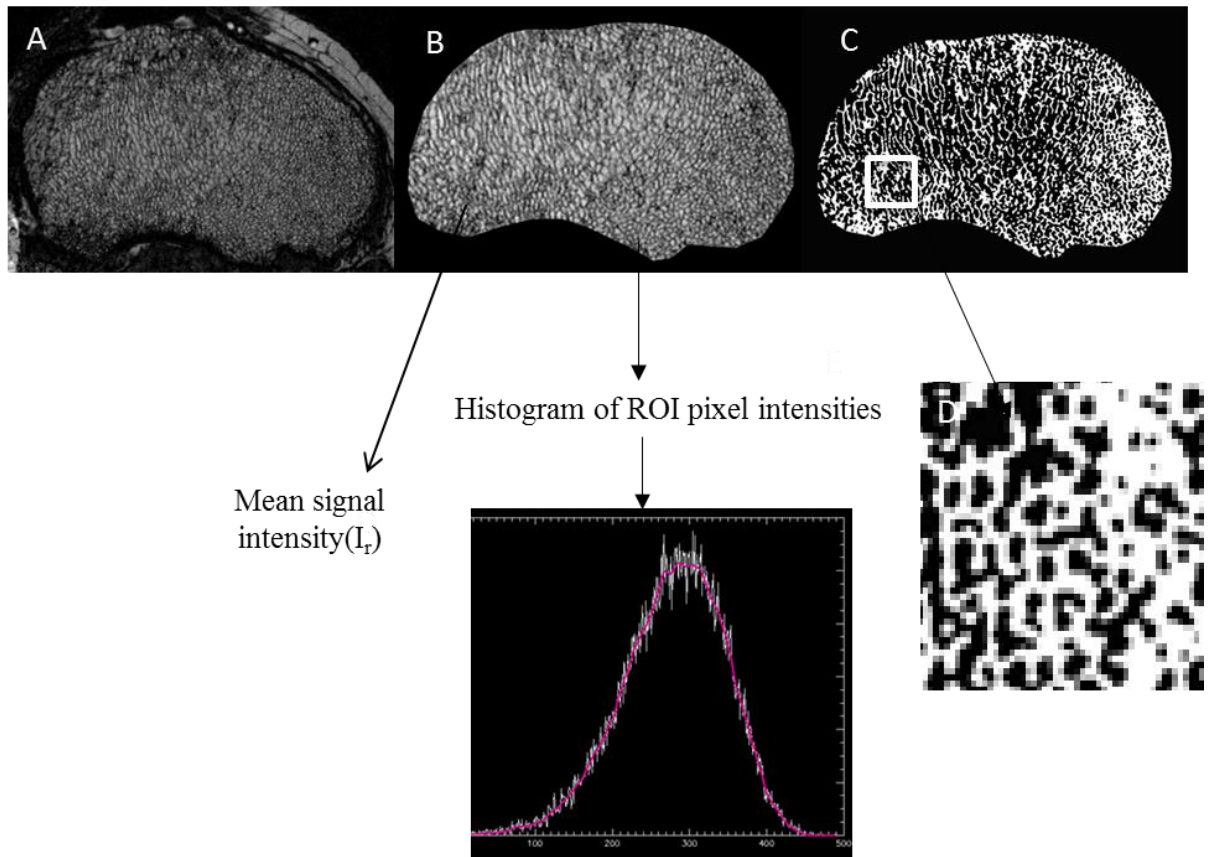


Figure 2.4: Representative MR Image through an axial section in the proximal tibia using MRI. (A) Micro-MR images. (B) The trabecular bone compartment (ROI), the intensity mean (I_r) over this ROI was measured. The histogram for this ROI is also shown. (C) The region of interest (ROI) is binarised to produce an image of a pure bone phase and a pure marrow phase. (D) Higher magnification view of section within the ROI.

2.2.2 MRS

2.2.2.1 Acquisition

MRS was performed using an 8-element spine coil, using the method described by McComb et al (434). Images of scan localisation are shown in (Figure 2.5). Spectra were obtained using a 20mm x 20mm x 20mm voxel positioned in the lumbar spine within the vertebral body of L3. A Point-RESolved Spectroscopy (PRESS) sequence with no water suppression was used with a short echo time (TE) to allow detection of lipids. The actual parameters of PRESS are shown in (Table 2.2).

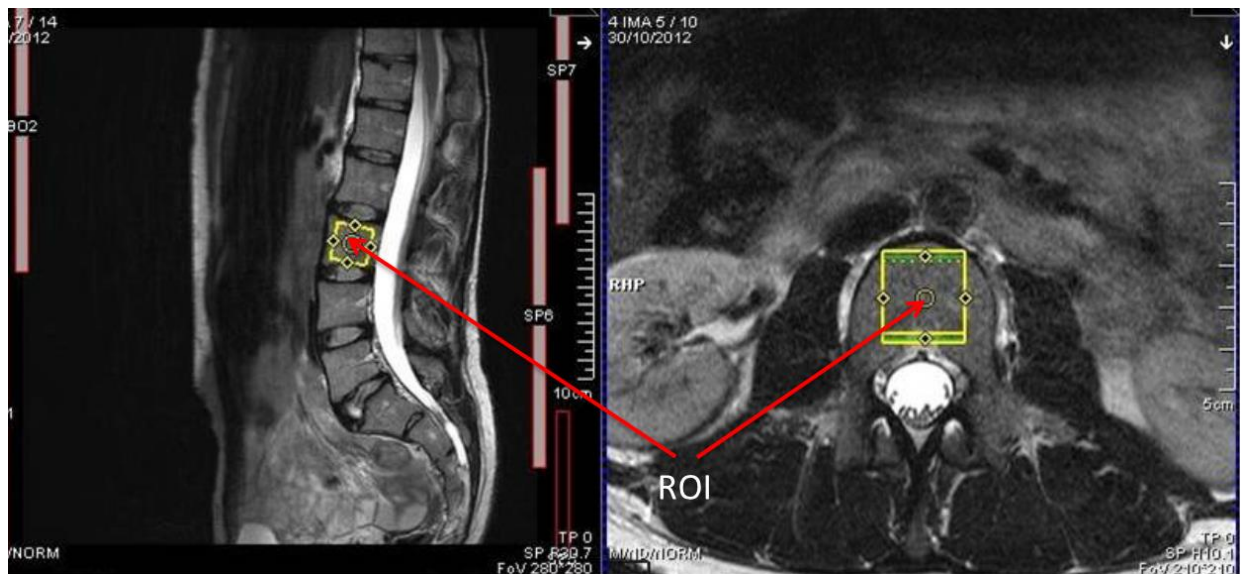


Figure 2.5: Representative MR image of spine showing the scan localisation at L3 vertebrae. Measurements were performed in automatically placed square region of interest (shimming box), yellow marked in the sagittal image and green marked in the axial image.

Table 2.2: Pulse sequence (PRESS) parameters for MRS

Parameters	Used value
TR	2000ms
TE	30ms
no. of averages	80
Scan time	2.48s
Voxel size	20 mm x 20 mm x 20 mm
Bandwidth	1200Hz

2.2.2.3 Analysis

MRS analysis was performed using Siemens Spectroscopy analysis software. The resulting spectrum shows peaks corresponding to water and fat are shown in (Figure 2.6). A best-fit Gaussian model was applied to the acquired spectrum, and the area under the resulting water peak (I_{water}) and lipid peak (I_{fat}) were measured. The percentage fat fraction (FF) was then calculated in the following way.

$$\% FF = \left(\frac{LWR}{LWR + 1} \right) \times 100$$

Equation 2-7. LWR; lipid water ratio.

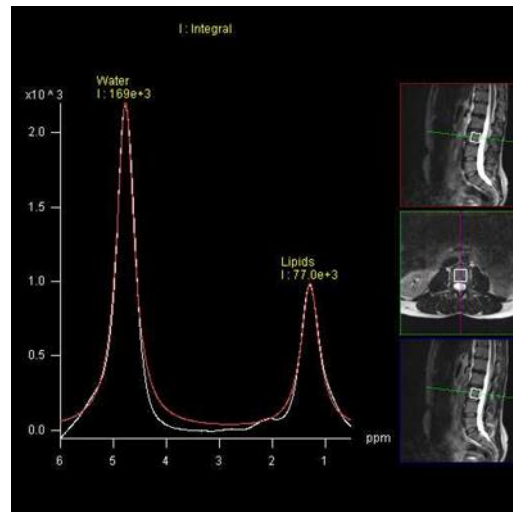


Figure 2.6: The method of frequency domain fitting using Gaussian line shape. The white line illustrates the original spectrum; the red line illustrates the fitting model.

2.2.3 Abdominal Fat Imaging

2.2.3.1 Acquisition

MRI images for abdominal fat quantification were obtained using the method described by Leinhard et al (496). Four element body coils with an 8-element spine coil were used to obtain images covering the abdominal region from the diaphragm to the bottom of the pelvis. A breath-hold sequence (approximately 17.2 Seconds per acquisition) was used to minimize the effects of respiratory motion on the images. To measure the abdominal fat contents, a T1 weighted turbo-spin-echo sequence was used to acquire 5 axial slices at the level of L3, the pulse sequences parameters are shown in (Table 2.3).

Table 2.3: Pulse sequence parameters for abdominal imaging

Parameters	Used value
Resolution	1.2 mm x 1.1mm
Slice thickness	4 mm
Repetition time (TR)	300 ms
Echo time (TE)	11ms
Flip angle	140
Bandwidth	260 Hz/pixel
Matrix size	205 x 320
Field of view	243 x 360 mm
Scan time	17.2 s

2.2.3.2 Analysis

The images were analysed with Slice-O-matic™ (version 4.3, Tomovision, Canada) for semi-automatic measurement of cross-sectional area (CSA), subcutaneous adipose tissue, (SAT), visceral adipose tissue (VAT) and total adipose tissue (TAT). The Morpho Mathematical TAG mode (Mosaic tagging) (Figure 2.7) has been used to create the TAG data. The main advantage of this technique is useful for segmenting tissue images that have a big enough surfaces and a well-defined image intensity gradient (e.g., abdominal adipose tissue). Five MR images at the level of L3 were opened in the software, the third central one was selected to be analysed for all participant.

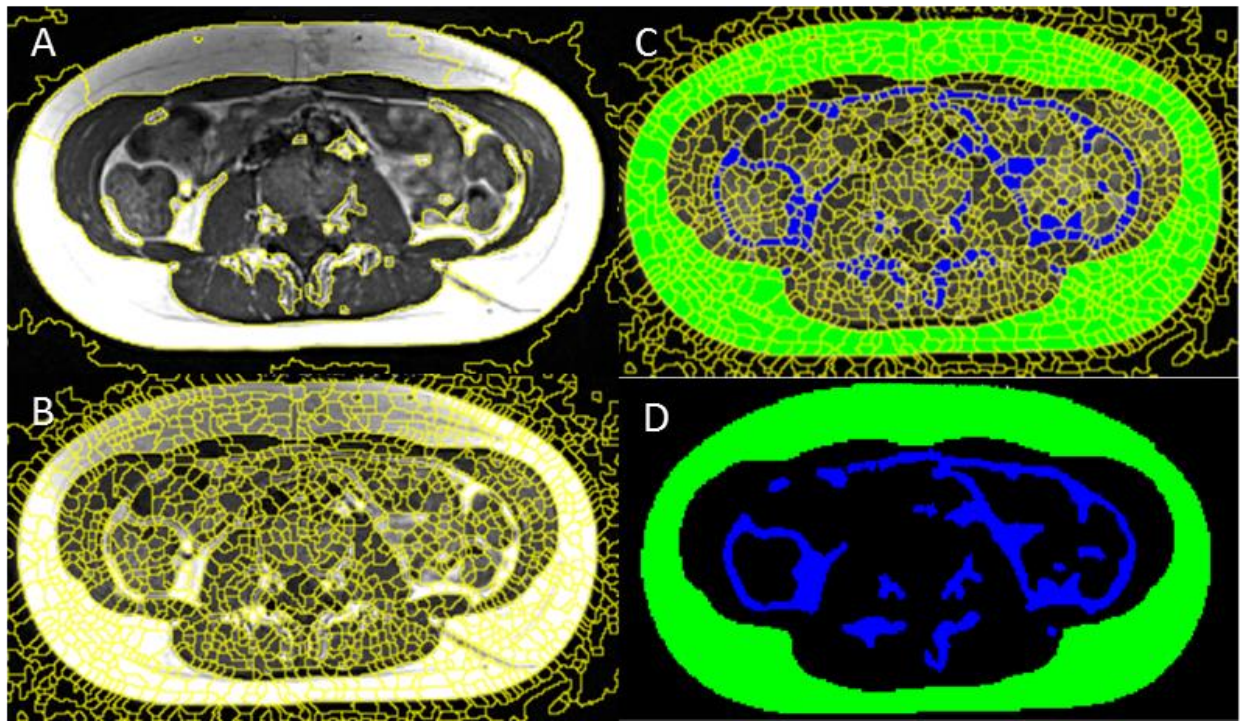


Figure 2.7: Representative MR Image through axial slice of abdomen at L3 vertebrae showing example of Slice-O-matic segmentation to delineate the subcutaneous (Green) and visceral (Blue) adipose tissue depots.

(A) Illustrating mosaic segmentation coarse scale setting for SCAT ;(B) mosaic segmentation fine scale setting for VAT; (C,D) coloured tagged image with morpho lines (C) and without morpho lines (D).

2.4 Dual-Energy X-ray Absorptiometry (DXA)

2.4.1 Principal of DXA

DXA scanning (Lunar Prodigy, GE Medical Systems, Waukesha, Wisconsin, USA) was performed to evaluate the bone and body composition parameters. DXA scanners comprise of mobile X-ray source, a couch for the patient, and a detection system that detects radiation emerging from the bones being examined. On a DXA device, the X-ray source is under the couch and moves together with the detection system, which is located opposite the X-ray source and over the patient's body (379). Principally, DXA is based on the difference in the attenuation properties of dual x-ray beams (high energy and low energy beam) when they pass through soft tissue and bone. As the dual beam passes through the body, the low-energy beam is attenuated more than the high-energy beam in both soft tissue and bone, but the difference is much greater in bone. With the use of a particular computing algorithm, the attenuation values of soft tissues are subtracted, leaving only the attenuation values of bone. By internal phantom calibration the bone attenuation can then be converted to give the measures of bone mineral density (498). The resulting measurements provide estimates of bone mineral content (BMC, measured in grams), bone mineral density (BMD, measured in g/cm^2), and bone area (BA, measured in cm^2). Bone area is the projected area in the coronal plane of the region scanned. The computer software calculates the bone mineral density (BMD, g/cm^2) by dividing BMC by the bone area, since BMD is determined using an area rather than a volume, it is referred to as areal BMD (aBMD) to emphasize that it is not a true volumetric density. Additionally, the dual beam allows for the delineation of soft tissue versus bone, thus in addition to measurement of BMD, DXA can assess body composition (fat mass, lean body mass, and percent body fat), on both total body (TB) and regional basis (379). The DXA also provide two standard deviations (SD) of BMD, which are described as T score and Z score. The T-score is a universally acceptable measure for diagnosis of osteoporosis; it compares the patient's BMD to the optimal peak bone density for the same gender. It is restricted in adult age over 50 and not applicable for children and young people. On other hand, the Z score is applicable for children, premenopausal women and men younger than 50 yrs. A z score is also SD score of BMD based on same age and sex, height and weight. Its measurement of -2.0 or lower is indicative of significantly decreased bone density for chronological age (499).

DXA can measure effectively any skeletal site, but its clinical use has been commonly concentrated on the lumbar spine, hip (femoral neck and total hip), forearm, and total body.

Mistakes in BMD measurement by DXA have been reported, and most of these pitfalls related to the scanner and its software, the positioning of patient and analysis of scans, and various patient-related artefacts (498, 500). A well-trained and experienced DXA technologist is required to avoid most of the errors in acquisition and analysis. Importantly, it is crucial to evaluate precisely patient position and region of interest (ROI) in each measurement before the scanning(501).

2.4.2 Outcomes of DXA

After proper positioning of the participants, DXA of the whole body, femoral neck and lumbar spine (L1-L4) was performed to determine the main study outcomes. The DXA scan took approximately 10-15 min to complete, and all of these scans were acquired by Dr Sheila Shepherd at RHC, Glasgow. The bone area (cm²), BMC (g), mean areal BMD (g/cm²) and BMD-z score of whole body, femoral neck (FN) and lumbar spine were measured. To minimise the size-related effects of DXA a BMD measurements, BMAD at lumbar spine was calculated by estimating the vertebral depth as the square root of the area measured by DXA (Bone area). Then, the vertebral volume is calculated by simply multiplying the height x width(BA) x depth (502). Body composition, including whole body- fat mass WB-FM (kg), WB-FM Z score and android/gynoid (kg) were obtained from the whole body DXA scan.

2.5 Blood analysis

Non-fasting blood samples were collected, centrifuged, and the supernatant stored at -80°C. Sample collection was standardized with collection performed in the afternoon to coincide with the clinic visit. Plasma total osteocalcin (OC) and serum bone-specific alkaline phosphatase (BAP) were analyzed by ELISA to assess bone formation (Immunodiagnostic Systems, Boldon, UK). Plasma undercarboxylated osteocalcin (uOC) was used to assess the inactive form of osteocalcin (Cusabio Life Science, Wuhan, PR China) and plasma C terminal telopeptide of type I collagen (CTX) was measured by ELISA to assess bone resorption (Immunodiagnostic Systems). The intra-assay variation for OC, uOC, BAP, and CTX was 5.3%, 13.2%, 0.8%, and 3.8%, respectively. Plasma leptin, preadipocyte factor-1, pentosidine, IGF-I and its binding proteins, IGFBP3, and the acid labile subunit (ALS) were also determined using ELISA (Mediagnost GmbH, Reutlingen, Germany). Intra-assay variabilities were 6.1%, 0.6%, 4.1%, 0.6%, 4.1%, and

3.4%, respectively. 25-Hydroxy vitamin D (25OHD) concentration was measured by a radioimmunoassay (Immunodiagnostic Systems).

2.6 Statistical Analysis

Statistical analyses were performed using Minitab 17 (Minitab Inc, PA, and USA) and SPSS 19 (IBM, New York, USA). Before performing any analysis, the data were checked for normality using an Anderson- Darling test. More information about the statistical tests used for data analysis is discussed in the relevant chapters.

Chapter 3

Deficits in Trabecular Bone Microarchitecture in Young Women With Type 1 Diabetes Mellitus

3.1 Abstract

Background: The pathophysiological mechanism of increased fractures in young adults with type 1 diabetes mellitus (T1DM) is unclear.

Aim: We conducted a case-control study of trabecular bone microarchitecture and vertebral marrow adiposity in young women with T1DM.

Subjects and methods: Thirty women with T1DM with a median age (range) age of 22.0 years (16.9, 36.1) attending one outpatient clinic with a median age at diagnosis of 9.7 years (0.46, 14.8) were compared with 28 age-matched healthy women who acted as controls. Measurements included MRI-based assessment of proximal tibial bone volume/total volume (appBV/TV), trabecular separation (appTb.Sp), vertebral bone marrow adiposity (BMA), and abdominal adipose tissue and biochemical markers of GH/IGF-1 axis (IGF-1, IGFBP3, ALS) and bone turnover.

Results: Median appBV/TV in cases and controls was 0.3 (0.22, 0.37) and 0.33 (0.26, 0.4), respectively ($p=0.018$) and median appTb.Sp in T1DM was 2.59 (2.24, 3.38) and 2.32 (2.03, 2.97), respectively ($p=0.012$). The median appBV/TV was 0.28 (0.22, 0.33) in those cases with retinopathy ($n=15$) compared with 0.33 (0.25, 0.37) in those without retinopathy ($p=0.02$). Although median visceral adipose tissue in cases was higher than in controls at 5733 mm³ (2030, 11,144) and 3460 mm³ (1808, 6832), respectively ($p=0.012$), there was no difference in median BMA, which was 31.1% (9.9, 59.9) and 26.3% (8.5, 49.8) in cases and controls, respectively ($p=0.2$). Serum IGF-1 and ALS were also lower in cases, and the latter showed an inverse association to appTbSp ($r=-0.30$, $p=0.04$).

Conclusion: Detailed MRI studies in young women with childhood-onset T1DM have shown clear deficits in trabecular microarchitecture of the tibia. Underlying pathophysiological mechanisms may include a microvasculopathy.

3.2 Introduction

The risk of hip fractures in those with type 1 diabetes mellitus (T1DM) is reported to be 7 to 12 times greater (336, 340) and this increased risk is also evident in young adults (221). The process of differentiation of mesenchymal stem cells into either adipocytes or osteoblasts is regulated by a number of growth factors including insulin, oxygen tension, and blood flow within the bone marrow (503, 504). T1DM is also associated with abnormalities of the growth hormone (GH)/insulin-like growth factor type 1 (IGF-1) axis with biochemical evidence of GH resistance (505). Growth hormone (GH) and IGF-1 also are important regulators of bone homeostasis and important for the maintenance of bone mass (506) and may also influence body composition and bone marrow adiposity (491). Mouse models of T1DM exhibit increased bone marrow adiposity (BMA), increased adipocyte markers, and increased numbers of lipid-dense adipocytes in the bone marrow (507). Childhood and adolescence are critical periods for skeletal development (508), and it is possible that those affected by T1DM at these ages may be especially susceptible. On dual-energy X-ray absorptiometry (DXA), adults with T1DM do show a reduction in bone mineral density (BMD) Z-score, reported in a meta-analysis at -0.22 at the lumbar spine and -0.37 at the hip (11) but their fracture risk is much higher (161, 221, 336, 340) than expected for this modest reduction in BMD. Recent advances in magnetic resonance (MR) imaging have led to the generation of high-resolution 3D images of bone structure that correlate with other techniques such as computed tomography (440, 509). In addition, MR can quantify the amount of intra-abdominal fat, and MR spectroscopy can also estimate the fat that is present within the bone marrow (457). There is, therefore, the potential to combine these MR-based techniques to obtain objective data on bone microarchitecture and fat content and study these in a condition such as T1DM.

With the increased reports of an association between marrow adiposity and bone health (510), the current study was designed to improve the understanding of the bone pathology in adults with childhood-onset T1DM by using high-resolution MRI and biochemical markers of GH action and bone turnover. To reduce the confounding effect of sex hormones, this study targeted young women with T1DM and compared them with a group of age-matched healthy women.

3.3 Material and method

3.3.1 Subjects

Figure 3.1 shows the pathway outlining participant recruitment and enrolment in this study. Between July 2012 and July 2013, 61 eligible women between the ages of 20 and 30 years and who were diagnosed before the age of 16 years were approached at one hospital clinic. From this group, 30 volunteered to participate. In addition, 28 age matched healthy control women working at the local university and hospital were also recruited. Exclusion criteria included the presence of metallic implants and pacemakers, active or planned pregnancy or lactation, kidney disease, chronic use of drugs that are known to affect bone health, and other chronic diseases that are known to be associated with an increased risk of fractures. Information on personal health and lifestyle habits, including cigarette smoking, alcohol consumption, current medication, use of vitamins or calcium, age at menarche, use of oral contraceptives, hours of weight-bearing physical activity per week, history of fractures, and a family history of early osteoporosis was also collected. Information on age at diagnosis, disease duration, insulin therapy, and presence of microvascular complications was obtained from the case records. A glycosylated hemoglobin (HbA1c) measurement within a 2-week period of the scan visit was used as current HbA1c. The study protocol was approved by the national research ethics service, and all participants provided written informed consent.

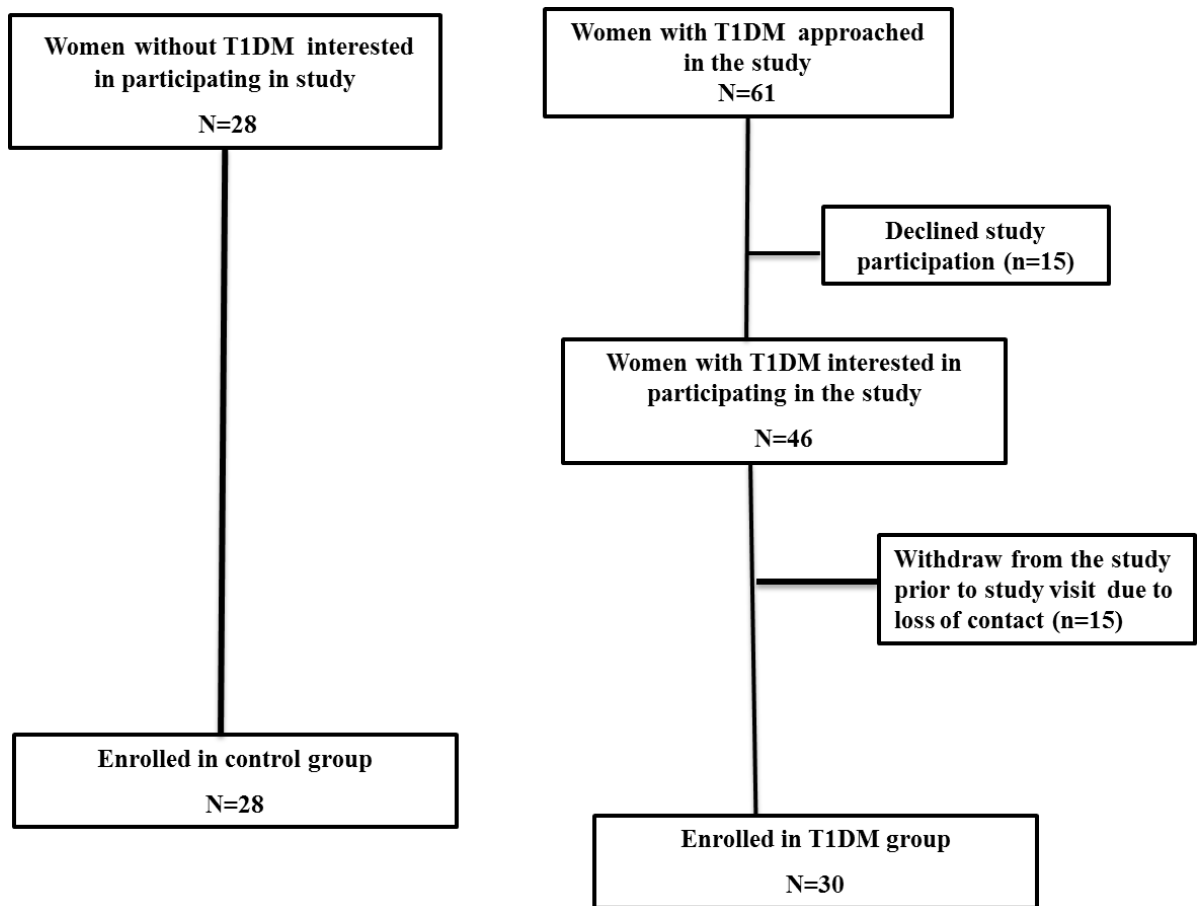


Figure 3.1: Pathway outlining participant recruitment and enrolment in the study.

3.3.2 Biochemical markers of bone metabolism, adiposity, and GH/IGF-1 axis

In 25 cases and 24 control participants, non-fasting blood samples were collected and analysed as described in chapter 2. We measured bone formation markers (plasma total osteocalcin (OC), serum bone-specific alkaline phosphatase (BAP), plasma undercarboxylated osteocalcin (uOC)), bone resorption marker (plasma C terminal telopeptide of type I collagen (CTX)), adiposity markers (Plasma leptin, Preadipocyte factor-1), growth hormone axis (IGF-I, IGF-BP3, the acid labile subunit (ALS)), pentosidine, and other regulator markers of bone turnover (PTH, 25-Hydroxy vitamin D (25OHD)).

3.3.3 Micro-MRI

30 slice images were acquired and analysed as described in Chapter 2. In 29 of 30 cases and in 27 of 28 control participants, the images were of a sufficiently good quality to be analysed. The analysis for each subject was repeated four times and averaged. Phantom validation of the used software has been performed previously by our diabetic endocrine

research group (DERG) (434). In addition, an assessment of repeatability was performed by two operators who independently analysed ten volunteer datasets four times each. Intra-operator repeatability was evaluated using coefficients of variation (CoV), and inter-operator repeatability was evaluated using Levene's test to compare the equality of variance between the results obtained by the two operators, and a Mann-Whitney test to compare the obtained values for each parameter. Five of the volunteers were scanned on two separate occasions, and the results were compared using a paired t-test.

3.3.4 MRS

MRS data were available in all 30 cases and 28 controls. Image acquisition and analysed are as described in chapter 2. Analysis was performed following fitting of the spectrum in the time domain using a nonlinear least-squares algorithm, AMARES (511), in the Java-based magnetic resonance user interface (jMRUI) software package (512). As for the micro-MRI data, an assessment of intra and inter-operator repeatability was performed by two operators who independently analysed ten datasets four times each. Five volunteers were also scanned on two separate occasions to assess the inter-scan repeatability.

3.3.5 MRI of abdominal fat

Of the participants who had MRS scans, in 24 cases and 19 controls, approval was also obtained to assess abdominal fat during the same scanning session. Five axial images at L3 level were acquired and analysed as described in chapter 2.

3.3.6 Calculation of sample size and statistical analysis

The primary hypothesis in the study was that cases with T1DM would have a lower appBV/TV and appTbN and a higher appTbSp compared with controls. Based on recent studies from our group (434) the estimated coefficient of variation (CV) of the microMRI measurements was less than 5%. To show a 10% difference between cases and controls with a significant difference at $p < 0.05$ with a power of 0.8, at least 16 cases and 16 controls were required for the above micro-MRI parameters. Data analysis was performed using Minitab 17 (Minitab Inc, PA, and USA). All data were described as medians and ranges; comparison between the cases and controls was performed, initially by the Mann-Whitney U test for continuous variables and by the chi-square test for categorical variables and then subsequently adjusted for multiple comparisons using false discovery rates (FDR)

(513). Univariate analysis between continuous variables was performed using the Pearson correlation coefficient.

3.4 Results

3.4.1 Clinical characteristics

There were no significant demographic or anthropometric differences between the cases and controls (Table 3.1). Notably, the median body mass index (BMI) in the cases and controls was 24.8 kg/m² (18.2, 31.2) and 22.9 kg/m² (18.3, 33.9), respectively ($p=0.1$) with similar amounts of physical activity reported in the cases and controls. Of the 30 cases and 28 controls, 9 (30%) and 3 (11%) reported a history of traumatic fractures ($p= 0.07$). In 2 cases, the fractures had occurred before the onset of diabetes, and in the other 7 cases, the duration of diabetes at the time of the fracture ranged between 2.5 years and 16 years. The median duration of T1DM was 12.8 years (7.9, 34.2) with a median age at diagnosis of 9.9 years (0.5, 15.0). Of the 30 cases, 7 were on twice daily insulin injections, 6 were on three-daily injections, and 17 were on four-daily injections. The median total daily insulin dose for body weight was 0.94 IU/kg/d (0.43, 1.52) and the median current HbA1C was 9.8% (5, 16), equivalent to 84 mmol/mol (31, 151). Of the 30 cases, 15 (50%) had retinopathy of which 12 had background retinopathy alone, 2 (7%) were being treated for hypertension, 1 (3%) had neuropathy and gastroparesis, and none had microalbuminuria. One of the cases had stable Crohn's disease requiring sulfasalazine therapy only for 2 years before the study and 2 cases were on a stable dose of thyroxine for acquired hypothyroidism, one of 3 years' duration and another of 5 years' duration.

Table 3.1: Clinical and biochemical details of study participants.

	T1DM	Controls	
N	30	28	p
Age (yrs)	22.0 (16.9, 36.1)	21.8 (18.6, 37.5)	0.7
BMI	24.8 (18.2, 31.2)	22.9 (18.3, 33.9)	0.1
Cigarette smoker (n)	4	0	0.05
Regular alcohol consumption (n)	25	27	0.9
Ca, VitD, Multivit supplements (n)	4	6	0.8
Age at menarche (yrs)	12 (10, 17.5)	13 (11, 15)	0.6
Previous pregnancy (n)	3	1	0.3
Oral contraceptive use (n)	21	22	0.9
Physical activity (hrs/wk)	4 (0, 10)	4 (0, 10)	0.9
PTH (pmol/l)	3.4 (1.1, 9)	4.2 (1.4, 12.5)	0.3
25OH D (nmol/l)	33 (19, 65)	45.5 (25, 84)	0.02
Osteocalcin (µg/l)	13.4 (3.6, 20.8)	14.3 (6.6, 40.5)	0.2
uOC (ng/mL)	1.8 (0.5, 13.9)	3.3 (0.5, 25.3)	0.18
Bone ALP (U/l)	16.2 (10.5, 44.3)	17.2 (4.6, 28.8)	0.9
CTX (µg/l)	0.15 (0.03, 0.39)	0.20 (0.05, 0.49)	0.04
IGF-1 (µg/l)	135.2 (66.5, 83.1)	182.4 (83.1, 293.4)	0.002
IGFBP-3 (µg/l)	2208 (1794, 3677)	2347 (1991, 3538)	0.17
ALS (mU/ml)	2064 (1005, 3009)	2549 (1929, 3682)	<0.0001
Leptin (µg/l)	12.4 (1.3, 105)	14.3 (2.6, 43.3)	0.96
Pref-1 (ng/ml)	0.19655(0.1105,0.3459)	0.22091(0.1128,0.3517)	0.3
Pentosidine (pmol/ml)	1007 (177, 2998)	829 (108,5923)	0.5

All continuous variables are described as median and range. PTH, Parathyroid hormone; OC, osteocalcin; 25OHD, 25-hydroxyvitamin D; ALP, Alkaline phosphatase; CTX, crosslinked C-terminal telopeptides of type I collagen; IGF-1, insulin-like growth factor 1; IGFBP-3, insulin-like growth factor binding protein 3; ALS, acid labile subunit; Pref-1, preadipocyte factor 1. Significance is assigned at p<0.05.

3.4.2 Biochemical markers of bone metabolism, adiposity, and GH/IGF-1 axis

Amongst the markers of bone metabolism, plasma 25OHD and CTX were significantly lower in cases compared with controls (Table 3.1). However, serum parathyroid hormone (PTH) and markers of bone formation were similar in both groups (Table 3.1). Amongst the markers of the GH/IGF-1 axis, plasma IGF-1 and ALS were significantly lower in the cases compared with controls, whereas IGFBP3 was similar in both groups (Table 3.1) (Figure 3.2). Serum pentosidine (1007 pmol/ml vs. 829 pmol/ml) was not different between both groups. Plasma leptin and Pref-1 were similar in the two groups and, as expected, Leptin showed a positive association with BMI ($r=0.33$; $p=0.02$). There was no association between age of diagnosis disease duration, HbA1c and the presence of retinopathy with the markers of bone metabolism, GH/IGF-1 axis, adiposity markers, or pentosidine.

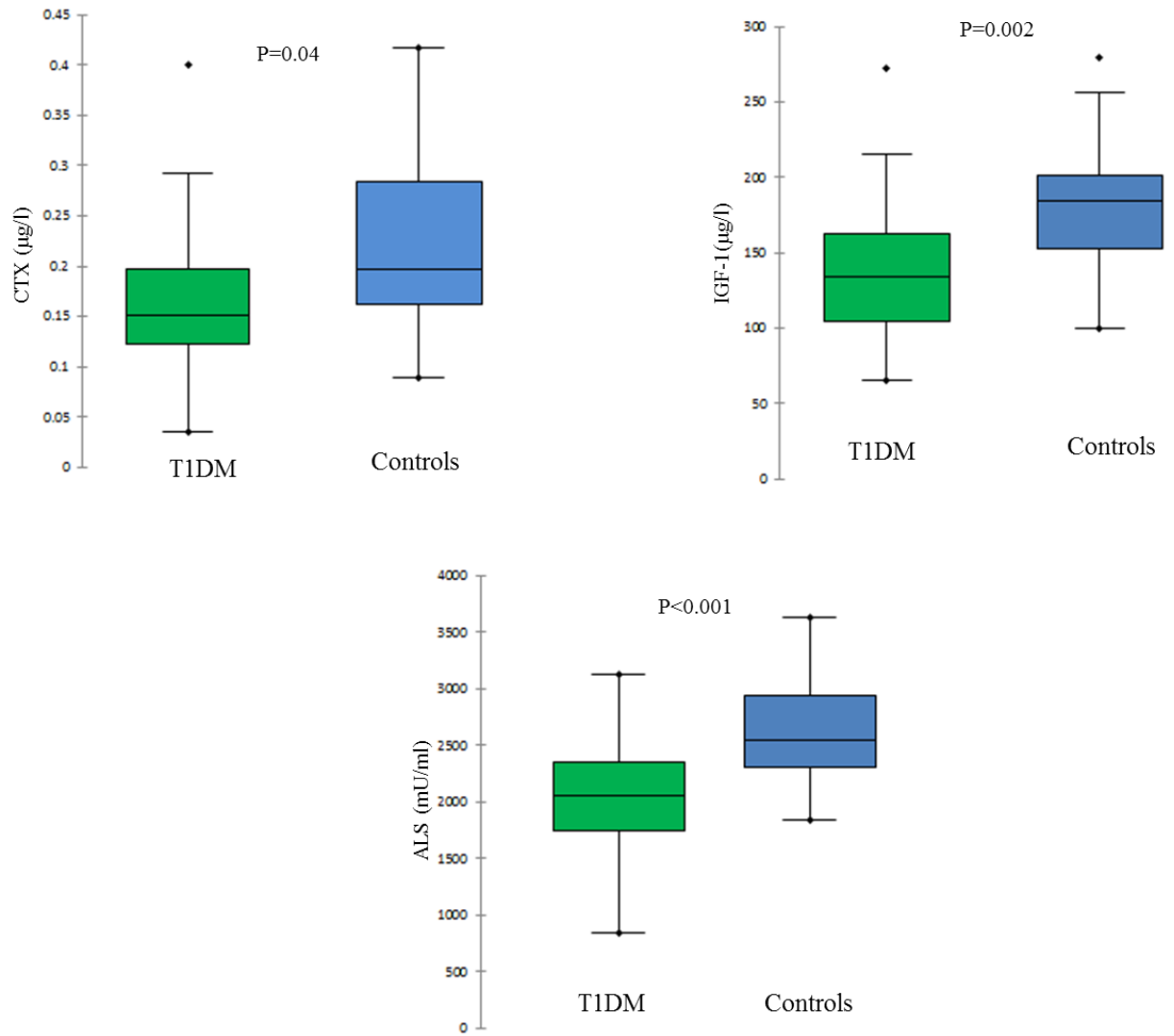


Figure 3.2: Box plot of serum CTX, IGF-1 and ALS in women with T1DM (Green box) and controls (Blue box).

CTX, crosslinked C-terminal telopeptides of type I collagen; IGF-1, insulin-like growth factor 1; ALS, acid labile subunit. The figure depicts the median and range for each plot, and p-value has been added.

3.4.3 MRI of abdominal fat

Despite no significant differences in the BMI and plasma leptin between cases and controls, abdominal adiposity including CSA, VAT, and TAT was significantly higher in cases compared with controls (Table 3.2) (Figure 3.3). However, SCAT was less markedly higher in cases, and the difference did not reach statistical significance. Serum leptin and pref-1 did not show an association with any of the MRI based markers of abdominal obesity. In addition, there was no association between adiposity with markers of control, markers of bone metabolism, GH/IGF-1 axis, leptin or pentosidine.

Table 3.2: MRI-based measures of abdominal adiposity, bone microarchitecture and vertebral bone marrow adiposity at L3

	T1DM	Controls	P*
N	30	28	
CSA (mm ²)	47,878 (30,134, 78,651)	39,918 (30,232, 69,789)	0.03
SCAT (mm ³)	21,583 (3,719, 42877)	15,582 (7,454, 40,807)	0.068
VAT (mm ³)	5,733 (2,030, 11,144)	3,460 (1,808, 6,832)	0.012
TAT (mm ³)	27,230 (6,584, 54,021)	19,130 (10,046, 47,639)	0.03
AppBV/TV	0.3 (0.22, 0.37)	0.33 (0.26, 0.4)	0.018
AppTb.N(mm-1)	0.26 (0.2, 0.3)	0.29 (0.23, 0.3)	0.012
AppTb.Sp(mm)	2.59 (2.24, 3.38)	2.32 (2.03, 2.97)	0.012
AppTbTh(mm)	1.14 (0.86, 1.49)	1.15 (0.96, 1.39)	0.3
L3 fat fraction (%)	25.4 (9.9, 72.8)	19.7 (8.5, 41.9)	0.2

All data are described as median and range. CSA- cross-sectional area of adipose tissue; SCAT – subcutaneous adipose tissue; VAT- visceral adipose tissue; TAT – total adipose tissue; AppBV/TV – apparent bone volume/total volume; AppTb.N – apparent trabecular number; AppTbSp – apparent trabecular separation; AppTbTh – apparent trabecular thickness. P-values have been adjusted for multiple comparisons using False Discovery Rates; significance has been assigned at adjusted p<0.05.

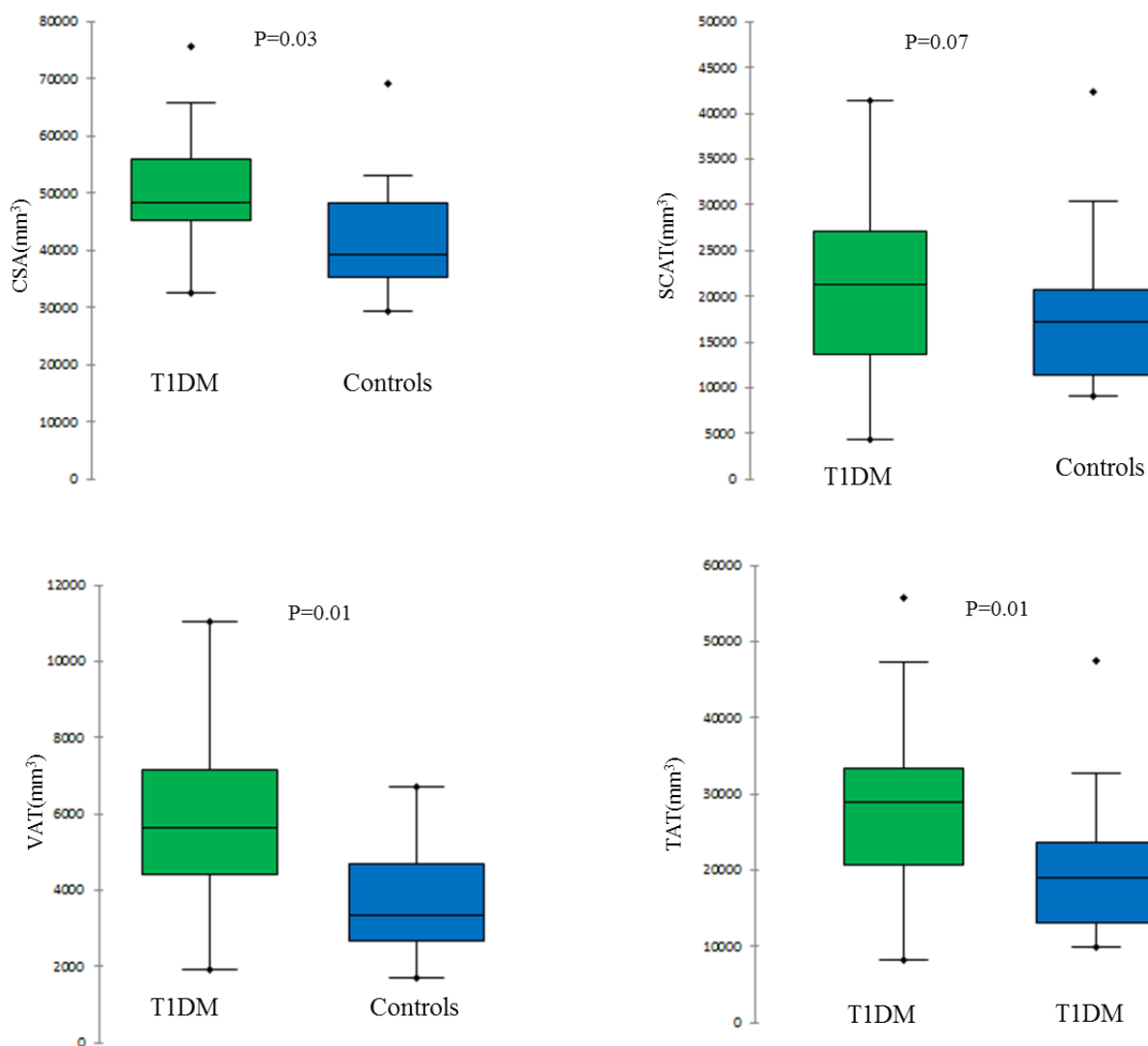


Figure 3.3: Box plot of MRI-measured abdominal adiposity parameters in women with T1DM (Green box) and controls (Blue box).

CSA- cross-sectional area of adipose tissue; SCAT, subcutaneous adipose tissue; VAT, visceral adipose tissue; TAT, total adipose tissue.

3.4.4 Bone microarchitecture by micro-MRI

Intra-operator repeatability was high, with an average CoV of 2.79 % for appBV/TV, 2.81 % for appTbTh, 1.36% for appTbN and 1.76% for appTbSp. Inter-operator repeatability was also high, with no statistically significant differences observed in the variance of the results obtained by the two operators, with the average CoV of 3.32 % for appBV/TV, 3.75 % for appTbTh, 2.02 % for appTbN and 2.58 % for appTbSp. Inter-scan repeatability for the same patient was also high with an average CoV of 3.4% for appBV/TV, 2.3% for appTbTh, 1.5% for appTbN and 2.8% for appTbSp. Comparison of bone microarchitecture variables revealed that appBV/TV and appTbN were significantly lower and appTbSp significantly higher in cases compared with controls (Table 3.2) (Figure 3.4). AppBV/TV

and appTbN did not show any association with any biochemical markers or MRI-based markers of abdominal obesity. However, appTbSp showed a significant inverse association to serum ALS ($r = -0.30$, $p = 0.04$) and OC ($r = 0.38$, $p = 0.009$) (Figure 3.5). This inverse association was not observed between appTbSp and uOC. An inverse association was also suggested between appTbSp and serum IGF-1, but this did not reach statistical significance ($r = -0.27$, $p = 0.06$). In the T1DM cases, there was no association of appBV/TV, appTbN, or appTbSp with HbA1c or daily insulin dose corrected for weight. However, there was a clear difference in median appBV/TV between those cases who had retinopathy and those who did not have retinopathy. The median appBV/TV was 0.285 (0.22, 0.33) in those cases with retinopathy compared with 0.33 (0.25, 0.37) in those cases without retinopathy ($p = 0.02$) (Figure 3.6). The HbA1c was 9.5% (5, 16) and 9.2% (5.5, 13) in the cases with and without retinopathy (NS). Additionally, appBV/TV and appTbSp showed significant correlation with age of the patients and disease duration ($p < 0.05$) (Figure 3.7).

Furthermore, when we stratified the cases into groups based on age of diagnosis <5yrs. of age, 5-10 yrs. of age and >10 yrs. of age, T1DM women diagnosed ≤ 5 yrs ($n = 5$) of age have trend toward lower appBV/TV than those with later age of diagnosis (0.29, 0.33, 0.30), respectively ($p = 0.08$) (Figure 3.8). When appBV/TV and appTbSp were entered as a dependent variable and age, disease duration, age of diagnosis, HbA1c, BMI and related microvascular complications (retinopathy) as independent variables in regression model, these correlations became insignificant. However, retinopathy was the only significant predictor of reduced bone volume ($r^2 = 44.77\%$, $p = 0.04$).

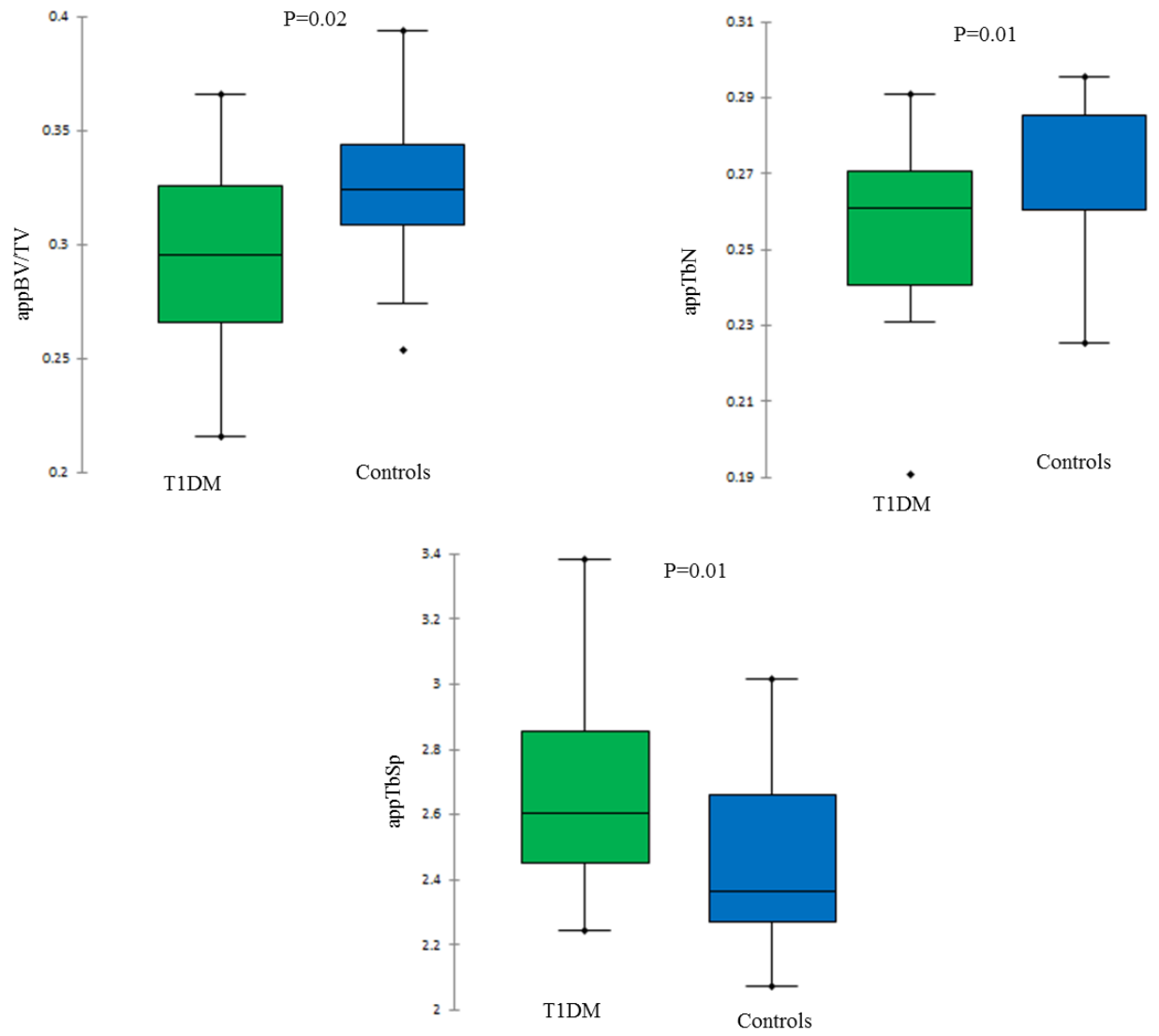


Figure 3.4: Boxplot of MRI-measured trabecular bone parameters in women with T1DM (Green box) and controls (Blue box).

AppBV/TV, apparent bone volume/total volume; AppTb.N, apparent trabecular number; AppTbSp, apparent trabecular separation; AppTbTh, apparent trabecular thickness

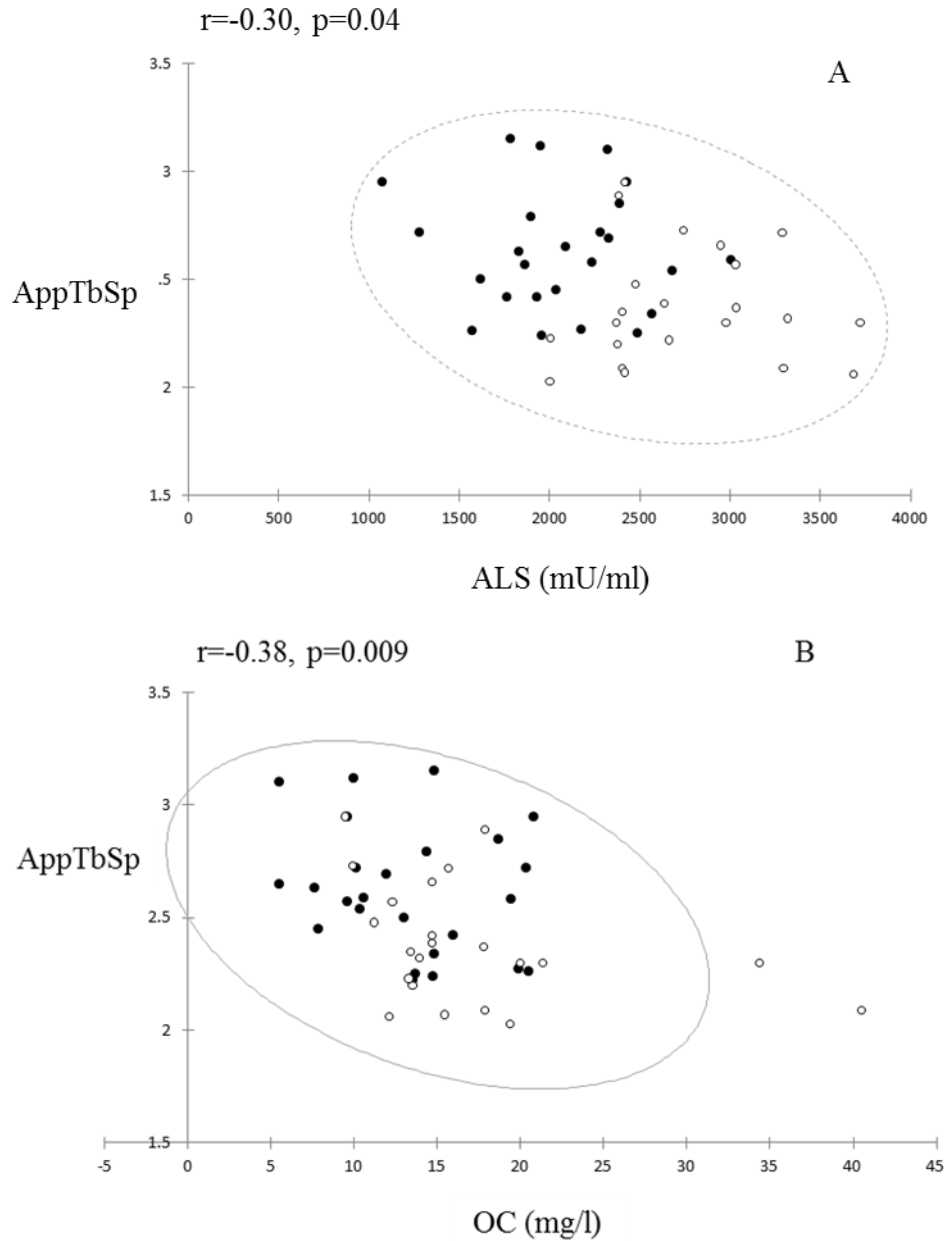


Figure 3.5: The relationship between apparent trabecular separation (appTbSp) as assessed by MRI and serum acid labile subunit (ALS) (A) and serum osteocalcin (OC) (B) in women with T1DM (filled circles) and controls (open circles).

A Gaussian ellipse of the data has been added to each plot, together with the correlation (r) and its p value (p). An inverse association between appTbSp and ALS and OC was observed.

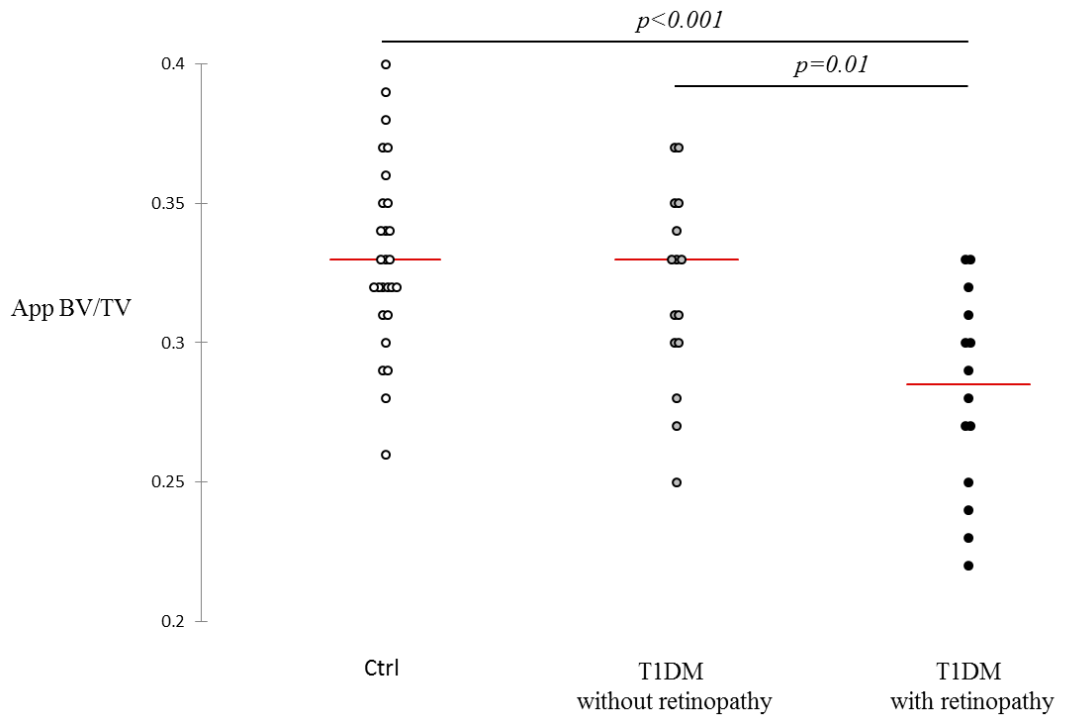


Figure 3.6: Apparent bone volume/total volume (appBV/TV) in women with T1DM with and without retinopathy and compared with control women

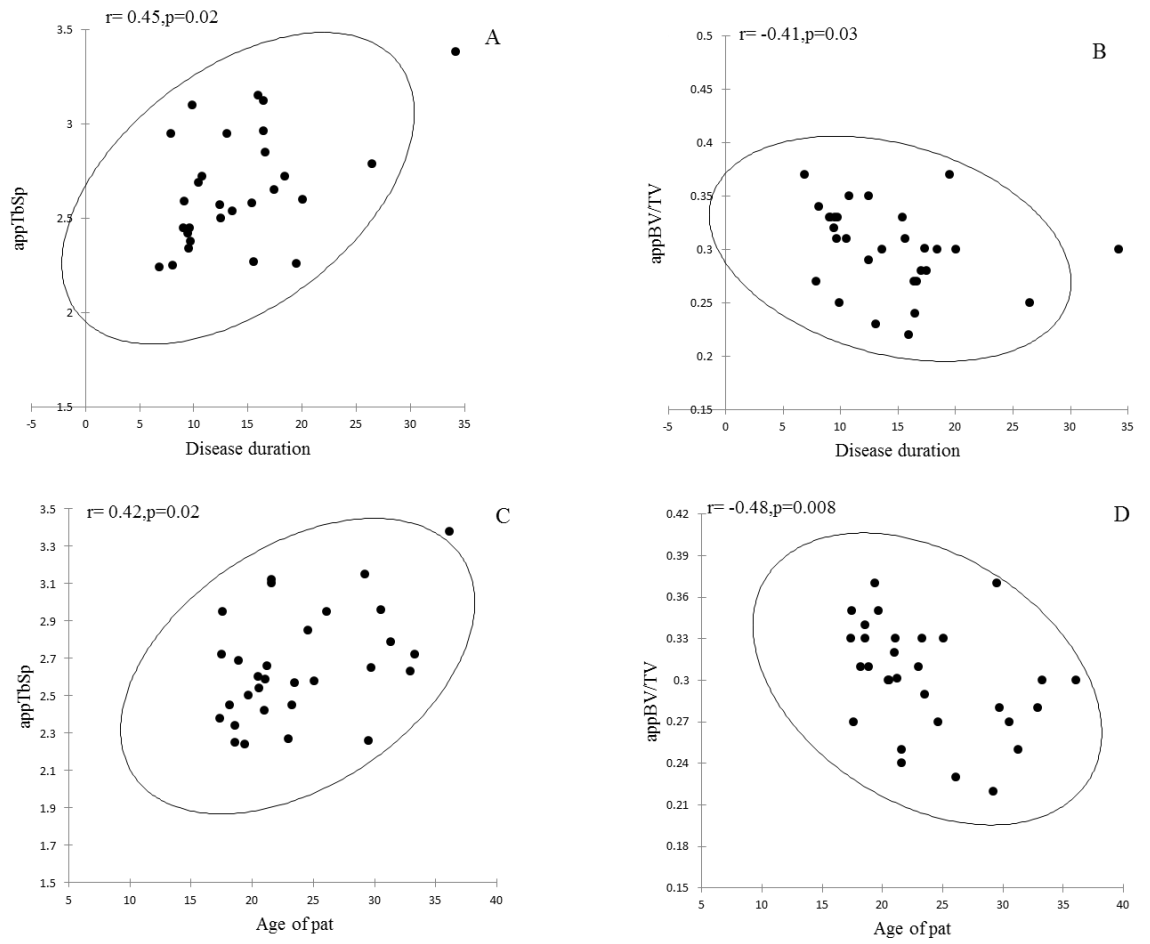


Figure 3.7: Unadjusted correlation of apparent trabecular separation (appTbSp) and appBV/TV with disease duration (A, B, respectively) and age of the patients (C, D, respectively) in women with T1DM.

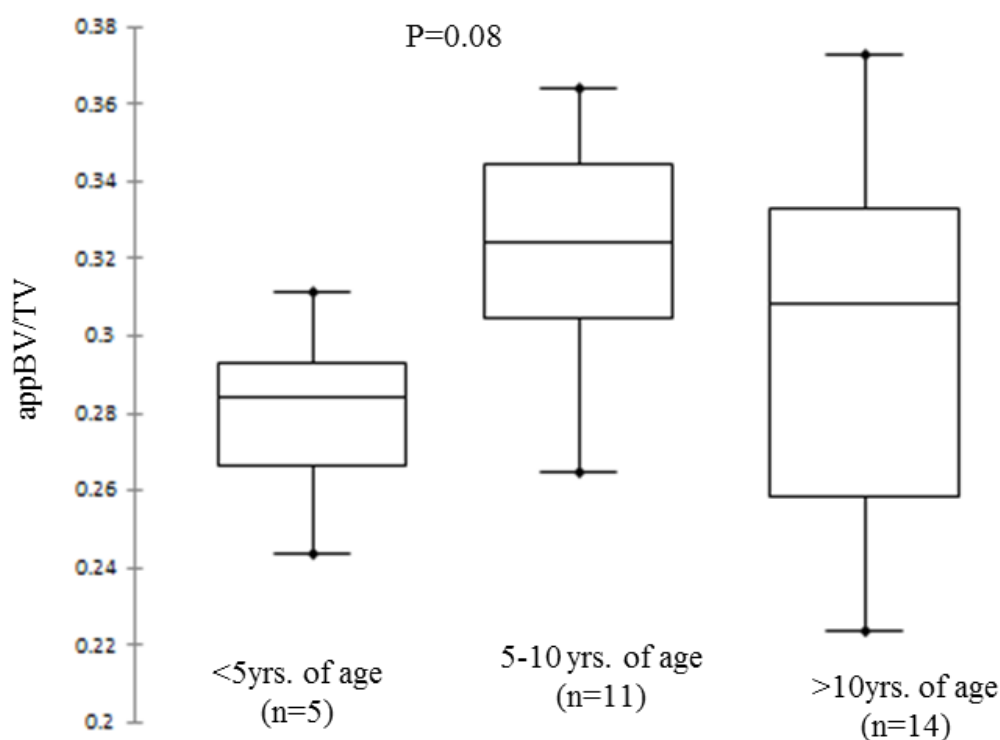


Figure 3.8: App BV/TV in relation to age of diagnosis. T1DM women with earlier age of diagnosis showed trend toward lower bone volume compared with women with later age of diagnosis ($p=0.08$).

3.4.5 Bone marrow adiposity

Intra-operator repeatability was high, with an average CoV of 2.5%. Inter-operator repeatability was also found to be high, with no statistically significant differences observed in the variance of the results obtained by the two operators. Additionally, No statistically significant inter-scan differences were observed. Median vertebral BMA, expressed as percentage fat fraction (%FF), was higher in cases than controls, but this did not reach statistical significant difference (Table 3.2). Vertebral BMA did not show association with biochemical markers of bone turnover, leptin, pref-1 or pentosidine. However, there was trend toward an inverse association of FF% with (OC) ($r=-0.20$, $p=0.2$) and ALS ($r=-0.25$, $p=0.08$) (Figure 3.9). Vertebral BMA showed significant a positive independent association with VAT ($r=0.34$, $p=0.03$) (Figure 3.10), which, as stated earlier, was higher in cases compared with controls. There was no association between vertebral BMA and MRI measured trabecular bone parameters. Median BMA was 30.5% (9.9, 59.9) in those cases with retinopathy compared with 31.6% (11.3, 50.1) in those cases without retinopathy ($p=0.97$). In T1DM, vertebral BMA showed significant positive association with mean current HbA1c ($r=0.45$, $P=0.02$) (Figure 3.11). Additionally, in the T1DM group, with HbA1c of $>7\%$ ($n=20$) showed significantly higher median vertebral BMA than diabetic subjects with HbA1c levels $\leq 7\%$ ($n=7$) ($p=0.02$)

(Figure 3.12). On the other hand, in T1DM, vertebral BMA did not show association with age of diagnosis or disease duration.

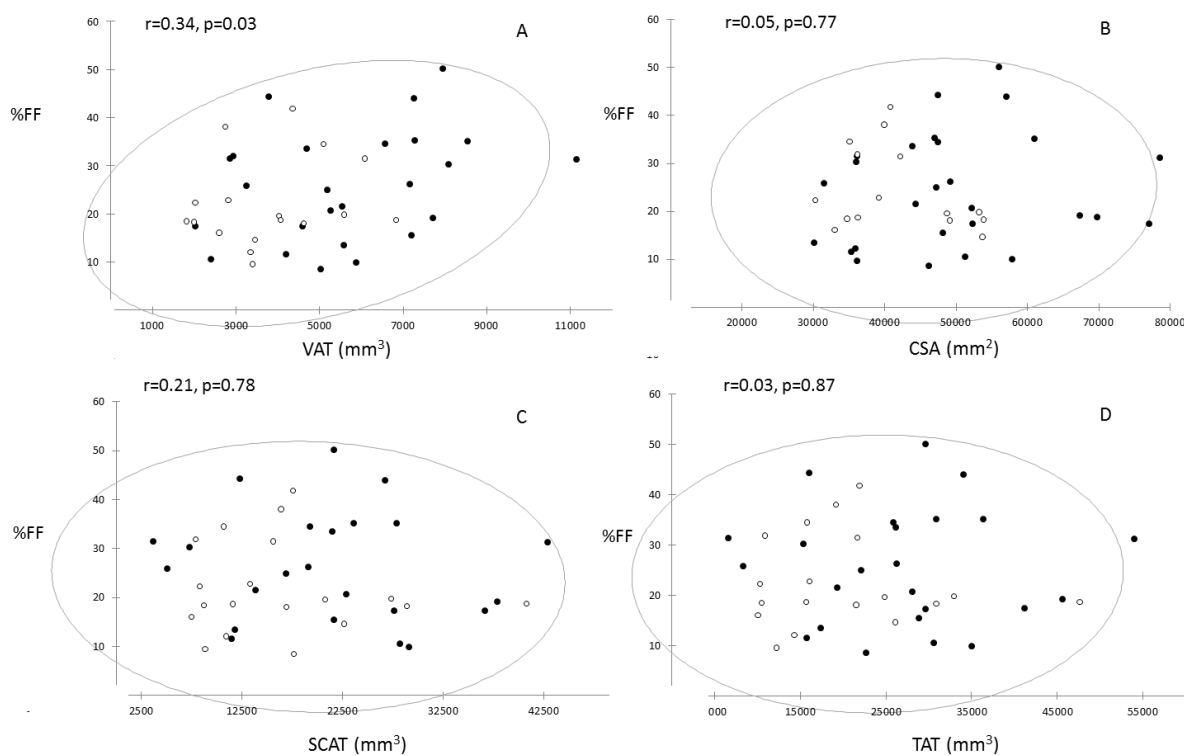


Figure 3.9 The relationship between vertebral bone marrow adiposity (FF%) as assessed by MRS and cross sectional area (CSA) (A), subcutaneous adipose tissue (SCAT) (B), visceral adipose tissue (VAT) (C) and total adipose tissue (TAT) (D) in women with T1DM (filled circles) and controls (open circles).

Positive significant association between FF% and VAT was observed.

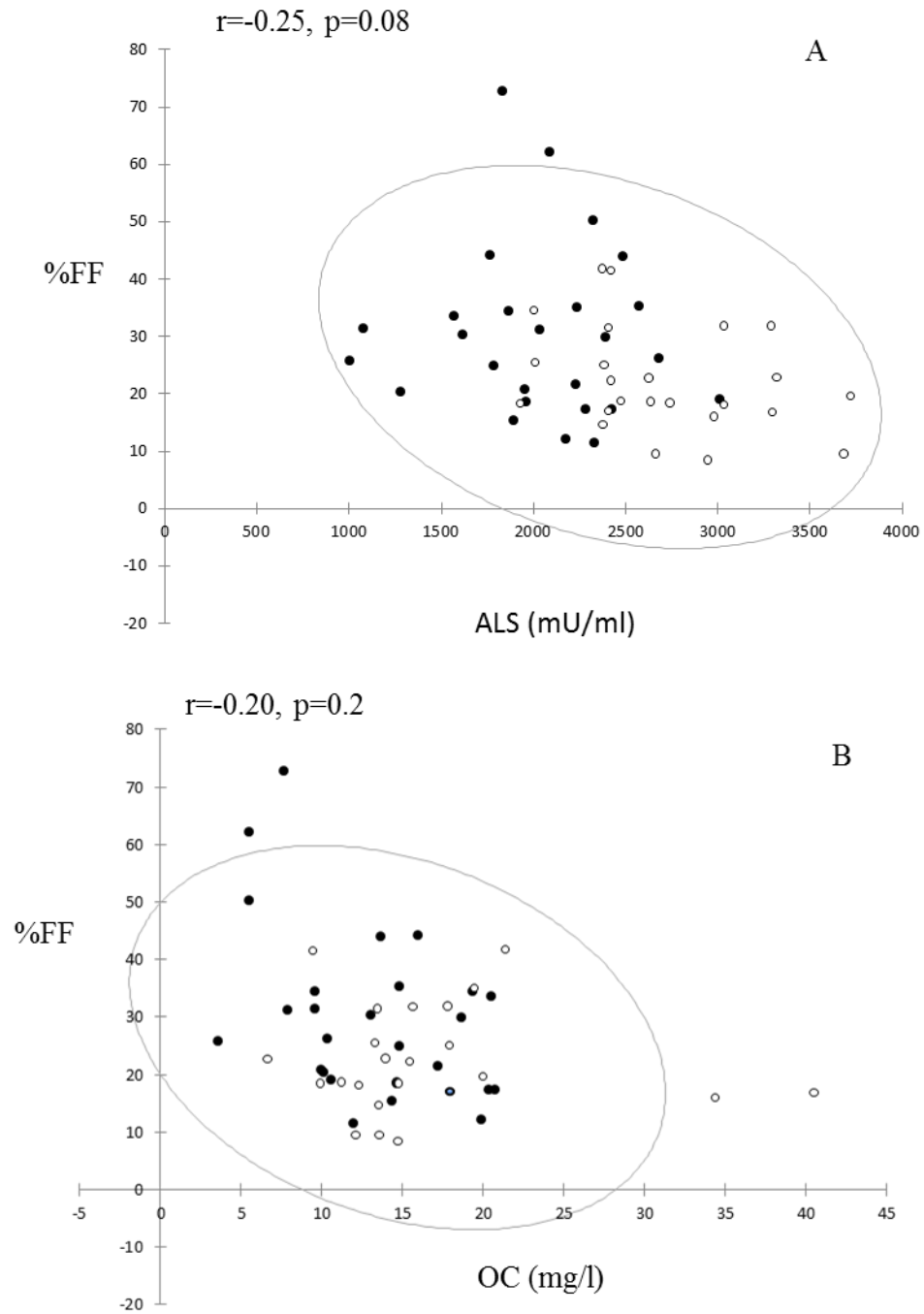


Figure 3.10: The relationship between vertebral bone marrow adiposity (FF%) as assessed by MRS and serum acid labile subunit (ALS) (A) and serum osteocalcin (OC) (B) in women with T1DM (filled circles) and controls (open circles).

A Gaussian ellipse of the data has been added to each plot, together with the correlation (r) and its p value (p). Trend toward an inverse association between FF% and ALS and OC was observed.

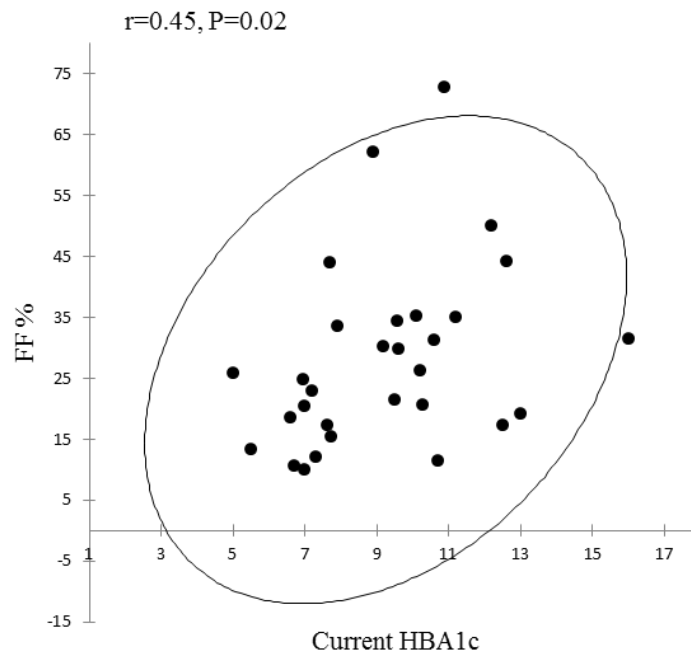


Figure 3.11: The relationship between vertebral BMA (FF %) and current HBA1c. Positive significant association was observed.

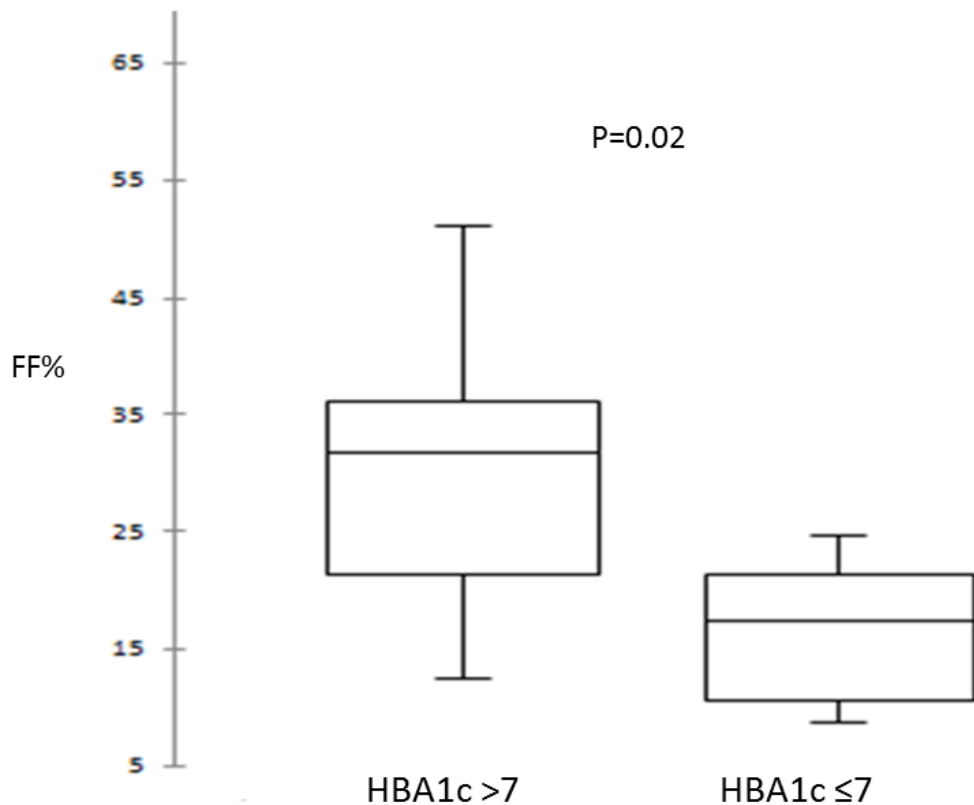


Figure 3.12 VBMA in relation to current HBA1c of >7% or ≤7%

Diabetic subjects with HbA1c levels >7% (n= 20) showed significantly ($P < 0.02$) higher mean vertebral bone marrow fat content than diabetic subjects with HbA1c levels ≤7% (n =7). The boxplot represents median of the vertebral bone marrow adiposity.

3.5 Discussion

The current study was primarily aimed at using MRI to compare the trabecular microarchitecture in young women with childhood-onset T1DM with that in healthy age-matched women. This is the first published clinical study to clearly show that this is altered in the former with reduced bone volume and trabecular number and increased trabecular separation. In addition, the study has also provided some insights into the underlying mechanisms that may lead to abnormality of skeletal development in adults with T1DM. In keeping with other reports of a higher prevalence of vitamin D deficiency in young people with T1DM, the women who participated in this study had lower vitamin D levels than the control group (514, 515). However, these levels were not particularly low and were not associated with a raised PTH or any other marker of bone formation or bone microarchitecture, and it is, therefore, unclear whether the lower vitamin D levels had a particularly marked contributory role. It is also unlikely that the women with T1DM had any other underlying genetic bone disorder because none had been revealed on history and examination. The reported rate of fractures in these cases seemed higher but not significantly different from controls and within the expected frequency for self-reported fractures in healthy women(516).

The findings in the current study suggest that the deficits in bone microarchitecture that were encountered in T1DM may have a multifactorial etiology. First, the negative association between total osteocalcin, a marker of bone formation, and trabecular separation in the study participants suggests that the osteopathy in T1DM may be linked to reduced bone formation rather than increased bone resorption. This was further reinforced by the lower levels of CTX, a marker of bone resorption, in the T1DM cases. This state of low bone turnover with reduced bone formation in T1DM has been reported previously (369, 517) and has been known to be associated with GH deficiency (518). To facilitate recruitment, the current study did not stipulate fasting blood samples. Markers of bone turnover and especially markers of bone resorption, such as CTX, show a diurnal variation and may be affected by fasting status (519) and future studies would benefit from standardization of sample collection.

The women with T1DM also had lower levels of circulating IGF-1 and ALS and the negative association of trabecular separation with ALS raises the possibility that the GH/IGF-1 axis and, in particular, reduced GH activity may contribute to the altered bone microarchitecture. GH and IGF-1 are important regulators of bone homeostasis and important for the maintenance of bone mass (506). GH stimulates osteoblastic proliferation through stimulation of circulating and local IGF-1 and it inhibits adipogenesis (520). In

humans, systemic availability of active IGF-1 is modulated through its binding to proteins such as IGFBP-3 and ALS(521), which, along with IGF-1, are primarily synthesized in the liver under the stimulation of GH(522). Insulin deficiency is reported to be associated with a state of GH resistance (523), an abnormality of posttranslational synthesis of ALS and ALS deficiency(524, 525), and with lower levels of ALS, circulating IGF-1 falls as a result of increased renal clearance. Because the insulin deficiency in the portal circulation exists despite insulin replacement in T1DM (526), it is likely that this state of GH resistance is not alleviated during treatment in T1DM, and the abnormal bone findings in this study may be a consequence of a persistent state of IGF-1 and ALS deficiency. The finding in the current study of an inverse association between trabecular separation and serum osteocalcin and ALS reinforces this view.

The other possible reason for the abnormality in bone microarchitecture in T1DM may be related to microvasculopathy. In our study, retinopathy was independent negative predictor of bone deficit irrespective of other diseases related factors. The clear association of reduced bone volume in those cases of T1DM who had retinopathy, albeit background retinopathy in most cases, suggests that it is possible that the underlying pathophysiology of retinopathy may also influence trabecular development. The pathology of diabetic retinopathy evolves in an environment of increased formation of reactive oxygen species, leukostasis, and breakdown of the blood-retinal barrier that is followed by formation of acellular capillaries and development of micro aneurysms (527). The superoxide-generating family of NADPH oxidase enzymes has not only been strongly implicated in the vascular complications of diabetes but also superoxide radicals may be associated with abnormalities of bone turnover (528, 529). The possibility of a microvasculopathy that affects bone in T1DM has not been studied widely and requires further exploration.

The women with T1DM in this study did not have a significantly higher BMI compared with controls, but they had markedly higher visceral adiposity and it is possible that this abnormality is also associated with functional GH deficiency (530). Although bone marrow adiposity was similar in the cases and controls, the cases did have increased trabecular spacing, which showed an inverse relationship to circulating ALS and osteocalcin. Increased trabecular spacing is not universally associated with increased bone marrow adiposity (510). Although this association may be encountered in GH deficiency (434, 531), in other conditions such as osteogenesis imperfecta, the two parameters do not show an association (434). It is also possible that in states of GH resistance such as T1DM, bone marrow adiposity may be increased. This hypothesis reinforced by the observed significant positive association of BMA with VAT in our study participants. Additionally,

the observed positive association between BMA and HbA1c level supporting the role of IGF-1 as regulator of adipogenic differentiation under hypoinsulinemic conditions (204). The current study was not powered to detect significant differences in bone marrow adiposity between the cases and controls, and it is possible that with a larger sample size this would also have been detected. The finding of an abnormality of bone microarchitecture and bone marrow adiposity would be consistent with a defect in bone marrow mesenchymal stem cell differentiation, which leads to a net reduction in bone formation in favour of adipogenesis (206) and, as previously described in streptozocin-induced T1DM mice (249), conditions that are associated with relative IGF-1 deficiency (491, 532)

The women with T1DM in this current group had a relatively high HbA1c and as expected for a population sample from an inner-city area in the west of Scotland (533). A relationship between HbA1c, pentosidine (AGEs markers) and trabecular bone parameters was not observed in the current study, and perhaps this investigation would have been facilitated if there was a wider range of HbA1c with large sample size. On the other hand, we observed positive significant correlation between BMA and HbA1c level ($r = 0.437$; $P < 0.02$) suggesting an effect of T1DM on the vertebral BMA. This became also apparent when the diabetic subjects were classified based on HbA1c levels and significantly higher vertebral BMA was found in subjects with HbA1c levels $>7\%$ ($p = 0.02$). More details about the association of glycaemic control and BMA will be discussed in Chapter 4.

Younger age of T1DM onset and long standing disease duration are other clinical factors which may have effect on bone health in people with T1DM. So far, there was no general agreement on the relative importance of these factors. In consistent with other studies (351, 377, 534-536), we did not observe significant association between bone parameters and disease duration. Younger age of onset of diabetes has been associated with bone deficits which continues to persist over years as noted in few studies (346), in our study, there was trend toward negative association between younger age of T1DM onset and bone deficit, with larger sample size this may be confirmed.

Finally, the current study highlights the objective versatility of MRI-based techniques in identifying differences in relatively small cohorts. Although there is now sufficient supporting evidence for the use of MRI for assessing bone microarchitecture (445), with the greater availability of 3T MRI scanners, there is a need to standardize the analytical techniques so that the clinical utility of MRI in metabolic conditions that are associated with abnormalities of bone health can be realized. With technological advances in hardware as well as analytical tools, an improvement in the current limited resolution of MRI as well as its ability to study cortical structure is highly likely. We chose to study

young women only, primarily because they are more likely to develop osteoporosis in the long term and to avoid the confounding effects of sex hormones, but given that the increased fracture incidence has been encountered in both sexes and bone marrow adiposity increases with old age (119, 537), there is a need to study older as well as younger people with diabetes in both sexes. We did not perform DXA in this group, but there is a need in future studies to assess the relationship of micro-MRI findings to DXA BMD as well as DXA-based methods of assessing trabecular architecture (223). Given that hip fractures are reported to be more common in people with T1DM (161, 336, 340), there is a place to examine the microarchitecture at this site, too. The lack of a sufficient number of cases with other complications associated with microvasculopathy limited the investigation of this association in the current study. The relationship between bone pathology and type 2 DM is less clear with a lower risk of fractures(221).However, a recent study that examined bone marrow adiposity in women with type 2 DM did report a higher level of vertebral bone marrow adiposity in those who had a history of a fracture (464).

3.6 Conclusion

In summary, detailed MRI studies in young women with T1DM have shown clear abnormalities of bone health that are characterized by reduced trabecular bone volume and reduced trabecular numbers. Possible underlying mechanisms that require further exploration include a microvasculopathy and GH resistance.

Chapter 4

Longitudinal Changes In Bone Marrow Adiposity And Its Relationship To Diabetes Control In Young Women With Type 1 Diabetes Mellitus

4.1 Abstract

Context: The pathophysiological mechanism of increased fractures in young women with Type 1 Diabetes Mellitus (T1DM) is unclear.

Objective: Prospective, longitudinal study of trabecular bone microarchitecture and vertebral marrow adiposity in young women with T1DM and a control group of healthy women.

Patients & Settings: 17 women with T1DM with a median (range) age of 22.2yrs (16.6, 32.4) attending one outpatient clinic with a median age at diagnosis of 10.1 yrs (4.8, 14.8) were compared to 11 age-matched healthy women who acted as controls.

Methods & Main Outcome Measures: Measurements included MRI-based assessment of abdominal adipose tissue, proximal tibial bone volume/total volume (appBV/TV), trabecular separation (appTb.Sp), vertebral bone marrow adiposity (BMA) at baseline and 12 months.

Results: Median appBV/TV in cases and controls was 0.31 (0.22, 0.37) and 0.33 (0.28, 0.4), respectively ($p=0.05$) and median appTb.Sp in T1DM was 2.57 (2.24, 3.15) and 2.32 (2.03, 2.73), respectively ($p=0.02$). There was no difference in median BMA which was 26.2% (12.1, 62.1) and 22.4% (9.6, 41.9) in cases and controls, respectively ($p=0.57$). Over the 12 month period, there was no significant change in these parameters. Although, there was no association between change in bone microarchitecture parameters and HbA1c in the cases, there was a strong correlation between change in HbA1c and change in BMA ($r, 0.8, p=0.002$).

Conclusion: Longitudinal MRI studies of trabecular bone show that over a period of one year, improvement in diabetes control is associated with a reduction in bone marrow adiposity but persistence of bone microarchitecture deficits

4.2 Introduction

The risk of hip fractures in those with Type 1 diabetes mellitus (T1DM) is reported to be 7–12 times greater (336, 340, 538). Although the underlying pathogenesis for this increased fracture risk may be multifactorial (539), bone marrow adiposity (BMA) may play an important role (463, 540). The process of differentiation of mesenchymal stem cells into either adipocytes or osteoblasts is regulated by a number of growth factors including insulin, oxygen tension and blood flow within the bone marrow (503, 504) and mouse models of T1DM exhibit increased BMA and increased adipocyte markers in the bone marrow (249).

On dual energy X-Ray absorptiometry (DXA), adults with T1DM show a reduction in bone mineral density (BMD) Z-score, reported in a meta-analysis at -0.22 at the lumbar spine and -0.37 at the hip (161), but the fracture risk in affected adults is much higher (161, 336, 340, 538) than expected for this modest reduction in BMD. Not only does MRI provide high resolution 3D images of bone structure that correlates with techniques such as computed tomography (440, 509) but it also allows MR spectroscopy for estimating BMA (541). Given the novelty of MRI-based assessment of bone microarchitecture and BMA, there is a need to assess the extent of longitudinal variation that may occur in healthy and disease states. Recent studies that use MRI and HR-CT have shown that people with T1DM may have a bone microarchitectural deficit (163, 542). However, an abnormality of BMA has not been observed to date in people with T1DM (542) and although the findings in those with T2DM are currently inconclusive, they suggest that there may be an association between chronic hyperglycemia and BMA (464, 466). Furthermore, there is scarce information on the extent of change when these measurements are repeated. The current study was, therefore, performed to assess longitudinal changes in MRI-based markers of bone health and their relationship to diabetes control in T1DM. This information will be vital for understanding the bone pathology in diabetes and for designing future intervention studies aimed at improving bone health.

4.3 Research Design & Methods

4.3.1 Subjects

Of the 29 women between the ages of 20 and 30 years and who were diagnosed with T1DM before the age of 16 years and who participated between July 2012 and July 2013 in a case: control study of bone health (542), 17 volunteered for another visit at 12-months. In addition, of the 28 healthy women who comprised the control group and were approached, 11 volunteered for a repeat visit at 12 months (Figure 4.1). Exclusion criteria included the presence of metallic implants and pacemakers, active or planned pregnancy or lactation, kidney disease, chronic use of drugs that are known to affect bone health and other chronic diseases that are known to be associated with an increased risk of fractures. Information on personal health and lifestyle habits, including cigarette smoking, alcohol consumption, current medication, use of vitamins or calcium, age at menarche, use of oral contraceptives, hours of weight bearing physical activity per week, history of fractures and a family history of early osteoporosis was also collected. Information on age of diagnosis, disease duration, insulin therapy and presence of microvascular complications was obtained from the case records. A glycosylated hemoglobin (HbA1c) measurement within the four-week period prior to the visit was used as current HbA1c. The study protocol was approved by the national research ethics service and all participants provided written informed consent.

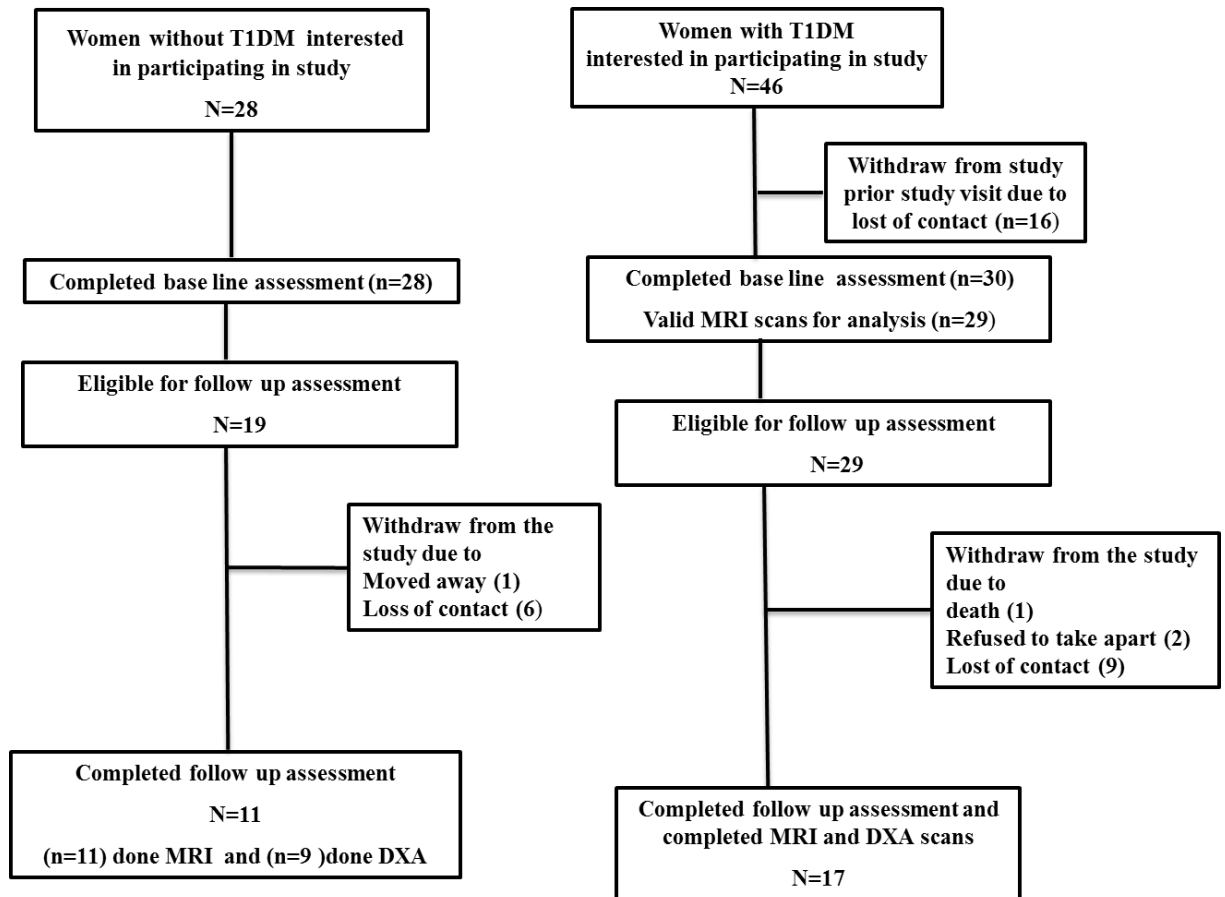


Figure 4.1: Path outlining study participant recruitment, enrollment and followup from baseline to follow-up assessment.

4.3.2 MRI acquisition and analysis

Micro MRI data were available in all 17 cases and 11 controls. MRS data were available in 16 case and all controls, MRI of abdominal fat are available in 17 case and 10 controls. All magnetic resonance images acquisitions and analysis were described previously in Chapter 2.

4.3.3 Statistical Analysis

Data analysis was performed using Minitab 17, Minitab Inc, State College, PA. All data were described as medians and ranges; comparison between the cases and controls was performed by the Mann-Whitney U test for continuous variables and by the Chi Squared test for categorical variables. Spearman correlation analysis was used to assess the univariate relationship between continuous variables and statistical significance was set at $p < 0.05$. Multivariable linear regression was performed on models with weight, age and adiposity to determine the baseline difference of bone parameters between cases and

controls, and to examine associations of changes in bone parameters in relation to changes in visceral adiposity. SPSS mixed modelling was employed where appropriate to explore the confounding effects of independent variables on the percentage change in bone parameters over the one year period.

4.4 Results

4.4.1 Clinical Characteristics

The median age at diagnosis of the cases was 10.1 yrs (4.8, 14.8) and the median duration of diabetes was 13.6 yrs (6.8, 26.5). There were no significant demographic or anthropometric differences between the cases and controls at baseline or at the 12-month follow-up visit (Table 4.1). In addition, there were no intra-group differences at the two time points (Table 4.2). Notably, the median BMI in the cases and controls was 24.4 kg/m² (18.7, 31.6) and 22.6 kg/m² (19.6, 28.0), respectively ($p=0.2$) at one year with similar amounts of physical activity reported in the cases and controls. Of the 17 cases, 5 (29%) reported a history of traumatic fractures and in 3, the fractures had occurred before the diagnosis of diabetes. No fractures were reported in the control group. None of the participants were on routine vitamin supplementation. Of the 17 cases, 9 (50%) had retinopathy of which 8 had background retinopathy alone, 2 (7%) were being treated for hypertension, and 3 (18%) had microalbuminuria. One of the cases had stable Crohn's disease over the study period requiring only sulfasalazine therapy for three years prior to the baseline assessment.

Table 4.1: Descriptive characteristic of study participants who were enrolled at baseline and follow-up. All continuous variables are described as median and range

	Baseline			1 year		
	Diabetes (17)	Controls (11)	p	Diabetes (17)	Controls (11)	p
Age (Years)	22.2 (16.6, 32.4)	20.0 (19.4, 23.1)	0.08	23.7 (17.4, 40.0)	21.0 (20.0, 23.9)	0.07
BMI (kg/m ²)	24.6 (18.2, 31.2)	22.6 (19.7, 27.8)	0.05	24.4 (18.7, 31.6)	22.6 (19.6, 3)	0.2
Smoker (n)	2	0	0.3	4	0	0.1
Alcohol consumption	13	10	0.8	13	9	0.9
Menarcheal Age (Years)	12.5 (10, 17.5)	12 (11, 15)	0.8	13 (10, 17.5)	12 (11, 15)	0.8
Pregnancy (n)	2	0	0.3	3	0	0.2
Oral Contraceptives (n)	12	9	0.8	10	10	0.5
Physical activity (hrs/wk)	4 (0, 10)	4 (0, 7)	0.7	3 (0, 10)	3 (1.5, 10)	0.7
Total insulin dose (IU/kg/d)	2.5 (1.2, 4.8)			2.5 (1.2, 3.7)		
Current HBA1c (mmol/mol)	77 (36.6, 114.2)			75 (51, 118)		
Ave HBA1C over 1yr (mmol/mol)	74.4 (41.3, 116.7)			75 (60.2, 110.4)		
Hypertension (n)	2			2		
Retinopathy (n)	8, (Mild, 7)			9, (Mild, 8)		
Microalbuminuria (n)	0			3		

Table 4.2: Differences in MRI baseline data for those who dropped out and those who completed the study.

	Diabetes			Controls		
	Dropout (n=13)	Completed the study (n=17)	P	Dropout (n=17)	Completed the study (n=11)	P
CSA (mm ²)	49186 (31489, 77086)	47878 (30134, 78651)	0.9766	47678 (32966, 69789)	36232 (30232, 53888)	0.1731
SCAT (mm ³)	25209 (3,719, 37936)	20458 (7,347, 42877)	0.660	17263 (7454, 40807)	11605 (7,885, 28875)	0.1731
VAT (mm ³)	5,065 (2,402, 7,715)	6,427 (2,030, 11144)	0.208	4042.5 (2,592, 6,832)	3,393 (1,808, 6,083)	0.3423
TAT (mm ³)	30788 (6,584, 45651)	26271 (15433, 54021)	0.660	22090 (10046, 47639)	15778 (10312, 30869)	0.2312
AppBV/TV	0.30 (0.23, 0.34)	0.33 (0.22, 0.37)	0.6	0.31 (0.22,0.37)	0.33 (0.28,0.40)	0.047
AppTb.N(mm-1)	0.26 (0.20, 0.29)	0.27 (0.24, 0.30)	0.5	0.27 (0.24,0.30)	0.29 (0.24,0.30)	0.031
AppTb.Sp(mm)	2.66 (2.25, 3.38)	2.57 (2.24, 3.15)	0.4	2.57 (2.24,3.15)	2.32 (2.03,2.73)	0.019
AppTbTh(mm)	1.18 (0.86, 1.49)	1.11 (0.91, 1.46)	0.5	1.11 (0.91, 1.46)	1.26 (1.05, 1.39)	0.144
BMA (FF%)	22.92 (9.86, 50.14)	26.20 (17.29, 59.60)	0.6	26.20 (12.05, 62.11)	22.35 (12.46, 49.82)	0.572

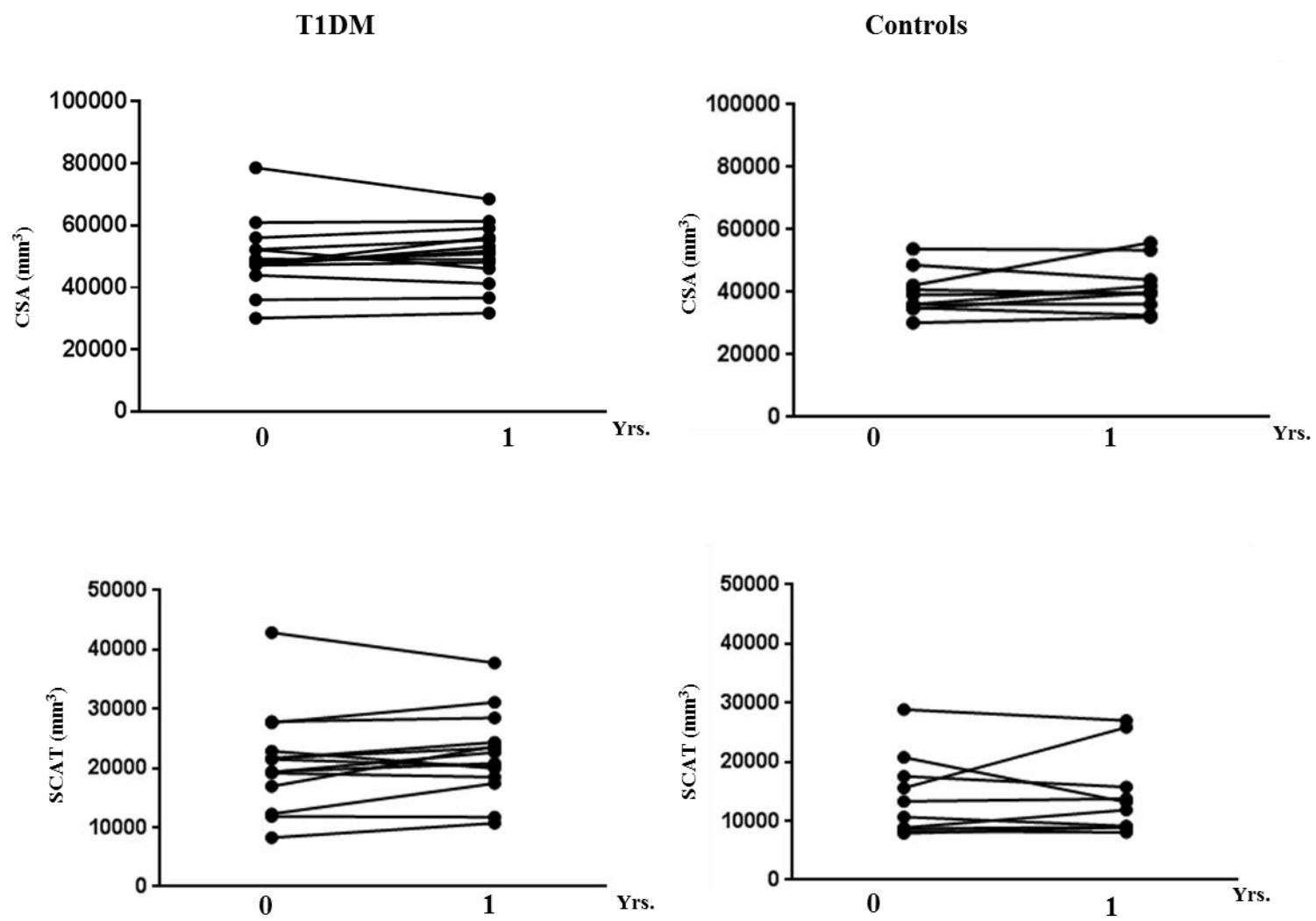
4.4.2 MRI of abdominal fat

While differences in BMI were not statistically different between cases and controls, the cases did have a higher BMI by 2kg/m^2 (Table 4.1). However, abdominal adiposity including CSA, SCAT, VAT and TAT, was clearly significantly higher in cases compared to controls at baseline and at 1 year and there was no significant change within these two groups for these respective parameters of adiposity (Table 4.3) (Figure 4.2, and 4.3). As expected, change in TAT showed a strong association to change in BMI ($r, 0.7, p<0.001$) and this association was similar in controls and those with T1DM (Figure 4.4). This relationship was also evident for weight and these two anthropometric measures were also strongly associated to CSA and SCAT (Figure 4.4). In the diabetes group, there was no association of abdominal adiposity parameters with current or annualized HbA1c, age at diagnosis and duration of T1DM at baseline or one-year. Furthermore, the percentage change in these markers of adiposity was not associated to a change in any of the markers of glycaemic control.

Table 4.3: MRI-based measures of abdominal adiposity, bone microarchitecture and vertebral bone marrow adiposity at L3 for controls and participants with T1DM (diabetes) at baseline and one year.

	Baseline			One Year			Change From Baseline (%)		
	Diabetes	Controls	p	Diabetes	Controls	p	Diabetes	Controls	p
CSA (mm ²)	47878 (30,134, 78,651)	36124 (30,232, 48,706)	0.009	51,829 (31,807, 73,485)	39707 (32,004, 55,860)	0.02	3.7 (-12.9, 18.2)	0.7 (-9.7, 32.4)	1
SCAT (mm ³)	20458 (8,278, 42,877)	10684 (7,885, 20,790)	0.009	22,662 (8,747, 38,179)	11881 (8,078, 25,829)	0.009	7.7 (-12.6, 41.8)	0.4 (-36.6, 65.8)	0.43
VAT (mm ³)	6,427 (2,030, 11,144)	3,393 (1,808, 6,083)	0.003	60,85.0 (2,112, 11,373)	3,818 (1,864, 7134)	0.003	2.5 (-27.6, 53.4)	4.2 (-4.1, 17.3)	0.39
TAT (mm ³)	26271 (15,433, 54,021)	15778 (10,312, 24819)	0.002	28,274 (14,727, 49,161)	15699 (10,343, 32,963)	0.003	5.6 (-9.7, 44.5)	1.8 (-31.4, 52.1)	0.58
AppBV/T V	0.31 (0.22, 0.37)	0.33 (0.28, 0.40)	0.05	0.29 (0.25, 0.38)	0.32 (0.27, 0.42)	0.1	2.7 (-21.6, 22.6)	-3.6 (-21.1, 36.7)	0.59
AppTb.N (mm ⁻¹)	0.27 (0.24, 0.30)	0.29 (0.24, 0.30)	0.03	0.26 (0.20, 0.32)	0.28 (0.24, 0.31)	0.1	0 (-25.0, 14.3)	0 (-17.0, 8.0)	0.85
AppTb.Sp (mm)	2.57 (2.24, 3.15)	2.32 (2.03, 2.73)	0.02	2.65 (2.06, 3.38)	2.47 (1.94, 2.79)	0.04	1.1 (-15.5, 49.6)	2.2 (-18, 24)	0.54
AppTbTh (mm)	1.11 (0.91, 1.46)	1.26 (1.05, 1.39)	0.14	1.17 (0.95, 1.46)	1.16 (1, 1.52)	1	6.9 (-26.7, 35.2)	-4.6 (-21.6, 36.9)	0.26
BMA (FF%)	26.20 (12.05, 62.11)	22.35 (9.57, 41.85)	0.57	26.91 (17.24, 58.49)	25.19 (8.34, 35.10)	0.44	17.9 (-35.1, 92.6)	5.9 (-21, 43.1)	0.41

All data are described as median and range. CSA- cross-sectional area of adipose tissue; SCAT – subcutaneous adipose tissue; VAT- visceral adipose tissue; TAT – total adipose tissue; AppBV/TV – apparent bone volume/total volume; AppTb.N – apparent trabecular number; AppTbSp – apparent trabecular separation; AppTbTh – apparent trabecular thickness; BMA– bone marrow adiposity; FF% -fat fraction.



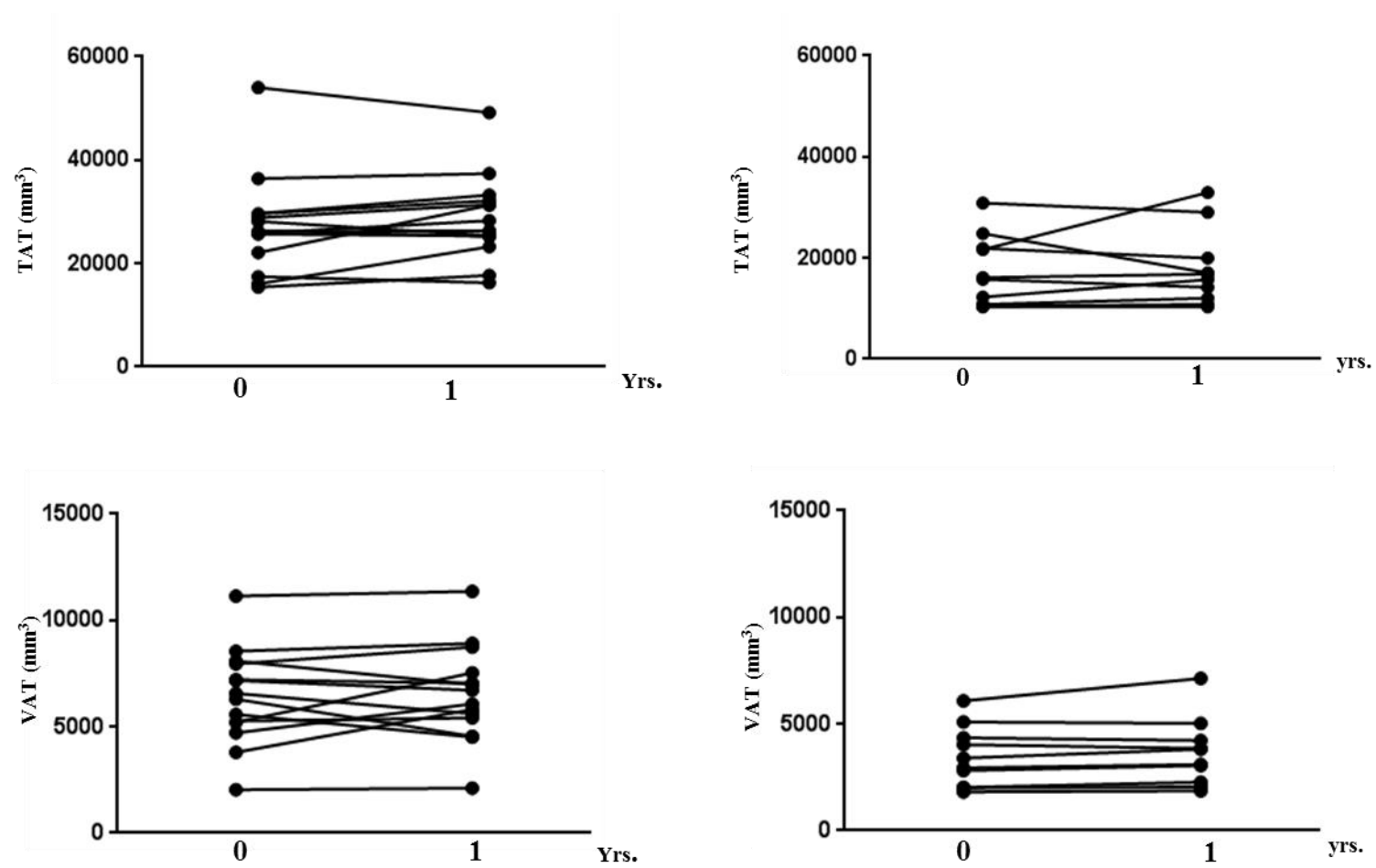


Figure 4.2: The absolute changes in the abdominal adiposity parameters over the one year period in both women with T1DM and controls.

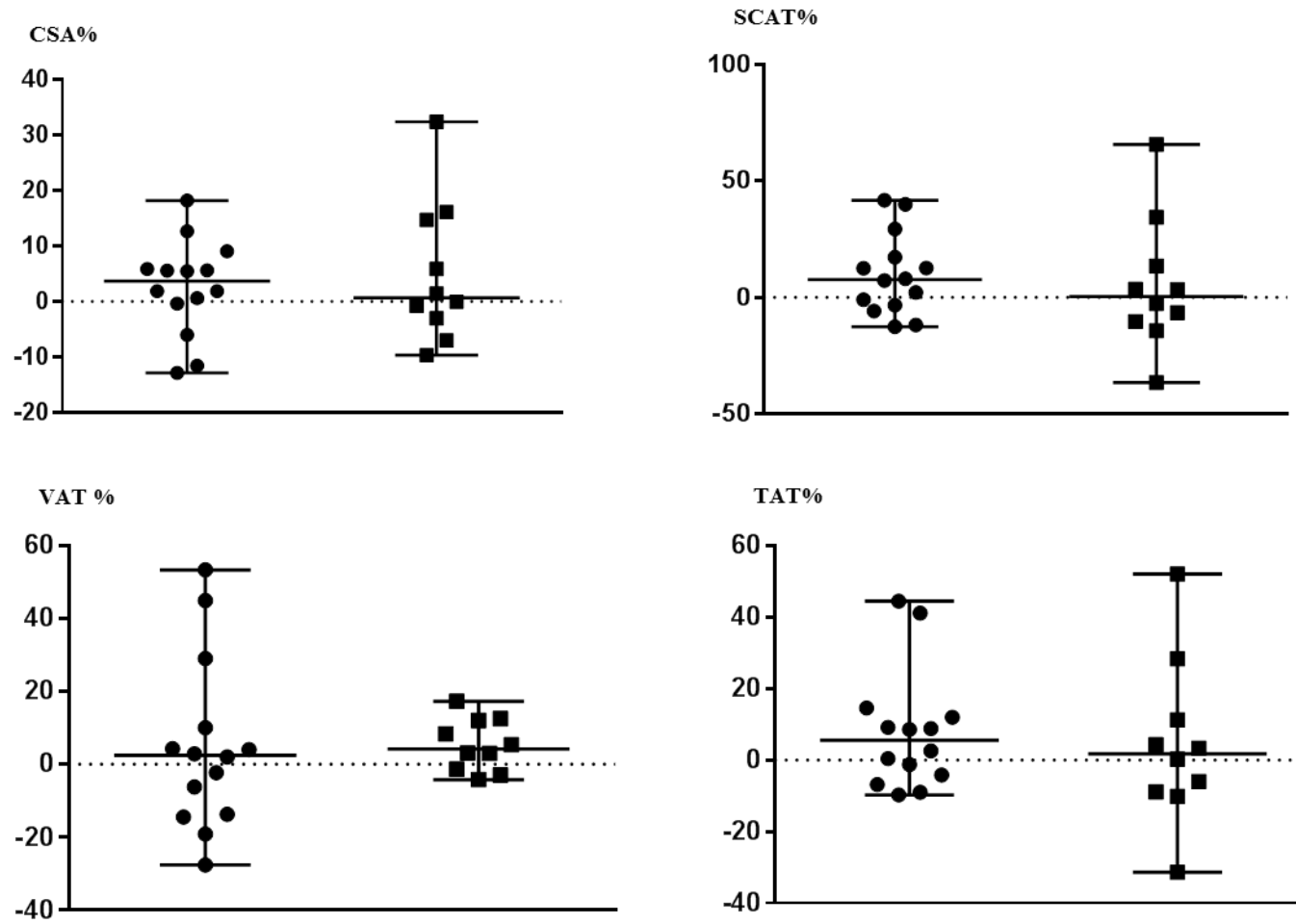


Figure 4.3: The median percentage changes in the abdominal adiposity parameters over the one year period in both T1DM (black circles) and controls (black squares).

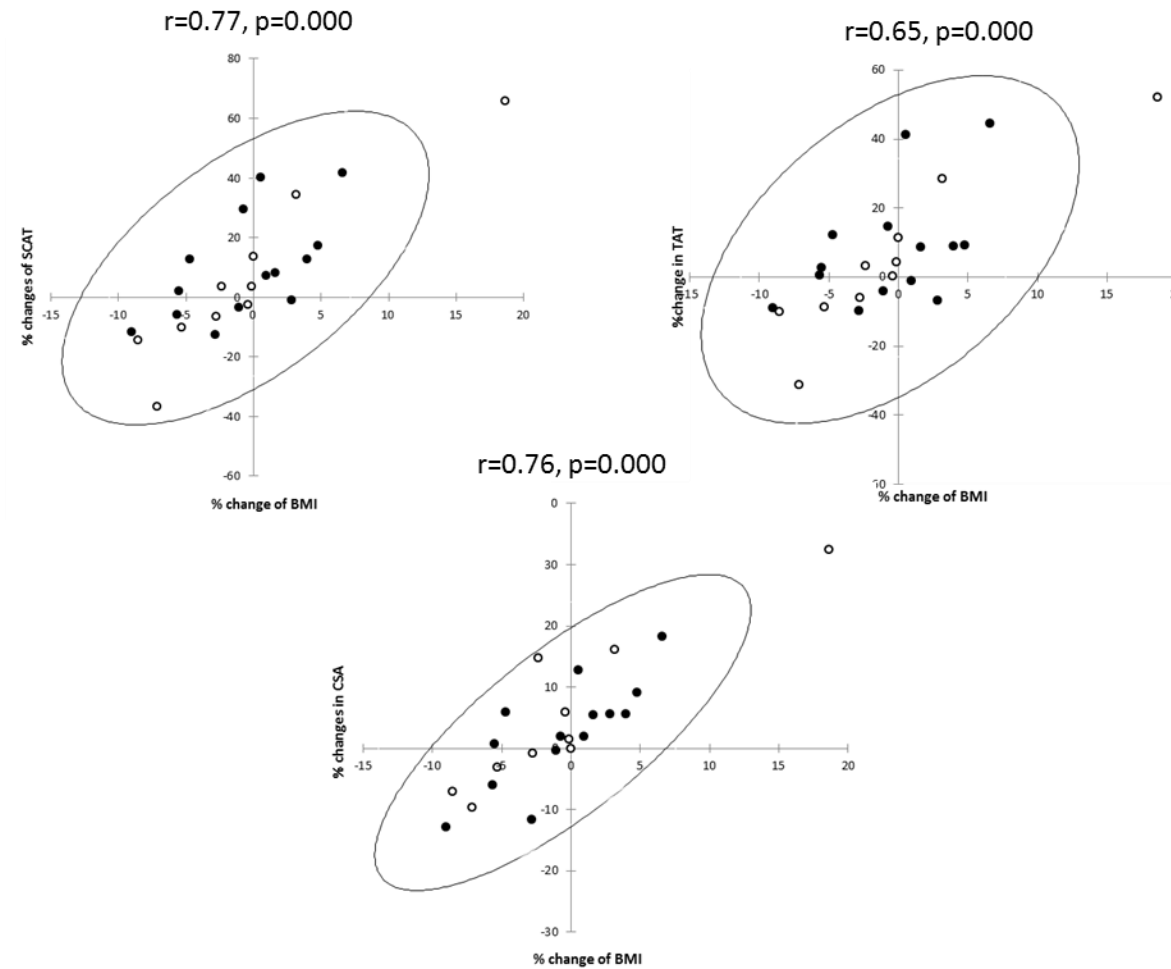


Figure 4.4: The relationship between % changes in CSA, SCAT and TAT as assessed by MRI and % change in BMI in women with T1DM (filled circles) and controls (open circles).

A positive association between % changes in CSA, SCAT and TAT and % change of BMI was observed.

4.4.3 Bone Marrow Adiposity

Absolute and median vertebral BMA, expressed as percentage fat fraction (%FF) did not change significantly during the study period in both cases and controls (Table 4.3) (Figure 4.5). Although, there was no association between the change in BMA and any of the anthropometric variables or markers of abdominal adiposity, in the women with T1DM, percentage change in BMA showed a strong positive association to percentage change in HbA1c when comparing most recent HbA1c at the two study time points ($r, 0.8, p=0.002$) (Figure 4.5). This association was still present but weaker when the percentage change in BMA was compared to the change in average HbA1c for the year prior to the MRI study ($r, 0.5, p=0.08$) (Figure 4.6). Of the 7 participants in whom the most recent HbA1c increased over the study period, 5 had increased BMA and of the 8 participants in whom HbA1c decreased, 4 had decreased BMA (Figure 4.7). Mixed model effect analysis showed that VAT was positively associated to a change in BMA ($p=0.02$).

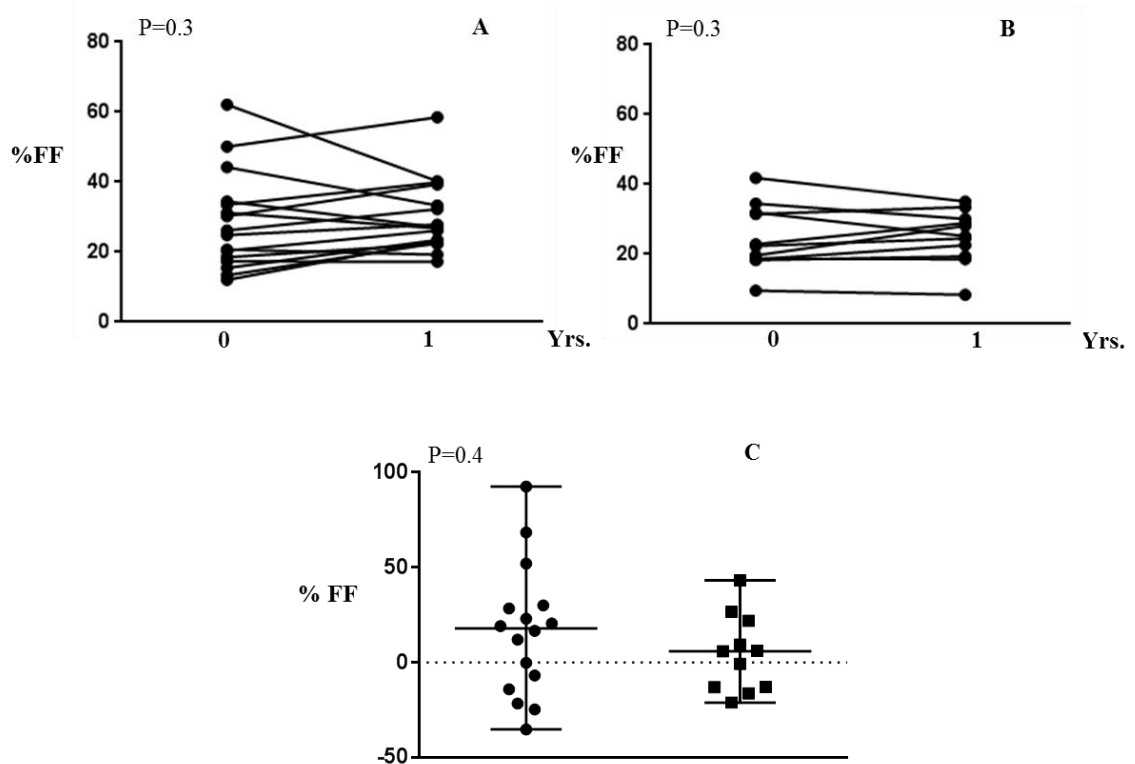


Figure 4.5: Absolute and median % changes in fat fraction (%FF) over one year period in both women with T1DM and controls. (A) absolute changes in FF% in T1DM, (B) absolute changes in FF% in controls and (C) % changes in FF% in both T1DM (Black circles) and controls (Black squares)

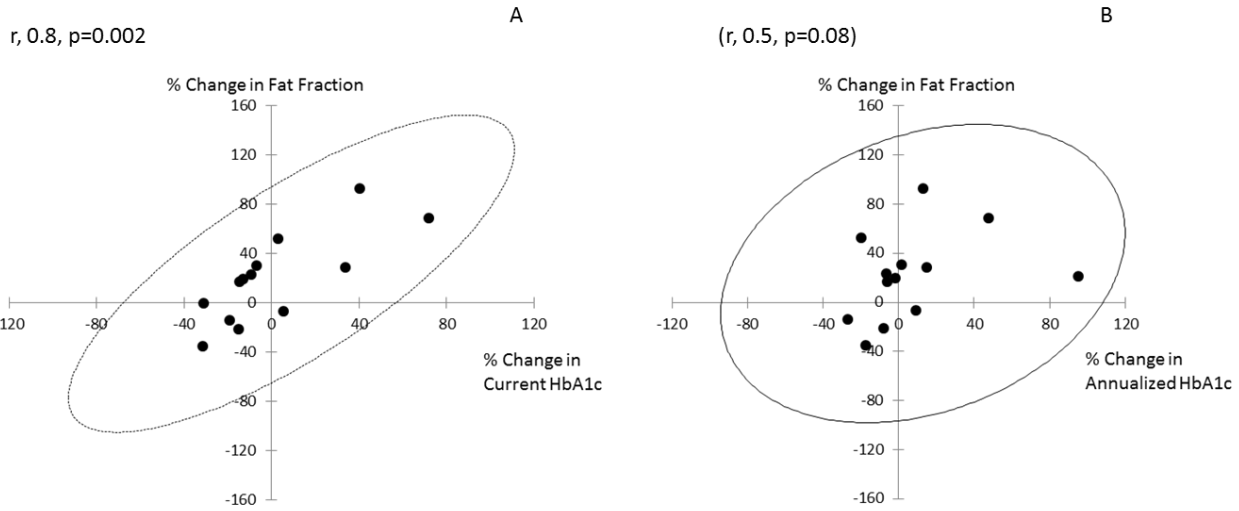


Figure 4.6: The relationship between percentage (%) change in fat fraction as a measure of vertebral Bone Marrow Adiposity (BMA) and % change in HbA1c measured within the 4 weeks prior to MRI scan at baseline and follow-up visit at 1 yr (A) and average HbA1c for the year prior to MRI scan at baseline and follow-up visit at 1 yr (B).

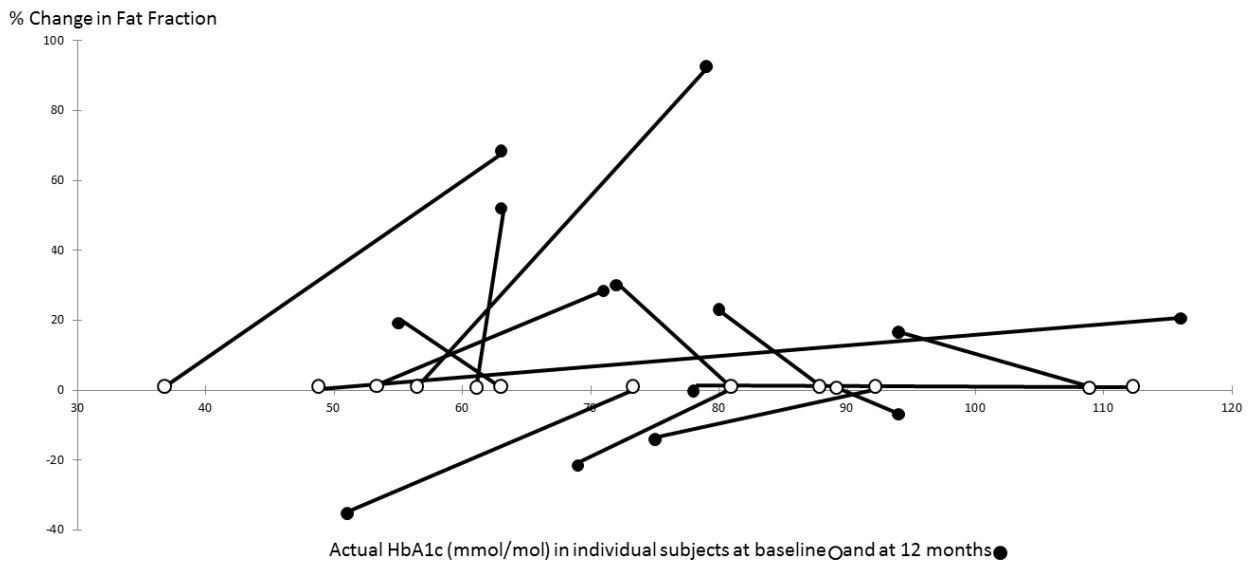


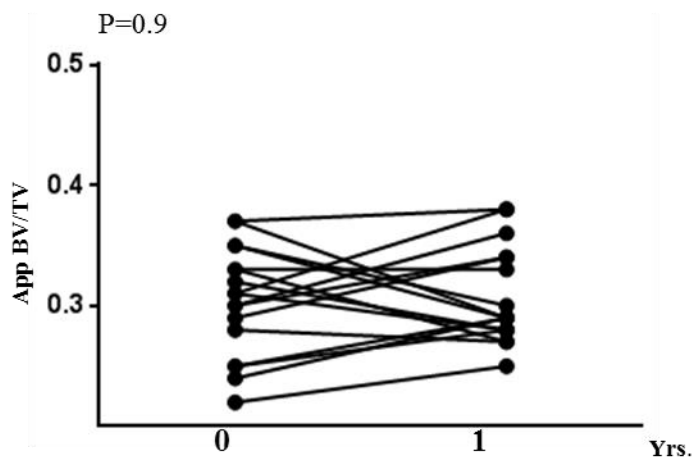
Figure 4.7: Percentage change (%) in fat fraction as a measure of vertebral Bone Marrow Adiposity (BMA) for each participant in relation to the extent of change in HbA1c from baseline to 12 months.

The open circle on the horizontal intersect denotes the actual HbA1c (mmol/mol) at baseline and the closed circle denotes the the actual HbA1c (mmol/mol) for the same subject at 12 months.

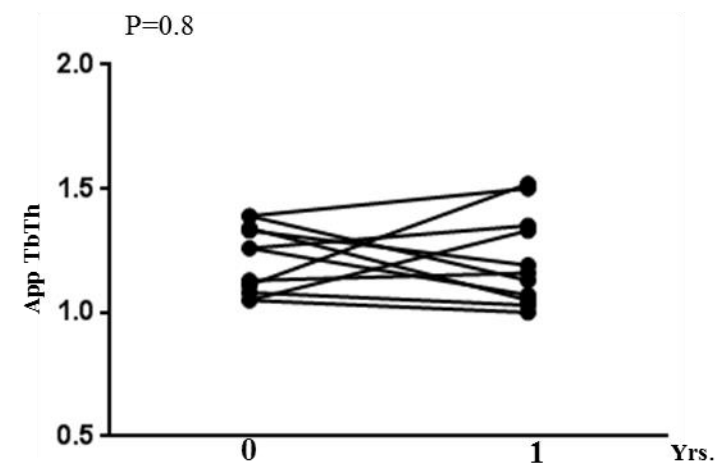
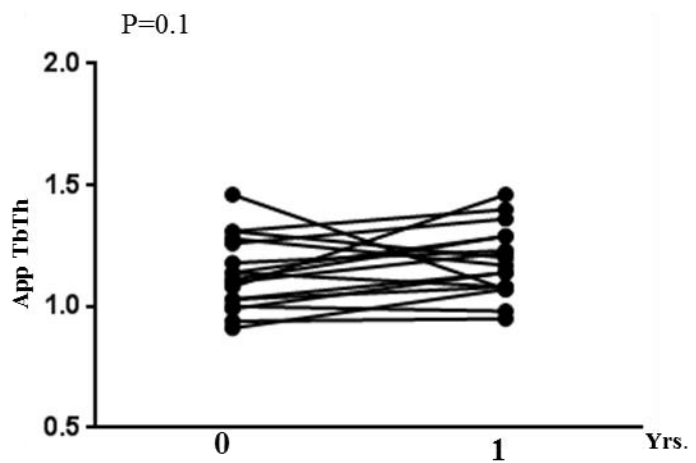
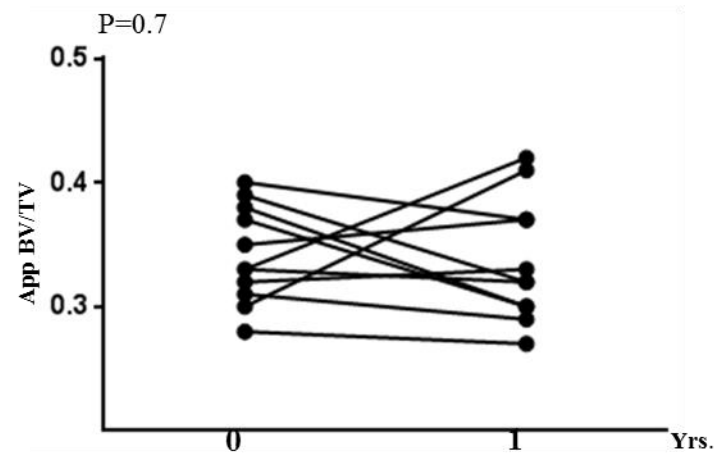
4.4.4 Bone Microarchitecture by Micro-MRI

Compared to controls, the cases had a lower median appTbN and a higher median appTbSp at baseline and 12 months (Table 4.3) and this difference persisted after adjusting for age, VAT and TAT. A clear difference existed for median appBV/TV and appTbSp between those cases who had retinopathy and those who did not have retinopathy. The median appBV/TV and appTbSp was 0.28 (0.25, 0.34), and 2.78 (2.44, 3.22), respectively, in those cases with retinopathy compared to 0.34 (0.28, 0.38) and 2.54 (2.06, 3.38) in those cases without retinopathy ($p=0.01$, 0.03 , respectively). There was no significant change in any of the bone microarchitecture parameters over the one year period in either group and the extent of change within each group was similar in the group of women with and without T1DM (Table 4.3) (Figure 4.8)(Figure 4.9). In the T1DM cases, there was no association of percentage change in appBV/TV, appTbN or app TbSp with percentage change in HbA1c, age at diagnosis, duration of T1DM or daily insulin dose adjusted for weight. Mixed model effect analysis showed that the age was negatively associated with the percent changes of app BV/TV, appTbN and appTbSp in both cases and controls ($p=0.02$, $p=0.02$, $p=0.002$, respectively). The percentage change in trabecular bone microarchitecture parameters did not show any association to the MRI-based markers of abdominal obesity and BMA, even after controlling for BMI.

T1DM



Controls



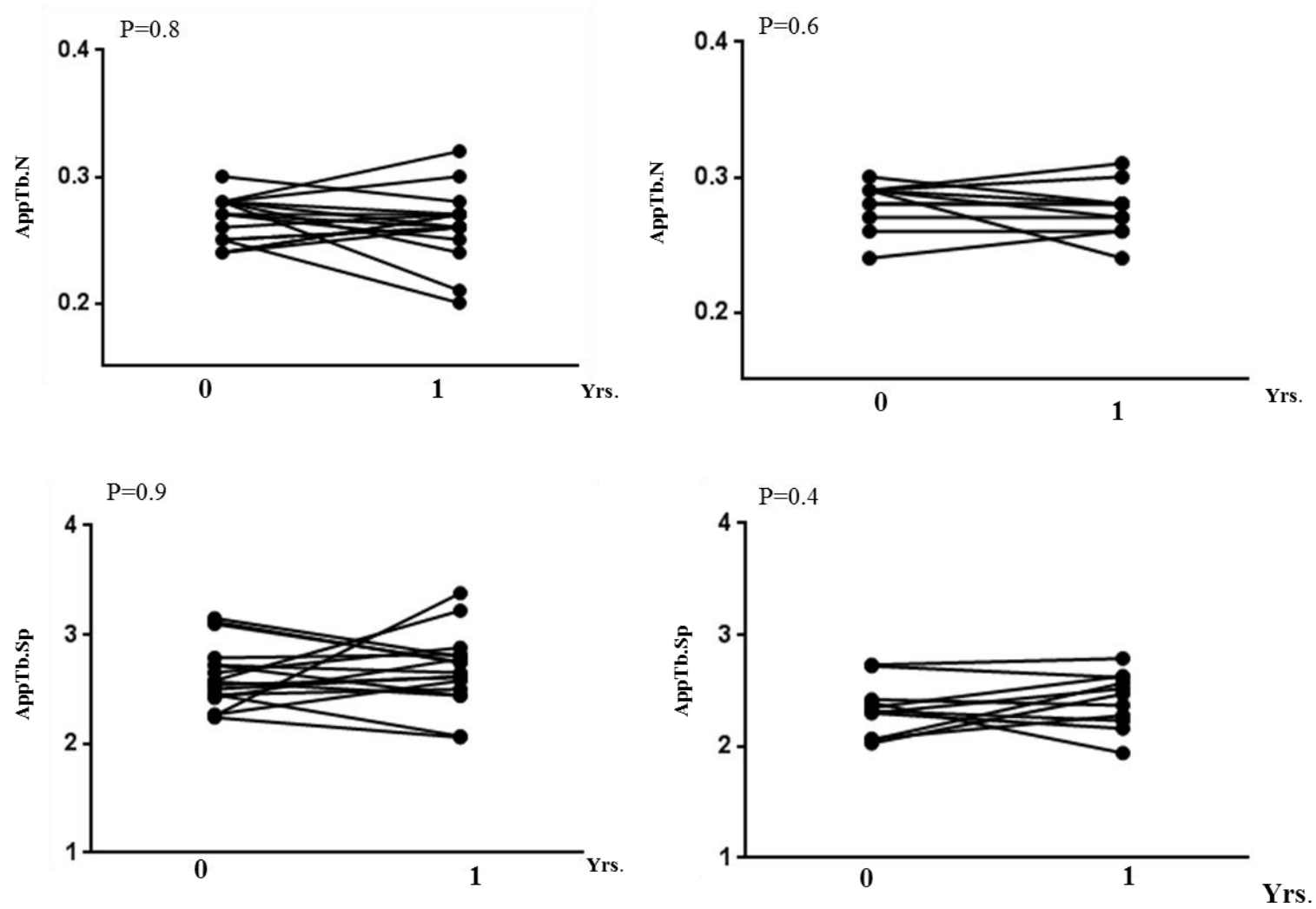


Figure 4.8: The median percentage changes in the bone microarchitecture parameters over the one year period in both women with T1DM and control groups.

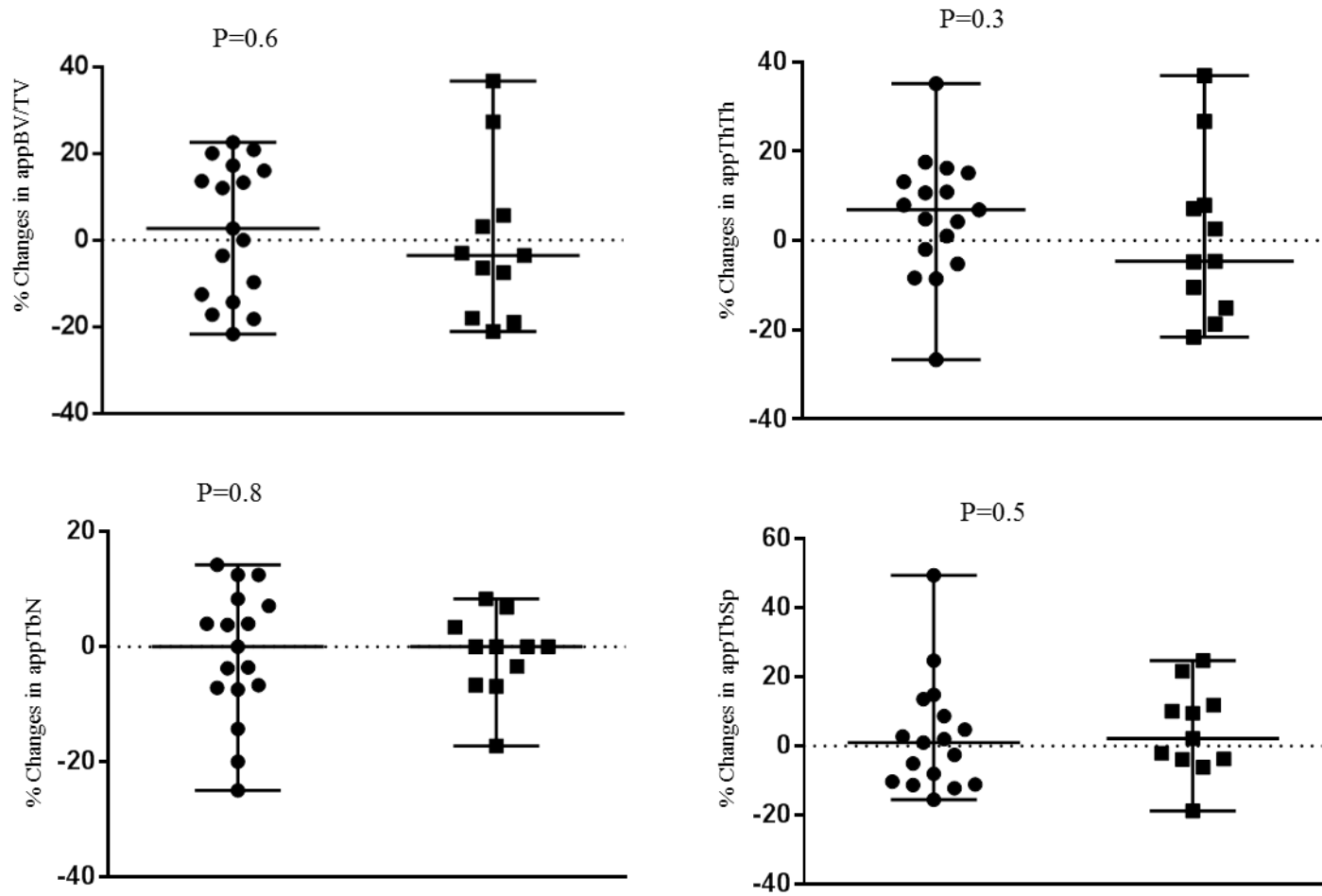


Figure 4.9: The median % changes in the bone microarchitecture parameters over one year period in both women with T1DM (Black circles) and controls (Black squares).

4.5 Discussion

The current study was primarily aimed at assessing the extent of change that may occur in MRI based parameters of bone health and adiposity in these women with T1DM, as well as in healthy young women. In addition, this study aimed to study the clinical factors that may be associated with longitudinal changes in MRI based measures of bone health. Although women with T1DM tended to be slightly overweight and their BMI was not significantly higher than the control group, abdominal adiposity as assessed by MRI was significantly raised in the women with T1DM. Although the overall change in the markers of abdominal adiposity did not show a significant difference between the cases and controls, the range of variation within the group of women with T1DM was greater. Raised abdominal adiposity in young people with T1DM is not a universal finding (543-545) and may perhaps be associated with overall control and lower socioeconomic status (546). A recent report of islet cell transplantation in a cohort of cases of T1DM of a similar socioeconomic status showed that improved control was also associated with a reduction in central obesity (546). However, in the current T1DM group, the changes in adiposity did not seem to be clearly related to any clinical variables. The average change in markers of abdominal adiposity was about 3% and this was similar to that published before in healthy young women and within the coefficient of variation for the technique which is about 5% (547).

In the previous case control study from our group, we did not show any statistical difference in BMA between cases with T1DM and controls (542) and, consistent with that, we did not detect a significant difference in the current smaller cohort. The average change in BMA over the year was about 12% and tended to be higher in the cases than the controls. Whilst there are several reports of increased BMA in mouse models of uncontrolled T1DM (249, 292, 507) there are currently no published reports of increased BMA in humans with T1DM and, given the extent of variation, a larger sample size may assist in conclusively evaluating this association. However, our current study has shown a clear and unequivocal association between a change in HbA1c and a change in BMA. Given that there is increasing evidence of a direct link between BMA and bone strength (467) we believe that this is a very important finding as it sheds further light on the aetiology of the osteopathy that is associated with increased bone fragility in T1DM. There is increasing evidence that the developmental origins of VAT and SCAT are different (185). The preliminary finding of an association between BMA and VAT but not TAT or SCAT needs to be confirmed in a larger group of individuals but suggests that the developmental origin of BMA may be more similar to VAT than SCAT.

The bone microarchitecture findings in the current study were also very striking and confirm our previous findings that a bone deficit exists in young women with T1DM and that this deficit is particularly marked in those with microvascular disease (542). These findings are especially notable as the association with retinopathy was statistically significant despite the relatively smaller number of cases in the current study sample. The average change in the trabecular parameters of bone microarchitecture over a period of the year was 3% and well below the upper level of variation of 7% in trabecular parameters in healthy volunteers (411). Unlike BMA, the range of change was lower for the bone microarchitecture parameters.

An association between change in BMA and markers of bone microarchitecture was not observed and although this may be due to the limited sample size, it is also possible that this could be explained by a lag phase between an effect of chronic hyperglycemia on BMA and its effect on bone microarchitecture and which may not have been adequately captured in this study and may require a longer period of study. The clear association of reduced bone volume in those cases of T1DM who had retinopathy, albeit background retinopathy in most cases, suggests that it is possible that the underlying microvasculopathy may also influence trabecular development.

Thus, the paradigm that these preliminary studies suggest is that BMA which might be associated to changes in HbA1c is the first marker of bone pathology and it is possible that this is followed over the longer term by abnormalities of bone microarchitecture which are less modifiable and mirror other microvascular conditions such as retinopathy. If this is true, then it would suggest that early identification of abnormalities of BMA may be a more effective approach for improving bone health in T1DM as well as other metabolic conditions that are associated with osteoporosis. Given that the increased risk of fractures in T1DM may also be present in older children and adolescents (219), there is a need to understand changes in BMA at an earlier stage of skeletal development than currently studied. The current study was limited to a relatively small group of cases and controls and there is a need to perform these studies in larger group of patients over a longer period to mitigate the effects of variability

4.7 Conclusion

In summary, detailed, longitudinal MRI studies of trabecular bone show that over a period of one year, improvement in diabetes control is associated with a reduction in bone marrow adiposity but bone microarchitecture deficits may persist. The chronological link between bone marrow adiposity and bone microarchitecture in pathological states needs further study.

Chapter 5

**An assessment of adiposity-based determinants of
bone density and microarchitecture in healthy young
women and women with T1DM**

5.1 Abstract:

Context: People with T1DM are at higher fracture risk yet the pathophysiological mechanism is unclear. Recent studies have demonstrated an important link between excess adiposity and bone deficits.

Aim of the study: The aim of this pilot study was primarily for assessing adiposity-based determinants of bone density and bone microarchitecture in healthy young women and women with T1DM. Secondly, to compare the feasibility of DXA and MRI measured bone parameters to differentiate between women with and without T1DM.

Methods: Measurements included MRI-based assessment of abdominal adipose tissue, proximal tibial bone volume/total volume (appBV/TV), trabecular separation (appTb.Sp), vertebral bone marrow adiposity (BMA). Additional measures included DXA based assessments of the whole body, femoral neck (FN) and lumbar spine bone area (cm²), BMC (g) and mean areal BMD (g/cm²). Body composition, including whole body fat mass (WB-FM (kg)), WM-FM Z- score and android/gynoid were also obtained from the whole body DXA scan.

Results: Women with T1DM had higher MRI based abdominal adiposity ($p < 0.05$) and greater WB-FM Z-score ($p = 0.03$) versus matched controls; BMI did not differ. Although, there was no difference in vertebral bone marrow adiposity (VBMA) which was 26.9 (17.2, 58.5) and 25.2 (8.3, 35.1) in cases and controls, respectively ($p = 0.51$), there was an inverse association between VBMA and DXA-measured BMD, BMD Z-score and BMC at all measured sites ($p < 0.05$). These correlations remained significant after controlling for age, BMI, WB-FM (Kg), VAT, TAT, SCAT. On the other hand, visceral adipose tissue (VAT) showed positive correlations with VBMA ($r = 0.42$, $p = 0.03$), and negative correlation with TB-BMD Z score ($r = -0.46$, $p = 0.02$). After controlling for TB-BMD Z-score and VAT, the correlation between VAT and vertebral bone marrow fat became insignificant ($P = 0.28$), but VBMA and BMD remained significant ($P = 0.04$). No significant difference in DXA and MRI measured bone parameters was evidenced between women with or without diabetes. In contrast, diabetic women with microvasculopathy demonstrated altered bone microarchitecture compared to healthy controls and those without microvasculopathy, but they did not show any significant differences in DXA measured bone parameters. AppTbSp showed a significant inverse association to TB BMD ($r = -0.40$, $p = 0.04$) and FN BMC ($r = -0.41$, $p = 0.04$).

Conclusions: In this young-aged population, a negative relationship existed between MRI-measured VBMA and femoral neck, lumbar spine and total body BMD independent of demographics and body composition. These observations support the growing evidence

linking BMA with low bone density. Comparing to DXA scan, micro-MRI appears promising to assess bone microarchitecture in term of its feasibility to detect disease-related changes in women with T1DM compared to healthy controls.

5.2 Introduction

T1DM is a chronic metabolic disorder that is characterized by a pathological quantity and distribution of adipose tissue (542). Looking at the literature, it is quite clear that patients with T1DM are at high risk of osteoporosis (548) and fracture (160, 161, 221). There is a growing body of evidence that suggests that the fat bone connection plays an important role in the pathophysiology of bone loss. Previous studies have reported an inverse association of BMA with BMD in patients with osteoporosis and other metabolic diseases (457, 466, 549). BMA is higher in mouse models with T1DM (249), however, the relationship of BMA and BMD in T1DM has scarcely been studied (369). Although, this is potentially related to altered mesenchymal stem cell differentiation into osteoblasts or adipocytes(199), the role of marrow adiposity and its relation to bone remains poorly understood. One important area of clinical investigation has considered the relationship between marrow adiposity and other body adiposity depots. However, several clinical and experimental studies indicate that adipose tissue itself is not functionally uniform, and different adipose depots have distinctive characteristics in terms of adipocytokine production(550, 551), and consequently may have distinct relationships with bone. Evidence regarding the relationship between VAT, BMA and bone health is inconsistent. Recent evidence suggests that VAT may negatively impact bone health. Decreased BMD and altered bone microarchitecture was associated with marrow adiposity and visceral adiposity in other different populations (460, 469, 491, 552). However, these relationships have not been examined in women with T1DM.

Our primary objective was to evaluate different measures of adiposity in healthy young women and women with T1DM, and to determine associations of these adiposity measures with BMD, BMC using DXA, and trabecular bone microarchitecture using high resolution MRI. The secondary objective was to compare the feasibility of DXA and MRI measured bone parameters to differentiate between women with and without T1DM.

5.3 Subjects and methods

5.3.1 Subjects

This was a cross-sectional, controlled study of 17 women between the ages of 17 and 34 years who were diagnosed with T1DM before the age of 16 years and who returned for a follow up visit between January 2014 and July 2014 in the previous longitudinal study of bone health (Chapter 4), and had a DXA scan. Of the 11 healthy women who comprised the control group, 9 had DXA scan. Exclusion criteria included the presence of metallic implants and pacemakers, active or planned pregnancy or lactation, kidney disease, chronic use of drugs that are known to affect bone health and other chronic diseases that are known to be associated with an increased risk of fractures. Information on personal health and lifestyle habits, including cigarette smoking, alcohol consumption, current medication, use of vitamins or calcium, age at menarche, use of oral contraceptives, hours of weight-bearing physical activity per week, history of fractures and a family history of early osteoporosis was also collected. Information on age of diagnosis, disease duration, insulin therapy and presence of microvascular complications was obtained from the case records. A glycosylated hemoglobin (HbA1c) measurement within a four-week period of the scan visit was used as current HbA1c. The study protocol was approved by the national research ethics service and all participants provided written informed consent.

5.3.2 MRI acquisition and analysis

Micro MRI data were available in all 17 cases and 11 controls. MRS data were available in 16 case and all controls, MRI of abdominal fat were available in 17 case and 9 controls. All magnetic resonance images acquisitions and analysis were described previously in Chapter 2.

5.3.3 DXA

DXA data were available in 17 cases and 9 matched controls. DXA of the whole body, femoral neck and lumbar spine (L1-L4) was performed to determine the main study outcomes. The bone area (cm^2), BMC (g) and mean areal BMD (g/cm^2) of whole body, femoral neck (FN) and lumbar spine were measured. In addition, bone mineral apparent density (BMAD) at lumbar spine was calculated. For the assessment of the bone mass in addition to the absolute values of bone mineral density presented in g/cm^2 we used the so called Z-score (number of standard deviations the patient's BMD differ from age- sex-

matched reference value). Because of the age characteristic (17-40 yrs.) of our study groups it was inappropriate to use T-score to determine BMD changes and WHO classification of osteopenia and osteoporosis could not be applied. Body composition, including WB-FM (kg), WB-FM Z -score and android/gynoid were obtained from the whole body DXA scan.

5.3.4 Statistical analysis

Statistical analyses were performed using Minitab 17, Minitab Inc, State College, PA. All data were described as medians and ranges; comparison between the cases and controls was performed by the Mann-Whitney U test for continuous variables and by the Chi Squared test for categorical variables. Spearman correlation analysis was used to assess the univariate relationship between continuous variables and statistical significance was set at $p < 0.05$. Multivariable linear regression was performed to examine associations of VBMA, BMD and visceral adiposity. BMA, age, BMI, WB-FM, VAT, SCAT were selected for the regression model because of their relatively high correlations with BMD.

5.4 Result

5.4.1 Clinical characteristics

There were no significant demographic or anthropometric differences between the cases and controls (Table 5.1). The study included 17 patients with T1DM, their median age was 23.7 yrs. (17.4, 34), the median age at diagnosis of the cases was 10.1 yrs. (4.8, 14.8) and the median duration of diabetes was 13.6 yrs (6.8, 26.5).

Table 5.1: Clinical characteristic of study participants

	Cases (n=17)	Control (n=9)	p
Age (yrs)	23.7 (17.4, 34)	21.6 (20, 23.8)	0.1
Ht SDS	-0.03 (-1.5, 1.9)	0.4 (-0.7, 3.2)	0.5
Wt (kg)	68.8 (50.2,91.5)	63.8 (54.4,76.5)	0.5
Wt SDS	1.2 (-1, 2.9)	0.7 (-0.4 , 2.9)	0.5
BMI	24.4 (18.7, 31.6)	22.6 (19.6, 28.0)	0.1
BMI SDS	0.82 (-1.4, 2.4)	0.2 (-0.9, 1.7)	0.1
Smoker	4	0	0.2
Regular alcohol	13	7	1
Menarcheal Age (yrs)	13 (10, 17.50)	12 (11, 15)	0.9
Pregnancy	3	0	0.2
Hormonal use pills (n)	10	9	0.4
Physical activity	3 (0, 10)	3 (1.5, 10)	0.8
Fracture (n)	5	0	
Hypertension	2	0	
Retinopathy	9, (background,8)	-	
Microalbuminuria	3	-	
Total insulin (IU/kg/d)	2.50(1.23, 3.74)	-	
Current HBA1c (mmol/mol)	75 (51,118)	-	

5.4.2 Body composition

Body composition results are summarized in (Table 5.2). MRI –measured abdominal adiposity parameters including CSA, SCAT, VAT and TAT were significantly higher in cases compared to controls. Additionally, women with T1DM had significantly higher DXA-measured whole- body fat mass z-score ($p=0.03$), and a tendency toward higher whole-body fat mass (WB-FM, Kg) and A/G ratio compared to matched healthy controls ($p=0.07$; $p=0.08$, respectively). Median vertebral BM (FF %) was not significantly different between cases and controls. Different body composition measures were significantly correlated among each other (Table 5. 3). BMI was positively correlated with DXA measured adiposity parameters and MRI-measured abdominal adiposity parameters. Age positively correlated with A/G, CSA, SCAT, VAT and TAT. There was no effect of disease related parameters on different body composition measures.

Table 5.2: Bone and body composition parameters in women with T1DM and matched controls

	Cases (n=17)	Controls (n=9)	p
Bone microarchitecture			
App BV/TV	0.29 (0.25, 0.38)	0.32 (0.27, 0.42)	0.1
App TbN (mm-1)	0.26 (0.20, 0.32)	0.27 (0.24, 0.31)	0.2
App TbSp (mm)	2.65 (2.06, 3.38)	2.52 (1.94, 2.79)	0.08
App ThTh (mm)	1.17 (0.95, 1.46)	1.19 (1.00, 1.52)	0.7
BMA L3 fat fraction (FF %)	26.9 (17.2, 58.5)	25.2 (8.3, 35.1)	0.5
TB BMC (g)	2504 (1669, 2967)	2636 (2147, 3)	0.3
TBMD g/cm ²	1.1 (1, 1.2)	1.1 (1, 1.3)	0.5
TB-BMD z score	-0.2 (-1.1, 1.5)	0.4 (-1.2, 2.0)	0.3
L2-L4 BMC (G)	49.8 (26.6, 60.8)	56.7 (38.2, 66.9)	0.2
L2-L4 BMD (g/cm ²)	1.18 (0.82, 1.39)	1.24 (0.99, 1.42)	0.8
L2-L4 BMD z score	-0.1 (-3.1, 1.6)	0.4 (-1.7, 1.8)	0.8
BMAD	0.38 (0.29, 0.42)	0.37 (0.27, 0.46)	0.7
Femoral BMC (G)	28.2 (21.3, 34.1)	31.1 (24.2, 35.8)	0.2
FN-BMD (g/cm ²)	0.94 (0.84, 1.13)	0.98 (0.88, 1.22)	0.6
FN-BMD Z-score	-0.6 (-1.2, 1)	-0.2 (-1.2, 1.7)	0.3
MRI-measured adiposity			
CSA (mm ³)	51829 (31807,73485)	39761 (32004, 55860)	0.04
SCAT (mm ³)	22662 (8747, 38179)	12529 (8078, 25829)	0.02
VAT (mm ³)	6085 (2112, 11373)	3460 (1864, 7134)	0.004
TAT (mm ³)	28274 (14727, 49161)	16251 (10343, 32963)	0.007
DXA-measured body fat			
Android/Gynoid	0.8 (0.5, 1.1)	0.8 (0.6, 0.9)	0.08
WB-FM (kg)	24.47(14.30,41.53)	17.56(14.01,31.76)	0.07
WB-FM z score	1.1 (0.5, 2.5)	0.3 (-0.2,1.9)	0.03

Table 5.3: Correlations among body fat measures in T1DM and Matched Controls

	CSA	SCAT	VAT	TAT	WB-FM(Kg)	WB-FM Z-score	A/G
SCAT (mm ³)	0.98 p=0.000						
VAT (mm ³)	0.55 p=0.003	0.51 p=0.006					
TAT (mm ³)	0.89 p=0.000	0.97 p=0.000	0.66 p=0.000				
WB-FM(Kg)	0.88 p=0.000	0.83, p=0.000	0.51 p=0.009	0.82 p=0.000			
WB-FM Z-score	0.78 p=0.000	0.74, p=0.000	0.69 p=0.000	0.75 p=0.000	0.96 p=0.000		
A/G	0.59 p=0.002	0.83, p=0.000	0.54 p=0.005	0.79 p=0.000	0.51 p=0.008	0.60 p=0.002	
BMA (FF %)	0.09 p=0.66	0.03 p=0.88	0.42 p=0.03	0.12 p=0.57	0.08 p = 0.68	0.19 P= 0.39	-0.01 p= 0.95

5.4.3 Bone measured parameters

Results of the measurement of bone mineral density and bone microarchitecture in women with T1DM and that in age matched healthy controls are presented in Table 5.2. All results are presented as median and range. No significant difference in DXA and MRI measured bone parameters was evidenced between women with or without diabetes. In contrast, diabetic women with microvasculopathy demonstrated altered bone microarchitecture compared to healthy controls and those without microvasculopathy, but they did not show any significant differences in DXA measured bone parameters (data not shown). DXA-measured BMD at different measured sites showed positive significant association with body weight, but this association was not observed between body weight and MRI-measured bone microarchitecture parameters. AppTbN and appTbSp showed significant association with the age of the whole participants ($r=-0.56$, $p=0.003$; $r=0.45$, $p=0.02$, respectively) and disease duration ($r=-0.49$, $p=0.04$; $r=0.54$, $p=0.03$, respectively) in patients with T1DM. This association was not observed between age and disease duration with BMD at all measured sites. In women with T1DM, by using regression analysis the negative association of AppTbN and appTbSp with age and disease duration became insignificant ($r^2=33.54\%$).

Correlation among different measured bone parameters are showed in Table 5.4. There was a significant correlation among DXA measured parameters at different skeletal sites ($P<0.05$). AppTbSp showed a significant inverse association to TB BMD ($r= -0.40$, $p=0.04$) and FN- BMC ($r =-0.41$, $p=0.04$) (Figure 5.1). Additionally, appTbSp showed a trend toward inverse association with TB BMC and FN-BMD($r=-0.37$, $p=0.07$) (Figure 5. 1).

Table 5.4: Correlation among bone measures in T1DM and matched controls.

	AppBV/TV	AppTb.N(m m)	AppTb.Sp(m m)	AppTbTh(m m)	TB BMC (g)	TB-BMD	TB-Z score	L2-L4 BMC	L2-L4 BMD	L2-L4 Z score	L2-L4 BMAD	FN- BMC (G)	FN- BMD
TB BMC (g)	0.24 p=0.2	0.25 p=0.2	-0.36 p=0.07	0.09 p=0.6									
TB-BMD	0.34 p=0.09	0.23 p=0.2	-0.40, p=0.04	0.21 p=0.3	0.88 p=0.000								
TB-Z score	0.23 p=0.3	0.17 p=0.4	-0.25 p=0.2	0.11 p=0.6	0.71 p=0.000	0.89 p=0.000							
L2-L4 BMC	0.30 p=0.1	0.10 p=0.6	-0.33 p=0.1	0.27 p=0.2	0.78, p=0.000	0.79 p=0.000	0.68 p=0.000						
L2-L4 BMD	0.27, p=0.2	0.07 p=0.7	-0.27, p=0.2	0.28, p=0.2	0.78 p=0.000	0.89 p=0.000	0.76 p=0.000	0.89 p=0.000					
L2-L4 Z score	0.29, p=0.1	0.09 p=0.6	-0.29, p=0.1	0.28, p=0.2	0.78 p=0.000	0.87 p=0.000	0.76 p=0.000	0.90 p=0.000	0.99 p=0.000				
L2-L4 BMAD	0.13, p=0.5	0.08 p=0.7	0.14, p=0.5	0.10, p=0.6	0.73 p=0.000	0.81 p=0.000	0.75 p=0.000	0.71 p=0.000	0.91 p=0.000	0.91, p=0.000			
FN-BMC (G)	0.30, p=0.1	0.28, p=0.1	-0.41, p=0.04	0.17, p=0.4	0.83 p=0.000	0.85 p=0.000	0.72 p=0.000	0.87 p=0.000	0.84 p=0.000	0.83, p=0.000	0.71, p=0.000		
FN-BMD	0.35, p=0.08	0.26 p=0.2	-0.37, p=0.07	0.20, p=0.3	0.61 p=0.001	0.72 p=0.000	0.68 p=0.000	0.69 p=0.000	0.75 p=0.000	0.76, p=0.000	0.72, p=0.000	0.81, p=0.000	
FN-Z score	0.30, p=0.1	0.26 p=0.2	0.29, p=0.1	0.15, p=0.4	0.45 p=0.02	0.85 p=0.000	0.68 p=0.000	0.57 p=0.000	0.65 p=0.000	0.67, p=0.000	0.64, p=0.000	0.68, p=0.000	0.93, p=0.000

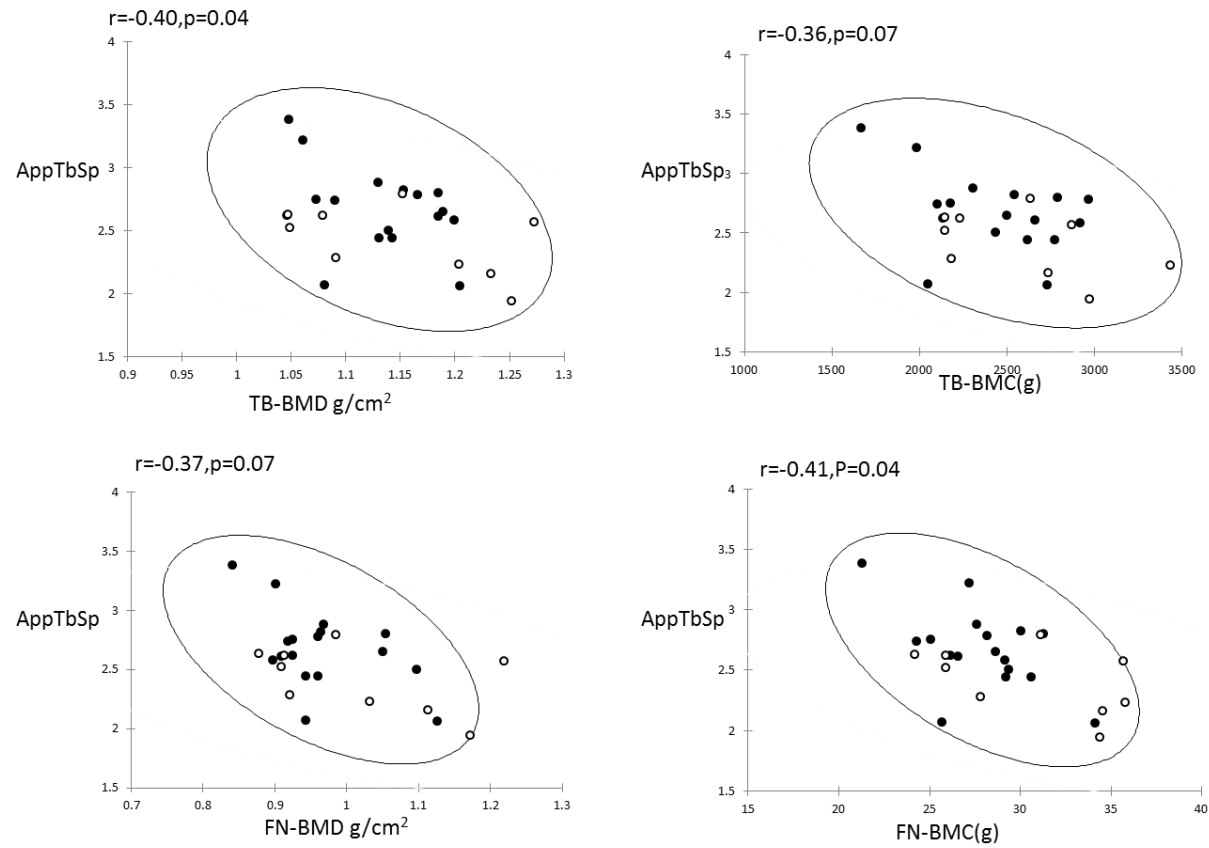


Figure 5.1: The relationship between apparent trabecular separation (appTbSp) as assessed by MRI and total body BMD (TB-BMD g/cm²), Total body BMC (TB-BMC (g)), Femoral neck BMD (FN-BMD (g/cm²)) and Femoral neck-BMC (FN-BMC (g)) in women with T1DM (filled circles) and controls (open circles). An inverse significant association between appTbSp and TB-BMD g/cm and FN-BMC (g) was observed

5.4.4 The relationship among different measures of body composition and bone measured parameters

Table 5 showed the correlation among different measures of body composition and bone measured parameters. MRI measured bone parameters did not show any significant association with vertebral BMA. However, VBMA showed significant negative correlation with TB-BMD, L2-L4 BMD and FN-BMD ($r=-0.54$, $P=0.005$; $r=-0.40$, $p=0.04$; $r=-0.44$, $p=0.03$; respectively) (Table 5.5) (Figure 5.2). This negative association was also observed with L2-L4 BMD Z score and FN- BMD Z score ($r=-0.41$, $P=0.04$; $r=-0.40$, $P=0.05$; respectively) (Table 5.5) (Figure 5.2). Femoral BMC (G) was also significantly associated with BMA ($r=-0.425$, $P=0.03$) (Table 5.5) (Figure 5.2). When BMD, BMD Z score and BMC were entered as a dependent variable and age, BMI, VBMA, SCAT, VAT and WB-FM as independent variables in regression model, vertebral bone marrow fat was a significant predictor of BMD ($p<0.05$) for all models (Table 5.6). On the other hand, Vertebral BMA showed positive correlations with VAT ($r=0.42$, $p=0.03$) (Table 5.5) (Figure 5.3). TB-BMD Z score negatively correlated with VAT ($r=-0.46$, $p=0.02$) (Table 5.5) (Figure 5.3). Because VAT is associated with TB-BMD Z score, we controlled for VAT and TB-BMD Z score using multivariate analysis. After controlling for TB-BMD Z-score, the correlation between vertebral bone marrow fat and VAT became insignificant ($P=0.28$). After controlling for VAT, the correlation between vertebral bone marrow fat and TB- BMD Z score remained significant ($P=0.04$).

Table 5.5: Correlations among bone measures, BMA, and body composition in T1DM and Matched Controls

	CSA	SCAT	VAT	TAT	Total tissue fat	Z- score fat	A/G	BMA
TBMD g/cm2	0.02, P= 0.9	-0.051,P= 0.8	-0.179,P= 0.4	-0.143,P= 0.5	0.060,P =0.8	0.012,p=0.6	0.062,P=0.8	-0.544,P=0.005
TB- BMD z score	-0.21, P= 0.3	-0.259,p= 0.2	-0.457,P= 0.022	-0.378,P = 0.06	-0.176,P= 0.4	-0.199,p=0.4	-0.128,P=0.5	-0.491,p=0.013
TB BMC (g)	0.11, P= 0.6	-0.052,P= 0.8	-0.182, P=0.385	-0.117,P= 0.6	0.212,P= 0.3	0.191,p=0.4	0.008,P=0.9	-0.284,p= 0.2
L2-L4 BMD (g/cm2)	0.14, P= 0.5	0.083,p= 0.7	0.042,p= 0.8	0.004,p= 0.9	0.129,P=0.5	0.155,p=0.5	0.226,P=0.3	-0.405,P= 0.04
L2-14 BMD Z score	0.11, p= 0.6	0.059,p= 0.8	0.023,p= 0.9	-0.022,p= 0.9	0.114,P=0.6	0.146,p=0.5	0.227,P=0.3	-0.410,P= 0.04
L2-L4 BMC (G)	-0.01, p= 1	-0.108,p= 0.6	-0.122,p = 0.5	-0.197,p= 0.3	-0.018,P=0.9	-0.013,p=0.9	0.061,P=0.8	-0.347,P= 0.08
BMAD	0.25, p= 0.2	0.193,p= 0.3	0.202,p= 0.3	0.137,= 0.5	0.283,P=0.2	0.162,p=0.5	0.349,P=0.09	-0.382,P= 0.06
Femoral N- BMD (g/cm2)	-0.050,P= 0.8	-0.122,p= 0.5	-0.105,p= 0.6	-0.169,p= 0.4	0.039,p=0.8	-0.021,p=0.9	0.067,P=0.7	-0.444,P= 0.03
FN- BMD Z-score	-0.232,p= 0.2	-0.274,p= 0.2	-0.201,p= 0.3	-0.304,p= 0.1	-0.136 ,p=0.5	-0.211,p=0.3	-0.027,P=0.9	-0.400,P= 0.05
FN- BMC (G)	-0.009,p = 1	-0.075,p= 0.7	-0.169,p= 0.4	-0.151,p= 0.5	0.045,p=0.8	0.032,p=0.9	0.008,P=-0.9	-0.425,P = 0.03
App BV/TV	-0.300,p=0.1	-0.279,p=0.2	-0.200,p=0.3	-0.289,p=0.1	-0.139, p=0.5	-0.072,p=0.7	-0.071,p=0.7	-0.287,p=0.1
App TbN (mm-1)	-0.404,p=0.04	-0.262,p=0.2	-0.292,p=0.1	-0.269,p=0.2	-0.033,p=0.9	0.072,p=0.7	-0.095,p=0.6	-0.280,p=0.2
App TbSp (mm)	0.369,p=0.06	0.315,p=0.1	0.312,p=0.1	0.348,p=0.07	0.120,p=0.6	0.003,p=0.9	0.130,p=0.5	0.358,p=0.08
App ThTh (mm)	-0.001,p=0.9	-0.032,p=0.9	0.090,p=0.6	-0.021,p=0.9	-0.019,p=0.9	-0.017,p=0.9	0.117,p=0.7	-0.028,p=0.9

Table 5.6: Regression model with BMD and FN-BMC as the dependent variable

Dependent variable	Independent variable		
	1	2	3
TBMD g/cm ²	-0.00348 (0.01)	-0.00374 (0.006)	-0.00361 (0.02)
TB- BMD z score	-0.0422 (0.01)	-0.0396 (0.02)	-0.0396 (0.02)
L2-L4 BMD (g/cm ²)	-0.00680 (0.03)	-0.00743 (0.02)	-0.00864 (0.02)
L2-L4 BMD Z score	-0.05739 (0.03)	-0.0624 (0.02)	-0.0720 (0.02)
Femoral N- BMD (g/cm ²)	-0.00452 (0.02)	-0.00466 (0.02)	-0.00541 (0.01)
FN- BMC (G)	-0.18919 (0.02)	-0.1951 (0.02)	-0.1976 (0.03)

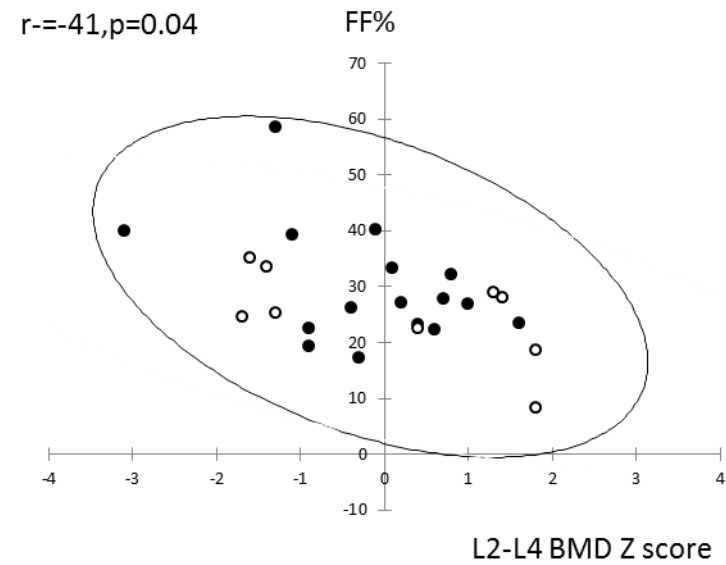
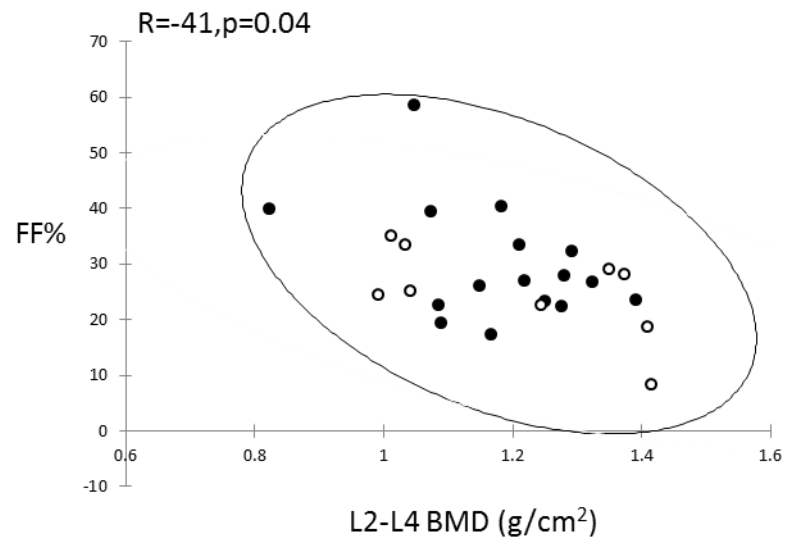
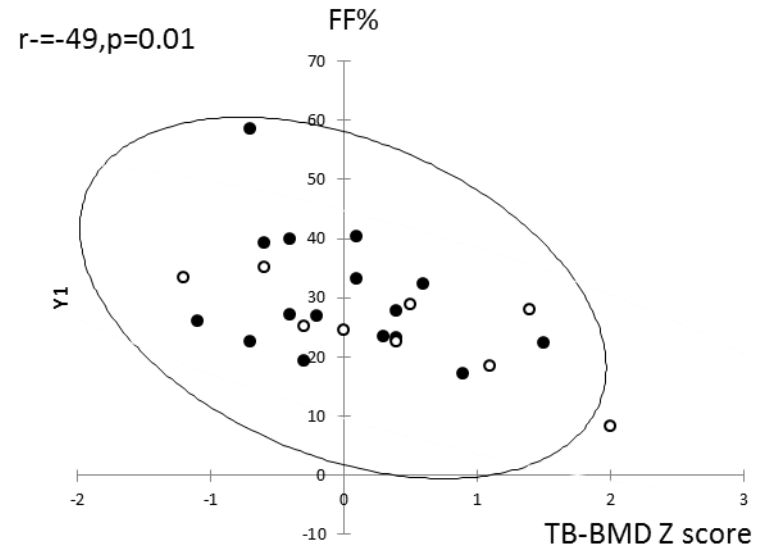
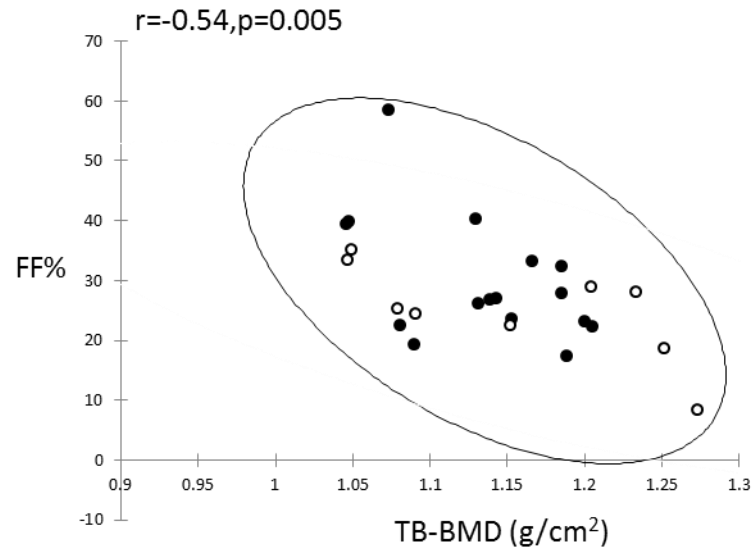
Note: Values are regression coefficients and p-value are in between the bracket. Abbr.: TB BMD; total body bone mineral density; L2-L4 BMD; lumbar spine bone mineral density; FN-BMD; femoral neck bone mineral density; FN-BMC; femoral neck bone mineral content.

Age is the covariate tested in each model:

Model 1 = VBMA + age + BMI

Model 2 = VBMA + age + WB-FM.

Model 3 = VBMA + age + SCAT + VAT.



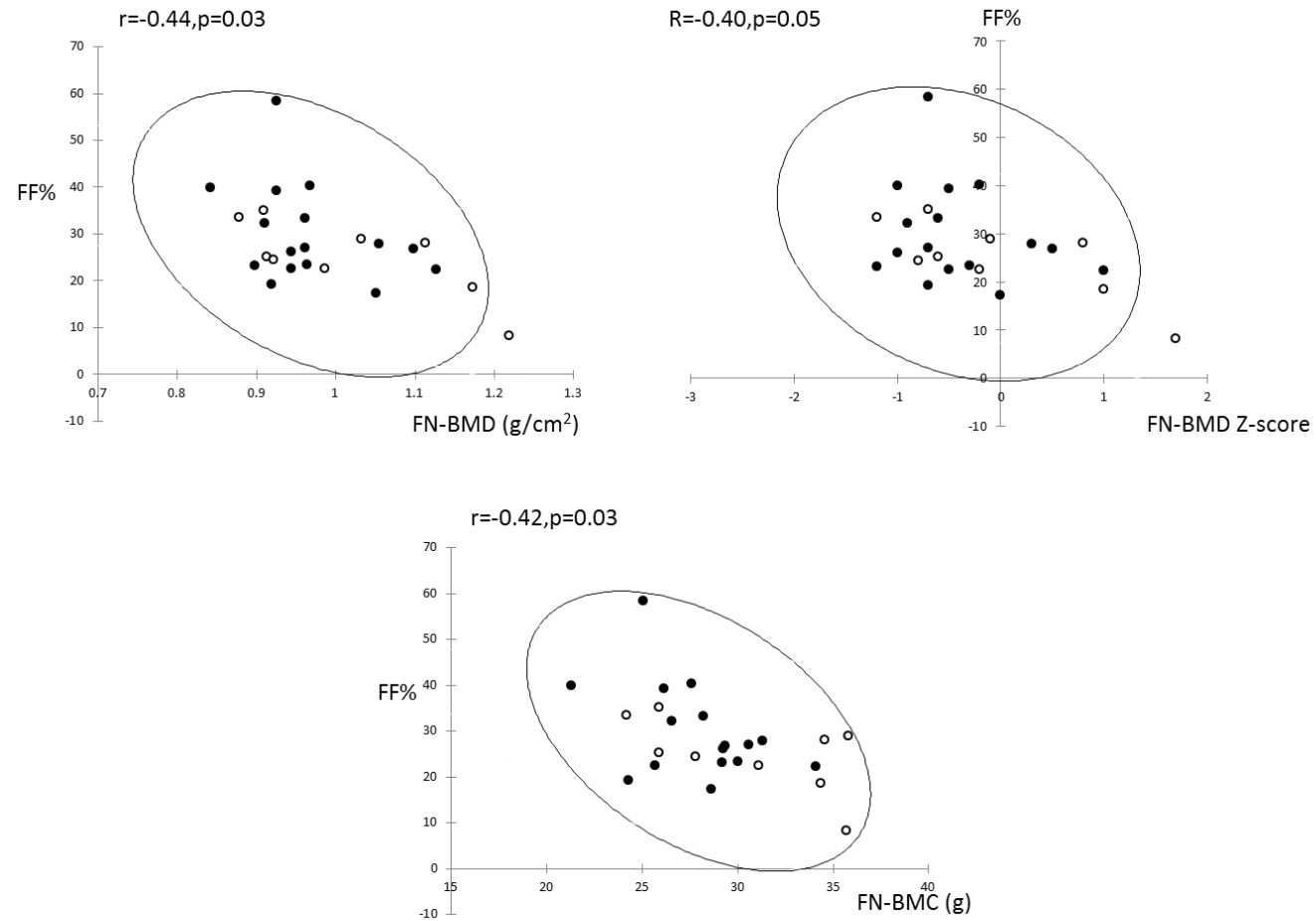


Figure 5.2: The relationship between VBMA and BMD and BMC at different measured sites (Whole body, FN, L2-L4) in women with T1DM (filled circles) and controls (open circles).

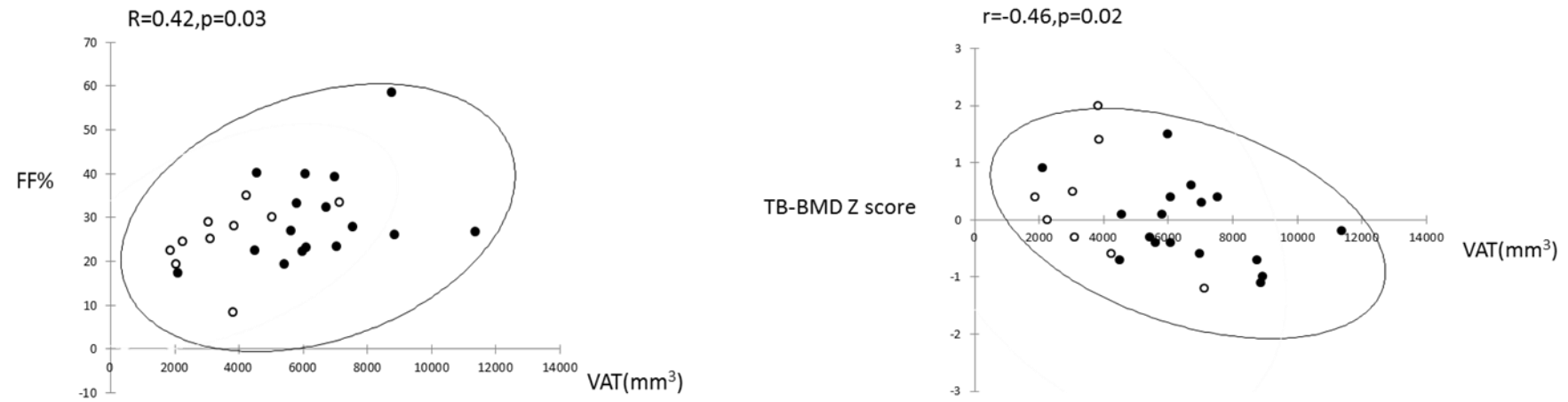


Figure 5.3: The relationship between visceral adipose tissue (VAT) as assessed by MRI and vertebral bone marrow adiposity (FF %) and Total body BMD (TB-BMD (g/cm²)) in women with T1DM (filled circles) and controls (open circles).

5.5 Discussion

To our knowledge, this is the first study to characterize relationships between detailed measures of body composition with DXA and MRI measured bone parameters in young healthy women and women with T1DM. Our study demonstrated that young women with T1DM had greater adiposity parameters compared to the healthy controls. Moreover, our data suggest that vertebral BMA is negative predictor of BMD despite normal BMD and trabecular bone microarchitecture.

The key finding in this study was demonstration of a striking inverse relationship between DXA measured bone parameters at different measured skeletal sites and BMA. Several studies have shown that BMD and BMA are reciprocally related in diverse population, e.g., anorexia nervosa, glucocorticoid therapy, healthy children, young adults, elderly and other osteoporotic conditions (443, 452, 457-461, 463, 537, 553, 554). Rodent models of T1DM showed that higher BMA, which occur in diabetes, correlates with decreased bone biomechanical quality and increased fractures (249). However, the relationship of BMA and BMD in people with T1DM has scarcely been studied, our finding is consistent with a recent study in type one diabetic people reported that BMA was not altered by T1-diabetes, but was inversely related to BMD (369). The current findings provide additional support at the macroscopic level for an inverse relationship between BMA and BMD. Since osteoblasts and adipocytes share a common precursor (i.e., the MSCs in bone marrow) (119, 194, 555), it is hypothesized that an increase in adipogenesis may impair bone integrity through reducing osteoblastogenesis (194). On the other hand, we did not observe this significant correlation with the measures of bone microarchitecture. There are few studies that have examined the association of bone microarchitecture with BMA (556, 557). Although, the effect of BMA on bone is different depending on the bone parameter of interest, bone marrow is highly concentrated in trabecular bone and the correlation between BMA and trabecular bone might be stronger than that with BMD, therefore, the lack of this association in our study might be due to small sample size. More studies with larger sample sizes are needed on the association between BMA and skeletal health. In particular, no prospective study has related BMF to fracture, the most important clinical consequence of osteoporosis.

In the present study, we observed an inverse relationship between BMA and BMD in an anatomically matched region (i.e., spine BMA and spine BMD), and non-anatomically matched region (i.e. spine BMA with femoral and total body BMD). Therefore, it is reasonable that both local level MSC differentiation and systemic level hormonal factors contribute to the observed inverse relationship between BMA and BMD. Our results add to

the body of literature that supports the competitive relationship between marrow fat and bone. Future studies may investigate potential targets to prevent and treat osteoporosis at both the MSC level and hormonal level.

In addition to the detrimental effect of BMA on bone health, VAT was negatively correlated with TB-BMD Z score and positively correlated with BMA, but this association became insignificant after regression analysis. The role of VAT on bone has not been elucidated yet; previous studies in other population have shown inconsistent association between body composition and bone measures (360, 494, 558-564). These studies were limited by the use of dual-energy x-ray absorptiometry (DXA), which is unable to distinguish VAT from SAT. In our study, despite high correlation between the DXA and MRI measured parameters of body composition, we found differences in their relation with BMA and bone measured parameters. Our data are in consistent with some reports (360, 564) that did not show any association between body composition assessed by DXA and BMD. In contrast, recent studies have reported that visceral fat has negative effects on bone health and correlates inversely with BMD and bone structure (486, 488-493). However, in our data we did not find this association with bone microarchitecture. In consistent with our findings, Bredella et al. (491) concluded that both BMA and VAT have detrimental effect on BMD whereas there was no difference in BMD, but these results remained significant even after adjustment for BMD. The effect of visceral adiposity is associated with dysregulation of the GH/IGF-I which is important regulators of bone homeostasis and importance for the maintenance of bone mass (506). Thus, further studies with larger sample size are needed to clarify this association in women with T1DM.

Another interesting finding, in consistent with Shanbhogue, V.V., et al (163) we have demonstrated that 3T MRI can detect deficit in bone microarchitecture which was only apparent in T1DM with microvasculopathy compared with the healthy controls. In contrast, we did not observe any differences in DXA measured bone parameters between T1DM with or without microvasculopathy and healthy controls. The discrepancy between DXA and trabecular bone results is consistent with previous studies in other population (153, 159, 565). Because DXA could not detect lower BMD in women with T1DM compared with the controls; the results suggest that MRI assessment of microarchitecture may potentially be more sensitive than DXA assessment of areal BMD as a method to assess changes in bone quality related to diabetes mellitus.

Although, there was discrepancy between DXA and MRI to determine bone deficit in severely affected diabetic women compared to healthy controls, we found minor positive correlation between the bone DXA-based measures and MRI-based measures. Previous

studies have reported this correlation (403, 431, 432, 566, 567). In our study the correlation was not observed with all MRI parameters, non-anatomically matched region was limitation of this study comparing to what previously described (567). The positive relationship between the MRI-based measures and the DXA-based measures provides some validation for the assessment of trabecular bone using MRI. Additionally, this minor correlation indicates that the MRI method of bone quantification is providing additional structural properties from trabecular bone that cannot be measured by DXA.

5.6 Conclusion

Our study group was relatively small and therefore conclusions must be drawn with some caution. However, in this population-based study group, with carefully matched control subjects, women with T1DM demonstrated greater pattern of adiposity compared to healthy controls. Additionally, we found that vertebral BMA was a significant predictor of BMD, whereas there was no difference in BMD, suggesting a distinct role of BMA in skeletal integrity

More importantly, in T1DM our study has demonstrated the feasibility of 3-T MRI to differentiate between women with and without microvasculopathy. On the other hand, 3-T MRI-derived measures showed positive correlations with DXA-derived BMD, suggesting that the two methodologies assess similar and complementary characteristics of bone. However, this is a small pilot study, and further validation with a large cohort is necessary.

Chapter 6

Discussion, conclusion and future perspective

6.1 General discussion

The studies presented in this thesis are the first clinical studies to investigate bone health by using high resolution micro-MRI (3T) in young women with childhood-onset T1DM compared with healthy women without T1DM. These studies add a number of novel findings to the knowledge base.

Deficit in trabecular bone microarchitecture in young adult women with childhood-onset T1DM compared with women without T1DM was demonstrated in Chapter 3. This cross-sectional study elucidated some possible underlying mechanisms that might contribute to deficits in trabecular bone microarchitecture, including: (1) patients with T1DM had a state of low bone turnover with reduced bone formation and resorption compared with healthy age matched controls; (2) deficit in the GH/IGF-1 axis; (3) associated diabetic microvascular complications. The deleterious effect of T1DM on trabecular bone microstructure is well established in rodent models of T1DM (568, 569). Currently, there is no published research about using MRI for studying trabecular bone microarchitecture in people with T1DM. However, as described in the introduction, two studies in humans have evaluated trabecular bone microarchitecture using HR-pQCT and histomorphometry and mCT techniques in adults with T1DM compared with healthy controls and the results were conflicting (163, 570). Since this study began, a single cross-sectional study has been published that evaluated bone structural parameters using HR-pQCT in adults with T1DM in comparison with healthy controls (163). This study reported that trabecular bone deficit was not characteristic of all T1DM patients, but of a subgroup characterized by the presence of microvascular complications. This finding is confirmed by our study; although bone deficits were observed in all the participants with T1DM, it was remarkably noticeable in those with microvascular complication. On the other hand, Armas *et al.* (570) reported no abnormalities in trabecular bone histomorphometric or mCT variables in a small cohort of adult with T1DM (n=18) in the absence of detectable microvascular complications. However, it was possible that the sample size in this study was not sufficient to detect between-group differences in multiple measures of trabecular bone microarchitecture. Previous *ex vivo* and *in vivo* studies have shown that trabecular bone microarchitecture parameters play an important role in the determination of bone strength and structural changes associated with bone pathology (403, 434, 571). Moreover, previous studies have shown that MRI-measured trabecular microarchitecture parameters are effective in differentiating subjects with and without fragility fractures (152). Therefore, our results suggest that the observed compromised trabecular bone microarchitecture may provide an explanation for increased fracture risk in women with T1DM. Further large

prospective studies will be required to determine whether MRI can potentially improve fracture prediction in this population.

Our study identified the association of microvascular complications with compromised bone microarchitecture as possible underlying mechanisms of diabetic osteopathy. This has been demonstrated in T1DM (163) as well in T2DM (572), and similarly our longitudinal study (Chapter 5) has confirmed this association. Although our sample size of participants with microvascular complications was very small ($n=8$), trabecular bone deficit was more noticeable in this group compared with those without microvascular complications and healthy controls. Interestingly, by using regression model and adjusting for multiple variables (age, BMI, disease duration, age of diagnosis, glycaemic control), microvascular complication was negative significant predictors of reduced bone volume. Thus, our data are consistent with abundant evidence which suggests that patients with T1DM are at significant risk for greater bone loss from diabetic complications such as vascular disease, retinopathy, nephropathy, and neuropathy (161, 162). The independent association of microvascular complications with reduced BMD and higher fracture risk has been reported previously (342, 345, 573-575). Some studies reported higher fracture risk in T1DM patients with microvascular complication, independent of BMD (161). This discrepancy could be explained by frequent falls that might result from associated microvascular complications (576). Therefore reduced BMD and compromised bone microarchitecture in combination with an increased susceptibility for falls likely explains the higher fracture risk in patients with T1DM.

Moreover, this study confirms the findings from previous reports that suggest that bone deficit in T1DM patients is associated with low bone turnover with reduced bone resorption (163, 224, 369) as described in section 1.4.3, and is accompanied by an inactive GH/IGF-1 pathway compared with healthy controls as described in section 1.4.4 (164). In our study this mechanism is elucidated and confirmed through the negative association of trabecular separation with total osteocalcin and ALS in women with T1DM. This study was the first to find the association between the markers of bone metabolism and trabecular bone microarchitecture parameters in women with T1DM. Insulin-like growth factor-1 (IGF-1) is an important local factor regulating bone turnover, promoting the proliferation and differentiation of osteoblasts, and its activity is modulated through its binding to proteins such as IGFBP-3 and ALS. Therefore, long-standing low bone turnover with an impaired IGF system which observed in T1DM may result in defective micro damage repair and increased bone micro crack accumulation that contributes to excess skeletal fragility and thus increased fracture risk. In non-diabetes subjects, bone turnover markers

are correlated with bone deficit and predicted fragility fractures (577) and accordingly bone turnover may be a marker of fracture risk in T1DM. However, this is not observed yet in T1DM. Additionally, IGF-1 is reported as a potential fracture predictor independent of BMD in postmenopausal women with T2DM (275). Therefore, it is possible that IGF-1 is also a predictor in T1DM. Further studies with larger sample sizes are needed to evaluate the association of fracture risk with trabecular bone deficit and bone metabolism to fully understand this mechanism.

Other possible explanations for bone deficit in young women with childhood onset T1DM include longer disease duration and poor glycaemic control. As mentioned in section 1.4.4, the existing data regarding these factors are still conflicting. Despite our study participants having childhood onset T1DM at a young age, the median age at diagnosis was 9.7 years (0.46, 14.8) and the median duration of T1DM was 12.8 years (7.9, 34.2), we did not observe any significant association of the observed bone deficit with age of diagnosis or disease duration. This finding may provide support to the inherent concept which suggests that childhood onset T1DM results in impairment of attaining peak bone mass and results in predisposition to more fragile bones later in life.

Additionally, the influence of glycaemic control on bone has not yet been well established as clinical studies exist to both support (346, 354) and rebut this idea (319, 564), but it has been well clarified in *in vitro* studies (226). The majority of the previous studies measured HbA1c at a single time point, which does not reflect long term hyperglycaemia. There are only a few studies that investigated repeated measures of HbA1c, and chronically poor glycaemic control has been found to correlate with low BMD (358, 370). Although our participants had poor glycaemic control and median HbA1c was 9.8% (5, 16), a relationship between HbA1c and MRI measured parameters was not demonstrated in the cross-sectional design. It has been shown that HbA1c levels above 9% compared with levels of 6-7% increase the risk of hip fracture (578). Our study was limited by the small sample size and limited range of HbA1c. Clearly, larger studies are required in the future to comprehensively establish how chronic hyperglycaemia influences trabecular bone parameters and other bone-related surrogate markers in particular fracture incidents. On the other hand, the adverse effects of chronic hyperglycaemia may be related to the accumulated AGEs (Pentosidine) which may impact bone quality (18). However, in the current study we did not observe any association of bone parameters with pentosidine. Larger sample size is needed to clarify this association.

Increasing BMA is another underlying pathophysiological mechanism for bone deficit in T1DM (204, 249), but it has not yet been clarified in patients with T1DM. Although our

study participants had greater abdominal adiposity parameters compared with healthy controls, consistent with those reported by Slade *et al.* (369), our baseline data did not allow us to demonstrate an abnormality of BMA in patients with T1DM. Additionally, we did not observe any association of BMA with MRI-measured trabecular bone parameters and biochemical markers of bone turnover, adiposity or GH/IGF-1 axis. The cross-sectional design and small sample size did not allow us to explore these associations; it is possible that a longitudinal design with larger sample size would allow these associations to be identified.

Based on this hypothesis, the study described in Chapter 4 was designed to explore the longitudinal changes in MRI-based measurements of bone health and adiposity in young women with T1DM compared with healthy controls. Furthermore, this study examined the possible underlying mechanism that might be associated with the expected changes. An advantage to using a prospective study design over a cross-sectional design is that insight can be gained into the time course of skeletal changes in T1DM compared with healthy controls, improve understanding of the bone pathology in diabetes and facilitate the design of future intervention studies aimed at preventing bone loss and thus reduce fracture risk. Although there were no differences between groups for bone marrow adiposity at the baseline, and no changes over time, this study has shown for the first time a clear positive association between changes in HBA1C and BMA in women with T1DM. This finding is reinforced by our baseline data which showed positive association between current HBA1c and BMA. There is a wealth of knowledge about the process and factors involved in adipogenesis and its association with bone loss in relation to T1DM; however, the current understanding of adipogenesis has largely emerged from *in vitro* studies (204). Consistent with our findings, it has been suggested that poor glycaemic control is a potential factor for accelerating adipogenesis in diabetes (579). It is also possible that the states of GH resistance associated with persistent hypoinsulinemia and poor glycaemic control might underlie mechanisms of increased bone marrow adiposity in T1DM. Currently, there are no longitudinal studies evaluated BMA in humans with T1DM, and given the extent of variation in our data, a larger sample size may assist in conclusively evaluating this association. Similar to our finding, poor glycaemic control has been demonstrated to lead to increased bone marrow adiposity in T2DM (466). There is increasing evidence of a direct link between BMA with bone strength (467) and fracture risk (464), so this is an important finding that may provide us not only with an understanding of diabetic adipogenesis but also with designing future intervention studies aimed at preventing bone loss.

Unlike BMA, the average changes were lower for the bone microarchitecture parameters and did not show any association with the changes of glycaemic control over a one year period. However, despite the wide variability of our data, the median of the percentage of these changes was still lower than that reported in healthy volunteers (411). With mixed modelling analysis, we observed that age was a negative predictor of these changes. This finding is consistent with recent a report which showed that alteration in trabecular microarchitecture occurs with aging (580). Interestingly despite the relatively smaller number of the cases, the study showed that bone deficit still exists in diabetic women compared with controls and this deficit is particularly marked in those with microvascular disease. These differences remained even after correction for age, BMI and abdominal adiposity parameters. The association of trabecular bone deficits with microvascular disease but not with glycaemic control suggested that both of these factors work independently. Theoretically, the lack of association between the changes in trabecular bone parameters and short-term changes in glycaemic control might indicate that poor glycaemic control at the onset and the initial years in the development of microvascular complications could dictate the long-term consequences to skeletal integrity. Currently, there are no longitudinal studies evaluating the changes of trabecular bone microarchitecture in T1DM, but because BMD measurements are related to trabecular bone microarchitecture measurements (431), prospective studies on BMD changes in patient with T1DM (345, 346, 535, 581-583) are informative and might help in understanding our findings. Consistent with our findings, one study has shown that young women with T1DM have lower bone mineral density that persists over time (346). However, some studies suggest that greater longitudinal decline in BMD occurs over time which was particularly observed in males with T1DM and those who develop microvascular complications over the follow-up period (345, 534, 581, 583). The inconsistency between existing studies may be due to the variability of included populations, as some data were not analysed by gender (583), and some studies observed that an increase in BMI and the improvement of glycaemic control may have a protective effect and contribute to the stabilization of BMD (345). Small sample sizes (583) and relatively short period of follow up (582) were other confounding factors. Overall, the lack of changes in the measures of trabecular bone microarchitecture in this study support the evidence that greater loss in BMD occurs within the years of achieving peak bone mass at the time of T1DM onset, which may explain why women with type 1 diabetes have skeletal fragility and an increased risk of fractures later in life. However, the small sample size, short period of follow up and wide variability of the data limited us in making a

definitive conclusion. Further longitudinal studies with a longer follow up interval including men and women and children at the time of T1DM onset are clearly warranted.

There is a growing body of evidence to indicate the association between fat and bone health. However, the way in which fat at different locations directly or indirectly influences bone strength has not been clarified to date. In addition to the systemic adverse effect (584), the location of fat deposition is implicated in adverse bone outcomes.

Essentially, increased BMA and greater visceral adipose tissue (VAT) are risk factors of reduced BMD, altered trabecular microarchitecture and increased fracture risk in a variety of populations (460, 469, 482, 491, 492, 552, 556, 557, 585). Given that T1DM is associated with greater body fat composition and abdominal adiposity which was reported previously and observed in our study as well, this study was designed to assess the detailed adiposity determinants of bone health in healthy young women and women with T1DM. In addition to MRI, we used DXA scans to measure the total body composition and BMD in both T1DM and healthy controls. Furthermore, our secondary aim was to compare the feasibility of MRI compared with DXA scans in detecting bone abnormality in those with T1DM compared with healthy controls. To our knowledge, this is the first study to characterize the relationship between detailed measures of body composition with DXA and MRI measured bone parameters in young healthy women and women with T1DM. A number of interesting findings emerged from this study.

Firstly, though the sample size was small, our study demonstrated that young women with T1DM still had greater adiposity parameters compared with the healthy controls.

Additionally, our data suggested that vertebral BMA is an independent negative predictor of BMD at both anatomically and non-anatomically matched regions, but we did not observe this association with trabecular microarchitecture parameters in the current study or in our previous studies (Chapter 3 and 4). This finding is consistent with previous studies that reported an association of BMA with decreased BMD and increased fracture risk in a diverse range of clinical conditions (Section 1.5.2.4.2). Consistent with our finding, one study on T1DM reported this inverse association between BMA and BMD (369). The reciprocal association of BMA and bone parameters is potentially related to altered mesenchymal stem cell differentiation into osteoblasts or adipocytes (199). The normal aging process and a variety of metabolic diseases are suggested to affect this process and favour adipogenesis versus osteoblastogenesis. This suggests that increased BMA will adversely affect bone metabolism and thus the bone strength surrogate markers, including BMD and trabecular microarchitecture parameters. The lack of association

between BMA and trabecular microarchitecture in our study might be due to the small sample size, and therefore more studies with larger sample sizes are needed to clarify this association.

The second result to be considered from our analysis was the significant positive association of VAT with BMA ($r = 0.42$, $p = 0.03$) and TB-BMD Z score ($r = -0.457$, $p = 0.02$), but only the association of BMA and TB-BMD Z score remained significant ($p = 0.04$) in the adjusted model. The positive association of VAT and BMA was also observed in our baseline data, but the lack of DXA results at the baseline unable us to correct it for BMD. This is important finding and support the emerging hypothesis that suggests that the developmental origin of BMA may be more similar to VAT. Lack of the association between abdominal adiposity measures and bone parameters in our study may be due to small sample size.

Another interesting finding was the discrepancy between DXA and MRI measured bone parameters in detecting bone deficits in T1DM patients with microvascular complications compared with those without microvascular complications and healthy controls. This discrepancy is consistent with previous studies in other populations (153, 159, 565). This finding suggested that MRI of trabecular bone microarchitecture may therefore serve as a novel tool for assessing BMD-independent skeletal fragility in T1DM patients.

Additionally, the lack of good correlation between MRI- measured trabecular parameters and DXA-measured BMD support the concept that MRI provides different information about bone quality beyond that provided by DXA. Thus, assessment of BMD and trabecular bone microarchitecture gives a more complete picture of bone health in people with T1DM.

6.2 Final conclusion

The initial hypotheses were evaluated and conclusions based on these hypotheses were:

1. Patients with T1DM had altered trabecular bone microarchitecture, low bone turnover state and a deficit in the GH/IGF-1 axis compared with women without T1DM. A difference in BMA was not discovered between cases and controls as the study was not powered to detect this difference.
2. The deficit in bone microarchitecture in patients with T1DM was associated with abnormal levels of biochemical markers of bone metabolism and the presence of microvascular complications. However, there was no association between this bone deficit and adiposity measures.

3. Although, there were no significant changes over a one year period in the measures of bone microarchitecture and adiposity in women with T1DM compared with women without T1DM, deficits in bone microarchitecture persisted.
4. Different body adiposity measures have different effects on DXA and MRI-measured bone parameters.
5. Vertebral BMA is negatively correlated with BMD and positively with VAT, but we did not demonstrate any association between VAT and DXA and MRI - measured bone parameters.
6. MRI-measured bone parameters were able to differentiate between T1DM patients with microvascular complications and those without microvascular complications, which was not detected by DXA.
7. Although we did not observe an association of markers of diabetic control and other possible clinical factors with bone microarchitecture and biochemical markers of bone metabolism and adiposity, BMA was positively correlated with current HBA1c, moreover, improvement in diabetes control was associated with a reduction in bone marrow adiposity.

Overall, this collection of work provides preliminary evidence that compromised bone microarchitecture, not deficits in BMD, is the underlying basis for excess skeletal fragility in young women with childhood onset T1DM. Moreover, our studies provide additional clues supporting this hypothesis including the association of altered trabecular microarchitecture with low bone turnover accompanied with reduced bone formation and resorption, deficit in the GH/IGF-1 axis and associated microvascular complications. Furthermore, although we did not demonstrate abnormality in vertebral BMA, the observed inverse association between changes in glycaemic control and changes in vertebral BMA may further our understanding of diabetic adipogenesis which may explain excess skeletal fragility in T1DM and point at possible beneficial effects of glycaemic control on bone health in patients with diabetes. This was further reinforced by an independent significant association of BMA with DXA-measured BMD at both anatomically matched and unmatched regions. Moreover, our preliminary finding of a positive association of BMA with VAT but not with BMI and the other body fat depots suggests distinct metabolic roles for visceral fat and other body fat depots, and further suggests that the developmental origin of BMA may be more similar to VAT than SCAT. More importantly, our observed positive correlation between VAT and BMA irrespective of BMD may provide clues to the underlying mechanism of the detrimental effects of

visceral fat on BMD and suggests a distinct role of BMA in skeletal integrity. The discrepancy between DXA and MRI-measured bone parameters in detecting bone deficits in T1DM with microvascular complications compared with those without microvascular complications and healthy controls highlights the sensitivity of MRI-measured bone parameters in identifying structural differences in relatively small cohorts and suggests that trabecular micro architectural parameters might be used as an additional tool to detect patients with poor bone quality who cannot be detected by DXA.

Collectively, these data have improved our understanding of how T1DM adversely impacts bone health, and clearly explain that T1DM is associated with structural bone abnormality that could not be captured with DXA. Therefore, the clinicians should be aware of the association between diabetes and osteoporosis, which is not reflected by the BMD. Thus, if osteoporosis is suspected more investigations should be done to rule out any suspected fracture. The suggestion that bone loss may be another manifestation of diabetes-related microvascular disease raises the possibility that assessment of bone health may become a routine component of screening for health complications in diabetes. Given the advances in routine clinical MRI imaging, our studies clearly show that MRI and MRS are both sensitive techniques for measuring bone quantity and bone quality, and can be readily translated into clinical practice and are likely to lead to improved targeted prevention of fractures in T1DM. Because T1DM is most commonly diagnosed in childhood and adolescence, the early assessment of bone health and skeletal risk factors in children with T1DM will be important, in an effort to maximise the acquisition of peak bone mass in these patients, and to minimise the impact of T1DM on the skeleton going forward.

6.3 Strengths and Limitations

The studies presented in this thesis have important strengths that should be highlighted. To our knowledge, this is the first study that has examined trabecular bone microarchitecture, BMA and the associations among fat distribution and bone outcomes in young women with childhood-onset T1DM using both high resolution MRI and DXA at the same time. Moreover, the well-characterised study population represents a significant strength. However, we acknowledge certain limitations in our studies. First, the sample size was relatively small. The initial power analysis was performed to detect differences in trabecular bone parameters (434). There was no option to calculate the power for a study of BMA to discriminate individuals with T1DM because data were lacking. Additionally, this relatively small sample size might be responsible for the lack of statistical significance in the relationship between BMA with trabecular bone parameters and biochemical markers

of bone metabolism, GH/IGF-1 axis and adiposity. Moreover, it is possible that additional underlying mechanisms would be discovered if a larger number of patients were evaluated; however, the significant findings that were noted suggest that there was adequate power to identify several important differences. Second, the cross sectional study design of Chapters 3 and 5 limits our ability to prove causality concerning the observed significant associations. To facilitate recruitment, we collected non-fasting blood samples; however, markers of bone turnover and especially markers of bone resorption, such as CTX, show a diurnal variation and may be affected by fasting status. Moreover, we did not collect blood samples at the second visit, and this limited our ability to study the longitudinal changes of biochemical markers of bone turnover, adiposity and GH axis, and to find their association with the changes in MRI-based measurements. In addition, studying only one skeletal site limits the ability to generalise our findings to the other skeletal sites. The lack of a sufficient number of cases with other microvascular complications limited the investigation of this association in the current study. Furthermore, many missing HBA1c measurements over a longer time period of 5 to 10 years in most of the cases did not allow us to study the long term effect of glycaemic controls on MRI-measured parameters. Despite the promising results of using micro MRI and MRS to better understand diabetic bone disease, there are still technical challenges to be overcome. In particular, the scan time was relatively long at 10 minutes, which could be restrictive in certain patient groups, and may increase the chance for motion artefact. Though we did not notice motion artefact on our images, in order to increase the applicability of the technique as part of routine clinical investigations, it will be necessary to reduce the scan time. Additionally, MRI has certain disadvantages in measuring trabecular bone microarchitecture as mentioned in the introduction section 1.6.3.4, e.g. partial volume effects, produced when imaging trabeculae that are smaller than the spatial resolution, may confound and overestimate measures of bone microarchitecture such as BV/TV and Tb.Th. Furthermore, MRI is technically demanding, and does not provide the option of measuring BMD and therefore we cannot compare or adjust for bone density at the measured site, and there are fewer reference data. Finally, measuring trabecular structures in the tibia and BMA in the lumbar spine is somewhat of a limitation, as it limited our ability to find the relationship between both parameters in the same location. This was not possible due to technical reasons – MRS was unsuccessful in the tibia, and the small FOV used in micro MRI was not compatible with spine imaging.

6.4 Future Perspectives

The studies presented in this thesis provide novel promising results on structural bone quality in young women with childhood onset T1DM that should be explored in future research studies. Firstly, future investigations should evaluate the association between MRI measured parameters and DXA data in cases of incident fractures which are the most important clinical consequence of osteoporosis. Given that hip fractures are reported to be more common in people with T1DM, examining the trabecular microarchitecture and BMA at this site would be more informative.

Moreover, a numbers of underlying pathophysiological mechanisms have emerged from the studies included in this thesis. More studies with larger sample sizes are needed to confirm these mechanisms and their relationship to the increased fracture risk observed in T1DM. Given the wide range of T1DM-related microvascular complications, there is a need to investigate the association of different microvascular abnormalities with MRI measured parameters. The data from our study could be used for future sample size calculations for a larger prospective study involving a wide spectrum of diabetic related microvascular complications. To draw definitive conclusions about the association of bone turnover markers with MRI-measured parameters, future large longitudinal studies are needed to study the changes of bone turnover marker and their association with changes in MRI parameters and fracture.

The study presented in Chapter 4 provides feasibility data but obviously larger longitudinal studies with longer time intervals are required to study the evolution of T1DM-related trabecular bone microarchitecture and marrow adiposity changes. In addition, more studies are also needed to confirm our findings regarding the potential mechanisms responsible for decreasing BMA in young women with T1DM. Good glycaemic control may decrease BMA; a future study looking at the effect of intensive insulin therapy may confirm this association.

The cumulative evidence suggests that changes in bone architecture are beginning early in childhood, particularly in those diagnosed at very young ages. Additionally, the increased fracture risk in T1DM has been encountered in both sexes and even in young children. Therefore, a definitive prospective study with adequate power comparing trabecular bone microarchitecture and BMA in children and adults of both sexes with T1DM and fragility fractures versus non-fracture T1DM controls is clearly warranted.

Altered bone marrow fat composition expressed as saturated, unsaturated and residual fat was related to T2DM and fragility fractures in postmenopausal women and women with T2DM (464). Consequently, there is a need to examine bone marrow composition in

patients with T1DM as well, and it will be more informative in those with fractures. The MRS acquisition in the current studies was not optimised to allow detection of saturated, unsaturated and residual fat. For future studies, the MRS pulse sequence should be optimised to allow these measurements to be made.

HR-pQCT based cortical abnormalities have been shown to play a key important role in increased skeletal fragility fracture in T2DM (157, 158, 586), and identified in those with T1DM as well (163). Further investigation of cortical bone parameters by using MRI would shed more insight into the pathophysiological mechanism of diabetic bone disease. In the current studies, because of some technical changes we were not able to do this. Firstly, we scanned the proximal tibia which is not the best place to assess cortical bone. Furthermore, the micro MRI images were designed to image trabecular bone, and the image contrast is such that it can be difficult to differentiate between cortical bone and muscle/tendons. For future studies, acquiring images from the distal femur where the cortical bone is thicker is needed. Additionally, ultra-short TE (UTE) pulse sequences are needed to assess cortical porosity. However, this type of pulse sequence was not available on the current scanner. Future studies could involve collaboration with other research groups to access this.

Finally, although there is now sufficient supporting evidence for the use of MRI for assessing bone microarchitecture, future research to expand upon the methodology employed in our studies will improve the clinical utility of 3 Tesla MRI and make it an acceptable option for widespread non-invasive assessment of bone health.

List of References

1. Clarke B. Normal bone anatomy and physiology. *Clinical journal of the American Society of Nephrology : CJASN*. 2008;3 Suppl 3:S131-9.
2. Johnell O, Kanis JA. An estimate of the worldwide prevalence and disability associated with osteoporotic fractures. *Osteoporosis international : a journal established as result of cooperation between the European Foundation for Osteoporosis and the National Osteoporosis Foundation of the USA*. 2006;17(12):1726-33.
3. Dempster DW, Raisz LG. Bone Physiology: Bone Cells, Modeling, and Remodeling. *Nutrition and Bone Health*: Springer; 2015. p. 37-56.
4. Zhou X, Novotny JE, Wang L. Anatomic variations of the lacunar-canalicular system influence solute transport in bone. *Bone*. 2009;45(4):704-10.
5. Saha PK, Liu Y, Chen C, Jin D, Letuchy EM, Xu Z, et al. Characterization of trabecular bone plate-rod microarchitecture using multirow detector CT and the tensor scale: Algorithms, validation, and applications to pilot human studies. *Medical physics*. 2015;42(9):5410.
6. Goldstein SA, Goulet R, McCubbrey D. Measurement and significance of three-dimensional architecture to the mechanical integrity of trabecular bone. *Calcified Tissue Int*. 1993;53(1):S127-S33.
7. Parkinson IH, Fazzalari NL. Interrelationships between structural parameters of cancellous bone reveal accelerated structural change at low bone volume. *Journal of bone and mineral research : the official journal of the American Society for Bone and Mineral Research*. 2003;18(12):2200-5.
8. Feldkamp LA, Goldstein SA, Parfitt AM, Jesion G, Kleerekoper M. The direct examination of three-dimensional bone architecture in vitro by computed tomography. *Journal of bone and mineral research : the official journal of the American Society for Bone and Mineral Research*. 1989;4(1):3-11.
9. Hildebrand T, Laib A, Muller R, Dequeker J, Ruegsegger P. Direct three-dimensional morphometric analysis of human cancellous bone: microstructural data from spine, femur, iliac crest, and calcaneus. *Journal of bone and mineral research : the official journal of the American Society for Bone and Mineral Research*. 1999;14(7):1167-74.
10. Bala Y, Seeman E. Bone's Material Constituents and their Contribution to Bone Strength in Health, Disease, and Treatment. *Calcified Tissue Int*. 2015;97(3):308-26.
11. Bala Y, Zebaze R, Ghasem-Zadeh A, Atkinson EJ, Iuliano S, Peterson JM, et al. Cortical porosity identifies women with osteopenia at increased risk for forearm fractures. *Journal of Bone and Mineral Research*. 2014;29(6):1356-62.
12. Weatherholt AM, Fuchs RK, Warden SJ. Specialized connective tissue: bone, the structural framework of the upper extremity. *Journal of Hand Therapy*. 2012;25(2):123-32.

13. Phan TC, Xu J, Zheng MH. Interaction between osteoblast and osteoclast: impact in bone disease. *Histology and histopathology*. 2004;19(4):1325-44.
14. Martin TJ, Sims NA. Osteoclast-derived activity in the coupling of bone formation to resorption. *Trends in molecular medicine*. 2005;11(2):76-81.
15. Boyce BF, Yao Z, Xing L. Osteoclasts have multiple roles in bone in addition to bone resorption. *Critical reviews in eukaryotic gene expression*. 2009;19(3):171-80.
16. Capulli M, Paone R, Rucci N. Osteoblast and osteocyte: games without frontiers. *Archives of biochemistry and biophysics*. 2014;561:3-12.
17. Fakhry M, Hamade E, Badran B, Buchet R, Magne D. Molecular mechanisms of mesenchymal stem cell differentiation towards osteoblasts. *World journal of stem cells*. 2013;5(4):136-48.
18. Marie PJ, Fromigie O. Osteogenic differentiation of human marrow-derived mesenchymal stem cells. *Regenerative medicine*. 2006;1(4):539-48.
19. Maeda K, Takahashi N, Kobayashi Y. Roles of Wnt signals in bone resorption during physiological and pathological states. *Journal of molecular medicine (Berlin, Germany)*. 2013;91(1):15-23.
20. Kapinas K, Kessler C, Ricks T, Gronowicz G, Delany AM. miR-29 modulates Wnt signaling in human osteoblasts through a positive feedback loop. *The Journal of biological chemistry*. 2010;285(33):25221-31.
21. Arfat Y, Xiao WZ, Ahmad M, Zhao F, Li DJ, Sun YL, et al. Role of microRNAs in osteoblasts differentiation and bone disorders. *Current medicinal chemistry*. 2015;22(6):748-58.
22. Montero A, Okada Y, Tomita M, Ito M, Tsurukami H, Nakamura T, et al. Disruption of the fibroblast growth factor-2 gene results in decreased bone mass and bone formation. *The Journal of clinical investigation*. 2000;105(8):1085-93.
23. Loebel C, Czekanska EM, Bruderer M, Salzmann G, Alini M, Stoddart MJ. In vitro osteogenic potential of human mesenchymal stem cells is predicted by Runx2/Sox9 ratio. *Tissue engineering Part A*. 2015;21(1-2):115-23.
24. Schaffler MB, Cheung WY, Majeska R, Kennedy O. Osteocytes: master orchestrators of bone. *Calcif Tissue Int*. 2014;94(1):5-24.
25. Tatsumi S, Ishii K, Amizuka N, Li M, Kobayashi T, Kohno K, et al. Targeted ablation of osteocytes induces osteoporosis with defective mechanotransduction. *Cell metabolism*. 2007;5(6):464-75.
26. Cullinane DM. The role of osteocytes in bone regulation: mineral homeostasis versus mechanoreception. *Journal of musculoskeletal & neuronal interactions*. 2002;2(3):242-4.
27. Downey PA, Siegel MI. Bone biology and the clinical implications for osteoporosis. *Physical therapy*. 2006;86(1):77-91.
28. Buckwalter JA, Glimcher MJ, Cooper RR, Recker R. Bone biology. I: Structure, blood supply, cells, matrix, and mineralization. *Instructional course lectures*. 1996;45:371-86.

29. Ural A, Vashishth D. Hierarchical perspective of bone toughness-from molecules to fracture. *International Materials Reviews*. 2014;59(5):245-63.
30. Ong HH, Wright AC, Wehrli FW. Deuterium nuclear magnetic resonance unambiguously quantifies pore and collagen-bound water in cortical bone. *Journal of bone and mineral research : the official journal of the American Society for Bone and Mineral Research*. 2012;27(12):2573-81.
31. Demais V, Audrain C, Mabilieu G, Chappard D, Basle MF. Diversity of bone matrix adhesion proteins modulates osteoblast attachment and organization of actin cytoskeleton. *Morphologie : bulletin de l'Association des anatomistes*. 2014;98(321):53-64.
32. Zohar R. Signals between cells and matrix mediate bone regeneration: INTECH Open Access Publisher; 2012.
33. Boivin G, Bala Y, Doublier A, Farlay D, Ste-Marie LG, Meunier PJ, et al. The role of mineralization and organic matrix in the microhardness of bone tissue from controls and osteoporotic patients. *Bone*. 2008;43(3):532-8.
34. Datta HK, Ng WF, Walker JA, Tuck SP, Varanasi SS. The cell biology of bone metabolism. *Journal of clinical pathology*. 2008;61(5):577-87.
35. Viguet-Carrin S, Garnero P, Delmas PD. The role of collagen in bone strength. *Osteoporosis international : a journal established as result of cooperation between the European Foundation for Osteoporosis and the National Osteoporosis Foundation of the USA*. 2006;17(3):319-36.
36. Christoffersen J, Landis WJ. A contribution with review to the description of mineralization of bone and other calcified tissues in vivo. *The Anatomical record*. 1991;230(4):435-50.
37. Saito M, Marumo K. Collagen cross-links as a determinant of bone quality: a possible explanation for bone fragility in aging, osteoporosis, and diabetes mellitus. *Osteoporosis international : a journal established as result of cooperation between the European Foundation for Osteoporosis and the National Osteoporosis Foundation of the USA*. 2010;21(2):195-214.
38. Depalle B, Qin Z, Shefelbine SJ, Buehler MJ. Influence of cross-link structure, density and mechanical properties in the mesoscale deformation mechanisms of collagen fibrils. *J Mech Behav Biomed Mater*. 2015 Dec;52:1-13.
39. Robling AG, Castillo AB, Turner CH. Biomechanical and molecular regulation of bone remodeling. *Annual review of biomedical engineering*. 2006;8:455-98.
40. Burr D. The complex relationship between bone remodeling and the physical and material properties of bone. *Osteoporosis Int*. 2015;26(3):845-7.
41. Seeman E. Bone Modeling and Remodeling. 2009;19(3):219-33.
42. Erben RG. Hypothesis: Coupling between Resorption and Formation in Cancellous bone Remodeling is a Mechanically Controlled Event. *Frontiers in endocrinology*. 2015;6:82.
43. Martin T, Gooi JH, Sims NA. Molecular mechanisms in coupling of bone formation to resorption. *Critical reviews in eukaryotic gene expression*. 2009;19(1):73-88.

44. Sims NA, Martin TJ. Coupling Signals between the Osteoclast and Osteoblast: How are Messages Transmitted between These Temporary Visitors to the Bone Surface? *Frontiers in endocrinology*. 2015;6:41.
45. Sims NA, Martin TJ. Coupling the activities of bone formation and resorption: a multitude of signals within the basic multicellular unit. *BoneKEY reports*. 2014;3.
46. Sapir-Koren R, Livshits G. Osteocyte control of bone remodeling: is sclerostin a key molecular coordinator of the balanced bone resorption-formation cycles? *Osteoporosis international : a journal established as result of cooperation between the European Foundation for Osteoporosis and the National Osteoporosis Foundation of the USA*. 2014;25(12):2685-700.
47. van Oers RF, Klein-Nulend J, Bacabac RG. The osteocyte as an orchestrator of bone remodeling: an engineer's perspective. *Clinical Reviews in Bone and Mineral Metabolism*. 2014;12(1):2-13.
48. Fogelman I, Gnanasegaran G, Van der Wall H. *Radionuclide and hybrid bone imaging*. Berlin: Springer; 2013.
49. Andreasen CM, Ding M, Overgaard S, Bollen P, Andersen TL. A reversal phase arrest uncoupling the bone formation and resorption contributes to the bone loss in glucocorticoid treated ovariectomised aged sheep. *Bone*. 2015;75:32-9.
50. Marie PJ. Osteoblast dysfunctions in bone diseases: from cellular and molecular mechanisms to therapeutic strategies. *Cellular and molecular life sciences : CMLS*. 2015;72(7):1347-61.
51. Sobacchi C, Schulz A, Coxon FP, Villa A, Helfrich MH. Osteopetrosis: genetics, treatment and new insights into osteoclast function. *Nat Rev Endocrinol*. 2013;9(9):522-36.
52. Recker R, Lappe J, Davies KM, Heaney R. Bone remodeling increases substantially in the years after menopause and remains increased in older osteoporosis patients. *Journal of bone and mineral research : the official journal of the American Society for Bone and Mineral Research*. 2004;19(10):1628-33.
53. Riggs BL, Khosla S, Melton LJ, 3rd. Sex steroids and the construction and conservation of the adult skeleton. *Endocrine reviews*. 2002;23(3):279-302.
54. Matsushita H, Wakatsuki A. [Osteoporosis: a gender specific disease]. *Nihon rinsho Japanese journal of clinical medicine*. 2015;73(4):639-43.
55. Lambert JK, Zaidi M, Mechanick JI. Male osteoporosis: epidemiology and the pathogenesis of aging bones. *Curr Osteoporos Rep*. 2011;9(4):229-36.
56. Parra-Torres AY, Valdés-Flores M, Orozco L, Velázquez-Cruz R. Molecular Aspects of Bone Remodeling. *Topics in Osteoporosis*. 2013:1-27.
57. Eriksen EF. Cellular mechanisms of bone remodeling. *Rev Endocr Metab Disord*. 2010;11(4):219-27.
58. Hauge EM, Qvesel D, Eriksen EF, Mosekilde L, Melsen F. Cancellous bone remodeling occurs in specialized compartments lined by cells expressing osteoblastic markers. *Journal of bone and mineral research : the official journal of the American Society for Bone and Mineral Research*. 2001;16(9):1575-82.

59. Dempster DW, Laming CL, Kostenuik PJ, Grauer A. Role of RANK ligand and denosumab, a targeted RANK ligand inhibitor, in bone health and osteoporosis: a review of preclinical and clinical data. *Clinical therapeutics*. 2012;34(3):521-36.
60. Weitzmann MN. The Role of Inflammatory Cytokines, the RANKL/OPG Axis, and the Immunoskeletal Interface in Physiological Bone Turnover and Osteoporosis. *Scientifica*. 2013;2013:125705.
61. Cauley JA. Bone health after menopause. *Current opinion in endocrinology, diabetes, and obesity*. 2015;22(6):490-4.
62. Burr DB, Allen MR. *Basic and applied bone biology*: Academic Press; 2013.
63. Vrahnas C, Sims NA. EphrinB2 Signalling in Osteoblast Differentiation, Bone Formation and Endochondral Ossification. *Current Molecular Biology Reports*. 2015;1(4):148-56.
64. Teti A. Bone development: overview of bone cells and signaling. *Current osteoporosis reports*. 2011;9(4):264-73.
65. Seeman E, Delmas PD. Bone quality—the material and structural basis of bone strength and fragility. *New England Journal of Medicine*. 2006;354(21):2250-61.
66. Starup-Linde J, Vestergaard P. Biochemical bone turnover markers in diabetes mellitus—a systematic review. *Bone*. 2016;82:69-78.
67. Garnero P. New biochemical markers of bone turnover. *IBMS BoneKEy*. 2008;5(3):84-102.
68. Vasikaran S, Eastell R, Bruyère O, Foldes A, Garnero P, Griesmacher A, et al. Markers of bone turnover for the prediction of fracture risk and monitoring of osteoporosis treatment: a need for international reference standards. *Osteoporosis Int*. 2011;22(2):391-420.
69. Johansson H, Odén A, Kanis J, McCloskey E, Morris H, Cooper C, et al. IFCC-IOF Joint Working Group on Standardisation of Biochemical Markers of Bone Turnover, A meta-analysis of reference markers of bone turnover for prediction of fracture. *Calcif Tissue Int*. 2014;94(5):560-7.
70. Khashayar P, Meybodi HA, Amoabediny G, Larijani B. Biochemical Markers of Bone Turnover and their Role in Osteoporosis Diagnosis: A Narrative Review. *Recent patents on endocrine, metabolic & immune drug discovery*. 2015;9(2):79-89.
71. Henriksen K, Christiansen C, Karsdal MA. Role of biochemical markers in the management of osteoporosis. *Climacteric : the journal of the International Menopause Society*. 2015;18 Suppl 2:10-8.
72. Fink E, Cormier C, Steinmetz P, Kindermans C, Le Bouc Y, Souberbielle JC. Differences in the capacity of several biochemical bone markers to assess high bone turnover in early menopause and response to alendronate therapy. *Osteoporosis international : a journal established as result of cooperation between the European Foundation for Osteoporosis and the National Osteoporosis Foundation of the USA*. 2000;11(4):295-303.
73. George A, Veis A. Phosphorylated proteins and control over apatite nucleation, crystal growth, and inhibition. *Chemical reviews*. 2008;108(11):4670-93.

74. Villafán-Bernal JR, Sánchez-Enríquez S, Muñoz-Valle JF. Molecular modulation of osteocalcin and its relevance in diabetes (Review). *International journal of molecular medicine*. 2011;28(3):283-93.
75. Lian J, Stewart C, Puchacz E, Mackowiak S, Shalhoub V, Collart D, et al. Structure of the rat osteocalcin gene and regulation of vitamin D-dependent expression. *Proceedings of the National Academy of Sciences of the United States of America*. 1989;86(4):1143-7.
76. Razzaque MS. Osteocalcin: a pivotal mediator or an innocent bystander in energy metabolism? *Nephrol Dial Transpl*. 2011;26(1):42-5.
77. Iwamoto J, Takeda T, Sato Y. Effects of vitamin K2 on osteoporosis. *Current pharmaceutical design*. 2004;10(21):2557-76.
78. Blumsohn A, Hannon RA, Eastell R. Apparent instability of osteocalcin in serum as measured with different commercially available immunoassays. *Clinical chemistry*. 1995;41(2):318-9.
79. Hauschka PV, Lian JB, Cole D, Gundberg CM. Osteocalcin and matrix Gla protein: vitamin K-dependent proteins in bone. *Physiological reviews*. 1989;69(3):990-1047.
80. Glowacki J, Lian JB. Impaired recruitment and differentiation of osteoclast progenitors by osteocalcin-deplete bone implants. *Cell differentiation*. 1987;21(4):247-54.
81. Ducy P, Desbois C, Boyce B, Pinero G, Story B, Dunstan C, et al. Increased bone formation in osteocalcin-deficient mice. *Nature*. 1996 Aug 1;382(6590):448-52.
82. Ducy P. The role of osteocalcin in the endocrine cross-talk between bone remodelling and energy metabolism. *Diabetologia*. 2011;54(6):1291-7.
83. Zoch ML, Clemens TL, Riddle RC. New insights into the biology of osteocalcin. *Bone*. 2016;82:42-9.
84. Ferron M, Hinoi E, Karsenty G, Ducy P. Osteocalcin differentially regulates beta cell and adipocyte gene expression and affects the development of metabolic diseases in wild-type mice. *Proceedings of the National Academy of Sciences of the United States of America*. 2008;105(13):5266-70.
85. Kanazawa I. Osteocalcin as a hormone regulating glucose metabolism. *World J Diabetes*. 2015;6(18):1345-54.
86. Ferron M, Wei J, Yoshizawa T, Del Fattore A, DePinho RA, Teti A, et al. Insulin signaling in osteoblasts integrates bone remodeling and energy metabolism. *Cell*. 2010;142(2):296-308.
87. Hinoi E, Gao N, Jung DY, Yadav V, Yoshizawa T, Myers MG, Jr., et al. The sympathetic tone mediates leptin's inhibition of insulin secretion by modulating osteocalcin bioactivity. *J Cell Biol*. 2008;183(7):1235-42.
88. Motyl KJ, McCabe LR, Schwartz AV. Bone and glucose metabolism: a two-way street. *Archives of biochemistry and biophysics*. 2010;503(1):2-10.
89. Lee NK, Sowa H, Hinoi E, Ferron M, Ahn JD, Confavreux C, et al. Endocrine regulation of energy metabolism by the skeleton. *Cell*. 2007;130(3):456-69.

90. Wolf G. Energy regulation by the skeleton. *Nutrition reviews*. 2008;66(4):229-33.
91. Karsenty G, Oury F. Regulation of male fertility by the bone-derived hormone osteocalcin. *Molecular and cellular endocrinology*. 2014;382(1):521-6.
92. Millán J. Alkaline Phosphatases: Structure, Substrate Specificity and Functional Relatedness to Other Members of a Large Superfamily of Enzymes. *Purinergic Signaling*, 2, 335-341. 2006.
93. Sharma U, Pal D, Prasad R. Alkaline phosphatase: an overview. *Indian Journal of Clinical Biochemistry*. 2014;29(3):269-78.
94. Fawley J, Gourlay D. Intestinal alkaline phosphatase: a summary of its role in clinical disease. *J Surg Res*. 2016 May 1;202(1):225-34.
95. Whyte MP. Hypophosphatasia [mdash] aetiology, nosology, pathogenesis, diagnosis and treatment. *Nature Reviews Endocrinology*. 2016;12(4):233-46.
96. Ralston SH. Paget's disease of bone. *New England Journal of Medicine*. 2013;368(7):644-50.
97. Belkhouribchia J, Bravenboer B, Meuwissen M, Velkeniers B. Osteomalacia with low alkaline phosphatase: a not so rare condition with important consequences. *BMJ case reports*. 2016;2016:bcr2015212827.
98. Avbersek-Luznik I, Gmeiner Stopar T, Marc J. Activity or mass concentration of bone-specific alkaline phosphatase as a marker of bone formation. *Clinical chemistry and laboratory medicine*. 2007;45(8):1014-8.
99. Hlaing TT, Compston JE. Biochemical markers of bone turnover - uses and limitations. *Annals of clinical biochemistry*. 2014;51(Pt 2):189-202.
100. Wheeler G, Elshahaly M, Tuck SP, Datta HK, van Laar JM. The clinical utility of bone marker measurements in osteoporosis. *J Transl Med*. 2013;11:201.
101. Swaminathan R. Biochemical markers of bone turnover. *Clin Chim Acta*. 2001;313(1-2):95-105.
102. Bergmann P, Body JJ, Boonen S, Boutsen Y, Devogelaer JP, Goemaere S, et al. Evidence-based guidelines for the use of biochemical markers of bone turnover in the selection and monitoring of bisphosphonate treatment in osteoporosis: a consensus document of the Belgian Bone Club. *International journal of clinical practice*. 2009;63(1):19-26.
103. Bjarnason N, Henriksen E, Alexandersen P, Christgau S, Henriksen D, Christiansen C. Mechanism of circadian variation in bone resorption. *Bone*. 2002;30(1):307-13.
104. Rogers RS, Dawson AW, Wang Z, Thyfault JP, Hinton PS. Acute response of plasma markers of bone turnover to a single bout of resistance training or plyometrics. *Journal of applied physiology*. 2011;111(5):1353-60.
105. Chiu KM, Ju J, Mayes D, Bacchetti P, Weitz S, Arnaud CD. Changes in bone resorption during the menstrual cycle. *Journal of Bone and Mineral Research*. 1999;14(4):609-15.
106. Hannon R, Eastell R. Preanalytical variability of biochemical markers of bone turnover. *Osteoporosis Int*. 2000;11(18):S30-S44.

107. Bauer D, Krege J, Lane N, Leary E, Libanati C, Miller P, et al. National Bone Health Alliance Bone Turnover Marker Project: current practices and the need for US harmonization, standardization, and common reference ranges. *Osteoporosis international : a journal established as result of cooperation between the European Foundation for Osteoporosis and the National Osteoporosis Foundation of the USA*. 2012;23(10):2425-33.
108. Travlos GS. Normal structure, function, and histology of the bone marrow. *Toxicologic pathology*. 2006;34(5):548-65.
109. Mendez-Ferrer S, Michurina TV, Ferraro F, Mazloom AR, MacArthur BD, Lira SA, et al. Mesenchymal and haematopoietic stem cells form a unique bone marrow niche. *Nature*. 2010;466(7308):829-34.
110. Moulopoulos LA, Koutoulidis Bone marrow MRI: a pattern based approach Springer Berlin Heidelberg, Berlin, Germany (2014)
111. Bracken J, Nandurkar D, Radhakrishnan K, Ditchfield M. Normal paediatric bone marrow: magnetic resonance imaging appearances from birth to 5 years. *Journal of medical imaging and radiation oncology*. 2013;57(3):283-91.
112. <http://depts.washington.edu/bonebio/ASBMRed/structure.html>. [cited 2016 8 January].
113. Babyn P, Stimec J. Bone Marrow. *Pediatric Orthopedic Imaging*: Springer; 2015. p. 873-901.
114. Hardouin P, Pansini V, Cortet B. Bone marrow fat. *Joint, bone, spine : revue du rhumatisme*. 2014;81(4):313-9.
115. Gurevitch O, Slavin S, Feldman AG. Conversion of red bone marrow into yellow - Cause and mechanisms. *Medical hypotheses*. 2007;69(3):531-6.
116. Di Iorgi N, Mo AO, Grimm K, Wren TA, Dorey F, Gilsanz V. Bone acquisition in healthy young females is reciprocally related to marrow adiposity. *The Journal of clinical endocrinology and metabolism*. 2010;95(6):2977-82.
117. Vande Berg BC, Malghem J, Lecouvet FE, Maldague B. [Normal bone marrow: dynamic aspects in magnetic resonance imaging]. *Journal de radiologie*. 2001;82(2):127-35.
118. Muruganandan S, Roman AA, Sinal CJ. Adipocyte differentiation of bone marrow-derived mesenchymal stem cells: cross talk with the osteoblastogenic program. *Cellular and molecular life sciences : CMLS*. 2009;66(2):236-53.
119. Rosen CJ, Bouxsein ML. Mechanisms of disease: is osteoporosis the obesity of bone? *Nature clinical practice Rheumatology*. 2006;2(1):35-43.
120. Shah LM, Hanrahan CJ. MRI of spinal bone marrow: part I, techniques and normal age-related appearances. *AJR American journal of roentgenology*. 2011;197(6):1298-308.
121. Guillerman RP. Marrow: red, yellow and bad. *Pediatric radiology*. 2013;43(1):181-92.
122. Lecka-Czernik B, Stechschulte LA. Bone and fat: a relationship of different shades. *Archives of biochemistry and biophysics*. 2014;561:124-9.

123. Gimble JM, Zvonic S, Floyd ZE, Kassem M, Nuttall ME. Playing with bone and fat. *J Cell Biochem.* 2006;98(2):251-66.
124. Consensus development conference: prophylaxis and treatment of osteoporosis. *The American journal of medicine.* 1991;90(1):107-10.
125. Melton LJ, 3rd, Chrischilles EA, Cooper C, Lane AW, Riggs BL. Perspective. How many women have osteoporosis? *Journal of bone and mineral research : the official journal of the American Society for Bone and Mineral Research.* 1992;7(9):1005-10.
126. Willson T, Nelson SD, Newbold J, Nelson RE, LaFleur J. The clinical epidemiology of male osteoporosis: a review of the recent literature. *Clinical epidemiology.* 2015;7:65-76.
127. Hernlund E, Svedbom A, Ivergard M, Compston J, Cooper C, Stenmark J, et al. Osteoporosis in the European Union: medical management, epidemiology and economic burden. A report prepared in collaboration with the International Osteoporosis Foundation (IOF) and the European Federation of Pharmaceutical Industry Associations (EFPIA). *Archives of osteoporosis.* 2013;8:136.
128. Cummings SR, Melton LJ. Epidemiology and outcomes of osteoporotic fractures. *The Lancet.* 2002;359(9319):1761-7.
129. Lorentzon M, Cummings SR. Osteoporosis: the evolution of a diagnosis. *Journal of internal medicine.* 2015;277(6):650-61.
130. Manolagas SC. Birth and death of bone cells: basic regulatory mechanisms and implications for the pathogenesis and treatment of osteoporosis. *Endocrine reviews.* 2000;21(2):115-37.
131. Assessment of fracture risk and its application to screening for postmenopausal osteoporosis. Report of a WHO Study Group. *World Health Organization technical report series.* 1994;843:1-129.
132. Black DM, Cummings SR, Karpf DB, Cauley JA, Thompson DE, Nevitt MC, et al. Randomised trial of effect of alendronate on risk of fracture in women with existing vertebral fractures. *Fracture Intervention Trial Research Group. Lancet (London, England).* 1996;348(9041):1535-41.
133. Cummings SR. How drugs decrease fracture risk: lessons from trials. *Journal of musculoskeletal & neuronal interactions.* 2002;2(3):198-200.
134. Bliuc D, Alarkawi D, Nguyen TV, Eisman JA, Center JR. Risk of subsequent fractures and mortality in elderly women and men with fragility fractures with and without osteoporotic bone density: the Dubbo Osteoporosis Epidemiology Study. *Journal of bone and mineral research : the official journal of the American Society for Bone and Mineral Research.* 2015;30(4):637-46.
135. Sale JE, Bogoch E, Meadows L, Gignac M, Frankel L, Inrig T, et al. Bone Mineral Density Reporting Underestimates Fracture Risk in Ontario. *Health.* 2015;7(5):566-71.
136. Cranney A, Jamal SA, Tsang JF, Josse RG, Leslie WD. Low bone mineral density and fracture burden in postmenopausal women. *CMAJ : Canadian Medical Association journal = journal de l'Association medicale canadienne.* 2007;177(6):575-80.

137. Wainwright SA, Marshall LM, Ensrud KE, Cauley JA, Black DM, Hillier TA, et al. Hip fracture in women without osteoporosis. *The Journal of clinical endocrinology and metabolism*. 2005;90(5):2787-93.
138. Schuit SC, van der Klift M, Weel AE, de Laet CE, Burger H, Seeman E, et al. Fracture incidence and association with bone mineral density in elderly men and women: the Rotterdam Study. *Bone*. 2004;34(1):195-202.
139. Sornay-Rendu E, Munoz F, Garnero P, Duboeuf F, Delmas PD. Identification of osteopenic women at high risk of fracture: the OFELY study. *Journal of bone and mineral research : the official journal of the American Society for Bone and Mineral Research*. 2005;20(10):1813-9.
140. Siris ES, Miller PD, Barrett-Connor E, Faulkner KG, Wehren LE, Abbott TA, et al. Identification and fracture outcomes of undiagnosed low bone mineral density in postmenopausal women: results from the National Osteoporosis Risk Assessment. *JAMA : the journal of the American Medical Association*. 2001;286(22):2815-22.
141. Mackey DC, Lui LY, Cawthon PM, Bauer DC, Nevitt MC, Cauley JA, et al. High-trauma fractures and low bone mineral density in older women and men. *JAMA : the journal of the American Medical Association*. 2007;298(20):2381-8.
142. Cummings SR, Karpf DB, Harris F, Genant HK, Ensrud K, LaCroix AZ, et al. Improvement in spine bone density and reduction in risk of vertebral fractures during treatment with antiresorptive drugs. *The American journal of medicine*. 2002;112(4):281-9.
143. Giangregorio LM, Leslie WD, Lix LM, Johansson H, Oden A, McCloskey E, et al. FRAX underestimates fracture risk in patients with diabetes. *Journal of bone and mineral research : the official journal of the American Society for Bone and Mineral Research*. 2012;27(2):301-8.
144. Kanis JA, Johnell O, Oden A, Johansson H, McCloskey E. FRAX and the assessment of fracture probability in men and women from the UK. *Osteoporosis international : a journal established as result of cooperation between the European Foundation for Osteoporosis and the National Osteoporosis Foundation of the USA*. 2008;19(4):385-97.
145. Kanis JA, Harvey NC, Johansson H, Oden A, Leslie WD, McCloskey EV. FRAX and fracture prediction without bone mineral density. *Climacteric : the journal of the International Menopause Society*. 2015:1-8.
146. Kanis JA, Johansson H, Oden A, McCloskey EV. Assessment of fracture risk. *European journal of radiology*. 2009;71(3):392-7.
147. NIH Consensus Development Panel on Osteoporosis Prevention, Diagnosis, and Therapy, March 7-29, 2000: highlights of the conference. *Southern medical journal*. 2001;94(6):569-73.
148. Zebaze RM, Ghasem-Zadeh A, Bohte A, Iuliano-Burns S, Mirams M, Price RI, et al. Intracortical remodelling and porosity in the distal radius and post-mortem femurs of women: a cross-sectional study. *Lancet (London, England)*. 2010;375(9727):1729-36.
149. Brandi ML. Microarchitecture, the key to bone quality. *Rheumatology (Oxford, England)*. 2009;48 Suppl 4:iv3-8.

150. Cheng XG, Lowet G, Boonen S, Nicholson PH, Brys P, Nijs J, et al. Assessment of the strength of proximal femur in vitro: relationship to femoral bone mineral density and femoral geometry. *Bone*. 1997;20(3):213-8.
151. Shimada Y, Miyakoshi N. *Osteoporosis in Orthopedics*. Springer Japan; 2016.
152. Chang G, Honig S, Liu Y, Chen C, Chu KK, Rajapakse CS, et al. 7 Tesla MRI of bone microarchitecture discriminates between women without and with fragility fractures who do not differ by bone mineral density. *J Bone Miner Metab*. 2015;33(3):285-93.
153. Chang G, Rajapakse CS, Regatte RR, Babb J, Saxena A, Belmont HM, et al. 3 Tesla MRI detects deterioration in proximal femur microarchitecture and strength in long-term glucocorticoid users compared with controls. *J Magn Reson Imaging*. 2015;42(6):1489-96.
154. Thomsen JS, Ebbesen EN, Mosekilde L. Relationships between static histomorphometry and bone strength measurements in human iliac crest bone biopsies. *Bone*. 1998;22(2):153-63.
155. Stein EM, Silva BC, Boutroy S, Zhou B, Wang J, Udesky J, et al. Primary hyperparathyroidism is associated with abnormal cortical and trabecular microstructure and reduced bone stiffness in postmenopausal women. *Journal of bone and mineral research : the official journal of the American Society for Bone and Mineral Research*. 2013;28(5):1029-40.
156. Silva BC, Leslie WD, Resch H, Lamy O, Lesnyak O, Binkley N, et al. Trabecular Bone Score: A Noninvasive Analytical Method Based Upon the DXA Image. *Journal of Bone and Mineral Research*. 2014;29(3):518-30.
157. Burghardt AJ, Issever AS, Schwartz AV, Davis KA, Masharani U, Majumdar S, et al. High-resolution peripheral quantitative computed tomographic imaging of cortical and trabecular bone microarchitecture in patients with type 2 diabetes mellitus. *The Journal of clinical endocrinology and metabolism*. 2010;95(11):5045-55.
158. Patsch JM, Burghardt AJ, Yap SP, Baum T, Schwartz AV, Joseph GB, et al. Increased cortical porosity in type 2 diabetic postmenopausal women with fragility fractures. *Journal of bone and mineral research : the official journal of the American Society for Bone and Mineral Research*. 2013;28(2):313-24.
159. Pritchard JM, Giangregorio LM, Atkinson SA, Beattie KA, Inglis D, Ioannidis G, et al. Association of larger holes in the trabecular bone at the distal radius in postmenopausal women with type 2 diabetes mellitus compared to controls. *Arthritis Care & Research*. 2012;64(1):83-91.
160. Zhukouskaya VV, Eller-Vainicher C, Vadzianava VV, Shepelkevich AP, Zhurava IV, Korolenko GG, et al. Prevalence of morphometric vertebral fractures in patients with type 1 diabetes. *Diabetes care*. 2013;36(6):1635-40.
161. Vestergaard P. Discrepancies in bone mineral density and fracture risk in patients with type 1 and type 2 diabetes - a meta-analysis. *Osteoporosis Int*. 2007;18(4):427-44.
162. Hofbauer LC, Brueck CC, Singh SK, Dobnig H. Osteoporosis in patients with diabetes mellitus. *Journal of Bone and Mineral Research*. 2007;22(9):1317-28.

163. Shanbhogue VV, Hansen S, Frost M, Jorgensen NR, Hermann AP, Henriksen JE, et al. Bone Geometry, Volumetric Density, Microarchitecture, and Estimated Bone Strength Assessed by HR-pQCT in Adult Patients With Type 1 Diabetes Mellitus. *Journal of bone and mineral research : the official journal of the American Society for Bone and Mineral Research*. 2015 Dec 1;30(12):2188-99.
164. Ishikawa K, Fukui T, Nagai T, Kuroda T, Hara N, Yamamoto T, et al. Type 1 diabetes patients have lower strength in femoral bone determined by quantitative computed tomography: A cross-sectional study. *J Diabetes Investig*. 2015;6(6):726-33.
165. Dawson-Hughes B. Calcium and vitamin D for bone health in adults. In *Nutrition and bone health 2015* (pp. 217-230). Springer New York.
166. Greco EA, Fornari R, Rossi F, Santiemma V, Prossomariti G, Annoscia C, et al. Is obesity protective for osteoporosis? Evaluation of bone mineral density in individuals with high body mass index. *International journal of clinical practice*. 2010;64(6):817-20.
167. Verma S, Rajaratnam JH, Denton J, Hoyland JA, Byers RJ. Adipocytic proportion of bone marrow is inversely related to bone formation in osteoporosis. *Journal of clinical pathology*. 2002;55(9):693-8.
168. Kim KC, Shin DH, Lee SY, Im JA, Lee DC. Relation between obesity and bone mineral density and vertebral fractures in Korean postmenopausal women. *Yonsei medical journal*. 2010;51(6):857-63.
169. Mpalaris V, Anagnostis P, Goulis DG, Iakovou I. Complex association between body weight and fracture risk in postmenopausal women. *Obesity reviews : an official journal of the International Association for the Study of Obesity*. 2015;16(3):225-33.
170. Greco EA, Lenzi A, Migliaccio S. The obesity of bone. *Therapeutic advances in endocrinology and metabolism*. 2015;6(6):273-86.
171. Reid IR. Fat and bone. *Archives of biochemistry and biophysics*. 2010;503(1):20-7.
172. Bermeo S, Gunaratnam K, Duque G. Fat and bone interactions. *Current osteoporosis reports*. 2014;12(2):235-42.
173. Bredella MA, Fazeli PK, Daley SM, Miller KK, Rosen CJ, Klibanski A, et al. Marrow fat composition in anorexia nervosa. *Bone*. 2014;66:199-204.
174. Thommesen L, Stunes AK, Monjo M, Grøsvik K, Tamburstuen MV, Kjølbi E, et al. Expression and regulation of resistin in osteoblasts and osteoclasts indicate a role in bone metabolism. *Journal of cellular biochemistry*. 2006;99(3):824-34.
175. Steeve KT, Marc P, Sandrine T, Dominique H, Yannick F. IL-6, RANKL, TNF-alpha/IL-1: interrelations in bone resorption pathophysiology. *Cytokine & growth factor reviews*. 2004;15(1):49-60.
176. Taguchi Y, Yamamoto M, Yamate T, Lin S-C, Mocharla H, DeTogni P, et al. Interleukin-6-type cytokines stimulate mesenchymal progenitor differentiation toward the osteoblastic lineage. *Proceedings of the Association of American Physicians*. 1997;110(6):559-74.

177. Ducy P, Amling M, Takeda S, Priemel M, Schilling AF, Beil FT, et al. Leptin inhibits bone formation through a hypothalamic relay: a central control of bone mass. *Cell*. 2000;100(2):197-207.
178. Thomas T. The complex effects of leptin on bone metabolism through multiple pathways. *Current opinion in pharmacology*. 2004;4(3):295-300.
179. Upadhyay J, Farr OM, Mantzoros CS. The role of leptin in regulating bone metabolism. *Metabolism*. 2015;64(1):105-13.
180. Lin YY, Chen CY, Chen CC, Lin HJ, Mersmann HJ, Wu SC, et al. The Effects of Adiponectin on Bone Metabolism. *Journal of Biomedical Science and Engineering*. 2014 Jul 4;7(09):621.
181. Conde J, Scotece M, Abella V, López V, Pino J, Gómez-Reino JJ, et al. Basic Aspects of Adipokines in Bone Metabolism. *Clinical Reviews in Bone and Mineral Metabolism*. 2015;13(1):11-9.
182. Srivastava S, Toraldo G, Weitzmann MN, Cenci S, Ross FP, Pacifici R. Estrogen decreases osteoclast formation by down-regulating receptor activator of NF- κ B ligand (RANKL)-induced JNK activation. *Journal of Biological Chemistry*. 2001;276(12):8836-40.
183. Cauley JA. Estrogen and bone health in men and women. *Steroids*. 2015;99:11-5.
184. Chau YY, Bandiera R, Serrels A, Martinez-Estrada OM, Qing W, Lee M, et al. Visceral and subcutaneous fat have different origins and evidence supports a mesothelial source. *Nature cell biology*. 2014;16(4):367-75.
185. Macotela Y, Emanuelli B, Mori MA, Gesta S, Schulz TJ, Tseng YH, et al. Intrinsic differences in adipocyte precursor cells from different white fat depots. *Diabetes*. 2012;61(7):1691-9.
186. Yeh L-CC, Ford JJ, Lee JC, Adamo ML. Palmitate attenuates osteoblast differentiation of fetal rat calvarial cells. *Biochemical and biophysical research communications*. 2014;450(1):777-81.
187. Gunaratnam K, Vidal C, Gimble JM, Duque G. Mechanisms of palmitate-induced lipotoxicity in human osteoblasts. *Endocrinology*. 2013;155(1):108-16.
188. Guo Y-f, Xiong D-h, Shen H, Zhao L-j, Xiao P, Guo Y, et al. Polymorphisms of the low-density lipoprotein receptor-related protein 5 (LRP5) gene are associated with obesity phenotypes in a large family-based association study. *Journal of medical genetics*. 2006;43(10):798-803.
189. Greco EA, Lenzi A, Migliaccio S. The obesity of bone. *Therapeutic advances in endocrinology and metabolism*. 2015;6(6):273-86.
190. Ribot C, Tremollieres F, Pouilles J-M, Bonneu M, Germain F, Louvet J-P. Obesity and postmenopausal bone loss: the influence of obesity on vertebral density and bone turnover in postmenopausal women. *Bone*. 1987;8(6):327-31.
191. Yang S, Nguyen ND, Center JR, Eisman JA, Nguyen TV. Association between abdominal obesity and fracture risk: a prospective study. *The Journal of Clinical Endocrinology & Metabolism*. 2013;98(6):2478-83.

192. Greco E, Fornari R, Rossi F, Santiemma V, Prossomariti G, Annoscia C, et al. Is obesity protective for osteoporosis? Evaluation of bone mineral density in individuals with high body mass index. *International journal of clinical practice*. 2010;64(6):817-20.
193. Sjøgaard AJ, Holvik K, Omsland TK, Tell GS, Dahl C, Schei B, et al. Abdominal obesity increases the risk of hip fracture. A population-based study of 43 000 women and men aged 60–79 years followed for 8 years. Cohort of Norway. *Journal of internal medicine*. 2015;277(3):306-17.
194. Pino AM, Rosen CJ, Rodriguez JP. In osteoporosis, differentiation of mesenchymal stem cells (MSCs) improves bone marrow adipogenesis. *Biological research*. 2012;45(3):279-87.
195. David V, Martin A, Lafage-Proust M-H, Malaval L, Peyroche S, Jones DB, et al. Mechanical loading down-regulates peroxisome proliferator-activated receptor γ in bone marrow stromal cells and favors osteoblastogenesis at the expense of adipogenesis. *Endocrinology*. 2007;148(5):2553-62.
196. Sethi J, Vidal-Puig A. Wnt signalling and the control of cellular metabolism. *Biochemical Journal*. 2010;427(1):1-17.
197. Xu C, Wang J, Zhu T, Shen Y, Tang X, Fang L, et al. Cross-Talking between PPAR and WNT Signaling and Its Regulation in Mesenchymal Stem Cell Differentiation. *Current stem cell research & therapy*. 2016 Apr 1;11(3):247-54.
198. James AW. Review of Signaling Pathways Governing MSC Osteogenic and Adipogenic Differentiation. *Scientifica*. 2013;2013:684736.
199. Rosen ED, MacDougald OA. Adipocyte differentiation from the inside out. *Nature reviews Molecular cell biology*. 2006;7(12):885-96.
200. Wan Y. PPAR γ in bone homeostasis. *Trends in endocrinology and metabolism: TEM*. 2010;21(12):722-8.
201. Christodoulides C, Lagathu C, Sethi JK, Vidal-Puig A. Adipogenesis and WNT signalling. *Trends in Endocrinology & Metabolism*. 2009;20(1):16-24.
202. During A, Penel G, Hardouin P. Understanding the local actions of lipids in bone physiology. *Progress in lipid research*. 2015;59:126-46.
203. Singh L, Brennan TA, Russell E, Kim J-H, Chen Q, Johnson FB, et al. Aging alters bone-fat reciprocity by shifting in vivo mesenchymal precursor cell fate towards an adipogenic lineage. *Bone*. 2016 Apr 30;85:29-36.
204. Piccinin MA, Khan ZA. Pathophysiological role of enhanced bone marrow adipogenesis in diabetic complications. *Adipocyte*. 2014;3(4):263-72.
205. Wang C, Meng H, Wang X, Zhao C, Peng J, Wang Y. Differentiation of Bone Marrow Mesenchymal Stem Cells in Osteoblasts and Adipocytes and its Role in Treatment of Osteoporosis. *Med Sci Monit*. 2016;22:226-33.
206. Kawai M, de Paula FJ, Rosen CJ. New insights into osteoporosis: the bone–fat connection. *Journal of internal medicine*. 2012;272(4):317-29.
207. van Belle TL, Coppieters KT, von Herrath MG. Type 1 diabetes: etiology, immunology, and therapeutic strategies. *Physiological reviews*. 2011;91(1):79-118.

208. Christoffersson G, Rodriguez-Calvo T, von Herrath M. Recent advances in understanding Type 1 Diabetes. *F1000Research*. 2016;5.
209. Kagohashi Y, Otani H. Role of nutritional factors at the early life stages in the pathogenesis and clinical course of type 1 diabetes. *BioMed research international*. 2015;2015.
210. Egro FM. Why is type 1 diabetes increasing? *Journal of molecular endocrinology*. 2013;51(1):R1-R13.
211. World Health Organization. *Global report on diabetes*. World Health Organization; 2016.
212. Whiting DR, Guariguata L, Weil C, Shaw J. IDF diabetes atlas: global estimates of the prevalence of diabetes for 2011 and 2030. *Diabetes research and clinical practice*. 2011;94(3):311-21.
213. Association AD. Standards of Medical Care in Diabetes—2014. *Diabetes Care* 2014; 37 (Suppl. 1): S14–S80. *Diagnosis and Classification of Diabetes Mellitus*. *Diabetes Care* 2014; 37 (Suppl. 1): S81–S90. *Diabetes care*. 2014;37(3):887-.
214. Association AD. 2. Classification and Diagnosis of Diabetes. *Diabetes care*. 2016;39(Supplement 1):S13-S22.
215. Association AD. Executive summary: standards of medical care in diabetes--2011. *Diabetes care*. 2011;34:S4.
216. Wenzlau JM, Juhl K, Yu L, Moua O, Sarkar SA, Gottlieb P, et al. The cation efflux transporter ZnT8 (Slc30A8) is a major autoantigen in human type 1 diabetes. *Proceedings of the National Academy of Sciences*. 2007;104(43):17040-5.
217. <https://www.diabetes.org.uk/Guide-to-diabetes/Managing-your-diabetes/Carb-counting/> [Cited 2016 4 February]. accessed on [04/02/2015].
218. Association. AD. Diagnosis and classification of diabetes mellitus. *Diabetes care*. 2012;35 Suppl 1:S64-71.
219. Weber DR, Haynes K, Leonard MB, Willi SM, Denburg MR. Type 1 Diabetes Is Associated With an Increased Risk of Fracture Across the Life Span: A Population-Based Cohort Study Using The Health Improvement Network (THIN). *Diabetes care*. 2015 Oct 1;38(10):1913-20.
220. Ramasamy R, Yan SF, Schmidt AM. The diverse ligand repertoire of the receptor for advanced glycation endproducts and pathways to the complications of diabetes. *Vascular pharmacology*. 2012;57(5-6):160-7.
221. Hothersall EJ, Livingstone SJ, Looker HC, Ahmed SF, Cleland S, Leese GP, et al. Contemporary risk of hip fracture in type 1 and type 2 diabetes: a national registry study from Scotland. *Journal of bone and mineral research : the official journal of the American Society for Bone and Mineral Research*. 2014;29(5):1054-60.
222. Janghorbani M, Feskanich D, Willett WC, Hu F. Prospective study of diabetes and risk of hip fracture: the Nurses' Health Study. *Diabetes Care*. 2006 Jul;29(7):1573-8.
223. Dhaliwal R, Cibula D, Ghosh C, Weinstock RS, Moses AM. Bone quality assessment in type 2 diabetes mellitus. *Osteoporosis Int*. 2014;25(7):1969-73.

224. Starup-Linde J, Eriksen SA, Lykkeboe S, Handberg A, Vestergaard P. Biochemical markers of bone turnover in diabetes patients-a meta-analysis, and a methodological study on the effects of glucose on bone markers. *Osteoporosis international : a journal established as result of cooperation between the European Foundation for Osteoporosis and the National Osteoporosis Foundation of the USA*. 2014;25(6):1697-708.
225. Cheng X, Ni B, Zhang Z, Liu Q, Wang L, Ding Y, et al. Polyol pathway mediates enhanced degradation of extracellular matrix via p38 MAPK activation in intervertebral disc of diabetic rats. *Connective tissue research*. 2013;54(2):118-22.
226. Inaba M, Terada M, Koyama H, Yoshida O, Ishimura E, Kawagishi T, et al. Influence of high glucose on 1, 25-dihydroxyvitamin D3-induced effect on human osteoblast-like MG-63 cells. *Journal of Bone and Mineral Research*. 1995;10(7):1050-6.
227. Cunha JS, Ferreira VM, Maquigussa E, Naves MA, Boim MA. Effects of high glucose and high insulin concentrations on osteoblast function in vitro. *Cell and tissue research*. 2014;358(1):249-56.
228. Botolin S, McCabe LR. Chronic hyperglycemia modulates osteoblast gene expression through osmotic and non-osmotic pathways. *Journal of cellular biochemistry*. 2006;99(2):411-24.
229. Hamada Y, Fujii H, Fukagawa M. Role of oxidative stress in diabetic bone disorder. *Bone*. 2009;45:S35-S8.
230. McCarthy A, Etcheverry S, Cortizo A. Effect of advanced glycation endproducts on the secretion of insulin-like growth factor-I and its binding proteins: role in osteoblast development. *Acta diabetologica*. 2001;38(3):113-22.
231. Yamamoto T, Ozono K, Miyauchi A, Kasayama S, Kojima Y, Shima M, et al. Role of advanced glycation end products in adynamic bone disease in patients with diabetic nephropathy. *American journal of kidney diseases*. 2001;38(4):S161-S4.
232. Bohlender JM, Franke S, Stein G, Wolf G. Advanced glycation end products and the kidney. *American Journal of Physiology-Renal Physiology*. 2005;289(4):F645-F59.
233. Vashishth D, Gibson G, Khoury J, Schaffler M, Kimura J, Fyhrie D. Influence of nonenzymatic glycation on biomechanical properties of cortical bone. *Bone*. 2001;28(2):195-201.
234. Silva MJ, Brodt MD, Lynch MA, McKenzie JA, Tanouye KM, Nyman JS, et al. Type 1 Diabetes in Young Rats Leads to Progressive Trabecular Bone Loss, Cessation of Cortical Bone Growth, and Diminished Whole Bone Strength and Fatigue Life. *Journal of Bone and Mineral Research*. 2009;24(9):1618-27.
235. Schwartz AV, Garnero P, Hillier TA, Sellmeyer DE, Strotmeyer ES, Feingold KR, et al. Pentosidine and increased fracture risk in older adults with type 2 diabetes. *The Journal of Clinical Endocrinology & Metabolism*. 2009;94(7):2380-6.
236. Saito M, Kida Y, Kato S, Marumo K. Diabetes, collagen, and bone quality. *Curr Osteoporos Rep*. 2014;12(2):181-8.

237. Saito M, Fujii K, Mori Y, Marumo K. Role of collagen enzymatic and glycation induced cross-links as a determinant of bone quality in spontaneously diabetic WBN/Kob rats. *Osteoporosis Int.* 2006;17(10):1514-23.
238. Tomasek JJ, Meyers SW, Basinger JB, Green DT, Shew RL. Diabetic and age-related enhancement of collagen-linked fluorescence in cortical bones of rats. *Life sciences.* 1994;55(11):855-61.
239. Yamamoto M, Yamaguchi T, Yamauchi M, Yano S, Sugimoto T. Serum pentosidine levels are positively associated with the presence of vertebral fractures in postmenopausal women with type 2 diabetes. *The Journal of clinical endocrinology and metabolism.* 2008;93(3):1013-9.
240. Hein GE. Glycation endproducts in osteoporosis—is there a pathophysiologic importance? *Clinica Chimica Acta.* 2006;371(1):32-6.
241. Kume S, Kato S, Yamagishi Si, Inagaki Y, Ueda S, Arima N, et al. Advanced Glycation End-Products Attenuate Human Mesenchymal Stem Cells and Prevent Cognate Differentiation Into Adipose Tissue, Cartilage, and Bone. *Journal of Bone and Mineral Research.* 2005;20(9):1647-58.
242. Stolzing A, Sellers D, Llewelyn O, Scutt A. Diabetes induced changes in rat mesenchymal stem cells. *Cells Tissues Organs.* 2010;191(6):453-65.
243. Okazaki K, Yamaguchi T, Tanaka K-i, Notsu M, Ogawa N, Yano S, et al. Advanced glycation end products (AGEs), but not high glucose, inhibit the osteoblastic differentiation of mouse stromal ST2 cells through the suppression of osterix expression, and inhibit cell growth and increasing cell apoptosis. *Calcified Tissue Int.* 2012;91(4):286-96.
244. Weinberg E, Maymon T, Weinreb M. AGEs induce caspase-mediated apoptosis of rat BMSCs via TNF α production and oxidative stress. *Journal of molecular endocrinology.* 2014;52(1):67-76.
245. Coe LM, Lippner D, Perez GI, McCabe LR. Caspase-2 deficiency protects mice from diabetes-induced marrow adiposity. *Journal of cellular biochemistry.* 2011;112(9):2403-11.
246. Miyata T, Notoya K, Yoshida K, Horie K, Maeda K, Kurokawa K, et al. Advanced glycation end products enhance osteoclast-induced bone resorption in cultured mouse unfractionated bone cells and in rats implanted subcutaneously with devitalized bone particles. *Journal of the American Society of Nephrology.* 1997;8(2):260-70.
247. Valcourt U, Merle B, Gineyts E, Viguet-Carrin S, Delmas PD, Garnero P. Non-enzymatic glycation of bone collagen modifies osteoclastic activity and differentiation. *Journal of Biological Chemistry.* 2007;282(8):5691-703.
248. Keats E, Khan ZA. Unique responses of stem cell-derived vascular endothelial and mesenchymal cells to high levels of glucose. *PLoS One.* 2012;7(6):e38752.
249. Botolin S, McCabe LR. Bone loss and increased bone adiposity in spontaneous and pharmacologically induced diabetic mice. *Endocrinology.* 2007;148(1):198-205.
250. Chuang CC, Yang RS, Tsai KS, Ho FM, Liu SH. Hyperglycemia enhances adipogenic induction of lipid accumulation: involvement of extracellular signal-

- regulated protein kinase 1/2, phosphoinositide 3-kinase/Akt, and peroxisome proliferator-activated receptor γ signaling. *Endocrinology*. 2007;148(9):4267-75.
251. Barbagallo I, Vanella A, Peterson SJ, Kim DH, Tibullo D, Giallongo C, et al. Overexpression of heme oxygenase-1 increases human osteoblast stem cell differentiation. *J Bone Miner Metab*. 2010;28(3):276-88.
 252. Keats EC, Dominguez JM, Grant MB, Khan ZA. Switch from Canonical to Noncanonical Wnt Signaling Mediates High Glucose-Induced Adipogenesis. *Stem cells (Dayton, Ohio)*. 2014;32(6):1649-60.
 253. Wang A, Midura RJ, Vasanji A, Wang AJ, Hascall VC. Hyperglycemia diverts dividing osteoblastic precursor cells to an adipogenic pathway and induces synthesis of a hyaluronan matrix that is adhesive for monocytes. *Journal of Biological Chemistry*. 2014;289(16):11410-20.
 254. Hough S, Russell JE, Teitelbaum SL, Avioli LV. Calcium homeostasis in chronic streptozotocin-induced diabetes mellitus in the rat. *American Journal of Physiology-Endocrinology and Metabolism*. 1982;242(6):E451-E6.
 255. Ikeda K, Matsumoto T, Morita K, Yamato H, Takahashi H, Ezawa I, Ogata E. The role of insulin in the stimulation of renal 1,25-dihydroxyvitamin D synthesis by parathyroid hormone in rats. *Endocrinology*. 1987 Nov;121(5):1721-6.
 256. Levy JR, Murray E, Manolagas S, Olefsky JM. Demonstration of Insulin Receptors and Modulation of Alkaline Phosphatase Activity by Insulin in Rat Osteoblastic Cells*. *Endocrinology*. 1986;119(4):1786-92.
 257. Thomas D, Hards D, Rogers S, Ng K, Best J. Insulin receptor expression in bone. *Journal of bone and Mineral Research*. 1996;11(9):1312-20.
 258. Hahn TJ, Westbrook SL, Sullivan TL, Goodman WG, Halstead LR. Glucose transport in osteoblast-enriched bone explants: Characterization and insulin regulation. *Journal of Bone and Mineral Research*. 1988;3(3):359-65.
 259. Canalis E. Effect of hormones and growth factors on alkaline phosphatase activity and collagen synthesis in cultured rat calvariae. *Metabolism*. 1983;32(1):14-20.
 260. Pun K. The importance of parathyroid hormone in inhibition of collagen synthesis and mitogenesis of osteoblastic cell. *Journal of biochemistry*. 1989;106(6):1090-3.
 261. Wergedal JE, Baylink DJ. Characterization of cells isolated and cultured from human bone. *Experimental Biology and Medicine*. 1984;176(1):60-9.
 262. Maor G, Karnieli E. The Insulin-Sensitive Glucose Transporter (GLUT4) Is Involved in Early Bone Growth in Control and Diabetic Mice, But Is Regulated through the Insulin-Like Growth Factor I Receptor 1. *Endocrinology*. 1999;140(4):1841-51.
 263. Fulzele K, Riddle RC, DiGirolamo DJ, Cao X, Wan C, Chen D, et al. Insulin receptor signaling in osteoblasts regulates postnatal bone acquisition and body composition. *Cell*. 2010;142(2):309-19.
 264. Thrailkill K, Bunn RC, Lumpkin C, Wahl E, Cockrell G, Morris L, et al. Loss of insulin receptor in osteoprogenitor cells impairs structural strength of bone. *Journal of diabetes research*. 2014 May 18;2014.

265. Díaz-López A, Bulló M, Juanola-Falgarona M, Martínez-González MA, Estruch R, Covas M-I, et al. Reduced serum concentrations of carboxylated and undercarboxylated osteocalcin are associated with risk of developing type 2 diabetes mellitus in a high cardiovascular risk population: a nested case-control study. *The Journal of Clinical Endocrinology & Metabolism*. 2013;98(11):4524-31.
266. Gower BA, Pollock NK, Casazza K, Clemens TL, Goree LL, Granger WM. Associations of total and undercarboxylated osteocalcin with peripheral and hepatic insulin sensitivity and β -cell function in overweight adults. *The Journal of Clinical Endocrinology & Metabolism*. 2013;98(7):E1173-E80.
267. Fukunaga Y, Minamikawa J, Inoue D, Koshiyama H. Does Insulin Use Increase Bone Mineral Density in Patients With Non—Insulin-Dependent Diabetes Mellitus? *Archives of internal medicine*. 1997;157(22):2668-9.
268. Weinstock RS, Goland RS, Shane E, Clemens TL, Lindsay R, Bilezikian JP. Bone mineral density in women with type II diabetes mellitus. *Journal of Bone and Mineral Research*. 1989;4(1):97-101.
269. Conover CA, Lee P, Riggs BL, Powell DR. Insulin-like growth factor-binding protein-1 expression in cultured human bone cells: regulation by insulin and glucocorticoid. *Endocrinology*. 1996;137(8):3295-301.
270. Rosen CJ. Insulin-like growth factor I and bone mineral density: experience from animal models and human observational studies. *Best Practice & Research Clinical Endocrinology & Metabolism*. 2004;18(3):423-35.
271. Horcajada-Molteni MN, Chanteranne B, Lebecque P, Davicco MJ, Coxam V, Young A, et al. Amylin and Bone Metabolism in Streptozotocin-Induced Diabetic Rats. *Journal of Bone and Mineral Research*. 2001;16(5):958-65.
272. Dacquin R, Davey RA, Laplace C, Levasseur R, Morris HA, Goldring SR, et al. Amylin inhibits bone resorption while the calcitonin receptor controls bone formation in vivo. *The Journal of cell biology*. 2004;164(4):509-14.
273. Bouxsein ML, Rosen CJ, Turner CH, Ackert CL, Shultz KL, Donahue LR, et al. Generation of a New Congenic Mouse Strain to Test the Relationships Among Serum Insulin-like Growth Factor I, Bone Mineral Density, and Skeletal Morphology In Vivo. *Journal of Bone and Mineral Research*. 2002;17(4):570-9.
274. Zhang M, Xuan S, Bouxsein ML, von Stechow D, Akeno N, Faugere MC, et al. Osteoblast-specific knockout of the insulin-like growth factor (IGF) receptor gene reveals an essential role of IGF signaling in bone matrix mineralization. *Journal of Biological Chemistry*. 2002;277(46):44005-12.
275. Kanazawa I, Yamaguchi T, Sugimoto T. Serum insulin-like growth factor-I is a marker for assessing the severity of vertebral fractures in postmenopausal women with type 2 diabetes mellitus. *Osteoporosis Int*. 2011;22(4):1191-8.
276. Zhang Y, Papasian C, Deng H-W. Alteration of vitamin D metabolic enzyme expression and calcium transporter abundance in kidney involved in type 1 diabetes-induced bone loss. *Osteoporosis Int*. 2011;22(6):1781-8.
277. McCabe L, Zhang J, Raetz S. Understanding the skeletal pathology of type 1 and 2 diabetes mellitus. *Critical reviews in eukaryotic gene expression*. 2011;21(2):187-206.

278. Schwartz AV. Diabetes mellitus: Does it affect bone? *Calcified Tissue Int.* 2003;73(6):515-9.
279. Hampson G, Evans C, Petitt R, Evans W, Woodhead S, Peters J, et al. Bone mineral density, collagen type 1 α 1 genotypes and bone turnover in premenopausal women with diabetes mellitus. *Diabetologia.* 1998;41(11):1314-20.
280. Verhaeghe J, Van Herck E, Visser WJ, Suiker AM, Thomasset M, Einhorn TA, et al. Bone and mineral metabolism in BB rats with long-term diabetes: decreased bone turnover and osteoporosis. *Diabetes.* 1990;39(4):477-82.
281. Frazer TE, White NH, Hough S, Santiago JV, McGee BR, Bryce G, et al. Alterations in Circulating Vitamin D Metabolites in the Young Insulin-Dependent Diabetic*. *The Journal of Clinical Endocrinology & Metabolism.* 1981;53(6):1154-9.
282. Del Pino-Montes J, Benito G, Fernandez-Salazar M, Covenas R, Calvo J, Bouillon R, et al. Calcitriol improves streptozotocin-induced diabetes and recovers bone mineral density in diabetic rats. *Calcified Tissue Int.* 2004;75(6):526-32.
283. Wang YH, Liu Y, Buhl K, Rowe DW. Comparison of the action of transient and continuous PTH on primary osteoblast cultures expressing differentiation stage-specific GFP. *Journal of Bone and Mineral Research.* 2005;20(1):5-14.
284. Motyl KJ, McCauley LK, McCabe LR. Amelioration of type I diabetes-induced osteoporosis by parathyroid hormone is associated with improved osteoblast survival. *Journal of cellular physiology.* 2012;227(4):1326-34.
285. Schmid C, Schlapfer I, Peter M, Boni-Schnetzler M, Schwander J, Zapf J, et al. Growth hormone and parathyroid hormone stimulate IGFBP-3 in rat osteoblasts. *American Journal of Physiology-Endocrinology and Metabolism.* 1994;267(2):E226-E33.
286. Porte D, Tuckermann J, Becker M, Baumann B, Teurich S, Higgins T, et al. Both AP-1 and Cbfa1-like factors are required for the induction of interstitial collagenase by parathyroid hormone. *Oncogene.* 1999;18(3):667-78.
287. Hamann C, Picke A-K, Campbell GM, Balyura M, Rauner M, Bernhardt R, et al. Effects of parathyroid hormone on bone mass, bone strength, and bone regeneration in male rats with type 2 diabetes mellitus. *Endocrinology.* 2014;155(4):1197-206.
288. Schnoke M, Midura SB, Midura RJ. Parathyroid hormone suppresses osteoblast apoptosis by augmenting DNA repair. *Bone.* 2009;45(3):590-602.
289. Lozano D, de Castro LF, Dapía S, Andrade-Zapata I, Manzarbeitia F, Alvarez-Arroyo MV, et al. Role of parathyroid hormone-related protein in the decreased osteoblast function in diabetes-related osteopenia. *Endocrinology.* 2009;150(5):2027-35.
290. Duque G. Bone and fat connection in aging bone. *Current opinion in rheumatology.* 2008;20(4):429-34.
291. Yaturu S, Humphrey S, Jain SK, Landry C. Decreased bone mineral density in men with metabolic syndrome alone and with type 2 diabetes. *Medical Science Monitor Basic Research.* 2008;15(1):CR5-CR9.

292. Botolin S, Faugere MC, Malluche H, Orth M, Meyer R, McCabe LR. Increased bone adiposity and peroxisomal proliferator-activated receptor- γ 2 expression in type I diabetic mice. *Endocrinology*. 2005;146(8):3622-31.
293. Motyl KJ, Raetz M, Tekalur SA, Schwartz RC, McCabe LR. CCAAT/enhancer binding protein β -deficiency enhances type 1 diabetic bone phenotype by increasing marrow adiposity and bone resorption. *American Journal of Physiology-Regulatory, Integrative and Comparative Physiology*. 2011;300(5):R1250-R60.
294. Vanella L, Kim DH, Asprinio D, Peterson SJ, Barbagallo I, Vanella A, et al. HO-1 expression increases mesenchymal stem cell-derived osteoblasts but decreases adipocyte lineage. *Bone*. 2010;46(1):236-43.
295. Rzonca S, Suva L, Gaddy D, Montague D, Lecka-Czernik B. Bone is a target for the antidiabetic compound rosiglitazone. *Endocrinology*. 2004;145(1):401-6.
296. Maurin AC, Chavassieux PM, Frappart L, Delmas PD, Serre CM, Meunier PJ. Influence of mature adipocytes on osteoblast proliferation in human primary cocultures. *Bone*. 2000;26(5):485-9.
297. Elbaz A, Wu X, Rivas D, Gimble JM, Duque G. Inhibition of fatty acid biosynthesis prevents adipocyte lipotoxicity on human osteoblasts in vitro. *J Cell Mol Med*. 2010;14(4):982-91.
298. Coe LM, Irwin R, Lippner D, McCabe LR. The bone marrow microenvironment contributes to type I diabetes induced osteoblast death. *Journal of cellular physiology*. 2011;226(2):477-83.
299. Steppan CM, Crawford DT, Chidsey-Frink KL, Ke H, Swick AG. Leptin is a potent stimulator of bone growth in ob/ob mice. *Regul Pept*. 2000;92(1-3):73-8.
300. Reseland JE, Syversen U, Bakke I, Qvigstad G, Eide LG, Hjertner O, et al. Leptin is expressed in and secreted from primary cultures of human osteoblasts and promotes bone mineralization. *Journal of bone and mineral research : the official journal of the American Society for Bone and Mineral Research*. 2001;16(8):1426-33.
301. Cornish J, Callon KE, Bava U, Lin C, Naot D, Hill BL, et al. Leptin directly regulates bone cell function in vitro and reduces bone fragility in vivo. *J Endocrinol*. 2002;175(2):405-15.
302. Luna R, Garcia-Mayor RV, Lage M, Andrade MA, Barreiro J, Pombo M, et al. High serum leptin levels in children with type 1 diabetes mellitus: contribution of age, BMI, pubertal development and metabolic status. *Clin Endocrinol (Oxf)*. 1999;51(5):603-10.
303. Karaguzel G, Ozdem S, Boz A, Bircan I, Akcurin S. Leptin levels and body composition in children and adolescents with type 1 diabetes. *Clin Biochem*. 2006;39(8):788-93.
304. Vasilkova O, Mokhort T, Sharshakova T, Hayashida N, Takamura N. Leptin is an independent determinant of bone mineral density in men with type 2 diabetes mellitus. *Acta Diabetol*. 2011;48(4):291-5.
305. Hamrick MW, Della-Fera MA, Choi YH, Pennington C, Hartzell D, Baile CA. Leptin treatment induces loss of bone marrow adipocytes and increases bone formation in leptin-deficient ob/ob mice. *Journal of bone and mineral research : the*

- official journal of the American Society for Bone and Mineral Research. 2005;20(6):994-1001.
306. Martin A, de Vittoris R, David V, Moraes R, Begeot M, Lafage-Proust MH, et al. Leptin modulates both resorption and formation while preventing disuse-induced bone loss in tail-suspended female rats. *Endocrinology*. 2005;146(8):3652-9.
 307. Motyl KJ, McCabe LR. Leptin treatment prevents type I diabetic marrow adiposity but not bone loss in mice. *Journal of cellular physiology*. 2009;218(2):376-84.
 308. Wu Y, Tu Q, Valverde P, Zhang J, Murray D, Dong LQ, et al. Central adiponectin administration reveals new regulatory mechanisms of bone metabolism in mice. *Am J Physiol Endocrinol Metab*. 2014;306(12):E1418-30.
 309. Buday B, Pach FP, Literati-Nagy B, Vitai M, Vecsei Z, Koranyi L. Serum osteocalcin is associated with improved metabolic state via adiponectin in females versus testosterone in males. Gender specific nature of the bone-energy homeostasis axis. *Bone*. 2013;57(1):98-104.
 310. Esser N, Legrand-Poels S, Piette J, Scheen AJ, Paquot N. Inflammation as a link between obesity, metabolic syndrome and type 2 diabetes. *Diabetes Res Clin Pract*. 2014;105(2):141-50.
 311. Bending D, Zacccone P, Cooke A. Inflammation and type one diabetes. *Int Immunol*. 2012;24(6):339-46.
 312. Motyl KJ, Botolin S, Irwin R, Appledorn DM, Kadakia T, Amalfitano A, et al. Bone inflammation and altered gene expression with type I diabetes early onset. *Journal of cellular physiology*. 2009;218(3):575-83.
 313. Roszer T. Inflammation as death or life signal in diabetic fracture healing. *Inflamm Res*. 2011;60(1):3-10.
 314. Spranger J, Kroke A, Mohlig M, Hoffmann K, Bergmann MM, Ristow M, et al. Inflammatory cytokines and the risk to develop type 2 diabetes: results of the prospective population-based European Prospective Investigation into Cancer and Nutrition (EPIC)-Potsdam Study. *Diabetes*. 2003;52(3):812-7.
 315. Irwin R, LaPres JJ, Kinser S, McCabe LR. Prolyl-hydroxylase inhibition and HIF activation in osteoblasts promotes an adipocytic phenotype. *J Cell Biochem*. 2007;100(3):762-72.
 316. Oikawa A, Siragusa M, Quaini F, Mangialardi G, Katare RG, Caporali A, et al. Diabetes mellitus induces bone marrow microangiopathy. *Arterioscler Thromb Vasc Biol*. 2010;30(3):498-508.
 317. Burkhardt R, Moser W, Bartl R, Mahl G. Is diabetic osteoporosis due to microangiopathy? *Lancet (London, England)*. 1981;1(8224):844.
 318. Johnston SS, Conner C, Aagren M, Ruiz K, Bouchard J. Association between hypoglycaemic events and fall-related fractures in Medicare-covered patients with type 2 diabetes. *Diabetes Obes Metab*. 2012;14(7):634-43.
 319. Eller-Vainicher C, Zhukouskaya VV, Tolkachev YV, Koritko SS, Cairolì E, Grossi E, et al. Low bone mineral density and its predictors in type 1 diabetic patients evaluated by the classic statistics and artificial neural network analysis. *Diabetes care*. 2011;34(10):2186-91.

320. Ali AA, Weinstein RS, Stewart SA, Parfitt AM, Manolagas SC, Jilka RL. Rosiglitazone causes bone loss in mice by suppressing osteoblast differentiation and bone formation. *Endocrinology*. 2005;146(3):1226-35.
321. Schwartz AV. TZDs and Bone: A Review of the Recent Clinical Evidence. *PPAR Res*. 2008;2008:297893.
322. Vestergaard P, Rejnmark L, Mosekilde L. Relative fracture risk in patients with diabetes mellitus, and the impact of insulin and oral antidiabetic medication on relative fracture risk. *Diabetologia*. 2005;48(7):1292-9.
323. Zinman B, Haffner SM, Herman WH, Holman RR, Lachin JM, Kravitz BG, et al. Effect of rosiglitazone, metformin, and glyburide on bone biomarkers in patients with type 2 diabetes. *The Journal of clinical endocrinology and metabolism*. 2010;95(1):134-42.
324. Cortizo AM, Sedlinsky C, McCarthy AD, Blanco A, Schurman L. Osteogenic actions of the anti-diabetic drug metformin on osteoblasts in culture. *Eur J Pharmacol*. 2006;536(1-2):38-46.
325. Gao Y, Xue J, Li X, Jia Y, Hu J. Metformin regulates osteoblast and adipocyte differentiation of rat mesenchymal stem cells. *J Pharm Pharmacol*. 2008;60(12):1695-700.
326. Kanazawa I, Yamaguchi T, Yano S, Yamauchi M, Sugimoto T. Metformin enhances the differentiation and mineralization of osteoblastic MC3T3-E1 cells via AMP kinase activation as well as eNOS and BMP-2 expression. *Biochemical and biophysical research communications*. 2008;375(3):414-9.
327. Ma P, Gu B, Ma J, E L, Wu X, Cao J, et al. Glimepiride induces proliferation and differentiation of rat osteoblasts via the PI3-kinase/Akt pathway. *Metabolism*. 2010;59(3):359-66.
328. Jang WG, Kim EJ, Bae IH, Lee KN, Kim YD, Kim DK, et al. Metformin induces osteoblast differentiation via orphan nuclear receptor SHP-mediated transactivation of Runx2. *Bone*. 2011;48(4):885-93.
329. Schurman L, McCarthy AD, Sedlinsky C, Gangoiti MV, Arnol V, Bruzzone L, et al. Metformin reverts deleterious effects of advanced glycation end-products (AGEs) on osteoblastic cells. *Exp Clin Endocrinol Diabetes*. 2008;116(6):333-40.
330. Zhen D, Chen Y, Tang X. Metformin reverses the deleterious effects of high glucose on osteoblast function. *Journal of diabetes and its complications*. 2010;24(5):334-44.
331. Mai QG, Zhang ZM, Xu S, Lu M, Zhou RP, Zhao L, et al. Metformin stimulates osteoprotegerin and reduces RANKL expression in osteoblasts and ovariectomized rats. *J Cell Biochem*. 2011;112(10):2902-9.
332. Jeyabalan J, Viollet B, Smitham P, Ellis SA, Zaman G, Bardin C, et al. The anti-diabetic drug metformin does not affect bone mass in vivo or fracture healing. *Osteoporosis international : a journal established as result of cooperation between the European Foundation for Osteoporosis and the National Osteoporosis Foundation of the USA*. 2013;24(10):2659-70.
333. Hegazy SK. Evaluation of the anti-osteoporotic effects of metformin and sitagliptin in postmenopausal diabetic women. *J Bone Miner Metab*. 2015;33(2):207-12.

334. Ljunggren O, Bolinder J, Johansson L, Wilding J, Langkilde AM, Sjostrom CD, et al. Dapagliflozin has no effect on markers of bone formation and resorption or bone mineral density in patients with inadequately controlled type 2 diabetes mellitus on metformin. *Diabetes Obes Metab.* 2012;14(11):990-9.
335. Bolinder J, Ljunggren O, Johansson L, Wilding J, Langkilde AM, Sjostrom CD, et al. Dapagliflozin maintains glycaemic control while reducing weight and body fat mass over 2 years in patients with type 2 diabetes mellitus inadequately controlled on metformin. *Diabetes Obes Metab.* 2014;16(2):159-69.
336. Nicodemus KK, Folsom AR. Type 1 and type 2 diabetes and incident hip fractures in postmenopausal women. *Diabetes care.* 2001;24(7):1192-7.
337. Lipscombe LL, Jamal SA, Booth GL, Hawker GA. The risk of hip fractures in older individuals with diabetes: a population-based study. *Diabetes care.* 2007;30(4):835-41.
338. Ahmed LA, Joakimsen RM, Berntsen GK, Fonnebo V, Schirmer H. Diabetes mellitus and the risk of non-vertebral fractures: the Tromso study. *Osteoporosis international : a journal established as result of cooperation between the European Foundation for Osteoporosis and the National Osteoporosis Foundation of the USA.* 2006;17(4):495-500.
339. Neumann T, Lodes S, Kastner B, Franke S, Kiehntopf M, Lehmann T, et al. High serum pentosidine but not esRAGE is associated with prevalent fractures in type 1 diabetes independent of bone mineral density and glycaemic control. *Osteoporosis international : a journal established as result of cooperation between the European Foundation for Osteoporosis and the National Osteoporosis Foundation of the USA.* 2014;25(5):1527-33.
340. Forsen L, Meyer HE, Midthjell K, Edna TH. Diabetes mellitus and the incidence of hip fracture: results from the Nord-Trondelag Health Survey. *Diabetologia.* 1999;42(8):920-5.
341. Neumann T, Samann A, Lodes S, Kastner B, Franke S, Kiehntopf M, et al. Glycaemic control is positively associated with prevalent fractures but not with bone mineral density in patients with Type 1 diabetes. *Diabetic medicine : a journal of the British Diabetic Association.* 2011;28(7):872-5.
342. Miao JM, Brismar K, Nyren O, Ugarph-Morawski A, Ye WM. Elevated hip fracture risk in type 1 diabetic patients. *Diabetes care.* 2005;28(12):2850-5.
343. Gunczler P, Lanes R, Paoli M, Martinis R, Villaroel O, Weisinger JR. Decreased bone mineral density and bone formation markers shortly after diagnosis of clinical type 1 diabetes mellitus. *Journal of pediatric endocrinology & metabolism : JPEM.* 2001;14(5):525-8.
344. Masse PG, Pacifique MB, Tranchant CC, Arjmandi BH, Ericson KL, Donovan SM, et al. Bone metabolic abnormalities associated with well-controlled type 1 diabetes (IDDM) in young adult women: a disease complication often ignored or neglected. *J Am Coll Nutr.* 2010;29(4):419-29.
345. Campos Pastor MM, Lopez-Ibarra PJ, Escobar-Jimenez F, Serrano Pardo MD, Garcia-Cervigon AG. Intensive insulin therapy and bone mineral density in type 1 diabetes mellitus: a prospective study. *Osteoporosis international : a journal established as result of cooperation between the European Foundation for*

- Osteoporosis and the National Osteoporosis Foundation of the USA. 2000;11(5):455-9.
346. Mastrandrea LD, Wactawski-Wende J, Donahue RP, Hovey KM, Clark A, Quattrin T. Young women with type 1 diabetes have lower bone mineral density that persists over time. *Diabetes care*. 2008;31(9):1729-35.
347. Pater A, Sypniewska G, Pilecki O. Biochemical markers of bone cell activity in children with type 1 diabetes mellitus. *Journal of pediatric endocrinology & metabolism : JPEM*. 2010;23(1-2):81-6.
348. Kayath MJ, Dib SA, Vieira JG. Prevalence and magnitude of osteopenia associated with insulin-dependent diabetes mellitus. *Journal of diabetes and its complications*. 1994;8(2):97-104.
349. Liu EY, Wactawski-Wende J, Donahue RP, Dmochowski J, Hovey KM, Quattrin T. Does low bone mineral density start in post-teenage years in women with type 1 diabetes? *Diabetes care*. 2003;26(8):2365-9.
350. Loureiro MB, Ururahy MA, Freire-Neto FP, Oliveira GH, Duarte VM, Luchessi AD, et al. Low bone mineral density is associated to poor glycemic control and increased OPG expression in children and adolescents with type 1 diabetes. *Diabetes Res Clin Pract*. 2014;103(3):452-7.
351. Brandao FR, Vicente EJ, Daltro CH, Sacramento M, Moreira A, Adan L. Bone metabolism is linked to disease duration and metabolic control in type 1 diabetes mellitus. *Diabetes Res Clin Pract*. 2007;78(3):334-9.
352. Lunt H, Florkowski CM, Cundy T, Kendall D, Brown LJ, Elliot JR, et al. A population-based study of bone mineral density in women with longstanding type 1 (insulin dependent) diabetes. *Diabetes Res Clin Pract*. 1998;40(1):31-8.
353. Kemink SA, Hermus AR, Swinkels LM, Lutterman JA, Smals AG. Osteopenia in insulin-dependent diabetes mellitus; prevalence and aspects of pathophysiology. *J Endocrinol Invest*. 2000;23(5):295-303.
354. Lopez-Ibarra PJ, Pastor MM, Escobar-Jimenez F, Pardo MD, Gonzalez AG, Luna JD, et al. Bone mineral density at time of clinical diagnosis of adult-onset type 1 diabetes mellitus. *Endocrine practice : official journal of the American College of Endocrinology and the American Association of Clinical Endocrinologists*. 2001;7(5):346-51.
355. Bridges MJ, Moochhala SH, Barbour J, Kelly CA. Influence of diabetes on peripheral bone mineral density in men: a controlled study. *Acta Diabetol*. 2005;42(2):82-6.
356. Strotmeyer ES, Cauley JA, Orchard TJ, Steenkiste AR, Dorman JS. Middle-aged premenopausal women with type 1 diabetes have lower bone mineral density and calcaneal quantitative ultrasound than nondiabetic women. *Diabetes care*. 2006;29(2):306-11.
357. Hamilton EJ, Rakic V, Davis WA, Chubb SA, Kamber N, Prince RL, et al. Prevalence and predictors of osteopenia and osteoporosis in adults with Type 1 diabetes. *Diabetic medicine : a journal of the British Diabetic Association*. 2009;26(1):45-52.

358. Danielson KK, Elliott ME, LeCaire T, Binkley N, Palta M. Poor glycemic control is associated with low BMD detected in premenopausal women with type 1 diabetes. *Osteoporosis Int.* 2009;20(6):923-33.
359. Botushanov N, Yaneva M, Orbetzova M, Botushanova A. Bone mineral density in bulgarian patients with type 1 diabetes mellitus. *Journal of Osteoporosis and Physical Activity.* 2014 Feb 27:1-6.
360. Ingberg CM, Palmer M, Aman J, Arvidsson B, Schvarcz E, Berne C. Body composition and bone mineral density in long-standing type 1 diabetes. *Journal of Internal Medicine.* 2004;255(3):392-8.
361. Heap J, Murray MA, Miller SC, Jalili T, Moyer-Mileur LJ. Alterations in bone characteristics associated with glycemic control in adolescents with type 1 diabetes mellitus. *J Pediatr.* 2004;144(1):56-62.
362. Moyer-Mileur LJ, Dixon SB, Quick JL, Askew EW, Murray MA. Bone mineral acquisition in adolescents with type 1 diabetes. *Journal of Pediatrics.* 2004;145(5):662-9.
363. Moyer-Mileur LJ, Slater H, Jordan KC, Murray MA. IGF-1 and IGF-binding proteins and bone mass, geometry, and strength: relation to metabolic control in adolescent girls with type 1 diabetes. *Journal of bone and mineral research : the official journal of the American Society for Bone and Mineral Research.* 2008;23(12):1884-91.
364. Saha MT, Sievanen H, Salo MK, Tulokas S, Saha HH. Bone mass and structure in adolescents with type 1 diabetes compared to healthy peers. *Osteoporosis Int.* 2009;20(8):1401-6.
365. Bechtold S, Dirlenbach I, Raile K, Noelle V, Bonfig W, Schwarz HP. Early manifestation of type 1 diabetes in children is a risk factor for changed bone geometry: data using peripheral quantitative computed tomography. *Pediatrics.* 2006;118(3):e627-34.
366. Bechtold S, Putzker S, Bonfig W, Fuchs O, Dirlenbach I, Schwarz HP. Bone size normalizes with age in children and adolescents with type 1 diabetes. *Diabetes care.* 2007;30(8):2046-50.
367. Roggen I, Gies I, Vanbesien J, Louis O, De Schepper J. Trabecular Bone Mineral Density and Bone Geometry of the Distal Radius at Completion of Pubertal Growth in Childhood Type 1 Diabetes. *Hormone Research in Paediatrics.* 2013;79(2):68-74.
368. Neumann T, Lodes S, Kastner B, Lehmann T, Hans D, Lamy O, et al. Trabecular bone score in type 1 diabetes-a cross-sectional study. *Osteoporosis international : a journal established as result of cooperation between the European Foundation for Osteoporosis and the National Osteoporosis Foundation of the USA.* 2016;27(1):127-33.
369. Slade JM, Coe LM, Meyer RA, McCabe LR. Human bone marrow adiposity is linked with serum lipid levels not T1-diabetes. *Journal of diabetes and its complications.* 2012;26(1):1-9.

370. Camurdan MO, Cinaz P, Bideci A, Demirel F. Role of hemoglobin A(1c), duration and puberty on bone mineral density in diabetic children. *Pediatrics International*. 2007;49(5):645-51.
371. Heilman K, Zilmer M, Zilmer K, Tillmann V. Lower bone mineral density in children with type 1 diabetes is associated with poor glycemic control and higher serum ICAM-1 and urinary isoprostane levels. *J Bone Miner Metab*. 2009;27(5):598-604.
372. Valerio G, del Puente A, Esposito-del Puente A, Buono P, Mozzillo E, Franzese A. The lumbar bone mineral density is affected by long-term poor metabolic control in adolescents with type 1 diabetes mellitus. *Hormone Research*. 2002;58(6):266-72.
373. Souza KSC, Ururahy MAG, Oliveira YM, Loureiro MB, Silva HPV, Bortolin RH, et al. Low bone mineral density in patients with type 1 diabetes: association with reduced expression of IGF1, IGF1R and TGF B 1 in peripheral blood mononuclear cells. *Diabetes/metabolism research and reviews*. 2016 Sep 1;32(6):589-95.
374. Pascual J, Argente J, Lopez MB, Munoz M, Martinez G, Vazquez MA, et al. Bone mineral density in children and adolescents with diabetes mellitus type 1 of recent onset. *Calcif Tissue Int*. 1998;62(1):31-5.
375. Gunczler P, Lanes R, Paz-Martinez V, Martins R, Esaa S, Colmenares V, et al. Decreased lumbar spine bone mass and low bone turnover in children and adolescents with insulin dependent diabetes mellitus followed longitudinally. *Journal of pediatric endocrinology & metabolism : JPEM*. 1998;11(3):413-9.
376. Hadjidakis DJ, Raptis AE, Sfakianakis M, Mylonakis A, Raptis SA. Bone mineral density of both genders in Type 1 diabetes according to bone composition. *Journal of diabetes and its complications*. 2006;20(5):302-7.
377. Leger J, Marinovic D, Alberti C, Dorgeret S, Chevenne D, Marchal CL, et al. Lower bone mineral content in children with type 1 diabetes mellitus is linked to female sex, low insulin-like growth factor type I levels, and high insulin requirement. *The Journal of clinical endocrinology and metabolism*. 2006;91(10):3947-53.
378. Simmons JH, Raines M, Ness KD, Hall R, Gebretsadik T, Mohan S, et al. Metabolic control and bone health in adolescents with type 1 diabetes. *International journal of pediatric endocrinology*. 2011;2011(1):13.
379. Korkusuz F. *Musculoskeletal Research and Basic Science*. Springer; 2015.
380. Guglielmi G, Muscarella S, Bazzocchi A. Integrated imaging approach to osteoporosis: state-of-the-art review and update. *Radiographics : a review publication of the Radiological Society of North America, Inc*. 2011;31(5):1343-64.
381. Baroncelli GI, Federico G, Bertelloni S, de Terlizzi F, Cadossi R, Saggese G. Bone quality assessment by quantitative ultrasound of proximal phalanxes of the hand in healthy subjects aged 3--21 years. *Pediatric research*. 2001;49(5):713-8.
382. Savino F, Viola S, Benetti S, Ceratto S, Tarasco V, Lupica MM, et al. Quantitative ultrasound applied to metacarpal bone in infants. *PeerJ*. 2013;1:e141.
383. McDevitt H, Ahmed SF. Quantitative ultrasound assessment of bone health in the neonate. *Neonatology*. 2007;91(1):2-11.

384. Gluer CC. Quantitative ultrasound techniques for the assessment of osteoporosis: expert agreement on current status. The International Quantitative Ultrasound Consensus Group. *Journal of bone and mineral research : the official journal of the American Society for Bone and Mineral Research*. 1997;12(8):1280-8.
385. Peyrin F, Muller C, Carillon Y, Nuzzo S, Bonnassie A, Briguët A. Synchrotron radiation microCT: a reference tool for the characterization of bone samples. *Advances in experimental medicine and biology*. 2001;496:129-42.
386. Majumdar S, Kothari M, Augat P, Newitt DC, Link TM, Lin JC, et al. High-resolution magnetic resonance imaging: Three-dimensional trabecular bone architecture and biomechanical properties. *Bone*. 1998;22(5):445-54.
387. Ito M. Radiation exposure in bone measurements. *Journal of Bone and Mineral Research*. 2006;21(5):803.
388. Griffith JF, Genant HK. New imaging modalities in bone. *Current rheumatology reports*. 2011;13(3):241-50.
389. Ashe M, Khan K, Kontulainen S, Guy P, Liu D, Beck T, et al. Accuracy of pQCT for evaluating the aged human radius: an ashing, histomorphometry and failure load investigation. *Osteoporosis Int*. 2006;17(8):1241-51.
390. Fuller H, Fuller R, Pereira RMR. High resolution peripheral quantitative computed tomography for the assessment of morphological and mechanical bone parameters. *Revista Brasileira de Reumatologia*. 2015 Aug;55(4):352-62.
391. Brown RW, Cheng Y-CN, Haacke EM, Thompson MR, Venkatesan R. *Magnetic resonance imaging: physical principles and sequence design*: John Wiley & Sons; 2014 May 2.
392. Vlaardingerbroek MT, Boer JA. *Magnetic resonance imaging: theory and practice*: Springer Science & Business Media; 2013 Mar 9.
393. Westbrook C KRC, Talbot J. . *MRI in Practice*. Third Edition ed: Wiley, ; 2005.
394. FW. W. Structural and functional assessment of trabecular and cortical bone by micro magnetic resonance imaging. *J Magn Reson Imaging* 2007;25 390-409.
395. Ridgway JP. Cardiovascular magnetic resonance physics for clinicians: part I. *Journal of cardiovascular magnetic resonance : official journal of the Society for Cardiovascular Magnetic Resonance*. 2010;12(1):71.
396. http://www.revisemri.com/questions/pulse_sequences/se_ge_differences. [cited 2015 28/10].
397. McRobbie DW ME, Graves MJ, Prince MR: . *MRI From Picture to Proton*. 2nd ed. ed. USA: : Cambridge University Press; 2010.
398. Blüml S, Panigrahy A. *MR Spectroscopy of Pediatric Brain Disorders*: Springer Science & Business Media; 2012.
399. Jansen JF, Backes WH, Nicolay K, Kooi ME. 1H MR Spectroscopy of the Brain: Absolute Quantification of Metabolites 1. *Radiology*. 2006;240(2):318-32.
400. S M. Magnetic resonance imaging of trabecular bone structure. *Top Magn Reson Imaging* 2002;12(5):323-34.

401. Ladinsky GA, Wehrli FW. Noninvasive assessment of bone microarchitecture by MRI. *Current osteoporosis reports*. 2006;4(4):140-7.
402. Majumdar S, Genant HK, Grampp S, Newitt DC, Truong VH, Lin JC, et al. Correlation of trabecular bone structure with age, bone mineral density, and osteoporotic status: In vivo studies in the distal radius using high resolution magnetic resonance imaging. *Journal of Bone and Mineral Research*. 1997;12(1):111-8.
403. Link TM, Majumdar S, Augat P, Lin JC, Newitt D, Lu Y, et al. In vivo high resolution MRI of the calcaneus: Differences in trabecular structure in osteoporosis patients. *Journal of Bone and Mineral Research*. 1998;13(7):1175-82.
404. Vieth V, Link TM, Lotter A, Persigehl T, Newitt D, Heindel W, et al. Does the trabecular bone structure depicted by high-resolution MRI of the calcaneus reflect the true bone structure? *Invest Radiol*. 2001;36(4):210-7.
405. Chung HW, Wehrli FW, Williams JL, Kugelmass SD, Wehrli SL. Quantitative analysis of trabecular microstructure by 400 MHz nuclear magnetic resonance imaging. *Journal of bone and mineral research : the official journal of the American Society for Bone and Mineral Research*. 1995;10(5):803-11.
406. Wehrli FW, Leonard MB, Saha PK, Gomberg BR. Quantitative high-resolution magnetic resonance imaging reveals structural implications of renal osteodystrophy on trabecular and cortical bone. *J Magn Reson Imaging*. 2004;20(1):83-9.
407. Iita N, Handa S, Tomiha S, Kose K. Development of a compact MRI system for measuring the trabecular bone microstructure of the finger. *Magnetic Resonance in Medicine*. 2007;57(2):272-7.
408. Krug R, Carballido-Gamio J, Banerjee S, Burghardt AJ, Link TM, Majumdar S. In vivo ultra-high-field magnetic resonance imaging of trabecular bone microarchitecture at 7 T. *J Magn Reson Imaging*. 2008;27(4):854-9.
409. Krug R, Stehling C, Kelley DAC, Majumdar S, Link TM. Imaging of the Musculoskeletal System In Vivo Using Ultra-high Field Magnetic Resonance at 7 T. *Invest Radiol*. 2009;44(9):613-8.
410. Chang G, Xia D, Chen C, Madelin G, Abramson SB, Babb JS, et al. 7T MRI detects deterioration in subchondral bone microarchitecture in subjects with mild knee osteoarthritis as compared with healthy controls. *Journal of magnetic resonance imaging : JMRI*. 2015;41(5):1311-7.
411. Hotca A, Rajapakse CS, Cheng C, Honig S, Egol K, Regatte RR, et al. In vivo measurement reproducibility of femoral neck microarchitectural parameters derived from 3T MR images. *J Magn Reson Imaging*. 2015 Nov 1;42(5):1339-45.
412. Wright AC, Lemdiasov R, Connick TJ, Bhagat YA, Magland JF, Song HK, et al. Helmholtz-pair transmit coil with integrated receive array for high-resolution MRI of trabecular bone in the distal tibia at 7T. *J Magn Reson*. 2011;210(1):113-22.
413. Magland JF, Wald MJ, Wehrli FW. Spin-Echo Micro-MRI of Trabecular Bone Using Improved 3D FLASE. *Magnetic resonance in medicine : official journal of the Society of Magnetic Resonance in Medicine / Society of Magnetic Resonance in Medicine*. 2009;61(5):1114-21.

414. Krug R, Han ET, Banerjee S, Majumdar S. Fully balanced steady-state 3D-spin-echo (bSSSE) imaging at 3 Tesla. *Magn Reson Med.* 2006;56(5):1033-40.
415. Jung BA, Weigel M. Spin echo magnetic resonance imaging. *J Magn Reson Imaging.* 2013;37(4):805-17.
416. Majumdar S, Link TM, Augat P, Lin JC, Newitt D, Lane NE, et al. Trabecular bone architecture in the distal radius using magnetic resonance imaging in subjects with fractures of the proximal femur. *Magnetic Resonance Science Center and Osteoporosis and Arthritis Research Group. Osteoporosis international : a journal established as result of cooperation between the European Foundation for Osteoporosis and the National Osteoporosis Foundation of the USA.* 1999;10(3):231-9.
417. Stampa B, Kuhn B, Liess C, Heller M, Gluer CC. Characterization of the integrity of three-dimensional trabecular bone microstructure by connectivity and shape analysis using high-resolution magnetic resonance imaging in vivo. *Top Magn Reson Imaging.* 2002;13(5):357-63.
418. Stein EM, Liu XS, Nickolas TL, Cohen A, Thomas V, McMahon DJ, et al. Abnormal microarchitecture and reduced stiffness at the radius and tibia in postmenopausal women with fractures. *Journal of bone and mineral research : the official journal of the American Society for Bone and Mineral Research.* 2010;25(12):2572-81.
419. Laib A, Newitt DC, Lu Y, Majumdar S. New model-independent measures of trabecular bone structure applied to in vivo high-resolution MR images. *Osteoporosis Int.* 2002;13(2):130-6.
420. Krug R, Banerjee S, Han ET, Newitt DC, Link TM, Majumdar S. Feasibility of in vivo structural analysis of high-resolution magnetic resonance images of the proximal femur. *Osteoporosis Int.* 2005;16(11):1307-14.
421. Chang G, Deniz CM, Honig S, Rajapakse CS, Egol K, Regatte RR, et al. Feasibility of three-dimensional MRI of proximal femur microarchitecture at 3 tesla using 26 receive elements without and with parallel imaging. *J Magn Reson Imaging.* 2014;40(1):229-38.
422. Hotca A, Ravichandra S, Mikheev A, Rusinek H, Chang G. Precision of volumetric assessment of proximal femur microarchitecture from high-resolution 3T MRI. *International journal of computer assisted radiology and surgery.* 2015;10(1):35-43.
423. Newitt DC, van Rietbergen B, Majumdar S. Processing and analysis of in vivo high-resolution MR images of trabecular bone for longitudinal studies: Reproducibility of structural measures and micro-finite element analysis derived mechanical properties. *Osteoporosis Int.* 2002;13(4):278-87.
424. Wehrli FW, Saha PK, Gomberg BR, Song HK, Snyder PJ, Benito M, et al. Role of magnetic resonance for assessing structure and function of trabecular bone. *Top Magn Reson Imaging.* 2002;13(5):335-55.
425. Hudelmaier M, Kollstedt A, Lochmuller EM, Kuhn V, Eckstein F, Link TM. Gender differences in trabecular bone architecture of the distal radius assessed with magnetic resonance imaging and implications for mechanical competence. *Osteoporosis Int.* 2005;16(9):1124-33.

426. Kirmani S, Christen D, van Lenthe GH, Fischer PR, Bouxsein ML, McCready LK, et al. Bone Structure at the Distal Radius During Adolescent Growth. *Journal of Bone and Mineral Research*. 2009;24(6):1033-42.
427. Christopher M. Modlesky a, □ DBa, JTKa, BMMA, , b DAR, et al. Sex differences in trabecular bone microarchitecture are not detected in pre and early pubertal children using magnetic resonance imaging. *Bone* 2011;49:1067–72.
428. Modlesky CM, Majumdar S, Dudley GA. Trabecular bone microarchitecture in female collegiate gymnasts. *Osteoporosis Int*. 2008;19(7):1011-8.
429. Modlesky C, Whitney D, Singh H, Barbe M, Kirby J, Miller F. Underdevelopment of trabecular bone microarchitecture in the distal femur of nonambulatory children with cerebral palsy becomes more pronounced with distance from the growth plate. *Osteoporosis Int*. 2015;26(2):505-12.
430. Modlesky CM, Subramanian P, Miller F. Underdeveloped trabecular bone microarchitecture is detected in children with cerebral palsy using high-resolution magnetic resonance imaging. *Osteoporosis international : a journal established as result of cooperation between the European Foundation for Osteoporosis and the National Osteoporosis Foundation of the USA*. 2008;19(2):169-76.
431. Modlesky CM, Majumdar S, Narasimhan A, Dudley GA. Trabecular bone microarchitecture is deteriorated in men with spinal cord injury. *Journal of bone and mineral research : the official journal of the American Society for Bone and Mineral Research*. 2004;19(1):48-55.
432. Modlesky CM, Bajaj D, Kirby JT, Mulrooney BM, Rowe DA, Miller F. Sex differences in trabecular bone microarchitecture are not detected in pre and early pubertal children using magnetic resonance imaging. *Bone*. 2011;49(5):1067-72.
433. Boutry N, Cortet B, Dubois P, Marchandise X, Cotten A. Trabecular bone structure of the calcaneus: preliminary in vivo MR imaging assessment in men with osteoporosis. *Radiology*. 2003;227(3):708-17.
434. McComb C, Harpur A, Yacoubian C, Leddy C, Anderson G, Shepherd S, et al. MRI-based abnormalities in young adults at risk of adverse bone health due to childhood-onset metabolic & endocrine conditions. *Clin Endocrinol (Oxf)*. 2014;80(6):811-7.
435. Folkesson J, Goldenstein J, Carballido-Gamio J, Kazakia G, Burghardt AJ, Rodriguez A, et al. Longitudinal evaluation of the effects of alendronate on MRI bone microarchitecture in postmenopausal osteopenic women. *Bone*. 2011;48(3):611-21.
436. Chesnut CH, Majumdar S, Newitt DC, Shields A, Van Pelt J, Laschansky E, et al. Effects of salmon calcitonin on trabecular microarchitecture as determined by magnetic resonance imaging: Results from the QUEST study. *Journal of Bone and Mineral Research*. 2005;20(9):1548-61.
437. Benito M, Vasilic B, Wehrli FW, Bunker B, Wald M, Gomberg B, et al. Effect of testosterone replacement on trabecular architecture in hypogonadal men. *Journal of bone and mineral research : the official journal of the American Society for Bone and Mineral Research*. 2005;20(10):1785-91.

438. Chang G, Pakin SK, Schweitzer ME, Saha PK, Regatte RR. Adaptations in trabecular bone microarchitecture in olympic athletes determined by 7T MRI. *J Magn Reson Imaging*. 2008;27(5):1089-95.
439. Pritchard JM, Giangregorio LM, Atkinson SA, Beattie KA, Inglis D, Ioannidis G, et al. Changes in trabecular bone microarchitecture in postmenopausal women with and without type 2 diabetes: a two year longitudinal study. *Bmc Musculoskeletal Disorders*. 2013;14.
440. Issever AS, Link TM, Newitt D, Munoz T, Majumdar S. Interrelationships between 3-T-MRI-derived cortical and trabecular bone structure parameters and quantitative-computed-tomography-derived bone mineral density. *Magn Reson Imaging*. 2010;28(9):1299-305.
441. Kazakia GJ, Hyun B, Burghardt AJ, Krug R, Newitt DC, de Papp AE, et al. In vivo determination of bone structure in postmenopausal women: a comparison of HR-pQCT and high-field MR imaging. *Journal of bone and mineral research : the official journal of the American Society for Bone and Mineral Research*. 2008;23(4):463-74.
442. Ladinsky GA, Vasilic B, Popescu AM, Wald M, Zemel BS, Snyder PJ, et al. Trabecular structure quantified with the MRI-based virtual bone biopsy in postmenopausal women contributes to vertebral deformity burden independent of areal vertebral BMD. *Journal of bone and mineral research : the official journal of the American Society for Bone and Mineral Research*. 2008;23(1):64-74.
443. Griffith JF, Yeung DKW, Antonio GE, Lee FKH, Hong AWL, Wong SYS, et al. Vertebral bone mineral density, marrow perfusion, and fat content in healthy men and men with osteoporosis: Dynamic contrast-enhanced MR imaging and spectroscopy. *Radiology*. 2005;236(3):945-51.
444. Tang GY, Lv ZW, Tang RB, Liu Y, Peng YF, Li W, et al. Evaluation of MR spectroscopy and diffusion-weighted MRI in detecting bone marrow changes in postmenopausal women with osteoporosis. *Clinical radiology*. 2010;65(5):377-81.
445. Li X, Kuo D, Schafer AL, Porzig A, Link TM, Black D, et al. Quantification of vertebral bone marrow fat content using 3 Tesla MR spectroscopy: reproducibility, vertebral variation, and applications in osteoporosis. *J Magn Reson Imaging*. 2011;33(4):974-9.
446. Yeung DK, Griffith JF, Antonio GE, Lee FK, Woo J, Leung PC. Osteoporosis is associated with increased marrow fat content and decreased marrow fat unsaturation: a proton MR spectroscopy study. *J Magn Reson Imaging*. 2005;22(2):279-85.
447. Griffith JF, Yeung DK, Antonio GE, Wong SY, Kwok TC, Woo J, et al. Vertebral marrow fat content and diffusion and perfusion indexes in women with varying bone density: MR evaluation. *Radiology*. 2006;241(3):831-8.
448. Schellinger D, Lin CS, Lim J, Hatipoglu HG, Pezzullo JC, Singer AJ. Bone marrow fat and bone mineral density on proton MR spectroscopy and dual-energy X-ray absorptiometry: their ratio as a new indicator of bone weakening. *AJR American journal of roentgenology*. 2004;183(6):1761-5.

449. Agrawal K, Agarwal Y, Chopra RK, Batra A, Chandra R, Thukral BB. Evaluation of MR Spectroscopy and Diffusion-Weighted MRI in Postmenopausal Bone Strength. *Cureus*. 2015;7(9):e327.
450. Bredella MA, Daley SM, Kalra MK, Brown JK, Miller KK, Torriani M. Marrow Adipose Tissue Quantification of the Lumbar Spine by Using Dual-Energy CT and Single-Voxel (1)H MR Spectroscopy: A Feasibility Study. *Radiology*. 2015;277(1):230-5.
451. Singhal V, Miller KK, Torriani M, Bredella MA. Short- and long-term reproducibility of marrow adipose tissue quantification by 1H-MR spectroscopy. *Skeletal Radiol*. . 2016 Feb 1;45(2):221-5.
452. Cohen A, Shen W, Dempster DW, Zhou H, Recker RR, Lappe JM, et al. Marrow adiposity assessed on transiliac crest biopsy samples correlates with noninvasive measurement of marrow adiposity by proton magnetic resonance spectroscopy (H-MRS) at the spine but not the femur. *Osteoporosis international : a journal established as result of cooperation between the European Foundation for Osteoporosis and the National Osteoporosis Foundation of the USA*. 2015.
453. Gao Y, Zong K, Gao Z, Rubin MR, Chen J, Heymsfield SB, et al. Magnetic resonance imaging-measured bone marrow adipose tissue area is inversely related to cortical bone area in children and adolescents aged 5-18years. *Journal of clinical densitometry : the official journal of the International Society for Clinical Densitometry*. 2015;18(2):203-8.
454. Kugel H, Jung C, Schulte O, Heindel W. Age-and sex-specific differences in the 1H-spectrum of vertebral bone marrow. *J Magn Reson Imaging*. 2001;13(2):263-8.
455. Griffith JF, Yeung DKW, Ma HT, Leung JCS, Kwok TCY, Leung PC. Bone marrow fat content in the elderly: A reversal of sex difference seen in younger subjects. *J Magn Reson Imaging*. 2012;36(1):225-30.
456. Schellinger D, Lin CS, Fertikh D, Lee JS, Lauerman WC, Henderson F, et al. Normal lumbar vertebrae: anatomic, age, and sex variance in subjects at proton MR spectroscopy--initial experience. *Radiology*. 2000;215(3):910-6.
457. Shen W, Chen J, Punyanitya M, Shapses S, Heshka S, Heymsfield SB. MRI-measured bone marrow adipose tissue is inversely related to DXA-measured bone mineral in Caucasian women. *Osteoporosis Int*. 2007;18(5):641-7.
458. Shen W, Chen J, Gantz M, Punyanitya M, Heymsfield SB, Gallagher D, et al. Ethnic and sex differences in bone marrow adipose tissue and bone mineral density relationship. *Osteoporosis international : a journal established as result of cooperation between the European Foundation for Osteoporosis and the National Osteoporosis Foundation of the USA*. 2012;23(9):2293-301.
459. Shen W, Chen J, Gantz M, Punyanitya M, Heymsfield SB, Gallagher D, et al. MRI-measured pelvic bone marrow adipose tissue is inversely related to DXA-measured bone mineral in younger and older adults. *European journal of clinical nutrition*. 2012;66(9):983-8.
460. Shen W, Scherzer R, Gantz M, Chen J, Punyanitya M, Lewis CE, et al. Relationship between MRI-measured bone marrow adipose tissue and hip and spine bone mineral density in African-American and Caucasian participants: the

- CARDIA study. *The Journal of clinical endocrinology and metabolism*. 2012;97(4):1337-46.
461. Shen W, Velasquez G, Chen J, Jin Y, Heymsfield SB, Gallagher D, et al. Comparison of the relationship between bone marrow adipose tissue and volumetric bone mineral density in children and adults. *J Clin Densitom*. 2014;17(1):163-9.
 462. Huovinen V, Viljakainen H, Hakkarainen A, Saukkonen T, Toiviainen-Salo S, Lundbom N, et al. Bone marrow fat unsaturation in young adults is not affected by present or childhood obesity, but increases with age: a pilot study. *Metabolism*. 2015;64(11):1574-81.
 463. Schwartz AV, Sigurdsson S, Hue TF, Lang TF, Harris TB, Rosen CJ, et al. Vertebral bone marrow fat associated with lower trabecular BMD and prevalent vertebral fracture in older adults. *The Journal of clinical endocrinology and metabolism*. 2013;98(6):2294-300.
 464. Patsch JM, Li X, Baum T, Yap SP, Karampinos DC, Schwartz AV, et al. Bone marrow fat composition as a novel imaging biomarker in postmenopausal women with prevalent fragility fractures. *Journal of Bone and Mineral Research*. 2013;28(8):1721-8.
 465. Schellinger D, Lin CS, Hatipoglu HG, Fertikh D. Potential value of vertebral proton MR spectroscopy in determining bone weakness. *AJNR American journal of neuroradiology*. 2001;22(8):1620-7.
 466. Baum T, Yap SP, Karampinos DC, Nardo L, Kuo D, Burghardt AJ, et al. Does vertebral bone marrow fat content correlate with abdominal adipose tissue, lumbar spine bone mineral density, and blood biomarkers in women with type 2 diabetes mellitus? *J Magn Reson Imaging*. 2012;35(1):117-24.
 467. Karampinos DC, Ruschke S, Gordijenko O, Grande Garcia E, Kooijman H, Burgkart R, et al. Association of MRS-Based Vertebral Bone Marrow Fat Fraction with Bone Strength in a Human In Vitro Model. *Journal of osteoporosis*. 2015 Apr 19;2015..
 468. Baum T, Yap SP, Dieckmeyer M, Ruschke S, Eggers H, Kooijman H, et al. Assessment of whole spine vertebral bone marrow fat using chemical shift-encoding based water-fat MRI. *J Magn Reson Imaging*. 2015 Oct 1;42(4):1018-23.
 469. Mostoufi-Moab S, Magland J, Isaacoff EJ, Sun W, Rajapakse CS, Zemel B, et al. Adverse Fat Depots and Marrow Adiposity Are Associated With Skeletal Deficits and Insulin Resistance in Long-Term Survivors of Pediatric Hematopoietic Stem Cell Transplantation. *Journal of bone and mineral research : the official journal of the American Society for Bone and Mineral Research*. 2015;30(9):1657-66.
 470. Shuster A, Patlas M, Pinthus JH, Mourtzakis M. The clinical importance of visceral adiposity: a critical review of methods for visceral adipose tissue analysis. *The British journal of radiology*. 2012;85(1009):1-10.
 471. Seidell JC, Bakker CJ, van der Kooy K. Imaging techniques for measuring adipose-tissue distribution--a comparison between computed tomography and 1.5-T magnetic resonance. *The American journal of clinical nutrition*. 1990;51(6):953-7.

472. Karcher HS, Holzwarth R, Mueller HP, Ludolph AC, Huber R, Kassubek J, et al. Body fat distribution as a risk factor for cerebrovascular disease: an MRI-based body fat quantification study. *Cerebrovascular diseases (Basel, Switzerland)*. 2013;35(4):341-8.
473. Karlsson AK, Kullberg J, Stokland E, Allvin K, Gronowitz E, Svensson PA, et al. Measurements of total and regional body composition in preschool children: A comparison of MRI, DXA, and anthropometric data. *Obesity (Silver Spring, Md)*. 2013;21(5):1018-24.
474. Heymsfield SB, Hu HH, Shen W, Carmichael O. Emerging Technologies and their Applications in Lipid Compartment Measurement. *Trends in Endocrinology & Metabolism*. 2015;26(12):688-98.
475. Lack CM, Lesser GJ, Umesi UN, Bowns J, Chen MY, Case D, et al. Making the most of the imaging we have: using head MRI to estimate body composition. *Clinical radiology*. 2016 Apr 30;71(4):402-e1.
476. Hu HH, Chen J, Shen W. Segmentation and quantification of adipose tissue by magnetic resonance imaging. *Magnetic Resonance Materials in Physics, Biology and Medicine*. 2015:1-18.
477. Antony J, McGuinness K, Welch N, Coyle J, Franklyn-Miller A, O'Connor N, et al. An interactive segmentation tool for quantifying fat in lumbar muscles using axial lumbar-spine MRI. *IRBM*. 2016 Feb 29;37(1):11-22.
478. Bonekamp S, Ghosh P, Crawford S, Solga SF, Horska A, Brancati FL, et al. Quantitative comparison and evaluation of software packages for assessment of abdominal adipose tissue distribution by magnetic resonance imaging. *International journal of obesity*. 2008;32(1):100-11.
479. Lee JJ, Beretvas SN, Freeland-Graves JH. Abdominal Adiposity Distribution in Diabetic/Prediabetic and Nondiabetic Populations: A Meta-Analysis. *Journal of obesity*. 2014 Nov 26;2014.
480. Fu X, Zhu F, Zhao X, Ma X, Zhu S. Central Fat Accumulation Associated with Metabolic Risks beyond Total Fat in Normal BMI Chinese Adults. *Annals of Nutrition and Metabolism*. 2014;64(2):93-100.
481. Yu Y, Venners SA, Wang B, Brickman WJ, Zimmerman D, Li Z, et al. Association of central adiposity with prediabetes and decreased insulin sensitivity in rural Chinese normal-weight and overweight women. *Metabolism*. 2010;59(7):1047-53.
482. Sheu Y, Cauley JA. The role of bone marrow and visceral fat on bone metabolism. *Curr Osteoporos Rep*. 2011;9(2):67-75.
483. Shen W, Wang Z, Punyanita M, Lei J, Sinav A, Kral JG, et al. Adipose tissue quantification by imaging methods: a proposed classification. *Obesity research*. 2003;11(1):5-16.
484. Ross R, Leger L, Morris D, de Guise J, Guardo R. Quantification of adipose tissue by MRI: relationship with anthropometric variables. *Journal of applied physiology*. 1992;72(2):787-95.
485. Pineau JC, Frey A. Comparison of skinfold thickness models with dexta: impact of visceral adipose tissue. *The Journal of sports medicine and physical fitness*. *The Journal of sports medicine and physical fitness*. 2016 May;56(5):541-5.

486. Gilsanz V, Chalfant J, Mo AO, Lee DC, Dorey FJ, Mittelman SD. Reciprocal relations of subcutaneous and visceral fat to bone structure and strength. *The Journal of clinical endocrinology and metabolism*. 2009;94(9):3387-93.
487. Hamdy O, Porramatikul S, Al-Ozairi E. Metabolic obesity: the paradox between visceral and subcutaneous fat. *Current diabetes reviews*. 2006;2(4):367-73.
488. Pollock NK, Bernard PJ, Wenger K, Misra S, Gower BA, Allison JD, et al. Lower bone mass in prepubertal overweight children with prediabetes. *Journal of bone and mineral research : the official journal of the American Society for Bone and Mineral Research*. 2010;25(12):2760-9.
489. Russell M, Mendes N, Miller KK, Rosen CJ, Lee H, Klibanski A, et al. Visceral fat is a negative predictor of bone density measures in obese adolescent girls. *The Journal of clinical endocrinology and metabolism*. 2010;95(3):1247-55.
490. Yamaguchi T, Kanazawa I, Yamamoto M, Kurioka S, Yamauchi M, Yano S, et al. Associations between components of the metabolic syndrome versus bone mineral density and vertebral fractures in patients with type 2 diabetes. *Bone*. 2009;45(2):174-9.
491. Bredella MA, Torriani M, Ghomi RH, Thomas BJ, Brick DJ, Gerweck AV, et al. Vertebral bone marrow fat is positively associated with visceral fat and inversely associated with IGF-1 in obese women. *Obesity (Silver Spring, Md)*. 2011;19(1):49-53.
492. Cohen A, Dempster DW, Recker RR, Lappe JM, Zhou H, Zwahlen A, et al. Abdominal fat is associated with lower bone formation and inferior bone quality in healthy premenopausal women: a transiliac bone biopsy study. *The Journal of clinical endocrinology and metabolism*. 2013;98(6):2562-72.
493. Ng AC, Melton LJ, 3rd, Atkinson EJ, Achenbach SJ, Holets MF, Peterson JM, et al. Relationship of adiposity to bone volumetric density and microstructure in men and women across the adult lifespan. *Bone*. 2013;55(1):119-25.
494. Edwards MH, Ward KA, Ntani G, Parsons C, Thompson J, Sayer AA, et al. Lean mass and fat mass have differing associations with bone microarchitecture assessed by high resolution peripheral quantitative computed tomography in men and women from the Hertfordshire Cohort Study. *Bone*. 2015;81:145-51.
495. Chen SC, Abdalrahman N, McComb C, Foster J, Ahmed SF. The precision of partial image analysis of trabecular bone microarchitecture by high-resolution magnetic resonance imaging in people with childhood-onset bone abnormalities. Presented at British Society for Paediatric Endocrinology and Diabetes BSPED 2015, Sheffield, UK, Endocrine Abstract 39 EP15
496. Leinhard OD, Johansson A, Rydell J, Smedby Ö, Nyström F, Lundberg P, et al., editors. Quantitative abdominal fat estimation using MRI. *Pattern Recognition, 2008 ICPR 2008 19th International Conference on*; 2008: IEEE.
497. Modlesky CM, Whitney DG, Carter PT, Allerton BM, Kirby JT, Miller F. The pattern of trabecular bone microarchitecture in the distal femur of typically developing children and its effect on processing of magnetic resonance images. *Bone*. 2014;60:1-7.
498. Peh WC. *WC. Pitfalls in Diagnostic Radiology*: Springer; 2014.

499. Cosman F, de Beur SJ, LeBoff MS, Lewiecki EM, Tanner B, Randall S, et al. Clinician's Guide to Prevention and Treatment of Osteoporosis. *Osteoporosis international : a journal established as result of cooperation between the European Foundation for Osteoporosis and the National Osteoporosis Foundation of the USA*. 2014;25(10):2359-81.
500. El Maghraoui A, Roux C. DXA scanning in clinical practice. *Qjm*. 2008;101(8):605-17.
501. Lenchik L, Rochmis P, Sartoris DJ. Optimized interpretation and reporting of dual X-ray absorptiometry (DXA) scans. *AJR American journal of roentgenology*. 1998;171(6):1509-20.
502. Carter DR, Bouxsein ML, Marcus R. New approaches for interpreting projected bone densitometry data. *Journal of bone and mineral research : the official journal of the American Society for Bone and Mineral Research*. 1992;7(2):137-45.
503. Chamberlain G, Fox J, Ashton B, Middleton J. Concise review: mesenchymal stem cells: their phenotype, differentiation capacity, immunological features, and potential for homing. *Stem cells (Dayton, Ohio)*. 2007;25(11):2739-49.
504. Wagegg M, Gaber T, Lohanatha FL, Hahne M, Strehl C, Fangradt M, et al. Hypoxia promotes osteogenesis but suppresses adipogenesis of human mesenchymal stromal cells in a hypoxia-inducible factor-1 dependent manner. *PloS one*. 2012;7(9):e46483.
505. Dunger DB, Regan FM, Acerini CL. Childhood and adolescent diabetes. *Endocrine development*. 2005;9:107-20.
506. Giustina A, Mazziotti G, Canalis E. Growth hormone, insulin-like growth factors, and the skeleton. *Endocrine reviews*. 2008;29(5):535-59.
507. Martin LM, McCabe LR. Type I diabetic bone phenotype is location but not gender dependent. *Histochemistry and cell biology*. 2007;128(2):125-33.
508. Zemel B. Bone mineral accretion and its relationship to growth, sexual maturation and body composition during childhood and adolescence. *World review of nutrition and dietetics*. 2013;106:39-45.
509. Genant HK, Engelke K, Fuerst T, Gluer CC, Grampp S, Harris ST, et al. Noninvasive assessment of bone mineral and structure: state of the art. *Journal of bone and mineral research : the official journal of the American Society for Bone and Mineral Research*. 1996;11(6):707-30.
510. Fazeli PK, Horowitz MC, MacDougald OA, Scheller EL, Rodeheffer MS, Rosen CJ, et al. Marrow fat and bone--new perspectives. *The Journal of clinical endocrinology and metabolism*. 2013;98(3):935-45.
511. Vanhamme L, van den Boogaart A, Van Huffel S. Improved method for accurate and efficient quantification of MRS data with use of prior knowledge. *J Magn Reson*. 1997;129(1):35-43.
512. Naressi A, Couturier C, Devos JM, Janssen M, Mangeat C, de Beer R, et al. Java-based graphical user interface for the MRUI quantitation package. *Magma (New York, NY)*. 2001;12(2-3):141-52.

513. Benjamini Y, Hochberg Y. Controlling the false discovery rate: a practical and powerful approach to multiple testing. *Journal of the Royal Statistical Society Series B (Methodological)*. 1995;289-300.
514. Svoren BM, Volkening LK, Wood JR, Laffel LM. Significant vitamin D deficiency in youth with type 1 diabetes mellitus. *The Journal of pediatrics*. 2009;154(1):132-4.
515. Al-Daghri NM, Al-Attas OS, Alokail MS, Alkharfy KM, Yakout SM, Aljohani NJ, et al. Lower vitamin D status is more common among Saudi adults with diabetes mellitus type 1 than in non-diabetics. *BMC public health*. 2014;14(1):153.
516. Donaldson L, Reckless I, Scholes S, Mindell JS, Shelton N. The epidemiology of fractures in England. *Journal of epidemiology and community health*. 2008;62(2):174-80.
517. Wędrychowicz A, Stec M, Sztefko K, Starzyk J. Associations between bone, fat tissue and metabolic control in children and adolescents with type 1 diabetes mellitus. *Experimental and clinical endocrinology & diabetes: official journal, German Society of Endocrinology [and] German Diabetes Association*. 2014;122(8):491-5.
518. Baroncelli GI, Bertelloni S, Ceccarelli C, Cupelli D, Saggese G. Dynamics of bone turnover in children with GH deficiency treated with GH until final height. *European Journal of Endocrinology*. 2000;142(6):549-56.
519. Qvist P, Christgau S, Pedersen B, Schlemmer A, Christiansen C. Circadian variation in the serum concentration of C-terminal telopeptide of type I collagen (serum CTx): effects of gender, age, menopausal status, posture, daylight, serum cortisol, and fasting. *Bone*. 2002;31(1):57-61.
520. Gevers EF, Loveridge N, Robinson IC. Bone marrow adipocytes: a neglected target tissue for growth hormone. *Endocrinology*. 2002;143(10):4065-73.
521. Guler H-P, Zapf J, Schmid C, Froesch ER. Insulin-like growth factors I and II in healthy man. *Acta endocrinologica*. 1989;121(6):753-8.
522. Baxter R, Martin JL, Beniac VA. High molecular weight insulin-like growth factor binding protein complex. Purification and properties of the acid-labile subunit from human serum. *Journal of Biological Chemistry*. 1989;264(20):11843-8.
523. Amiel SA, Sherwin RS, Hintz RL, Gertner JM, Press CM, Tamborlane WV. Effect of diabetes and its control on insulin-like growth factors in the young subject with type I diabetes. *Diabetes*. 1984;33(12):1175-9.
524. Bereket A, Wilson TA, Blethen SL, Sakurai Y, Herndon DN, Wolfe RR, et al. Regulation of the acid-labile subunit of the insulin-like growth factor ternary complex in patients with insulin-dependent diabetes mellitus and severe burns. *Clinical endocrinology*. 1996;44(5):525-32.
525. Dai J, Baxter RC. Regulation in vivo of the acid-labile subunit of the rat serum insulin-like growth factor-binding protein complex. *Endocrinology*. 1994;135(6):2335-41.
526. Brismar K, Fernqvist-Forbes E, Wahren J, Hall K. Effect of insulin on the hepatic production of insulin-like growth factor-binding protein-1 (IGFBP-1), IGFBP-3,

- and IGF-I in insulin-dependent diabetes. *The Journal of Clinical Endocrinology & Metabolism*. 1994;79(3):872-8.
527. Santos JM, Mohammad G, Zhong Q, Kowluru RA. Diabetic retinopathy, superoxide damage and antioxidants. *Current pharmaceutical biotechnology*. 2011;12(3):352-61.
 528. Goettsch C, Babelova A, Trummer O, Erben RG, Rauner M, Rammelt S, et al. NADPH oxidase 4 limits bone mass by promoting osteoclastogenesis. *The Journal of clinical investigation*. 2013;123(11):4731-8.
 529. Almeida M, O'Brien CA. Basic biology of skeletal aging: role of stress response pathways. *The journals of gerontology Series A, Biological sciences and medical sciences*. 2013;68(10):1197-208.
 530. Miller K, Biller B, Lipman J, Bradwin G, Rifai N, Klibanski A. Truncal adiposity, relative growth hormone deficiency, and cardiovascular risk. *The Journal of Clinical Endocrinology & Metabolism*. 2005;90(2):768-74.
 531. Menagh PJ, Turner RT, Jump DB, Wong CP, Lowry MB, Yakar S, et al. Growth hormone regulates the balance between bone formation and bone marrow adiposity. *Journal of Bone and Mineral Research*. 2010;25(4):757-68.
 532. Fazeli PK, Bredella MA, Freedman L, Thomas BJ, Breggia A, Meenaghan E, et al. Marrow fat and preadipocyte factor-1 levels decrease with recovery in women with anorexia nervosa. *Journal of Bone and Mineral Research*. 2012;27(9):1864-71.
 533. Govan L, Maietti E, Torsney B, Wu O, Briggs A, Colhoun H, et al. The effect of deprivation and HbA1c on admission to hospital for diabetic ketoacidosis in type 1 diabetes. *Diabetologia*. 2012;55(9):2356-60.
 534. Salvatoni A, Mancassola G, Biasoli R, Cardani R, Salvatore S, Broggin M, et al. Bone mineral density in diabetic children and adolescents: a follow-up study. *Bone*. 2004;34(5):900-4.
 535. Bechtold SM, Putzker S, Bonfig W, Fuchs O, Isa D, Schwarz H. Bone geometry normalizes with age in children and adolescents with type 1 diabetes mellitus. *Bone*. 2007;40(6):S25-S6.
 536. Joshi A, Varthakavi P, Chadha M, Bhagwat N. A study of bone mineral density and its determinants in type 1 diabetes mellitus. *Journal of osteoporosis*. 2013;2013:397814.
 537. Justesen J, Stenderup K, Ebbesen EN, Mosekilde L, Steiniche T, Kassem M. Adipocyte tissue volume in bone marrow is increased with aging and in patients with osteoporosis. *Biogerontology*. 2001;2(3):165-71.
 538. Hothersall. Contemporary risk of hip fracture in type 1 and type 2 diabetes: a national registry study from Scotland. *J Bone Miner Res*. 2013;29(5).
 539. Naiemh Abdalrahman SCC, Jessie Ruijun Wang, and Syed Faisal Ahmed. An update on diabetes related skeletal fragility. *Expert Review of Endocrinology & Metabolism*. 2015;10(2):193-210.
 540. Cohen A, Dempster DW, Stein EM, Nickolas TL, Zhou H, McMahon DJ, et al. Increased Marrow Adiposity in Premenopausal Women with Idiopathic

- Osteoporosis. *Journal of Clinical Endocrinology & Metabolism*. 2012;97(8):2782-91.
541. Paccou J, Hardouin P, Cotten A, Penel G, Cortet B. The Role of Bone Marrow Fat in Skeletal Health: Usefulness and perspectives for clinicians. *The Journal of clinical endocrinology and metabolism*. 2015;jc20152338.
 542. Abdalrahman N, McComb C, Foster J, McLean J, Lindsay R, McClure J, et al. Deficits in Trabecular Bone Microarchitecture in Young Women with Type 1 Diabetes Mellitus. *Journal of bone and mineral research : the official journal of the American Society for Bone and Mineral Research*. 2015;30(8):1386-93.
 543. Dube MC, Joanisse DR, Prud'homme D, Lemieux S, Bouchard C, Perusse L, et al. Muscle adiposity and body fat distribution in type 1 and type 2 diabetes: varying relationships according to diabetes type. *International journal of obesity (2005)*. 2006;30(12):1721-8.
 544. Kabadi UM, Vora A, Kabadi M. Hyperinsulinemia and central adiposity: influence of chronic insulin therapy in type 1 diabetes. *Diabetes care*. 2000;23(7):1024-5.
 545. Greenfield JR, Samaras K, Chisholm DJ. Insulin resistance, intra-abdominal fat, cardiovascular risk factors, and androgens in healthy young women with type 1 diabetes mellitus. *The Journal of clinical endocrinology and metabolism*. 2002;87(3):1036-40.
 546. Forbes S, McGowan NW, Duncan K, Anderson D, Barclay J, Mitchell D, et al. Islet transplantation from a nationally funded UK centre reaches socially deprived groups and improves metabolic outcomes. *Diabetologia*. 2015;58(6):1300-8.
 547. Marina A, von Frankenberg AD, Suvag S, Callahan HS, Kratz M, Richards TL, et al. Effects of dietary fat and saturated fat content on liver fat and markers of oxidative stress in overweight/obese men and women under weight-stable conditions. *Nutrients*. 2014;6(11):4678-90.
 548. Pan H, Wu N, Yang T, He W. Association between bone mineral density and type 1 diabetes mellitus: a meta-analysis of cross-sectional studies. *Diabetes/metabolism research and reviews*. 2014;30(7):531-42.
 549. Wren TAL, Chung SA, Dorey FJ, Bluml S, Adams GB, Gilsanz V. Bone Marrow Fat Is Inversely Related to Cortical Bone in Young and Old Subjects. *Journal of Clinical Endocrinology & Metabolism*. 2011;96(3):782-6.
 550. Loh NY, Neville MJ, Marinou K, Hardcastle SA, Fielding BA, Duncan EL, et al. LRP5 Regulates Human Body Fat Distribution by Modulating Adipose Progenitor Biology in a Dose-and Depot-Specific Fashion. *Cell metabolism*. 2015;21(2):262-72.
 551. Fontana L, Eagon JC, Trujillo ME, Scherer PE, Klein S. Visceral fat adipokine secretion is associated with systemic inflammation in obese humans. *Diabetes*. 2007;56(4):1010-3.
 552. Singhal V, Maffazioli GDN, Cano Sokoloff N, Ackerman KE, Lee H, Gupta N, et al. Regional fat depots and their relationship to bone density and microarchitecture in young oligo-amenorrheic athletes. *Bone*. 2015;77:83-90.

553. Shih TT, Chang CJ, Hsu CY, Wei SY, Su KC, Chung HW. Correlation of bone marrow lipid water content with bone mineral density on the lumbar spine. *Spine*. 2004;29(24):2844-50.
554. de Paula FJ, de Araujo IM, Carvalho AL, Elias J, Jr., Salmon CE, Nogueira-Barbosa MH. The Relationship of Fat Distribution and Insulin Resistance with Lumbar Spine Bone Mass in Women. *PloS one*. 2015;10(6):e0129764.
555. Gimble JM, Robinson CE, Wu X, Kelly KA. The function of adipocytes in the bone marrow stroma: an update. *Bone*. 1996;19(5):421-8.
556. Bredella MA, Lin E, Gerweck AV, Landa MG, Thomas BJ, Torriani M, et al. Determinants of bone microarchitecture and mechanical properties in obese men. *The Journal of clinical endocrinology and metabolism*. 2012;97(11):4115-22.
557. Schnitzler CM, Mesquita J. Bone marrow composition and bone microarchitecture and turnover in blacks and whites. *Journal of bone and mineral research : the official journal of the American Society for Bone and Mineral Research*. 1998;13(8):1300-7.
558. Janicka A, Wren TA, Sanchez MM, Dorey F, Kim PS, Mittelman SD, et al. Fat mass is not beneficial to bone in adolescents and young adults. *The Journal of clinical endocrinology and metabolism*. 2007;92(1):143-7.
559. Travison TG, Araujo AB, Esche GR, Beck TJ, McKinlay JB. Lean mass and not fat mass is associated with male proximal femur strength. *Journal of bone and mineral research : the official journal of the American Society for Bone and Mineral Research*. 2008;23(2):189-98.
560. Jiang Y, Zhang Y, Jin M, Gu Z, Pei Y, Meng P. Aged-Related Changes in Body Composition and Association between Body Composition with Bone Mass Density by Body Mass Index in Chinese Han Men over 50-year-old. *PloS one*. 2015;10(6):e0130400.
561. Liu PY, Ilich JZ, Brummel-Smith K, Ghosh S. New insight into fat, muscle and bone relationship in women: determining the threshold at which body fat assumes negative relationship with bone mineral density. *International journal of preventive medicine*. 2014;5(11):1452-63.
562. Ho-Pham LT, Nguyen ND, Lai TQ, Nguyen TV. Contributions of lean mass and fat mass to bone mineral density: a study in postmenopausal women. *BMC Musculoskelet Disord*. 2010;11:59.
563. Weiler HA, Janzen L, Green K, Grabowski J, Seshia MM, Yuen KC. Percent body fat and bone mass in healthy Canadian females 10 to 19 years of age. *Bone*. 2000;27(2):203-7.
564. Joshi A, Varthakavi P, Chadha M, Bhagwat N. A study of bone mineral density and its determinants in type 1 diabetes mellitus. *J Osteoporos*. 2013;2013:397814.
565. Chang G1 HS, Liu Y, Chen C, Chu KK, Rajapakse CS, Egol K, Xia D, Saha PK, Regatte RR. 7 Tesla MRI of bone microarchitecture discriminates between women without and with fragility fractures who do not differ by bone mineral density. *J Bone Miner Metab*. 2015;33(3)::285-93.
566. Ouyang X, Selby K, Lang P, Engelke K, Klifa C, Fan B, et al. High resolution magnetic resonance imaging of the calcaneus: age-related changes in trabecular

- structure and comparison with dual X-ray absorptiometry measurements. *Calcif Tissue Int.* 1997;60(2):139-47.
567. Link TM, Vieth V, Langenberg R, Meier N, Lotter A, Newitt D, et al. Structure analysis of high resolution magnetic resonance imaging of the proximal femur: in vitro correlation with biomechanical strength and BMD. *Calcif Tissue Int.* 2003;72(2):156-65.
568. Nyman JS, Even JL, Jo CH, Herbert EG, Murry MR, Cockrell GE, et al. Increasing duration of type 1 diabetes perturbs the strength-structure relationship and increases brittleness of bone. *Bone.* 2011;48(4):733-40.
569. Casazza K, Hanks LJ, Clines GA, Tse HM, Eberhardt AW. Diabetes-related impairment in bone strength is established early in the life course. *World journal of diabetes.* 2013;4(4):145-50.
570. Armas LAG, Akhter MP, Drincic A, Recker RR. Trabecular bone histomorphometry in humans with Type 1 Diabetes Mellitus. *Bone.* 2012;50(1):91-6.
571. Newitt DC, Majumdar S, van Rietbergen B, von Ingersleben G, Harris ST, Genant HK, et al. In vivo assessment of architecture and micro-finite element analysis derived indices of mechanical properties of trabecular bone in the radius. *Osteoporosis international : a journal established as result of cooperation between the European Foundation for Osteoporosis and the National Osteoporosis Foundation of the USA.* 2002;13(1):6-17.
572. Shanbhogue VV, Hansen S, Frost M, Jørgensen NR, Hermann AP, Henriksen JE, et al. Compromised cortical bone compartment in type 2 diabetes mellitus patients with microvascular disease. *European Journal of Endocrinology.* 2016;174(2):115-24.
573. Rix M, Andreassen H, Eskildsen P. Impact of peripheral neuropathy on bone density in patients with type 1 diabetes. *Diabetes care.* 1999;22(5):827-31.
574. Ivers RQ, Cumming RG, Mitchell P, Peduto AJ. Diabetes and risk of fracture: The Blue Mountains Eye Study. *Diabetes care.* 2001;24(7):1198-203.
575. Vestergaard P, Rejnmark L, Mosekilde L. Diabetes and its complications and their relationship with risk of fractures in type 1 and 2 diabetes. *Calcif Tissue Int.* 2009;84(1):45-55.
576. Schwartz AV, Sellmeyer DE. Diabetes, fracture, and bone fragility. *Curr Osteoporos Rep.* 2007;5(3):105-11.
577. Szulc P, Delmas PD. Biochemical markers of bone turnover: potential use in the investigation and management of postmenopausal osteoporosis. *Osteoporosis international : a journal established as result of cooperation between the European Foundation for Osteoporosis and the National Osteoporosis Foundation of the USA.* 2008;19(12):1683-704.
578. Li CI, Liu CS, Lin WY, Meng NH, Chen CC, Yang SY, et al. Glycated hemoglobin level and risk of hip fracture in older people with type 2 diabetes: a competing risk analysis of Taiwan diabetes cohort study. *Journal of Bone and Mineral Research.* 2015;30(7):1338-46.

579. Monickaraj F, Aravind S, Gokulakrishnan K, Sathishkumar C, Prabu P, Prabu D, et al. Accelerated aging as evidenced by increased telomere shortening and mitochondrial DNA depletion in patients with type 2 diabetes. *Molecular and cellular biochemistry*. 2012;365(1-2):343-50.
580. Shanbhogue VV, Brixen K, Hansen S. Age- and Sex-Related Changes in Bone Microarchitecture and Estimated Strength. A Three-Year Prospective Study Using HR-pQCT. *Journal of bone and mineral research : the official journal of the American Society for Bone and Mineral Research*. 2016 Aug 1;31(8):1541-9.
581. Hamilton EJ, Rakic V, Davis WA, Paul Chubb SA, Kamber N, Prince RL, et al. A five-year prospective study of bone mineral density in men and women with diabetes: the Fremantle Diabetes Study. *Acta Diabetol*. 2012;49(2):153-8.
582. Miazgowski T, Czekalski S. A 2-year follow-up study on bone mineral density and markers of bone turnover in patients with long-standing insulin-dependent diabetes mellitus. *Osteoporosis international : a journal established as result of cooperation between the European Foundation for Osteoporosis and the National Osteoporosis Foundation of the USA*. 1998;8(5):399-403.
583. Mathiassen B, Nielsen S, Johansen JS, Hartwell D, Ditzel J, Rodbro P, et al. Long-term bone loss in insulin-dependent diabetic patients with microvascular complications. *The Journal of diabetic complications*. 1990;4(4):145-9.
584. Goodpaster BH, Krishnaswami S, Harris TB, Katsiaras A, Kritchevsky SB, Simonsick EM, et al. Obesity, regional body fat distribution, and the metabolic syndrome in older men and women. *Archives of internal medicine*. 2005;165(7):777-83.
585. Schorr M, Dichtel LE, Gerweck AV, Torriani M, Miller KK, Bredella MA. Body composition predictors of skeletal integrity in obesity. *Skeletal Radiol*. 2016;45(6):813-9.
586. Yu EW, Putman MS, Derrico N, Abrishamian-Garcia G, Finkelstein JS, Bouxsein ML. Defects in cortical microarchitecture among African-American women with type 2 diabetes. *Osteoporosis international : a journal established as result of cooperation between the European Foundation for Osteoporosis and the National Osteoporosis Foundation of the USA*. 2015;26(2):673-9.

Appendices

7.2 Appendix A: Study protocol

1. Title

Pilot Study Of Bone Health In Young People With Type 1 Diabetes Mellitus

2. Introduction

Although the association between diabetes and increased fracture risk is well recognised (Schwartz, 2003), the underlying mechanisms for this increased fracture predisposition are unclear. Adults with Type 1 diabetes mellitus (T1DM) tend to have mild osteopenia as adults, with bone mineral density (BMD) values which are about 10% lower than normal (Bouillon, 1991, Hofbauer, 2007). This modestly low BMD should lead to an increase in hip fracture risk of about 2-fold, yet prospective studies indicate that postmenopausal women with type 1 diabetes have 7–12 times greater risk of hip fracture compared with age-matched non-diabetics (Forsen, 1999, Nicodemus, 2001). People with type 2 diabetes (T2DM) tend to have normal or modestly increased BMD, which should be associated with reduced fracture risk. However, these patients' fracture risk is increased at the hip, proximal humerus, and lower extremity by about 2-fold compared with normal (Forsen, 2008, Schwartz, 2001). Thus, ***clinical evidence indicates that fracture risk in diabetic patients is disproportionately high relative to BMD as assessed by DXA.***

Abnormalities of bone microarchitecture as well as geometry that may lead to a reduction in material properties of bone cannot be assessed by DXA and the use of other techniques such as quantitative CT (QCT) have revealed alterations in bone geometry in adults and adolescents with DM (Saha, 2009, Melton III, 2008). In a large study of children and young adults with T1DM, markers of bone formation were lower than normal (Bouillon, 1995). Studies in animal models of diabetes as well as studies of biochemical markers of bone turnover in humans with diabetes suggest that the defect may be related to poor osteoblastic function (McCabe, 2007) and may also be related to disease duration and metabolic control (Brandao, 2007). Lastly, pentosidine is a non-enzymatic collagen cross-link which rises with age (Saito and Marumo, 2010) and a rise in this advanced glycation end product has been reported to be associated with a reduction in the maximal load of bone without a notable reduction in BMD in a rodent model of diabetes (Saito M, 2006) as well as patients with T2DM (Schwartz, 2009).

T1DM mice exhibit increased bone marrow adiposity, increased adipocyte markers and increased numbers of lipid-dense adipocytes in the bone marrow (Martin and McCabe, 2007). Whereas osteoclasts belong to the macrophage family, osteoblasts and adipocytes share a common precursor and are derived from mesenchymal stem cells. The process of differentiation into either adipocytes or osteoblasts is regulated by a number of growth factors including insulin (Chamberlain, 2007), oxygen tension and blood flow within the bone marrow (Wang, 2007). It is possible that the increased marrow adiposity in the T1DM rats is due to a combination of these factors as well as hyperglycaemia, hyperlipidaemia and reduced insulin action. The increased adiposity may itself have a lipotoxic effect on osteoblasts and may even stimulate local osteoclast activity (Duque, 2008). It is also possible that in older people with T1DM, other factors such as peripheral neuropathy and susceptibility to falls may also play a part in the increased fracture risk (Patel, 2008). Recently, insulin itself, acting through its cognate insulin receptor has been shown to have a direct role on osteoblast signalling and postnatal bone acquisition (Fulzele, 2010).

As bone, itself, may influence insulin sensitivity, the relationship between osteopenia and DM may be difficult to tease out in T2DM (Lee, 2007). The underlying aetiology of T2DM, itself, is complex and these factors may themselves have an effect on bone health which is independent of the effect of DM. The bone pathology which is associated with T1DM may serve as a more straightforward system to understand the effect of suppressed insulin signalling, hyperglycaemia,

and metabolic abnormalities on the regulation of bone formation. Given that childhood and adolescence is a period of net bone acquisition and T1DM is relatively common in this age group, a detailed study of the bone and fat link in this group of subjects would be particularly useful and provide valuable insight into the development of the osteopathy. However, there is a need to explore suitable non-invasive methods that can reliably investigate these features longitudinally.

Recent advances in MR imaging have allowed the generation of 3D images of bone structure (Wehrli, 2006) where bone structure can be assessed indirectly by microMRI via measurements of the surrounding marrow and other soft tissues. The 'apparent' trabecular properties that are derived from these images correlate with trabecular architecture obtained with higher-resolution techniques (Majumdar, 1996, Link, 1999). Until recently, evaluation of trabecular bone morphology was limited to appendicular sites. However, innovative surface coils and pulse sequences show potential for MR-based assessments of trabecular structure in the proximal femur and MR-derived trabecular microarchitecture measurements can reflect age- and disease-specific differences (Benito, 2003, Wehrli, 2007). Recent studies show good correlation between MRI & CT derived measures of bone health (Issever, 2010). There are, however, limited data on treatment related changes (Cheshunt, 2005, Zhang, 2008). Recently, MR spectroscopy has also raised the potential to quantify the amount of fat that is present within the marrow in the lumbar spine (Griffith, 2006, Shen, 2007, Liu, 2010, Li, 2011). There is, therefore, the potential to combine the two MR based techniques to obtain objective longitudinal data on bone microarchitecture and fat content and abdominal adipose tissue and study its relationship to T1DM and its metabolic control in a group of children and young people.

There is a need to explore whether microMRI can discriminate between groups of patients in a way that other measures of bone health cannot and, thus, act as a diagnostic biomarker of alterations in bone health.

It was also observed that visceral adipose tissue positively correlated with vertebral bone marrow fat content in obese women and in postmenopausal women with T2DM, (Bredella MA, et al 2011, Baum et al 2012). However, this relationship has not been examined in women with T1DM. Therefore, we aimed to determine whether vertebral bone marrow fat content correlates with the volume of abdominal adipose tissue in young women with T1DM by using MRI.

However, before using microMRI in a larger group of children and adolescents of varying ages, there is a need to perform these studies in a small group of young adults with T1DM. These preliminary studies will provide data that can then facilitate the development of a more comprehensive study of bone health in children and adolescents with T1DM.

3. Translational Aspects Of The Research

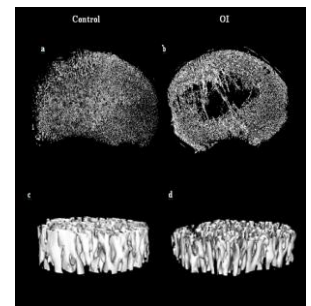
- A. MicroMRI promises to be a clinically useful technique for assessing bone health. Suitable MRI scanners are increasingly available across the health service as well as research institutes and there is a need to explore the utility of these scanners in assessing bone health.
- B. In the field of osteoporosis and fragility fractures, there are at least three groups of patients who pose a major clinical challenge - those who have a fragility fracture but have a normal DXA BMD, those with osteoporosis who do not show an increase in DXA BMD despite receiving bone-protective therapy and, finally, those with osteoporosis who have a fracture on bone-protective therapy. Another method of assessing bone health may improve the management of these patients.
- C. A practical, non-invasive method of assessment of bone health that provides details of microarchitecture and bone quality will be of value in the management

of challenging cases of metabolic bone disease. Its non-invasive nature may obviate the need for bone biopsies.

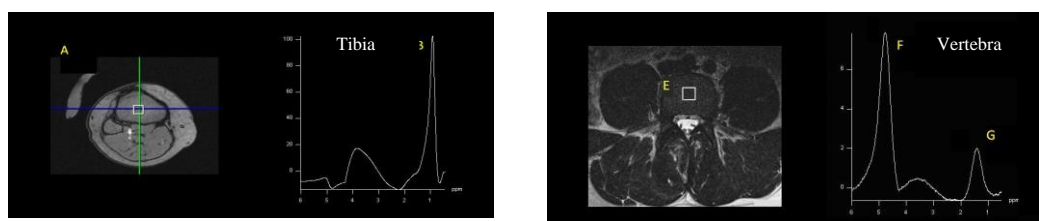
- D. Improved methods of assessing and understanding diabetes-related osteopathy will pave the way for interventional studies that are aimed at improving bone health.
- E. Alterations in insulin sensitivity and bone health are commonly encountered in people with chronic inflammation and the lessons learnt from these studies can be applied to children and adults with chronic inflammation.
- F. Lessons learnt from these studies can also be applied to investigating the concerns about bone health in patients with T2DM.
- G. Targeting bone marrow adipogenesis is an attractive option for improving bone health and treating possible osteoporosis. However, before this is considered as a novel therapy, there will be a need to develop innovative methods of imaging bones.

4. Results of any pilot studies

The MRI Department in Glasgow and the Developmental Endocrinology Research Group (DERG) have successfully performed some pilot studies exploring the utility of 1.5T and 3.0T MRI in assessing the microarchitecture of bone in healthy volunteers and some young adults with concerns about bone health. We were successful in developing a program that allowed quantification of four key bone parameters; apparent bone volume to total volume ratio (appBV/TV), apparent trabecular thickness (appTb.Th), apparent trabecular number (appTb.N) and apparent trabecular separation (appTb.Sp). Validation of the software has been performed with a purpose-built phantom with known trabecular thickness and separation, and a good correlation was found between the actual and measured values. Repeat scanning of four healthy individuals allowed the CoV to be assessed for appBV/TV, appTb.Th, appTb.N and appTb.Sp, and all values were found to be 7% or less. Figure above shows a binarised image of a slice from the proximal tibia of a control subject versus that of a person with osteogenesis imperfecta (OI). As expected, patients with OI had a significantly lower appBV/TV and appTb.N and a significantly higher appTb.Sp. AppTb.Th was also lower in the OI group but this did not reach statistical significance. A further pilot study was performed in volunteers with growth hormone deficiency (GHD), who are expected to have less severe bone abnormalities than in OI. In this study, there was a statistically significant decrease in appBV/TV, increase in appTb.Sp and decrease in appTbN in the GHD group, and again appTbTh was reduced but this did not reach statistical significance.



Pilot data have also been obtained for MRS the lumbar vertebral site, and also in the tibia, showing that the methodology can be applied to obtain reliable data for fat and water content. The figure below shows a sample of the spectra that has been obtained from the proximal tibia and L2.



In addition to the above pilot study, DERG has an active interest in assessing bone health in children with chronic disease with active research studies in children with inflammatory bowel disease, leukaemia and extreme prematurity. The group uses a range of densitometry techniques including DXA, peripheral quantitative CT and quantitative ultrasound. It has collected DXA data on school-children in Glasgow

and contributed these data towards the creation of UK reference range. The MRI physics team has extensive experience of performing MR spectroscopy in various organs in the body, for example the brain, liver and heart, using both 1.5T and 3T MRI scanners.

5. Aims

The primary aim of this study is to perform a cross-sectional study of bone health and markers of metabolic control in a group of young adults with T1DM. The innovative methods that we propose to use will provide us with novel data that can inform the development of a case-control study of bone health in children and adolescents with T1DM.

6. Research questions & Hypotheses

In young adults:-

- A. Is T1DM associated with a normal bone health as assessed by microMRI?
- B. What is the variation in microMRI parameters over a period of one year?
- C. Is T1DM associated with increased bone marrow adiposity as assessed by bone marrow MRS?
- D. Is T1DM associated with an abnormality in dual x-ray absorptiometry (DXA)-based total body (TB), Femoral Neck (FN) and lumbar spine (LS) bone mineral content (BMC)?
- E. Is there a relationship between microMRI bone parameters, DXA BMC and adiposity parameters?
- F. Is there an association between abdominal fat and bone marrow fat as assessed by MRI?
- G. What is the relationship between these parameters and markers of diabetes control?
- H. Is T1DM associated with abnormal biochemical markers of bone health and adiposity?

Primary Null Hypotheses

- A. There is no difference in the measurements of key bone parameters obtained from micro-MRI images of people with T1DM compared to healthy controls
- B. There is no difference in bone adiposity measurements obtained using MRS in patients with T1DM compared to healthy controls

7. Plan, methods, expertise available, statistical power

7.A. Recruitment

Ethics approval is already available to perform MRI scans for assessment of bone health in individuals over the age of 16 years but a revised application will be submitted. The subjects shall be recruited from the diabetes clinics that are linked with the clinical diabetes service network in the West of Scotland. All patients with childhood-onset T1DM, ie diagnosis of T1DM before the age of 16 yrs and their sisters and female friends within the same age band shall be invited to participate in the study. For this pilot study, 30 cases and 30 controls between the ages of 16 and 40yrs shall be recruited. Any adult with T1DM shall be invited to participate in the study. For this study, 20 cases shall be recruited.

Eligible participants who cannot sit or lie still for 15 minutes, are pregnant, have a known bone disease or cannot have a MRI scan for routine technical reasons shall be excluded from the study. Height and weight will be measured using standard validated techniques. Age at menarche and a menstrual history shall be recorded. Information about T1DM including age at diagnosis, current HBA1C, total insulin dose shall be obtained.

7.B. Scan Procedure

Participants will be required to come for an MRI scan at the BHF Glasgow Cardiovascular Research Centre on two occasions.

Visit one:

MRI scan and a blood sample– this has been completed already.

Visit 2:

This visit shall be undertaken one year after the first one. It involves two scans: a MRI

Scan which will be performed by the same team at BHF and a DXA scan which shall be

Performed at Yorkhill hospital. The patients shall be invited by a letter to discuss the information about the study.

Prior to taking part in the research, participants will be taken through the MR safety checklist by a member of the research team. Any subject who fails to satisfy any of the safety criteria e.g. has metal inside their body will not be allowed to take part in the research.

Participants shall have a scan of the right knee, L2 and the abdomen. The participant will initially be positioned on the MR scanner bed with their right knee inside a receiver coil, which is effectively a cylinder which surrounds the knee. Padding will be placed between the knee and the coil to reduce the potential for movement and help the volunteer to remain as still as possible during the scan. The volunteer will be moved into the scanner feet first, and their head and shoulders will remain outside of the scanner for the duration of the scan.

The scan protocol will consist of 3 short localiser scans which allow the area of interest to be identified, followed by a 10 minute micro MRI scan. The knee coil will then be removed, and a further 3 short localiser scans followed by approximately 10 minutes of MRS will be performed in the lumbar spine (L2). The spine coil is built into the scanner bed, and it will not be necessary for the volunteer to move. A surface body coil will then be positioned over the abdomen, and a further 3 short localiser scans followed by approximately 10 minutes of image acquisition to allow quantification of abdominal fat will be performed. Again, it will not be necessary for the volunteer to move. The total time in the MRI scanner will be a maximum of 1 hour.

The MRI scanner generates acoustic noise whilst it is operating. For this reason all research participants will be provided with adequate ear protection before entering the scanner e.g. earphones. This is a standard procedure used in clinical practice. Volunteers may also find the scanning process unpleasant, particularly if they suffer from claustrophobia. The research team will be able to communicate with the volunteer during the scanning process and reassure them if necessary. The volunteer will have an alarm that they can press to stop the scan at any time. Should the volunteer become distressed at any point, the scan will be stopped. Each volunteer will have the opportunity to listen to some music during the scan to help them feel relaxed.

7.C. Primary Outcome

MicroMRI parameters of bone health – High resolution MRI images of the proximal tibia at the 8% site will be acquired using a 3T MRI scanner (Siemens Verio) with the use of a transmit/receive extremity coil. Following immobilisation, localiser scans shall be performed in the sagittal, axial and coronal planes to identify the region of interest. A TrueFISP sequence shall be used at a resolution of 0.2 x 0.2 x 0.4mm. Acquisition of the high resolution images shall be achieved with a scan time of 10 minutes. Images shall be coded and analysed blindly. Quantitative analysis will be performed using software developed in-house (based

on the method described by Majumdar et al and Issever et al) to obtain measures of cortical thickness, apparent bone volume to total volume ratio (appBV/TV), apparent trabecular thickness (appTb.Th), apparent trabecular number (appTb.N) and apparent trabecular separation (appTb.Sp).

7.D. Secondary Outcomes

Bone Marrow Adiposity – MR spectroscopy will be performed in the lumbar spine using a 3T MRI scanner during the same scanning session as the microMRI image acquisition, using the method described by Tang et al. Spectra will be obtained from a volume of interest of approximately 2 x 2 x 2mm within the vertebral body using a Point-REsolved Spectroscopy (PRESS) sequence with a short echo time (TE) to allow detection of lipids. Analysis of the spectra will be performed using software provided by the MRI scanner manufacturer for this purpose. The peak amplitudes of the resulting water peak (I_{water}) and lipid peak (I_{fat}) will be measured, and the percentage fat fraction (FF) will be calculated in the following way:

$$FF(\%) = \frac{I_{fat}}{I_{fat} + I_{water}} \times 100$$

Abdominal Adiposity – MRI images will be acquired using a 3T MRI scanner during the same scanning session as the microMRI and MRS acquisitions, using the method described by Leinhard et al. A four element body coil will be used to obtain images covering the abdominal region from the diaphragm to the bottom of the pelvis. A dual echo, multi slice, spoiled, fast gradient echo pulse sequence will be used. To measure the fat, Dixon method will be used, it is performed by acquiring two separate images: one where the signals from fat and water are 180° out of phase ($I_1 = w - f$) and one where they are in phase ($I_2 = w + f$). Ideally, water and fat can then be obtained as the sum and difference of these images, respectively, and the total fat content in any region of interest can then easily be calculated.

Bone Densitometry

Measurement by DXA (total body, lumbar spine vertebrae 2-4 and femoral neck) using the Lunar Prodigy DXAScanner. Instrument precision has been determined onsite to be <1% forTB, LS and femoral neck.

Blood sample - A blood sample (10mls) shall be collected when patients attend for the MRI scan. This sample shall be used for measuring markers of bone turnover as well as adiposity.

8. Expertise Available

Prof SF Ahmed is a clinical investigator who leads the Developmental Endocrinology Research Group (DERG) at Yorkhill. He has a particular interest in the assessment and management of bone health of children and adolescents with chronic disease. His research group is currently engaged in a range of projects on bone health and skeletal development. Dr J Foster is Academic Supervisor and Consultant MR Physicist with 20 years of MRI experience and a team of MR Physicist, including Christie McComb who has been involved in the pilot work and is funded through the Academic Health Sciences Collaboration to support such studies. Christie McComb will continue to remain closely involved in the work. Dr Naiemh Abdalrahman who is a research fellow studying for a PhD at Glasgow University and is funded by Govt of Libya and the Medical Fund of the University of Glasgow. Dr G Shaikh and Dr K Robertson are closely involved in the Children's and Adolescent Diabetes Service in the West of Scotland which is the largest children's diabetes service in the UK. Dr C Perry, Dr A McLennan and Dr R Lindsay manage young people with T1DM. Dr J McClure at the Glasgow Cardiovascular Research centre has provided statistical input into the calculation of the sample size. DXA scans shall be performed by Sheila Khanna in bone densitometry.

9. Sample Size and Statistical Analyses

Based on our current studies of healthy controls and the cases of osteogenesis imperfecta, we estimate the CV to be about 7-10%. If a greater than 10% difference between case and controls is aimed to show a significant difference at $p < 0.05$ with a power of 0.8, at least 16 cases and 16 controls will be required for assessing apparent trabecular separation (appTb.Sp) and at least 14 cases and 14 controls will be required to assess apparent trabecular number (appTb.N). Group differences will be analysed by Students t-tests using, where necessary, normalised data and Chi square for categorical variables. Measurements of bone health, adiposity and metabolic status will be tested using ANOVA.

10. Timetable

Months -6 to -2: Obtain ethics approval. Design study database.

Months -3 to 0: Identify suitable patients and send paperwork

Months 1 to 12: Recruit subjects, begin assessments and follow-up

Months 12 to 15: Perform preliminary analysis

Month 15: Consider the feasibility of a study in children with T1DM

11. Existing Facilities

All the expertise, equipment and techniques required for the study are available in Glasgow within the Royal Hospital for Sick Children, Yorkhill and the BHF Cardiovascular Research Centre, Glasgow, and have previously been used in adolescents and adults to ensure the techniques are acceptable and reproducible.

12. Justification of Requirements

We are requesting support for:-

12.A. Scans

- MRI scans – Each 3 hour session will accommodate 3 scans and preliminary analysis. These scans will be supervised by Ms C McComb. Based on a scan cost of £320, total MRI scan cost shall be £12,800.

12.B. Patient Visits

Visits – Each participant will receive £20 to cover travel expenses for the MRI. Total costs £800.

The funding for this pilot work has been secured from the Medical Fund at the University of Glasgow as well as the bench fees of a PhD studentship.

13. Future exploitation plan, including potential funding sources, to achieve NHS benefit

The data and skills that are collected and developed from the proposed study can help develop research in and clinical practice in a number of ways:-

A. We propose to use resources and skills that are readily available in the current research and NHS settings in Glasgow and adapt them for our needs, thus allowing us to perform research that could in the future be performed at multiple sites.

B. T1DM has an approximate prevalence of 1 in a 1000 children in Scotland. The lessons we learn can be used to initially design cross-sectional case-control study in children and then design a longitudinal study that has an intervention arm which compares the effect of two forms of treatment (in T1DM) on the bone health. Funding could be sought from a number of diabetes-related charities.

C. Using MRI to assess bone health may provide a better insight into those cases of osteoporosis who do not respond to bisphosphonates and those who fracture despite relatively normal DXA results. Using a technology that is readily available in the NHS already may facilitate implementation. Identification of this group would allow better targeting of anti-osteoporosis drugs.

D. There is increasing realisation that abnormalities of bone health, glucose homeostasis, and cardiovascular health may be a common manifestation of a chronic inflammatory process that is linked to ageing. Novel methods of assessing

bone health will become an integrated part of assessing the chronic effects of inflammation and fit within the theme of current research in Glasgow and many funding institutions.

E. The results that will be generated from these studies have the potential to influence clinical practice within the next 5 years.

14. Public Engagement In Science

The study is currently being discussed with older patients who attend the Diabetes Service at Yorkhill which will also include details and progress of the study on its website <http://www.diabetes-scotland.org/ggc/>. The study will also be personally discussed within the diabetes team and in patient discussion groups. Although physical activity is stressed regularly, there is little awareness of maintaining good bone health in children and adults with diabetes. Engaging the CYP and their families in this project will fit within the general strategy of diabetes management of promoting physical activity.

15. Dissemination

The initial data shall be presented at an international MRI meeting in 2011 in Montreal and are currently being prepared for submission for publication. The findings from this study will be presented at national and international scientific meetings and submitted to scientific peer-reviewed journals for publication. Bodies such as Diabetes UK and the National Osteoporosis Society will also be informed on the outcomes of the study. The data shall be used to design further studies of a larger cohort.

16. References

- Benito M et al, J Clin Endocrinol Metab, 2003;
 Baum et al, 2012
 Bouillon R, Calcif Tissue Int.1991;
Bredella MA, et al 2011.
 Brandao FR et al, Diab Res & Clin Pract 2007;
 Chamberlain G et al, Stem Cells, 2007;
 Chesnut J et al, J Bone Miner Res, 2005;
 Chinapaw MJ et al, Sports Med, 2010;
 Corder K et al, Am J Clin Nutr, 2009;
 Duque G, Curr Opin Rheumatol, 2008;
 Forsen L et al, Diabetologia, 1999;
 Fulzele K et al, Cell, 2010;
 Griffith JF et al, Radiology, 2006;
 Hofbauer LC et al, J Bone Miner Res 2003;
 Issever AS, Magn Reson Imaging, 2010;
 Lee NK et al, Cell 2007;
 Leinhard et al, 2008;
 Li X et al, J Mag Reson Imaging, 2011;
 Link TM et al, Eur Radiol, 1999;
 Liu Y et al, Chin Med J, 2010;
 Majumdar S et al, OI, 1996;
 Majumdar S et al, J Bone Miner Res, 1997;
 Martin LM and McCabe LR, Histochem Cell Biol,2007;
 Masson LF, Pub Health Nutr, 2003;
 Mccabe LR, J Cell Biochem 2007;
 Melton LJ III et al, J Clin Endocrinol Metab, 2008;
 Melton LJ III et al, J Bone Miner Res 2008;
 Nicodemus KK, Diabetes Care, 2001;
 Owen CG, Diabetologia, 2010;
 Patel S et al, Calcif Tissue Int, 2008;
 Saha MT et al, Osteoporos Int 2009;
 Saito M and Marumo K, Osteoporos Int, 2010;
 Saito M et al, Osteopor Int, 2006;
 Schwartz AV, J Clin Endocrinol Metab, 2001;

Schwartz AV, *Calcif Tissue Int*, 2003;
Schwartz AV, *J Clin Endocrinol Metab*, 2009;
Shen W et al, *Osteoporos Int* 2007;
Tang GY et al, *Clin Radiol*, 2010;
Wang Y et al, *Ann N Y Acad Sciences* 2007;
Wehrli FW et al, *NMR Biomed*, 2006;
Wehrli FW et al, *J Magn Res Imaging*, 2007;
Wong SC et al, 2008, *Arch Dis Child*;
Zhang XH et al, *J Bone Miner Res*, 2008.

7.3 Appendix B: Pilot Study Of Bone Health In Young People With Type 1 Diabetes Mellitus, Case Report Form.

Hospital number:

Study number:

Date of visit:

Demographic and anthropometric data:

<p>Patient ID:</p> <p>Patient initials <input type="text"/> <input type="text"/> <input type="text"/></p> <p>Tel number:</p>	<p>Sex:</p> <p>Female <input type="checkbox"/></p> <p>Male <input type="checkbox"/></p>	<p>Date of birth <input type="text"/> <input type="text"/> <input type="text"/></p> <p>Age in year <input type="text"/></p>	<p>Height=</p> <p>Weight=</p>
--	--	---	---

Details of diabetes:

<p>Age at diagnosis:</p> <p>Disease duration:</p> <p>Current HbA1c:</p> <p>Total insulin dose:</p> <p>Pump or injection:</p>

Health behaviour and diet

Smoker:	current.	Past.	Never.
Drinker (unites).	/Day	/Week	/Month
Calcium (mg/day):			
Vitamin D (IU/day):			
Multivitamin use:			
Physical activity:			

Reproductive history

Onset of puberty (years):
Menarche (years):
Average menstrual cycle length:
Amenorrhea for ≥ 3 months:
Ever pregnant:
Number of pregnancies:
Current hormone use:
Estrogen + progesterone
Progesterone only

Medical History

<table border="1" style="width: 100%;"> <tr> <td style="text-align: center;">Patient History</td> </tr> <tr> <td>High blood pressure: Last BP= /</td> </tr> <tr> <td>Thyroid disorder: Last TFT at/...../..... Result</td> </tr> <tr> <td>Orthopaedic: Joint problems Fracture</td> </tr> </table>	Patient History	High blood pressure: Last BP= /	Thyroid disorder: Last TFT at/...../..... Result	Orthopaedic: Joint problems Fracture	<table border="1" style="width: 100%;"> <tr> <td style="text-align: center;">Family History</td> </tr> <tr> <td>Family history of osteoporosis:</td> </tr> <tr> <td>Family history of fracture:</td> </tr> </table>	Family History	Family history of osteoporosis:	Family history of fracture:
Patient History								
High blood pressure: Last BP= /								
Thyroid disorder: Last TFT at/...../..... Result								
Orthopaedic: Joint problems Fracture								
Family History								
Family history of osteoporosis:								
Family history of fracture:								

<p>Heart disease:</p> <p>Peripheral vascular disease (varicose veins):</p> <p>Renal complication (Microalbuminuria): Date/...../..... Result</p> <p>Retionopathy: Last follow up at/...../..... Result</p> <p>Neuropathy: Statin use or any other drug</p>	
---	--

Blood Investigation:

Biochemistry	Leptin	Adiponectine	IGF-I
Date of blood taken			
Result			
Reference Range			
Measurement unit			

Biochemistry	OC	CTX	25VitD	PTH	B-ALP
Date of blood taken					
Result					
Reference Range					
Measurement unit					

Radiological Investigation:

Radiography	site	Yes	No
Micro MRI	Proximal tibia		
MRI	Abdominal fat		
MRS	Lumbar spine		

